Exploiting pre-existing non-cognate T cell help to enhance humoral vaccine responses



Tom Hills MBChB (Otago) MSc (Oxon)

St John's College

A thesis submitted for the degree of Doctor of Philosophy

to the Department of Oncology, University of Oxford

Michaelmas Term 2014

Abstract

Vaccination is one of the most powerful examples of scientific endeavour resulting in clear benefits for the population. Successes in vaccinology have largely been due to empirical approaches. However, the list of diseases for which there is still no effective vaccine remains long and it is likely that a more rational approach to vaccine design will be needed for these targets. Increasingly, this appears possible with technological advances and an improved understanding of the adaptive and innate immune systems. There is a pressing need for novel B cell vaccines to target pathogens such as malaria, influenza, and human immunodeficiency virus. Well-designed humoral vaccine approaches could also be valuable in the growing field of cancer immunotherapy.

This thesis describes a novel particle-based vaccine strategy designed to elicit rapid antibody responses by exploiting pre-existing non-cognate CD4+ T cell help. Vaccine particles were engineered to display target B cell antigens exclusively on the particle surface, while helper CD4+ T cell epitopes were contained in the particle core. In principle, corresponding vaccine particles could be produced by physical formulation (e.g. using a liposomal vector) or by genetic engineering (e.g. using a recombinant measles virus). Greater success was observed in this study using a liposomal platform that allows flexible particle engineering, avoids biological challenges such as achieving adequate viral titres, and is readily scalable.

Data generated with these liposomal nanoparticles show that pre-existing CD4+ T cell immunity induced by vaccination with ovalbumin (OVA) can enhance anti-circumsporozoite protein (CSP) antibody responses following the administration of CSP-coated liposomal particles that encapsulate OVA epitopes. Anti-CSP antibodies were produced faster, reached higher levels, were of a greater affinity, and contained more isotype-switched antibody in mice pre-vaccinated with OVA. The inclusion of TLR9 agonists to give ‘self-adjuvanting’ particles further increased the immunogenicity of the vaccine platform. Next, other sources of pre-existing CD4+ T cells were examined. Many chronic viral infections induce dramatic T cell responses. Experiments using murine cytomegalovirus (MCMV) demonstrate that pre-existing anti-viral CD4+ T cells can also be re-purposed to provide non-cognate help to enhance antibody responses to CSP. Lastly, preliminary results show the utility of this approach in breaking tolerance to a cancer antigen.

The vaccine platform described in this thesis and the principles that it exploits could contribute to future rationally-designed vaccine strategies against infectious disease or cancer antigens.

Declaration of Authentication

The work presented in this thesis is my own and, where relevant, any contributions made by others have been acknowledged. The material submitted here in no way forms part of another thesis in this or any other university. This work was performed under the supervision of Professor Leonard Seymour and Doctor Ryan Cawood, Department of Oncology, Division of Medical Sciences, University of Oxford.

Tom Hills

Oxford

December 2014

Acknowledgements

Firstly, I would like to thank Professor Len Seymour and Dr Ryan Cawood for giving me the opportunity to undertake the work presented in this thesis and for their support and supervision over the last few years.

Members of the Seymour research group have been instrumental – and tolerant – in my transformation from a lab-shy clinician to something resembling a scientist. I am indebted to Drs Alison Tedcastle, Clemens Thoma, and Gray Kueberuwa for the invaluable advice and guidance they have provided over the course of my studies. The process of completing a DPhil was made easier and more enjoyable thanks to the assistance and comradeship of my fellow immunology DPhil students Dr Aliaa Alamoudi, Phil Jakeman, and Dr Geoffrey Lynn. Other members of the Seymour lab have, to a person, been welcoming, helpful, and eager to share their knowledge; I am grateful to them all. Outside of the laboratory, I would like to thank my wonderful group of Oxford friends for ensuring these last few years have been so much fun.

My family has always been a source of inspiration and support. I would like to acknowledge that my progress through school and university was only possible thanks to sacrifices made by my parents. Further, over the course of my journey in formal education, numerous devoted teachers have helped to shape both my mind and the academic path that I've taken. It is thanks to these teachers and mentors that I have found myself in such a privileged position.

I am grateful for the incredible opportunities that have fallen my way due to the kindness of strangers. The Rhodes Trust elected to provide me with a generous scholarship to undertake this work, along with an invitation to join an inspiring and nurturing community of scholars. A huge number of people have gone to considerable lengths to fundraise so that groups like Professor Seymour's can undertake scientific research; I am grateful for the dedication of these volunteers.

Lastly, and most importantly, I would like to thank my partner Alice for her love and support.

Table of contents

Abstract 2
Declaration of Authentication 3
Acknowledgements 4
Table of contents 5
List of abbreviations 12
1. Introduction 16
1.1. Vaccinology 16
1.1.1 History of vaccination 16
1.1.2. An overview of existing vaccine technologies 18
1.1.3. Challenges and future directions 20
1.2. Vaccines targeting tumour antigens 22
1.2.1. Cancer and cancer treatment 22
1.2.2. Immunotherapy for cancer 22
1.2.3. Monoclonal antibodies in cancer therapy 23
1.2.4. Cancer vaccines – history and challenges 25
1.2.5. Cancer vaccines – success stories from the clinic and future directions 29
1.3. Immunology of the humoral immune response 30
1.3.1. B cell receptor engagement 30
1.3.2. CD4+ T cell help 30
1.3.3. Toll-like receptors in the humoral immune response 32
1.3.4. Shaping the developing antibody response 33
1.4. Exploiting pre-existing non-cognate CD4+ T cells to enhance vaccine responses 37
1.4.1. Overview of the proposed mechanism of action 37
1.4.2. Conjugate vaccines 38
1.4.3. Proposed vaccine particle structure 40
1.4.4. Sources of pre-existing CD4+ T cells 41
1.5. Thesis aims and overview 43
1.5.1. Thesis aims 43
1.5.2. Thesis hypotheses 43
1.5.3. Thesis overview 44

2. Materials and methods 45
2.1. Molecular biology 45
2.1.1. Plasmid amplification in prokaryotic cells 45
2.1.2. Bacterial cells 45
2.1.3. Plasmid purification 46
2.1.4. DNA restriction digests (preparative and qualitative) 46
2.1.5 Agarose gel electrophoresis 46
2.1.6. DNA quantification 47
2.1.7. PCR amplification 47
2.1.8. DNA ligation 47
2.2. Cell culture 48
2.2.1. Growth of cell lines 48
2.2.2 DNA transfection 49
2.2.3. Generation of cell lines by transfection 50
2.2.4. Lenti-X Tet-On Advanced Inducible Expression System 50
2.2.5. Production of lentiviral constructs 50
2.2.6. Generation of cell lines by lentiviral infection 51
2.3. Flow cytometry 51
2.3.1. Overview of flow cytometry methods 51
2.3.2. Antibodies used in flow cytometry 52
2.4. Microscopy 53
2.5. Western and dot blotting 53
2.5.1. Cellular samples 53
2.5.2. Liposomal samples 53
2.6. Function-spacer-lipid (FSL) modification of cells and viruses 54
2.7. Production of Recombinant Measles Virus 54
2.7.1. Rescue of MV-RFP from cDNA 54
2.7.2. MV-RFP propagation and production in Vero cells 55
2.7.3. Purification of MV-RFP iodixanol banding 55
2.7.4. Assessment of MV titre by $TCID_{50}$ 56
2.8. Liposome production and purification 57
2.8.1. Lipid film methodology 57

2.8.2. Lipid composition of liposomal preparations 58
2.8.3. Antigens and TLR9 agonists 59
2.8.4. Dialysis 61
2.9. Vaccine particle characterisation 61
2.9.1. Dynamic light scattering (DLS) to determine particle size 61
2.9.2. Determination of particle zeta potential 61
2.9.3. Flow cytometry to detect viruses and liposomes 61
2.9.4. Electron microscopy 62
2.9.5. ssDNA oligo quantification 62
2.9.6. ELISA for quantification of particle-associated antigens 62
2.9.7. Dose calculations 63
2.10. Animal studies 64
2.10.1. General statement 64
2.10.2. Housing conditions and diet 64
2.10.3. Details of procedures 64
2.11. Assessment of cellular responses to vaccination 65
2.11.1. Preparation of mouse splenocytes 65
2.11.3. Enzyme-Linked ImmunoSpot (ELISPOT) assays 65
2.11.4. Tetramer staining 66
2.11.5. Cytokine multiplex assay 66
2.12. Assessment of humoral responses to vaccination 68
2.12.1. Enzyme-linked immunosorbant (ELISA) assay for total antigen-specific immunoglobulin response 68
2.12.2. ELISA assay for antigen-specific isotype response 69
2.12.3. ELISA to determine endpoint titre 69
2.12.4. Antigens used to coat ELISA plates 70
2.12.5. Antibodies used in ELISA studies 71
2.12.6. Assessing avidity using sodium thiocyanate 72
2.13. Statistical analyses 72
3. Production and characterisation of liposomal vaccine particles with spatially separated B and T cell epitopes 73
3.1. Introduction 73
3.2. Chapter aims 74

3.3. Results 75
3.3.1. Assessment of particle size distribution 75
3.3.2. Visualisation of liposomal vaccine particles by flow cytometry 77
3.3.3. Demonstration that liposomal vaccine particles contain OVA323-339 78
3.3.4. Demonstration of particle-bound CSP 80
3.3.5. Confirmation that CSP is present on the surface of vaccine particles 82
3.3.6. Characterising the biological activity of B cell and CD4+ T cell antigens delivered by liposomal vaccine particles 84
3.3.7. Assessment of liposomal stability 85
3.4. Chapter conclusions 86
3.5. Chapter discussion 86
3.5.1. Discussion of results 86
3.5.2. Limitations and future work 87
4. Exploiting pre-existing vaccine-induced immunity to provide non-cognate CD4+ T cell help 89
4.1. Introduction 89
4.2. Chapter aims 90
4.3. Results 90
4.3.1. Development of a vaccination regime to establish CD4+ T cell immunity 90
4.3.2. Characterisation of the antibody response to OVA323-339 + TiterMax Gold vaccination 96
4.3.3. Exploiting pre-existing immunity to full-length ovalbumin to enhance anti-CSP antibody responses 97
4.3.4. Exploiting pre-existing immunity to OVA323-339 to enhance anti-CSP antibody responses 100
4.3.5. Confirming the proposed mechanism of action 102
4.3.6. The effect of pre-existing, non-cognate, CD4+ T cell immunity on anti-CSP isotypes 103
4.3.7. The effect of pre-existing, non-cognate, CD4+ T cell immunity on anti-CSP antibody avidity 105
4.3.8. Distinguishing between the local immunostimulatory effect of TiterMax Gold and pre-existing, non-cognate, CD4+ T cell help 107

4.3.9. Exploiting systemic CD4+ T cell immunity at anatomically distinct vaccination sites 108
4.3.10. Assessing the relative importance of liposomal vaccine dose and pre-existing, non-cognate, CD4+ T cell immunity 111
4.4. Chapter conclusions 114
4.5. Chapter discussion 115
4.5.1. Discussion of results 115
4.5.2. Limitations and future work 117
5. Incorporating TLR9 agonists as the 'third signal' for B cell activation 119
5.1. Introduction 119
5.2. Chapter aims 120
5.3. Results 120
5.3.1. Incorporation of unmethylated CpG DNA oligonucleotides in liposomal vaccine constructs 120
5.3.2. *In vitro* characterisation of liposomal vaccine particle TLR9 agonism 121
5.3.3. *In vivo* safety studies of TLR9-incorporating liposomes 123
5.3.4. Pilot *in vivo* studies assessing the effect of TLR9 agonism on anti-CSP antibody responses 124
5.3.5. *In vivo* studies with a single lower dose of vaccine for further characterisation of the effect of TLR9 agonism on anti-CSP responses 126
5.4. Chapter conclusions 128
5.5. Chapter discussion 128
5.5.1. Discussion of results 128
5.5.2. Limitations and future work 131
6. Exploiting pre-existing anti-viral immunity to provide non-cognate T cell help 132
6.1. Introduction 132
6.2. Chapter aims 133
6.3. Results 134
6.3.1. Evaluating OT-II transgenic mice as a source of anti-OVA323-339 CD4+ T cells to support anti-CSP antibody responses 134
6.3.2. Production of liposomes containing the immunodominant murine cytomegalovirus MHCII epitope 135

6.3.3. Characterising the immune response of MCMV-infected mice 135
6.3.4. Pilot *in vivo* studies exploiting anti-MCMV CD4+ T cell help to enhance anti-CSP responses 140
6.3.5. *In vivo* studies to characterise the effect of anti-MCMV CD4+ T cell immunity and TLR9 agonism on anti-CSP responses 144
6.4. Chapter conclusions 150
6.5. Chapter discussion 150
6.5.1. Discussion of results 150
6.5.2. Limitations and future directions 152
7. Pilot studies targeting the self-antigen ErbB2/neu 154
7.1. Introduction 154
7.2. Chapter aims 155
7.3. Results 155
7.3.1. Production of liposomes with surface ErbB2/neu 155
7.3.2. A pilot *in vivo* study targeting ErbB2/neu in C57Bl/6 mice 157
7.3.3. Evaluating this vaccine strategy in BALB/C mice 158
7.3.4. Targeting ErbB2/neu in BALB/C mice 161
7.4. Chapter conclusions 162
7.5. Chapter discussion 162
7.5.1. Discussion of results 162
7.5.2. Limitations and future directions 163
8. Modifying measles virus particles with B cell target antigens as a strategy to exploit pre-existing anti-measles CD4+ T cells 165
8.1. Introduction 165
8.2. Chapter aims 167
8.3. Results 168
8.3.1. Genetic modification of MV to replace the surface glycoproteins with fusion proteins containing the extracellular domains of target antigens 168
8.3.2. Confirming the functionality of target Ag-F chimeric proteins 170
8.3.3. Development and characterisation of a tetracycline-responsive rescue system to provide the MV glycoproteins *in trans* during rescue and propagation of genetically modified vaccine constructs 171

8.3.4. Attempts at MV-CSP, MV-gp100, and MV-Her2 rescue in a tetracycline inducible MV glycoprotein expression cell line 176
8.3.5. Development and characterisation of an alternative rescue cell line based on the Cre-loxP system 177
8.3.6. Attempts at MV-CSP, MV-gp100, and MV-Her2 rescue in an inducible MV glycoprotein expression cell line based on a Cre-loxP system 182
8.3.7. Production of MV-RFP as a modified version of the Edmonston vaccine strain of MV 183
8.3.8. Labelling the surface of MV-RFP with FSL technology 184
8.3.9. Modifying the surface of MV-RFP with CSP antigen 185
8.3.10. Pilot in vivo studies exploiting pre-existing anti-MV immunity to enhance responses to CSP 187
8.4. Chapter conclusions 189
8.5. Discussion 189
8.5.1. Discussion of results 189
8.5.2. Limitations and future directions 190
9. Discussion: 192
9.1. Summary and discussion of results 192
9.1.1. Exploiting pre-existing non-cognate CD4+ T cells 192
9.1.2. Modifying the vaccine platform to make particles 'self-adjuvanting' 193
9.1.3. Exploiting pre-existing anti-viral immunity 194
9.1.4. Breaking tolerance to self-antigens 194
9.1.5. Modifying viral vectors to display target antigens 195
9.2. Final discussion and future directions 196
9.2.1. Future directions for this vaccine platform 196
9.2.2. Broader applications of this thesis 197
9.2.3. Final conclusions 201
References 202

List of abbreviations

/	Per
3’ or 5’	Three or five prime end of a DNA/RNA molecule
µ	Micro
Ag	Antigen
ALP	Alkaline phosphatase
ANOVA	Analysis of variance
AP-1	Activator protein 1
APAR	Advanced protein assay reagent
bNAb	Broadly neutralising antibody
BSA	Bovine serum albumin
CPE	Cytopathic effect
CSP	Circumsporozoite protein from *Plasmodium falciparum.* Primarily used in this thesis to refer to the NANP repeat B cell epitope.
CTLA-4	Cytotoxic T lymphocyte associated protein 4
Da	Daltons
DBCO	Dibenzocyclooctyl
dH_20	Deionized water
DMEM	Dulbecco’s Modified Eagle’s Media
DNA	Deoxyribonucleic acid
EDTA	Ethylenediamine tetra-acetic acid
EGFR	Epidermal growth factor receptor
Fc	Fragment crystallisable
FcR	Fc receptor
FCS	Fetal calf serum

FITC	Fluorescein isothiocyanate
FSL	Function-spacer-lipid
g	Grams
g	Gravitational force
GFP	Green fluorescent protein
GM-CSF	Granulocyte-macrophage colony-stimulating factor
H2-IAb	Designation of the MHCII haplotype of C57Bl/6 mice
H2-IAd	Designation of MHCII haplotype of BALB/C mice
HCMV	Human cytomegalovirus
HEPES	4-(2-hydroxyethyl)-1-piperazineethanesulfonic acid
HLA	Human leukocyte antigen
HRP	Horseradish peroxidase
i.m.	Intramuscular
Ig	Total immunoglobulin
IgG	Mouse immunoglobulin isotype G
IgG1	Mouse/human immunoglobulin isotype G1
IgG2	Human immunoglobulin isotype G2
IgG2a	Mouse immunoglobulin isotype G2a
IgG2b	Mouse immunoglobulin isotype G2b
IgG2c	Mouse immunoglobulin isotype G2c
IgG3	Mouse/human immunoglobulin isotype G3
IgG4	Human immunoglobulin isotype G4
IgA	Human immunoglobulin isotype A
IgD	Human immunoglobulin isotype D
IgE	Human immunoglobulin isotype E

IgM	Mouse immunoglobulin isotype M
kb	kilobase
L	Measles virus large polymerase
LB	Luria Bertani
M09	Murine cytomegalovirus M09 peptide 133-147
MCMV	Murine cytomegalovirus
mAb	Monoclonal antibody
MOI	Multiplicity of infection
mmHg	Millimetres of mercury
MV	Measles virus (Edmonston vaccine strain)
MV-RFP	Measles virus expressing the red fluorescent protein
MVA-T7	Modified Vaccinia Ankara expressing the bacteriophage T7 RNA polymerase
n	number
N	Measles virus nucleocapsid
N/A	Not applicable
NF-κB	Nuclear factor kappa-light-chain-enhancer of activated B cells
OD	Optical density
OTII	Transgenic mice bearing TCRs that recognise the OVA323-339 epitope in the context of I-A-b
P	Measles virus phosphoprotein
PBS	Phosphate Buffered Saline
PCR	Polymerase chain reaction
PE	Phycoerythrin
PVDF	Polyvinylidene fluoride
RAG	Recombination activating gene
RFP	Red fluorescent protein

RNA	Ribonucleic acid
RPMI	Roswell Park Memorial Institute media
sd	Standard deviation
SEAP	Secreted form of embryonic alkaline phosphatase
ssDNA	Single stranded DNA
subcut	Subcutaneous
T7	Bacteriophage T7 RNA polymerase
$TCID_{50}$	50% tissue culture infectious dose
TCR	T cell receptor
T_H	T helper cell
TLR9	Toll-like receptor 9
TMB	3,3′,5,5′-tetramethylbenzidine
TMG	TiterMax Gold adjuvant
UK	United Kingdom
VEGF	Vascular endothelial growth factor
VLP	Virus-like particle
VV-T7	Vaccinia virus expressing the bacteriophage T7 RNA polymerase
wt	Wild-type
x	Multiplied by

1. Introduction

1.1. Vaccinology

1.1.1 History of vaccination

Vaccination is the use of an antigenic substance prepared from the causative agent of a disease or a synthetic substitute that is administered to provide immunity against one or several ailments. The history of vaccination probably traces back to China, where as early as the 10th century liquid from smallpox lesions was taken by insufflation in an effort to induce immunity to the disease (Fenner et al. 1988). Other strategies, such as scarification were prominent in India and either arose there or arrived from China (Plotkin 2005). Cutaneous variolation eventually made its way via the Middle East to Europe. It was here, however, that vaccinology as we conceive of it today began. In the late 18th century, Edward Jenner – perhaps intrigued by a dairymaid who observed that she was protected from smallpox because she had suffered cowpox – demonstrated that cowpox inoculation could prevent smallpox (Baxby 1999). In the 19th century, Louis Pasteur began to study methods of attenuating microorganisms for the purpose of producing vaccines and vaccinology was born as a scientific endeavour (Pasteur 1880).

While smallpox vaccination and eradication holds places as both the origin of vaccinology and its crowning achievement, it is the breadth of reach that vaccinology achieved in the 20th century that is most impressive. It has become cliché to state that vaccines have had a greater effect on mortality than any other intervention except clean water (Plotkin 2005). Nonetheless, there are now licensed vaccines for more than 25 diseases, many of which once ravaged the human population (Smith et al. 2011). The benefits of vaccination are clearly demonstrated in table 1.1, which compares historical and current rates of diseases that are now preventable with vaccines. Advantages to combating diseases with vaccines include cost-effectiveness, safety, the prevention of disease – rather than its cure – with an associated reduction in suffering, and the potential for disease eradication.

Disease	20th Century pre-vaccine annual cases	2009 cases	Relative decrease
Measles	503,282	71	99.9%
Diphtheria	175,885	0	100%
Mumps	152,209	1,991	98.7%
Pertussis	147,271	13,214	91.0%
Smallpox	48,164	0	100%
Rubella	47,745	3	99.9%
Polio	16,316	0 / 1*	100%
Tetanus	1,314	18	98.6%
Haemophilus influenzae type B	20,000	35	99.8%

Table 1.1. The effect of vaccination. A comparison of vaccine-preventable disease rates in the United States for diseases in the era before vaccination with levels in 2009. * Single case of vaccine-strain associated Polio in 2009. Source: (Centers for Disease Control and Prevention 2009).

Simple and empirical vaccine design strategies – such as the use of related but non-pathogenic viruses pioneered by Jenner or the attenuation of pathogens established by Pasteur – have brought these effective vaccines to the clinic. There are undoubtedly many gains still to be made by overcoming barriers to access and uptake of the existing range of vaccines and this will be the key to realising goals such as polio eradication. However, the utility of the empirical approach to vaccine design seems limited in the face of more challenging vaccine targets. Indeed, the list of diseases for which empirical approaches have failed and where we are still without effective vaccines remains long.

1.1.2. An overview of existing vaccine technologies

The majority of licensed vaccines have been derived through the attenuation or inactivation of pathogens, or by administering pathogen components in adjuvant (table 1.2). These successful vaccines emerged largely without the rational application of immunological science. The precise mechanism of action was typically not considered during vaccine design and in some cases remains only partially understood (Plotkin 2005). The vast majority of these vaccines elicit their protective effect by inducing antibody responses. Indeed, with the exception of the Bacille Calmette-Guérin (BCG) vaccine for tuberculosis, the protective effect of all licensed vaccines is primarily mediated by antibody responses (Plotkin 2010).

Despite the overwhelming success of vaccines in the last two centuries, many challenges remain; it seems that the empirical approach to vaccine design that was initially so effective will be inadequate in designing vaccines for the future (Lambert et al. 2005). Numerous strategies are under investigation to produce novel vaccine platforms. In particular, approaches built on genetic platforms (such as viral vectors) and nanotechnologies (such as liposomes) are showing promise (table 1.2).

Live vaccines strategies, targets, and their approximate times of availability		
Use of a related animal virus	1798	Smallpox
Chemical attenuation	1885	Rabies
	1881	Anthrax
Passage *in vitro*	1927	BCG
	1935	Yellow fever
Cell culture passage	1962	OPV
	1963	Measles
	1971	Adenoviruses
	1995	Varicella
	2005	Rotavirus 89-12
Cell culture passage with cold adaptation	1969	Rubella
	2003	Live influenza
Auxotrophy	1989	Ty21a typhoid
Use of reassortants	1970s	Inactivated influenza seed
	2003	Live influenza
	2005	Rotavirus bovine-human
Non-living vaccines and their approximate times of availability		
Inactivated whole organisms	1896	Typhoid
	1896	Cholera
	1897	Plague
	1926	Whole-cell pertussis
	1938	Influenza
	1955	IPV
	1995	Hepatitis A
Use of extracts and subunits	1944	Japanese encephalitis
	1970s	Influenza
	1960	Anthrax
	1976	Cell-culture rabies
Use of toxoids	1923	Diphtheria
	1927	Tetanus
Use of capsular polysaccharides	1977	Pneumococcal
	1974	Meningococcal
	1995	Typhoid
Use of protein-conjugated capsular polysaccharides	1987	H. influenzae type b
	2002	Pneumococcal
	2002	Meningococcal
Use of purified or recombinant proteins	1986	Hepatitis B
	1996	Acellular pertussis
	1998	Lyme disease
Newer strategies with a genetic foundation (either developed as vaccines or showing promise in trials)		
Recombinant protein production	Hepatitis B S Ag, pertussis toxin, Lyme outer surface protein A, CMV gB protein	
Recombinants with genes from related agents	Dengue genes in yellow fever 17D, M. tuberculosis genes in BCG, etc	
Recombinant viral vectors with pathogen genes	HIV, CMV	
Alpha virus replicons	HIV, Haemorrhagic Fevers	
Replication-defective particles	HPV, SARS	
'Naked' DNA plasmids	HIV and many others	
Prime boost using DNA and/or vectors	HIV, malaria, tuberculosis	
Reverse vaccinology	Meningococcus B	
Synthetic peptides	Cancer, cytotoxic T cell vaccines	
Synthetic capsular polysaccharides	Hib	
Reverse genetics	Influenza, parainfluenza, RSV	
Nanotechnology strategies under development		
Cationic liposomes	Influenza, TB, etc.	
Synthetic polymer-based nanotechnologies	Influenza, Hepatitis B, HIV, etc	
Natural polymers (e.g. chitosan nanoparticles)	Hepatitis B,	
Carbon nanoparticles	TB	
MF59 (<250 nm oil-in-water droplets)	Influenza, HIV, Hepatitis B, CMV, etc.	
ISCOM or ISCOMATRIX	Influenza, HIV, Hepatitis C, Cancer peptides etc	

Table 1.2. An overview of important vaccine technologies, the approximate time they became available for use in humans, and selected novel approaches to vaccine design. Modified from: (Plotkin 2005), (Peek et al. 2008), and (Kim et al. 2014).

1.1.3. Challenges and future directions

There are many examples of vaccine targets where existing vaccine strategies are proving inadequate, but HIV, tuberculosis (TB), and malaria are particularly noteworthy. A successful vaccine strategy in each of these conditions must overcome a unique set of challenges. For example, the lack of clearly understood naturally acquired immunity to HIV, the rapid mutation rate of the virus, and the complex structure of the viral glycoproteins have rendered HIV vaccine design difficult (Burton et al. 2004)(Gaschen et al. 2002). In light of these challenges, experimental vaccine strategies have sought to elicit broadly neutralising antibody responses or cytotoxic T cells that recognise conserved epitopes. While the BCG vaccine for TB has been used for almost 100 years, its efficacy is limited due to a variety of factors such as strain variation, genetics, geographical area, and prior exposure to environmental mycobacterial species (Luca & Mihaescu 2013). A rise in antibiotic resistant strains of *Mycobacterium tuberculosis* has reinvigorated the search for a better vaccine. Approaches being evaluated include attempts to boost BCG-induced T cell responses with newer strategies such as viral vectors in heterologous prime-boost regimens (Parida & Kaufmann 2010).

While some patients infected with malaria do develop naturally acquired immunity, malaria vaccine development has been hampered by a multi-stage parasite life cycle, the lack of a clearly superior vaccine target, variability in potential target antigens, and a lack of a clear understanding of the complex interactions between the parasite and the human immune system (Arama & Troye-Blomberg 2014)(Crompton et al. 2010). While many experimental vaccines exist targeting different stages of the parasite lifecycle, RTS,S, a particle vaccine that combines immunodominant epitopes from the circumsporozoite protein with the surface antigen of Hepatitis B (HBsAg) to form particles that are immunogenic in proprietary adjuvants (Casares et al. 2010)(Gordon et al. 1995). Vaccination elicits antibody responses to both CSP and HBsAg (Casares et al. 2010). In Phase III clinical trials, RTS,S achieved a protective efficacy of 50.4% in children at 14 months post-vaccination, and 30.1% in infants (Agnandji et al. 2011)(Agnandji et al. 2012). Despite this modest success, questions remain about the durability of protection (Abdulla et al. 2013) and it may be that a combination approach (perhaps with a vaccine targeting the liver stage of infection) or an altogether different strategy, is required to achieve greater efficacy.

Despite the number of unmet vaccine needs, there has been important progress made in developing new technologies that may help fill this void. Innovative approaches to vaccine design include fusion proteins, reverse vaccinology, recombinant viral vectors, novel adjuvants such as Toll-like receptor agonists, virus-like particles, attenuation via codon de-optimisation, and nanoparticle delivery platforms (Plotkin 2009). These newer vaccine strategies – informed by advances in related scientific fields such as immunology, virology, microbiology, and nanotechnology – point to a future where vaccines will consolidate their position as a leading intervention to improve population health.

1.2. Vaccines targeting tumour antigens

1.2.1. Cancer and cancer treatment

Cancer describes a collection of different conditions unified by cellular proliferation and a propensity for invasion (Hanahan & Weinberg 2011). The life time risk of cancer is 37% and 40% for females and males, respectively (Sasieni et al. 2011), and cancer is responsible for more than one in four deaths in the United Kingdom (CRUK 2012). Advances in cancer treatment, along with improvements in early detection and screening, have reduced the mortality rate in many malignancies (Siegel et al. 2013). However, these conventional treatments have limitations. Surgery is very effective at removing primary lesions, but has limited value when distal metastases exist. Radiotherapy is a potent treatment modality in certain malignancies, but its utility is also limited by the anatomical location of the lesion and a not inconsiderable side effect profile due to damage of normal tissue. Chemotherapy is able to target distant metastases and is incredibly effective in a small number of malignancies, such as testicular cancer (Einhorn 1997). Nonetheless, in the majority of cancers the benefit of chemotherapy is more modest – even when used as a combination of chemotherapeutic agents or in multi-modal treatment regimens. These benefits are not without costs, as traditional chemotherapeutic agents have off-target effects that can manifest as severe side effects for patients undergoing treatment.

1.2.2. Immunotherapy for cancer

The field of cancer immunotherapy is maturing and immunotherapy is increasingly recognised as a powerful class of anti-cancer therapeutic. Historically, however, the question of whether or not the immune system could play a therapeutic anti-cancer role was contentious. In 1957, Burnet and Thomas first proposed the existence of tumour immune surveillance: a concept that the immune system could recognise malignant cells and could play a role in the prevention of cancer. Burnet wrote:

"It is by no means inconceivable that small accumulations of tumour cells may develop and because of their possession of new antigenic potentialities provoke an effective immunological reaction with regression of the tumour and no clinical hint of its existence" (Burnet 1957).

The existence of a role for the immune system in controlling or preventing tumour growth was challenged for decades because of a lack of direct experimental evidence. However, experimental data assessing tumour formation in mouse models with specific immune deficiencies (e.g. perforin$^{-/-}$ mice or RAG$^{-/-}$ mice) steadily accumulated, as did epidemiological evidence that individuals with immune deficiencies were more prone to both virally and non-virally induced cancers (G. P. Dunn et al. 2002). By 2003, the concept of tumour immune surveillance was widely accepted (Pardoll 2003).

Cancerous cells express different antigens to normal cells and these tumour antigens are the target of cancer immunotherapies. The existence of tumour antigens was first demonstrated in studies that found mice immunised with chemically induced tumours were protected against subsequent re-challenge with the same tumour (Old & Boyse 1964). Tumour antigens can be derived from foreign agents – such as oncogenic viruses. However, most tumour antigens arise from 'self'. For example, genetic mutations in cancer cells can give rise to neo-antigens. Alternatively, altered gene expression can lead to over-expression of proteins or the expression of proteins ordinarily restricted to specific developmental stages (Pardoll 2003). Because these tumour antigens arise from 'self', they can be poorly immunogenic. Indeed, a growing tumour develops numerous strategies to minimise tumour antigenicity and to subvert anti-tumour immunity (Zou 2005). Cancer immunotherapies typically seek to stimulate immune responses to tumour antigens or to counter tumour immune suppression, but it may be that a combination of these two approaches will prove most successful.

1.2.3. Monoclonal antibodies in cancer therapy

Monoclonal antibody (mAb) therapies are one of the great medical advances in recent decades. Administering a mAb is, in some ways, a passive form of immunotherapy. The efficacy of the mAb rituximab – which targets the B cell antigen CD20 – has paved the way for licensure of a number of anti-cancer mAbs. There are now several mAb licensed for use in cancer patients; widely used agents are described in table 1.3.

mAb	Target	Target location/function	Malignancy
Alemtuzumab	CD52	Monocytes, dendritic cells, and mature lymphocytes.	Chronic lymphocytic leukaemia and T-cell lymphomas.
Bevacizumab	VEGF	Vascular endothelial growth factor.	Colorectal, lung, breast, and renal cancer.
Cetuximab	EGFR	Receptor for epidermal growth factor.	Colorectal cancer.
Ipilimumab	CTLA-4	Negative regulatory molecule on the surface of T cells.	Melanoma.
Rituximab	CD20	Widely expressed on B cells, but not plasma cells.	Non-Hodgkin's Lymphoma.
Trastuzumab	ErbB2	Epidermal growth factor receptor dimerization partner.	Breast cancer.

Table 1.3. Anti-cancer monoclonal antibodies. A number of monoclonal antibodies are now recognised as efficacious anti-cancer agents. This table highlights important agents licensed for use in human patients. Adapted from (Oldham & Dillman 2008) and (Scott et al. 2012). For a more detailed review of mAb in cancer, including experimental agents, see: (Scott et al. 2012).

Anti-cancer mAbs may exert their effect through a variety of different mechanisms. The destruction of cancer cells can be mediated by immune effects, such as complement dependent cytotoxicity or antibody dependent cellular cytotoxicity (ADCC). Alternatively, mAbs might act by modulating signalling. Trastuzumab, for example, prevents the dimerization of Her2 receptors and subsequently reduces cellular proliferation signals (Mir et al. 2007). Bevacizumab sequesters vascular endothelial growth factor (VEGF), reducing the blood supply to tumours (Shih & Lindley 2006). Ipilimumab is an antagonist of the T cell inhibitory molecule CTLA-4 and can thus unshackle anti-cancer T cell responses, although antibody-mediated depletion of T regulatory cells may also contribute to its efficacy (Simpson et al. 2013).

Despite their success, mAb therapies have their drawbacks. The manufacture of clinical grade mAb is an intensive process, contributing to the high cost of these medications. Additionally, short half-lives can mean that the mAb must be repeatedly administered to achieve therapeutic levels (Levêque et al. 2005). A therapeutic vaccine strategy could overcome these issues. Further, it is possible that a vaccine-induced antibody response – with affinity maturation and epitope spreading – could be more efficacious than mAb therapy. However, it is also possible that a more focused antibody response – with a restricted specificity to, for example, an epitope critical in target molecule signalling – would be more efficacious. Flexible B cell vaccine platforms could be designed to allow the study of either polyclonal or mAb-like responses.

1.2.4. Cancer vaccines – history and challenges

Cancer vaccines are an inherently attractive approach – both intellectually and practically – to generate potentially powerful anti-cancer immune responses. Vaccines for infectious diseases have established themselves as the most important medical intervention of the last century (Plotkin 2005). However, vaccines against tumour antigens have not achieved similar success (Finn 2003).

In the 1890s, William Coley began treating patients with bacterial extracts ('Coley's toxins') which might have augmented immune responses targeting cancerous cells (Coley 1893). More than a century later, increasingly sophisticated and targeted approaches have been developed to generate anti-cancer immune responses. There are many detailed reviews of these strategies and their effectiveness (Pardoll 1998)(Klebanoff et al. 2011)(Schlom 2012). Conspicuously, and in stark contrast to vaccination against infectious diseases, cancer vaccines have demonstrated only limited efficacy in human patients. Table 1.4 summarises key clinical trials of cancer vaccines in recent years where standard criteria for measuring clinical responses have been reported. It provides a non-exhaustive list of different cancer vaccine strategies that have entered recent clinical trials and details their immunogenicity and clinical response rates.

Class	Vaccine	Malignancy	Reference	Immune response	Clinical response
Peptide	NY-ESO-1 + CpG	Melanoma	(Fourcade et al. 2008)	CD8	0/8
	Multi-epitope vaccine alone	Melanoma	(Slingluff et al. 2008)	CD4	2/17 (PR)
	gp100 + IFA ± GM-CSF	Melanoma	(Celis 2007)	CD8	0/28
	NY-ESO-1 + IFA	Melanoma	(Khong et al. 2004)	CD8 + CD4	1/37 (PR)
	Multi-epitope vaccine + IFA	Kidney	(Suekane et al. 2007)	CD8 + Ab	0/10
	CA9 multi-epitope vaccine + IFA	Kidney	(Uemura et al. 2006)	CD8 + Ab	3/23 (PR)
	Multi-epitope vaccine + IFA	Lung	(Barve et al. 2008)	CD8 + CD4	2/63 (1 PR, 1 CR)
	Telomerase peptides + IFA	Lung	(Bolonaki et al. 2007)	CD8	0/22
	Multi-epitope vaccine + IFA	Lung	(Suzuki et al. 2013)	CD8	0/15
	Survivin peptide ± IFA	Breast	(Tsuruma et al. 2008)	CD8	0/17
	WT1 + IFA	Brain	(Izumoto et al. 2008)	Not detected	2/21 (PR)
	Multi-epitope vaccine + IFA	Oesophagus	(Kono et al. 2009)	CD8	1/10 (CR)
	Survivin peptide + IFA	Urothelial	(Honma et al. 2009)	CD8	0/9
	WT1 peptide + IFA	Gynaecological	(Ohno et al. 2009)	Not reported	0/12
	Glypican-3 + IFA	Hepatocellular	(Sawada et al. 2012)	CD8	1/33
	Chimeric Her2 peptide + ISA 720	Multiple	(Kaumaya et al. 2009)	Ab	1/24 (PR)
	WT1 + IFA	Multiple	(Morita et al. 2006)	Not reported	1/10 (PR)
	Telomerase peptides + IFA	Multiple	(Mavroudis et al. 2006)	CD8	0/19
	Multi-epitope vaccine + IFA	Biliary tract	(Aruga et al. 2013)	CD8	0/9
	OVERALL RESPONSE RATE				**14/387 (3.6%)**
Dendritic cell	Transduced with MART-1	Melanoma	(Butterfield et al. 2008)	CD8 + CD4	0/17
	Pulsed with allogeneic tumour lysate	Melanoma	(von Euw et al. 2008)	CD8	0/7
	Pulsed with allogeneic tumour lysate	Melanoma	(Palucka et al. 2006)	CD8	2/20 (1 PR, 1 CR)
	Pulsed with autologous tumour lysate	Melanoma	(O'Rourke et al. 2007)	Not reported	6/46 (3 PR, 3 CR)
	Transfected with RNA	Melanoma	(Kyte et al. 2006)	CD8 + ?CD4	0/20
	Pulsed with peptides	Melanoma	(Lesimple et al. 2006)	CD8	0/12
	Pulsed with wt & modified gp100 peptides + KLH	Melanoma	(Lesterhuis et al. 2011)	CD8	2/27
	Pulsed with peptides	Kidney	(Berntsen et al. 2008)	CD8	0/30
	Allogeneic DC fused with autologous tumour	Kidney	(Avigan et al. 2007)	CD8 + CD4	2/20 (PR)
	Pulsed with peptides	Breast	(Svane et al. 2007)	CD8	0/26
	Pulsed with allogeneic tumour lysate	Thyroid	(Bachleitner et al. 2009)	?CD8	0/10
	Pulsed with CEA peptide	Multiple	(Babatz et al. 2006)	CD8	0/9
	Pulsed with mannan-MUC1 fusion protein	Multiple	(Loveland et al. 2006)	CD8 + CD4 + Ab	0/10
	Modified by pox-virus expressed CEA + TRICOM	Multiple	(Morse et al. 2005)	CD8 + CD4	0/13
	OVERALL RESPONSE RATE				**12/247 (4.9%)**
Viral vector	Heterologous prime-boost poxvirus-tyrosinase	Melanoma	(Lindsey et al. 2006)	CD8 + Ab	0/13
	Heterologous prime-boost poxvirus-NY-ESO-1	Melanoma	(Odunsi et al. 2012)	CD8 + CD4 + Ab	3/21 (2 CR, 1 PR)
	Poxvirus-encoded 5T4	Kidney	(Amato et al. 2008)	CD8 + Ab	0/13
	Poxvirus-encoded PSA + TRICOM	Prostate	(Arlen et al. 2007)	CD8	0/7
	Poxvirus-encoded 5T4	Colorectal	(Harrop et al. 2006)	?CD8 + ?CD4 + Ab	0/17
	Poxvirus-encoded CEA + TRICOM	Multiple	(Marshall et al. 2005)	Ab + CD8	1/68 (CR)
	Poxvirus-encoded MUC-1 + CEA + TRICOM	Multiple	(Mohebtash et al. 2011)	CD8 + CD4 + Ab	2/26 (1 PR, 1 CR)
	OVERALL RESPONSE RATE				**6/155 (3.9%)**
Protein	CHP-NY-ESO-1 + CHP-Her2 proteins + OK-432	Oesophagus	(Aoki et al. 2009)	Ab	0/8
	NY-ESO-1 protein + ISCOMATRIX	Melanoma	(Nicholaou et al. 2009)	CD8 + Ab	0/27
	MAGE-A3 + AS15 in a liposomal formulation	Melanoma	(Kruit et al. 2013)	CD4 + Ab	4/36 (1 PR, 3 CR)
	CHP-Her2 ± GM-CSF or OK-432	Multiple	(Kitano et al. 2006)	CD4 + CD8	0/9
	OVERALL RESPONSE RATE				**4/80 (5.0%)**
OTHERS					
Ganglioside	Ganglioside + IFA	Melanoma	(Osorio et al. 2008)	Ab	1/22 (PR)
RNA	Autologous tumour mRNA	Melanoma	(Weide et al. 2008)	?CD8 + ?CD4 + Ab	0/8
Tumour cells	Tumour cells mixed with a GM-CSF cell line	Lung	(Nemunaitis et al. 2006)	Ab	0/49
	Autologous tumour + GM-CSF	Mesothelioma	(Powell et al. 2006)	Ab	0/22

Table 1.4. An overview of selected recent cancer vaccine clinical trials. Where evidence used atypical assays (i.e. not ELISPOT, tetramer, or antigen specific proliferation assays) CD4+ or CD8+ T cell responses are appended with a '?'. Delayed type hypersensitivity responses were not recorded. This list is not exhaustive. Rather, it gives an idea of the range of cancer vaccines that have recently completed early stage clinical trials and summarises their immunogenicity and efficacy. Updated from (Klebanoff et al. 2011).

In contrast to vaccination against infectious disease antigens, therapeutic cancer vaccination faces significant additional hurdles both to immunogenicity and effector function. Firstly, many cancer antigens are protected by both central and peripheral self-tolerance mechanisms. Breaking tolerance is a considerably more challenging goal than generating an immune response to an antigen derived from a foreign pathogen. Secondly, a more recently developed understanding of the immune-suppressive local immune microenvironment cultured by solid tumours has emerged as an additional barrier to efficacy. It follows that cancer vaccines capable of inducing systemic immune responses may not mediate anti-tumour immune effects as key effector cell functions can be attenuated in the tumour microenvironment (Zou 2005). Indeed, many of the vaccine strategies outlined in table 1.4 elicited readily detectable antibody, CD4+, or CD8+ T cell responses in cancer patients, but these did not necessarily translate into clinical responses. It is not clear whether this is due to suboptimal immune responses or due to the inability of these mediators to act effectively in the tumour microenvironment.

The low response rate across a range of different vaccine approaches is striking, although this should be interpreted in light of the overall response rate for all early-stage clinical trials of anti-cancer agents, which is reported as 3.8% or 4.4% (although the overall response rate in trials that included a licensed agent with known efficacy rate is 17.8%) (Horstmann et al. 2005)(Roberts et al. 2004). This low response rate for cancer vaccines is troubling, but not totally disheartening. This table used strict criteria for determining response rates – taking only complete and partial responses by Response Evaluation Criteria in Solid Tumours (RECIST) criteria as a positive result. Frequently, correlations between clinical and immune responses were observed, suggesting an efficacious vaccine response. Additionally, many patients experienced stabilisation of their disease – sometimes for extended periods of time – but stable disease was not classified as a response in this analysis due to difficulties drawing conclusions about what constitutes stable disease in a range of different malignancies described in studies that were largely single-arm. Lastly, as with many cancer immunotherapies, the efficacy of cancer vaccines may be understated when measured with conventional tools for assessing radiological responses. For example, immunotherapy may induce an inflammatory response locally that results in an increase in tumour volume that reduces over several months. If assessed with metrics such as RECIST, this would be scored as ‘progressive disease’. Accordingly, many investigators have called for different response

criteria to be used in immunotherapy trials to reflect the distinct mechanism of action and to better capture meaningful clinical responses (Wolchok et al. 2009).

Overall survival is potentially both a more important and less subjective study endpoint than response rates measured with RECIST or similar tools. Despite modest response rates by conventional criteria, some cancer vaccines have produced significant improvements in progression-free or overall survival. For example, a heterologous prime-boost regimen where poxviruses encoding prostate specific antigen (PSA) and a triad of costimulatory molecules (TRICOM) demonstrated an 8.5 month overall survival benefit in metastatic castration resistant prostate cancer (Kantoff, Schuetz, et al. 2010). This approach had previously been shown to elicit immunological responses and reductions in PSA in a phase I trial, but no responses had met RECIST criteria (Arlen et al. 2007).

CD8+ T cell responses have been the goal of the vast majority of cancer vaccine strategies. This may reflect parallel advances in the understanding of cytotoxic T cell biology, the correlation of certain T cell responses with favourable outcomes in many cancers (Galon et al. 2006), and the efficacy of adoptive T cell therapies in specific malignancies (Hinrichs & Rosenberg 2014). However, the generation of an effective CD8+ T cell response by vaccination faces at least two major hurdles. First, many tumour antigens – being 'self' or 'modified self' molecules – are protected by central tolerance mechanisms; negative selection during thymic T cell development may result in a paucity of effector T cells capable of recognising and responding to epitopes derived from tumour antigens. Secondly, vaccine-induced cytotoxic T cells must be able to function in the immune-suppressive tumour microenvironment. B cell vaccine strategies do not face the exact same challenges. Auto-reactive B cells are deleted during development, but this process is less stringent than for T cells and many B cells capable of mounting response against 'self' exist in the periphery. These cells are generally anergic or 'antigen ignorant', with important control mechanisms including the absence of CD4+ T cell help. Occasionally, autoantibodies are produced and these drive the pathogenesis of a range of different autoimmune conditions by destroying normal cells in organs such as the thyroid, pancreas, and skin (Davidson & Diamond 2001). The observation that auto-antibodies can have powerful cytotoxic effects, coupled with the success of mAb therapy for cancer, suggests that B cell vaccine approaches could be successful in cancer. Further, antibodies elicited by cancer vaccines may be less likely to be impeded by local immune-suppressive mechanisms than vaccine-induced cellular responses.

1.2.5. Cancer vaccines – success stories from the clinic and future directions

Many cancer vaccines have been evaluated in clinical trials, but response rates have been low. It is not clear whether this is a result of inadequate immunogenicity – either quantitatively or qualitatively – or because of immune dysfunction in the tumour microenvironment. After years of disappointing results, there are now success stories emerging in cancer vaccinology.

Sipuleucel-T is now a licensed prostate cancer vaccine. This approach uses autologous peripheral-blood mononuclear cells that have been activated *ex vivo* with a recombinant fusion protein consisting of the tumour antigen prostatic acid phosphatase fused to the immune cell-activating granulocyte–macrophage colony-stimulating factor (GM-CSF). In a pivotal phase III trial, sipuleucel-T prolonged survival in castration-resistant prostate cancer by 4.1 months (Kantoff, Higano, et al. 2010). Numerous other therapies using more complex and potent strategies to enhance the function of antigen presenting cells (APCs) are also showing promise (Palucka & Banchereau 2012), and it is likely that as our understanding of APC biology improves so too will the efficacy of APC-based cancer vaccines.

Another class of cancer immunotherapy that could be considered a vaccine is the oncolytic virus 'T-VEC'. This is a cancer-selective replicating 'oncolytic' Herpes Simplex virus that liberates tumour antigens during replication and lysis of cancer cells. It is proposed that the presence of a replicating virus, alongside secreted virally-encoded GM-CSF, potentiates an anti-cancer immune response. Potentially, this strategy could directly alter the immunosuppressive immune microenvironment to allow effective immune destruction of tumour cells. T-VEC elicited anti-tumour responses in both injected and non-injected lesions. A phase III trial in metastatic melanoma demonstrated an objective response rate of 26% and a complete response rate of 11%, compared with 5.7% and 0.7% respectively in the GM-CSF alone control arm (Andtbacka et al. 2013). Durable responses were seen in 16.3% of T-VEC treated patients, compared with only 2.1% in the control arm (Kaufman et al. 2014). These results seemingly leave T-VEC poised for clinical approval. It is possible that the future of cancer immunotherapy will lie in combination treatment with agents that stimulate immune responses and address local immune suppression.

1.3. Immunology of the humoral immune response

1.3.1. B cell receptor engagement

The humoral immune response is initiated by B cell receptor (BCR) engagement – 'signal one' of the three signals necessary for full B cell activation. This initial recognition stage typically occurs in secondary lymphoid organs, such as lymph nodes (Kelsoe 1995). Smaller antigens – less than 70 kDa – can diffuse freely via the lymphatics and subcapsular sinus to lymph node follicles where they encounter B cells (Pape et al. 2007). Larger antigens, however, do not diffuse through this conduit system. Particles in the 200 nm size range are trapped in the subcapsular synapse by a sheet of macrophages (Carrasco & Batista 2007). Increasingly, it is recognised that B cells do not always engage soluble antigen and that larger antigens are acquired by B cells following interactions with macrophages in this subcapsular follicle region, or through interactions with other APCs such as follicular dendritic cells (Carrasco & Batista 2007)(Batista & Harwood 2009). Recent insights have identified the acquisition of membrane associated antigen as particularly important for generating B cell responses *in vivo* (Wykes et al. 1998)(Batista et al. 2001)(Carrasco & Batista 2006).

1.3.2. CD4+ T cell help

BCR binding and cross-linking results in internalisation of target antigen. In the endosomal pathway, protease activity gives rise to small peptides that can be loaded onto MHCII molecules for presentation at the cell surface (Watts 2001). These MHCII-peptide complexes are recognised by CD4+ T helper cells bearing T cell receptors (TCRs) specific for the MHCII-peptide complex (Parker 1993). This interaction between a CD4+ T cell and a B cell presenting antigenic peptides in the context of MHCII can result in helper signals – via a combination of contact-dependent mediators (e.g. CD40-CD40L interactions) and soluble molecules such as cytokines – that drive B cell proliferation, antibody affinity maturation, isotype switching, and the formation of B cell memory (Parker 1993) (Garside et al. 1998)(McHeyzer-Williams et al. 2011).

Germinal centres are specialised structures in secondary lymphoid organs where somatic hypermutation, isotype switching, and the selection of high-affinity B cells occurs (Kelsoe 1995)(Liu et al. 1996). T follicular helper cells are particularly important in the developing humoral immune response. These are a specialised, antigen-experienced CD4+ T cell

population that express the germinal centre homing marker CXCR5, high levels of CD40L, and secrete the 'helper cytokine' IL-21 (King et al. 2008). In the germinal centre, CD4+ T cells provide helper signals to naïve B cells to drive the formation of high affinity antibody responses and, crucially, long-lasting humoral immunity (Manz et al. 2005). B cells can mature into memory B cells, antibody-secreting plasma cells, or long-lived plasma cells, which can reside in sites such as the bone marrow and produce high levels of antibody for long periods of time (McHeyzer-Williams et al. 2011).

In the absence of CD4+ T cell help, antibody production can still occur. However, germinal centres do not form and B cell isotype switching, affinity maturation, and memory formation are greatly impaired (Parker 1993)(Kawabe et al. 1994). Carbohydrate antigens do not contain peptide epitopes for presentation to CD4+ T cells on MHCII. They do, however, often contain highly organised repeated units and so can effectively bind and cross link BCRs (Mond et al. 1995). Alone, these 'type II T-independent' antigens generate significant IgM but often do not elicit high titre IgG antibodies or effective B cell memory responses (Bachmann & Zinkernagel 1997)(Buskas et al. 2009). In clinical trials, carbohydrate antigens generated IgM and IgG2 responses, but these were transient and a booster response was not able to be elicited on repeat administration (Käyhty et al. 1984). Conjugate vaccines attempt to overcome this limitation by coupling carbohydrate antigens to a protein carrier to provide epitopes for CD4+ T cell help (section 1.4.2). In contrast, type I T-independent antigens generate polyclonal antibody responses by non-specifically activating B cells. Examples of type I T-independent antigens include the Toll-like receptor (TLR) agonists such as lipopolysaccharide or CpG DNA (Bachmann & Zinkernagel 1997).

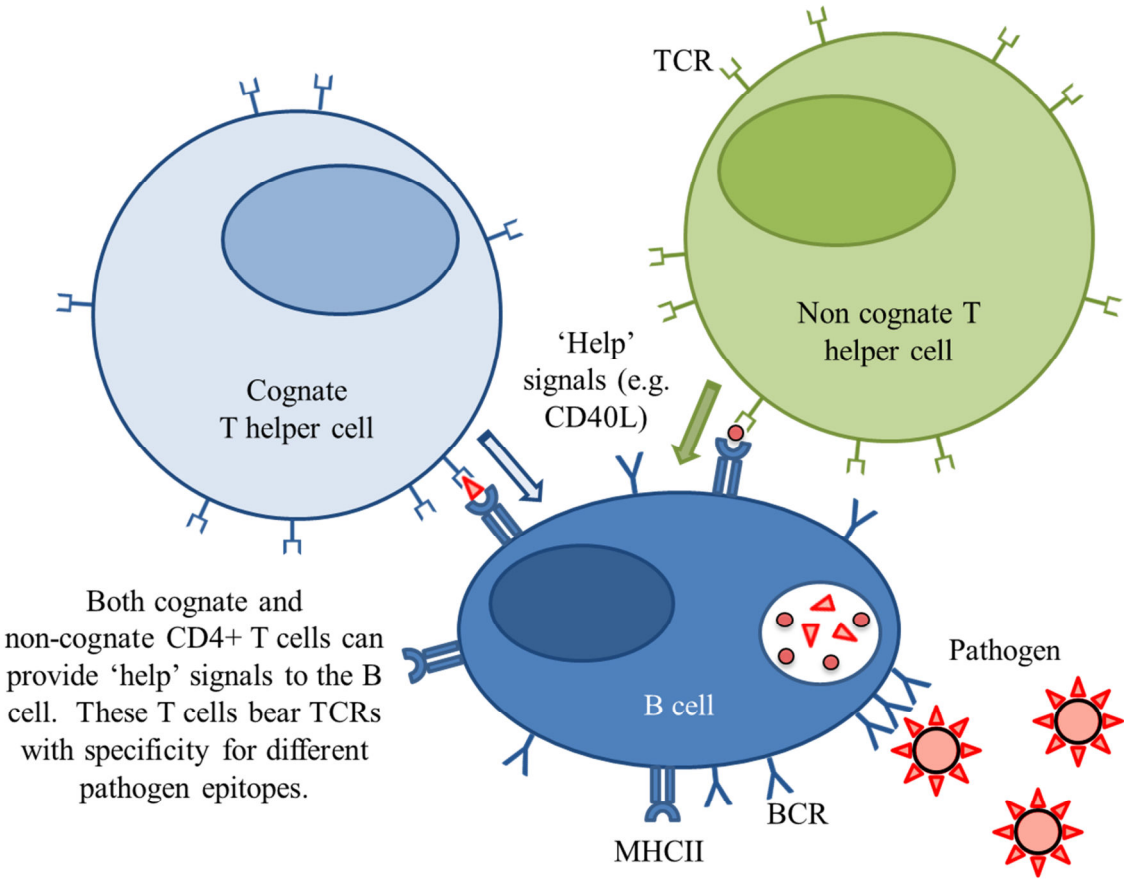


Figure 1.1. An overview of the humoral immune response to pathogens. B-cell activation begins with extracellular antigens binding to BCRs on naïve B-cells. This results in receptor crosslinking and internalisation of the antigen into the endosomal system, where protease activity generates peptides that are loaded onto MHCII and expressed at the cell surface. CD4+ T cells bearing a TCR that recognises MHCII-Ag complexes (either specific for the same [cognate] antigen that was bound by the BCR, or a different co-internalised [non-cognate] antigen) then interact with the stimulated B-cell to provide 'help' signals that result in B-cell proliferation, differentiation, antibody production, somatic hypermutation, and isotype switching.

1.3.3. Toll-like receptors in the humoral immune response

TLR agonists have long been known to non-specifically stimulate naïve B cells to proliferate and produce antibody (Krieg et al. 1995). However, the dogma of an antigen specific B cell response involved the sequential integration of two signals: BCR activation and CD4+ T cell help. It is increasingly recognised that even in the context of antigen specific B cell responses TLR agonism is an important driver of a fully developed antibody response. TLR agonism can synergise with BCR triggering and CD4+ T cell help for full differentiation of naïve human B cells into long-lived, class-switched, antibody-secreting plasma cells (Ruprecht & Lanzavecchia 2006)(Liu et al. 2003). This response resulted from the direct action of TLR agonists on B cells, rather than being mediated indirectly through other antigen presenting cells or via CD4+ T cells (Ruprecht & Lanzavecchia 2006).

B cells express a range of different TLRs and signalling through these receptors has been shown to influence many different B cell functions (Iwasaki & Medzhitov 2004). When considering the effect of TLR agonism on B cells, it is worth reflecting on the unique position of B cells in immunology as both a VDJ-rearranged effector cell of the adaptive immune system and an APC charged with detecting pathogenic threats and coordinating appropriate immune responses. TLR agonism in B cells has been demonstrated to stimulate B cell proliferation, differentiation, antigen presentation, class-switch recombination, and cytokine secretion (Bekeredjian-Ding & Jego 2009). TLR2, TLR4, TLR7, and TLR9 are critical B cell pattern recognition receptors, although their relative importance differs between murine and human B cells. Most notably, human B cells are not responsive to TLR4 agonists such as lipopolysaccharide (Mandler et al. 1993)(Bekeredjian-Ding & Jego 2009).

TLR agonists are increasingly included adjuvant strategies to enhance vaccine responses (Maisonneuve et al. 2014). Often, this strategy seeks to enhance antigen presentation in dendritic cells, but a direct effect on B cells is likely to be important in a number of situations. TLR9 is a particularly influential pattern recognition receptor in both murine and human B cells, as well as in a number of other leukocytes (Iwasaki & Medzhitov 2004). TLR9 detects unmethylated CpG DNA motifs, which are more numerous in pathogenic DNA when compared with mammalian genomes (Krieg et al. 1995). In murine B cells, TLR9 agonism can stimulate B cell proliferation and immunoglobulin secretion (Gururajan et al. 2007)(Krieg et al. 1995). TLR9 agonists have emerged as important adjuvants capable of stimulating powerful antibody and cell-mediated immune responses (Vollmer & Krieg 2009)(Lin et al. 2004).

1.3.4. Shaping the developing antibody response

A fully-developed humoral immune response is achieved by three signals: BCR triggering, CD4+ T cell help, and B cell TLR agonism. In the rational design of a novel vaccine strategy, it is important to consider how each of these signals will be achieved and the desired effect on the developing B cell response.

Alongside T_{fh} cells, other CD4+ T cell subsets are critical in shaping the humoral immune response. The original paradigm of T helper cell differentiation divided CD4+ T helper cells into T_H1 or T_H2 populations (Mosmann et al. 1986). These subsets were primarily defined by which effector cytokines dominated the cytokine secretion profile – IFNγ, IL-2, and TNFα for T_H1 cells, and IL-4, IL-5, and IL-13 for T_H2 cells, although production of some of these

cytokines was not exclusively restricted by subset (Mosmann & Sad 1996)(Zhu et al. 2010). Cytokines are critical for directing a naïve T helper cells fate. The complex cytokine milieu that exists where a CD4+ T cell encounters its cognate antigen directs its polarisation. Broadly speaking, IL-12 and IFNγ evoke a T_H1 phenotype whereas IL-4 drives towards T_H2 polarisation (Zhu et al. 2010).

The T_H1/T_H2 profile of CD4+ T cells that provide helper signals to B cells influences the isotype of antibody produced during the developing humoral immune response (Coffman et al. 1988). B cells are capable of producing a range of different antibody isotypes each with distinct functions (table 1.5). Immature B cells express IgM on their surface and initially secrete IgM when they encounter their cognate antigen. As the B cell response develops, signals – typically from CD4+ T cells and including contact dependent signals such as CD40-CD40L interactions and contact independent signals such as the cytokines IFNγ and IL-4 – result in isotype switching (Parker 1993)(Coffman et al. 1988). CD4+ T cell help induces the expression of enzymes such as activation-induced cytosine deaminase (AID), a key mediator of class-switch recombination and somatic hypermutation (Muramatsu et al. 2000)(Dedeoglu et al. 2004). Isotype switching occurs primarily through non-homologous end-joining of repaired, deaminated, switch regions (Stavnezer et al. 2008). These cytosine-rich switch regions are located upstream of the genes encoding for the different heavy chain genes that give rise to IgM, IgD, IgE, IgA, and IgG antibodies. How the T_H1/T_H2 balance of CD4+ T_H cells affects the isotype of the antibody response is not necessarily simple, and may depend on the antigen and the context it is encountered. However, IgG1 is the dominant T_H2 isotype produced in a mouse setting, whereas IgG2a (or IgG2c in C57Bl/6 mice) production requires T_H1-polarised CD4+ T cell help (Coffman et al. 1988)(Stevens et al. 1988).

	Human IgG isotypes				Mouse IgG isotypes			
	IgG1	**IgG2**	**IgG3**	**IgG4**	**IgG1**	**IgG2a IgG2c**	**IgG2b**	**IgG3**
Pathogen neutralisation	+++	++	++	++	+	+++	++	+
Antibody dependent cellular cytotoxicity	++	-	++	-	-	+++	++	+
Complement dependent cytotoxicity	++	+	+++	-	-	+++	+++	-
Association with T_H1/T_H2	T_H1/ T_H2	T_H1/ T_{indep}	? T_H1	T_H2	T_H2	T_H1	T_H1	? T_H1

Table 1.5. An overview of the function of human and mouse IgG subclasses. Comparisons between different isotype subclasses in different species are inherently problematic due to diverse experimental systems, including assays where the functionality of murine IgG subclasses is measured in human models. Hence, this table aims to act as a guide only. For clarity, non-IgG isotypes have been omitted. This is not to understate their importance in the immune response, or their functional capabilities. For example, IgM a powerful activator of the complement cascade whereas IgE potently sensitises mast cells. Produced with data collated from (Janeway et al. 2001), (Nimmerjahn & Ravetch 2005), (Nimmerjahn & Ravetch 2007), (Schroeder Jr & Cavacini 2010), (Stevens et al. 1988), (Banerjee et al. 2010), and (Lin et al. 2004).

Different antibody isotypes have different functions *in vivo*, although making comparisons between isotypes is difficult due to differences between murine and human IgG subclasses and the diversity of techniques used to measure antibody subclass function. The Fc region of IgG antibodies is critical in determining its functionality, as it influences the interaction with soluble mediators such as complement and immune cells bearing a range of different activatory and inhibitory Fc receptors (Nimmerjahn & Ravetch 2005). In humans, IgG1 and IgG3 bind the activatory Fc receptors with a higher affinity than IgG2 or IgG4, resulting in more antibody-dependent cellular cytotoxicity (ADCC). Similarly, in mice, IgG2a and IgG2b antibodies bind activatory receptors with a higher affinity than the inhibitory FcγRIIB, whereas IgG1 antibodies readily bind FcγRIIB. These differences translate to significantly more ADCC when antibodies are an IgG2a or IgG2b subclass (Nimmerjahn & Ravetch 2007).

As the B cell response matures, the affinity of the secreted antibody can also change. AID expression results in the deamination of deoxycytidine residues in DNA, transforming C:G pairs into U:G mispairs. The resulting base-pair mismatches are subsequently repaired to give a variety of single nucleotide substitutions (Di Noia & Neuberger 2007). Somatic hypermutation results in affinity maturation as B cells bearing BCRs with higher affinity for antigen are selected for (Neuberger & Milstein 1995).

Signals from T_{fh} cells or other CD4+ T cell subsets – such as T_H1 or T_H2 cells – that shape the developing B cell response can be delivered by CD4+ T cells that recognise the same antigenic molecule that the BCR engaged ('cognate' help) or a distinct molecule also taken up and presented on MHCII by the B cell ('non-cognate' help) (Russell & Liew 1979)(Russell & Liew 1980)(Scherle & Gerhard 1986). This non-cognate help (also termed 'intermolecular' or 'heterotypic' help) has been shown to be crucial for the development of protective immune responses to vaccinia virus vaccination (Yin et al. 2013). This observation forms the mechanistic basis for the proposed particle vaccine design presented in this thesis, which seeks to exploit pre-existing non-cognate CD4+ T cell populations to enhance antibody responses to target antigens.

1.4. Exploiting pre-existing non-cognate CD4+ T cells to enhance vaccine responses

1.4.1. Overview of the proposed mechanism of action

This thesis proposes a humoral vaccine strategy that exploits pre-existing non-cognate CD4+ T cell responses to enhance antibody responses to target antigens. In doing so, it describes a platform technology that could be used to target a range of different antigens. In the context of infectious diseases, this approach could generate rapid antibody responses to pandemic threats, such as influenza. Alternatively, if developed as a cancer vaccine, exploiting pre-existing non-cognate CD4+ T cells might allow the breaking of tolerance to tumour antigens. Indeed, vaccines could be designed to display antigens that represent target epitopes of efficacious mAb with a view to generating anti-cancer immune responses *in vivo*.

A fully developed humoral immune response requires both B cells and CD4+ T cells (Parker 1993). An absent or inadequate CD4+ T cell response may limit the magnitude and speed of antibody production to pathogens such as influenza (Alam et al. 2014). Similarly, a lack of CD4+ T cell help may limit the efficacy of vaccine approaches for certain vaccine targets such as carbohydrate antigens which do not contain any peptides for presentation on MHCII or cancer antigens where cognate T cells may have been deleted during thymic development. Indeed, CD4+ T cell responses have been shown to be critical to efficacy of cancer vaccine approaches that elicit efficacious antibody responses in preclinical models (Overwijk et al. 1999). To achieve adequate CD4+ T cell help, vaccine particles can be designed to contain both target and 'helper' antigens (see section 1.4.2). In keeping with the 'intermolecular help' model, CD4+ T cells specific for a helper antigen ('non-cognate' CD4+ T cells) can support B cell responses against a distinct target antigen, provided the two antigens are both taken up by a B cell bearing a BCR specific for the target antigen (figure 1.2).

Exploiting non-cognate CD4+ T cells is not in itself a novel idea. Indeed, conjugate vaccines exploit CD4+ T cell responses to carrier proteins to enhance the immunogenicity of 'weak' carbohydrate antigens. However, this thesis proposes that spatial segregation of these B cell and T cell epitopes – with helper T cell epitopes 'hidden' within the vaccine particle core – will focus the immune response on the target B cell antigen. Further, it is hypothesised that these particles will be capable of exploiting *pre-existing* non-cognate CD4+ T cells to drive

rapid production of higher titre, higher affinity, and isotype-switched antibodies against target antigens.

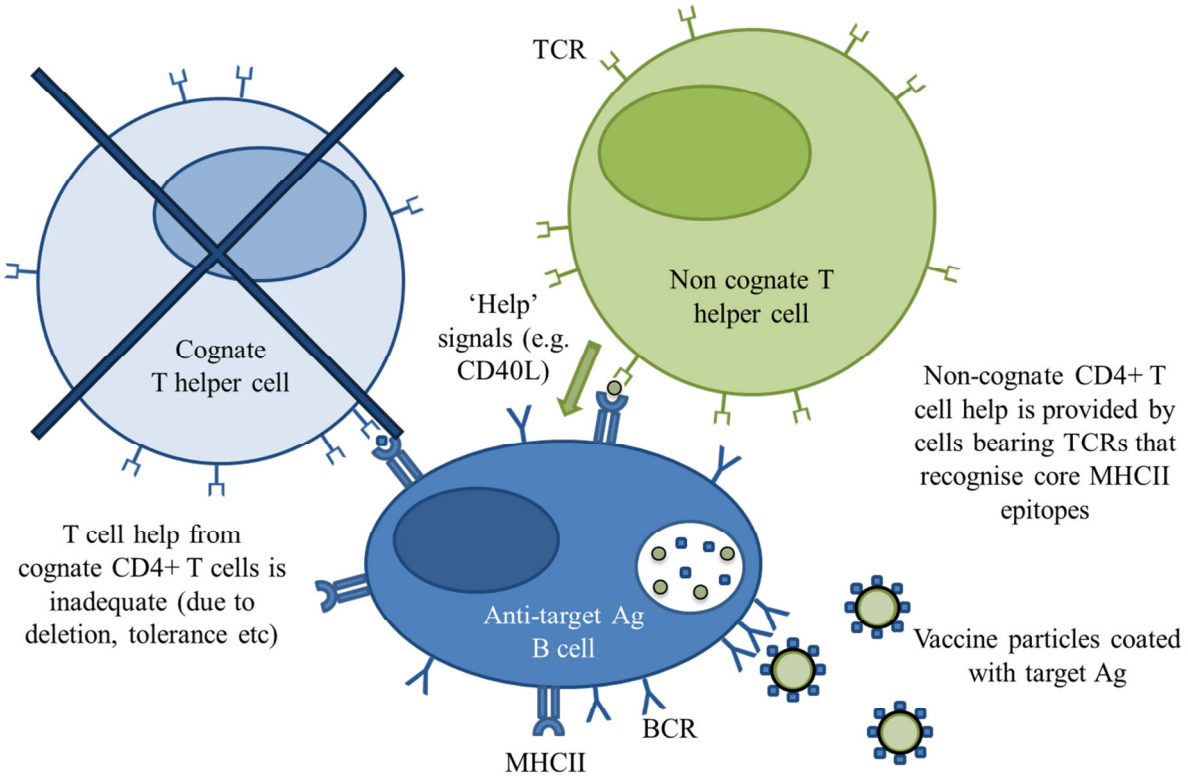


Figure 1.2. Proposed vaccine mechanism of action. Pre-existing non-cognate CD4+ T cell help is exploited to enhance antibody responses to target antigens. B-cells with BCRs specific for the antigen on the particle surface are engaged by vaccine particles. Following internalisation, endosomal proteases generate peptide fragments from both the surface antigen and the helper antigen entrapped within the vaccine particle. These are presented on MHC class II to cognate T cells (i.e. those that recognise the same antigen as the BCR – which may be rare for weak antigens) and non-cognate T cells (i.e. those that recognise the strong helper MHCII epitopes). Pre-existing CD4+ T cells that recognise the helper antigen (generated by pre-vaccination or viral infection) can then provide co-stimulatory signals to the B-cell, resulting in confirmation of antibody production. These signals may drive B-cell proliferation, differentiation, antibody production, somatic hypermutation, and isotype switching. Because the specificity of this antibody response was determined at the point of BCR-mediated antigen-recognition, the antibody produced will be directed against the target antigen on the vaccine particle surface, and not against the core helper components.

1.4.2. Conjugate vaccines

Conjugate vaccines also look to combine B cell epitopes with 'helper' T cell antigens. Carbohydrate antigens can generate T-independent responses, but these are suboptimal. Practically, the most important limitation of T-independent vaccine strategies is the failure to elicit significant and sustained antibody responses in children under 18 months of age (Goldblatt 2000). Conjugate vaccines are produced by chemically linking carbohydrate antigens to protein carriers containing helper epitopes. In 1931, Avery & Goebel were the

first to demonstrate the ability of carrier proteins to overcome the poor immunogenicity of carbohydrate antigens (Avery & Goebel 1929)(Avery & Goebel 1931). Nowadays, conjugate vaccines are an important part of the routine immunisation schedule, where they induce robust antibody responses to carbohydrate antigens in young children where the disease burden of some encapsulated pathogens is highest.

For example, the *Haemophilus influenzae* type b (Hib) vaccine comprises the polysaccharide from the bacterial capsule conjugated to an immunogenic protein carrier – often a tetanus or diphtheria toxoid. B cells with Hib polysaccharide-specific BCRs bind the polysaccharide component of the conjugate vaccine and internalise the whole molecule. After endosomal processing, peptide from the carrier protein component can be presented on MHC class II for recognition by toxoid-specific CD4+ T cells. These toxoid-specific CD4+ T cells provide helper signals that activate Hib-specific B cells, driving the production of a protective antibody response to the Hib polysaccharide. In contrast to the strategy proposed in this thesis, conjugate vaccines do not necessarily exploit *pre-existing* non-cognate CD4+ T cells. The T and B cell responses may both develop following the administration of a conjugate vaccine. Further, immunisation schedules frequently combine multiple vaccines in single dose products, and the Hib conjugate vaccine is sometimes combined with the tetanus and diphtheria toxoid vaccines (National Health Service 2014). However, it is worth noting that the effect of combining vaccines on the developing immune responses can be complex and single dose formulations do not always result in enhanced responses (Greenberg et al. 2000).

It should be noted that the structure of conjugate vaccines may leave both the carbohydrate antigen and the helper protein available for B cell binding. Consequently, conjugate vaccines may elicit significant antibody responses against protein carriers (Del Giudice 1992) and it is possible that this response may detract from that mounted against the polysaccharide target. In fact, linking a carbohydrate antigen to a protein carrier does not guarantee an improved antibody response to the carbohydrate target. In fact, in different contexts, conjugation to a protein carrier can enhance or inhibit antibody response to carbohydrate antigens (Peeters et al. 1991)(Schutze et al. 1985)(Pobre et al. 2014).

A large number of conjugate vaccines targeting carbohydrate tumour antigens have been developed through to clinical trials. Both the technologies and the clinical progress of these trials have been reviewed in detail (Danishefsky & Allen 2000)(Dube & Bertozzi 2005)(Buskas et al. 2009). Like many cancer vaccination strategies, conjugate cancer

vaccines shown some promise, and antibody responses in clinical trials have correlated with improved clinical outcomes (Buskas et al. 2009). However, this approach has failed to consistently demonstrate anti-tumour efficacy in large numbers of patients. The reasons for this lack of efficacy could be many and varied. Of note, conjugate vaccines face surmountable problems such as linkage chemistry which can damage antigens and result in variations between batches (Buskas et al. 2009), but perhaps the biggest challenge in conjugate cancer vaccinology is the design of particles capable of eliciting high-titre antibody responses to self-antigens.

Numerous carrier proteins and peptides have been investigated to enhance the immunogenicity of carbohydrate tumour antigens. However, a major problem in conjugate cancer vaccinology is that anti-carrier or anti-linker antibody responses can dominate over the response to the weak carbohydrate antigen (Buskas et al. 2004)(Ni et al. 2006). It may be that more sophisticated methods of displaying B and T cell antigens are required. In fact, one of the most promising strategies comprises a totally synthetic, three component vaccine particle. A carbohydrate antigen is conjugated to a peptide CD4+ T cell epitope and displayed on the surface of a liposomal particle (Buskas et al. 2005)(Ingale et al. 2007). The multivalent display of the B cell epitope on the particle surface is believed to be critical for the enhanced immunogenicity, but it is worth considering whether a key benefit of this strategy is that the spatial arrangement of the antigens effectively shields the CD4+ T cell epitope from B cell recognition (Bundle 2007).

1.4.3. Proposed vaccine particle structure

Vaccine particles studied in this thesis are coated in target antigen but, unlike conjugate vaccines, do not have exposed helper epitopes. Instead, these are encapsulated inside the particle core where they are unavailable for BCR binding but can still be accessed for presentation to CD4+ T cells on MHCII. This spatial separation of B and T cell antigens may elicit an antibody response focused on the target B cell antigen. To produce particles with these characteristics, two strategies were investigated.

Liposomal particles can be engineered to carry protein antigens in the particle core. Additionally, by incorporating more complex lipids with pendant functional groups, it is possible to conjugate proteins to the particle surface. The use of a liposomal platform carries the advantage of flexible engineering to include established model antigens or novel targets. Additionally, it is possible to incorporate other vaccine components – such as Toll-like

receptor agonists – in a vaccine particle. An alternative strategy modifying a viral vector was also explored. When designing viral vectors for gene therapy, it is common to 'pseudotype' viruses by replacing native glycoproteins with those of another virus (Naldini et al. 1996). Here, a similar strategy was employed but the genes encoding the native glycoproteins of the Edmonston strain of Measles Virus (MV) were replaced with target B cell antigens, rather than glycoproteins from other viruses.

This thesis aims to test the effect of pre-existing immunity to core components of these vaccine particles on the developing humoral immune response to surface-displayed target antigens. Interestingly, it has long been known that the immune response to core viral components can influence responses to subsequent infection with distinct serotypes (Russell & Liew 1979)(Russell & Liew 1980), but vaccine particles have not been designed to directly exploit this phenomenon, as is proposed in this thesis.

1.4.4. Sources of pre-existing CD4+ T cells

From a translational perspective, two major populations of pre-existing CD4+ T cells could be exploited to enhance antibody responses to target antigens.

The first population is vaccine-induced CD4+ T cells. Many vaccines currently included in the routine immunisation schedule elicit long-lived populations of CD4+ T cells. Some well-studied vaccines – such as the Edmonston strain of measles virus (Naniche et al. 2004), vaccinia virus (Amara et al. 2004), or the tetanus toxoid vaccine (Diethelm-Okita et al. 2000) – can induce durable CD4+ T cell responses that can persist for years after vaccination. Immunodominant CD4+ T cell epitopes restricted to common HLA class II haplotypes have been described for many of these vaccines (Diethelm-Okita et al. 1997). Importantly, there has also been work to define 'universal' helper epitopes from tetanus and diphtheria toxoids – capable of acting as CD4+ T cell epitopes in a diverse population with an array of different MHCII molecules (Diethelm-Okita et al. 2000). Incorporating these universal helper epitopes to exploit pre-existing anti-tetanus or anti-diphtheria vaccine-induced immunity is an appealing strategy. A benefit of exploiting vaccine-induced populations of CD4+ T cells is the ability to boost this response as required. For example, pre-vaccination could cultivate an optimal population of non-cognate CD4+ T cells before the particle vaccine designed to exploit these cells was administered.

An alternative approach would be to exploit CD4+ T cells raised by chronic infection. There are many pathogens that are near ubiquitous in human populations. However, it is chronic viral infections that elicit the highest frequency of T cells. The magnitude of the anti-viral CD4+ T cell response to human cytomegalovirus (HCMV) infection is striking. One third of infected adults have HCMV-specific populations comprising >20% of their circulating CD4+ and/or CD8+ memory T cell repertoire. These T cell responses can be oligoclonal and even inflationary; up to 23% of CD8+ T cells from a healthy seropositive donor have been reported to recognise just one viral epitope (Khan et al. 2002). Approximately 5% of the CD4+ T cell pool is directed against HCMV epitopes in healthy seropositive individuals, but this can be as high as 40% (H. S. Dunn et al. 2002)(Harcourt et al. 2006)(Sester et al. 2002). Within this population, CD4+ T cells with specificity for one viral epitope can represent 0.3-1.5% of the total peripheral CD4+ T cell population (Weekes et al. 2004). Anti-HCMV CD4+ T cells have a memory phenotype and secrete IFNγ and TNFα (Vescovini et al. 2007)(Sester et al. 2002).

Both seroprevalence and detectable cellular immune responses to HCMV increase with age (Staras et al. 2006)(H. S. Dunn et al. 2002). Consequently, it may be best to exploit anti-HCMV CD4+ T cells in vaccine strategies designed for use in elderly patients, such as cancer vaccines. It is worth noting that, unlike the situation with other chronic infections such as lymphocytic choriomeningitis virus (LCMV), the phenomenon of exhaustion is not seen in T cell responses to HCMV (Crawford et al. 2014). Designing a particle vaccine that encapsulates immunodominant HCMV epitopes so as to exploit these high frequency anti-HCMV T_H1 CD4+ T cells to enhance humoral immune responses is an attractive strategy.

1.5. Thesis aims and overview

1.5.1. Thesis aims

The overarching aim of this thesis is to exploit pre-existing non-cognate CD4+ T cells to support antibody responses to target antigens. To test this hypothesis, pre-existing CD4+ T cell populations could be raised in mice by vaccination, mimicking the CD4+ T cell populations elicited by vaccination in humans. Alternatively, by infecting mice with a chronic viral pathogen such as murine cytomegalovirus (MCMV), anti-viral CD4+ T cells could be generated in a model representative of human cytomegalovirus (HCMV) infection. Pilot immunogenicity studies will then assess whether these anti-vaccine or anti-viral CD4+ T cells can be co-opted to provide helper signals to B cells that recognise target antigens on the surface of vaccine particles that also encapsulate immunodominant CD4+ T cell epitopes from the antigen targeted by pre-vaccination or from MCMV. The effect of pre-existing non-cognate CD4+ T cell immunity on the magnitude, isotype, and avidity of the antibody response will be measured. The utility of this platform as a strategy to 'break tolerance' to tumour antigens will then be assessed. As an alternative to a liposomal particle platform measles virus (MV) vaccine particles will be modified to display target antigens on the surface of particles to assess whether viral vectors can also be used to exploit pre-existing non-cognate CD4+ T cell responses.

1.5.2. Thesis hypotheses

1. Pre-existing CD4+ T cells generated by vaccination with ovalbumin peptides will support higher magnitude antibody responses to *Plasmodium falciparum* circumsporozoite protein (CSP) following the administration of CSP-coated liposomes that encapsulate CD4+ T cell epitopes from ovalbumin.

2. Anti-CSP antibody responses generated with non-cognate CD4+ T cell help will be produced faster, be of a higher avidity, and will contain more isotype-switched antibody.

3. Antibody responses will be further augmented by the inclusion of Toll-like receptor agonists in liposomal vaccine particles that are designed to exploit pre-existing non-cognate CD4+ T cell help.

4. Pre-existing anti-viral immunity – generated by chronic infection with MCMV – will be able to provide non-cognate CD4+ T cell help to support anti-CSP antibody responses to CSP-coated liposomal vaccine particles that encapsulate immunodominant MCMV CD4+ epitopes.

5. By exploiting pre-existing CD4+ T cell help, liposomal particles coated with the cancer antigen Erbb2/neu will be able to elicit anti-Erbb2/neu antibody responses.

6. Measles virus particles engineered to display target antigens on the particle surface will elicit higher anti-target antigen antibody responses in the presence of pre-existing non-cognate anti-MV CD4+ T cell immunity.

1.5.3. Thesis overview

1. Producing liposomal vaccine particles with B cell epitopes on the particle surface and MHCII epitopes for CD4+ T cell help in the particle core (chapter three).

2. Exploiting pre-existing non-cognate CD4+ T cell immunity raised by vaccination to enhance antibody responses to target antigens (chapter four).

3. Augmenting B cell responses by incorporating TLR9 agonists in the core of liposomal vaccine particles (chapter five).

4. Exploiting pre-existing non-cognate CD4+ T cell immunity raised by MCMV infection to enhance antibody responses to target antigens (chapter six).

5. Pilot studies assessing whether this vaccine platform can ‘break tolerance’ to tumour antigens (chapter seven).

6. Modifying measles virus particles to assess whether pre-existing non-cognate CD4+ T cells can be exploited by a viral particle coated in target antigen (chapter eight).

2. Materials and methods

2.1. Molecular biology

2.1.1. Plasmid amplification in prokaryotic cells

Transformation of *Escherichia coli (E.coli)* allows amplification of recombinant plasmid DNA. Transformation of bacterial cells was performed by thawing competent *E. coli* cells on ice, followed by the addition of 10-100 ng of plasmid DNA per reaction. Competent cells were incubated with DNA on ice for 20 minutes and then subjected to heat shock by placing tubes in a water bath at 37 ºC for 3 minutes. Subsequently, 0.9 mL of Luria Bertani (LB) medium was added to each tube and then incubated for a further 30 minutes at 37 ºC (for Ampicillin-resistant vectors) or 60 minutes at 37 ºC (for Kanamycin-resistant vectors). Samples were poured onto nutrient agar plates containing the relevant selection antibiotic, or 100 µL of each sample was streaked out to allow individual colony isolation.

Culture media and culture plate agar were prepared using LB broth base (20 g/L, Sigma-Aldrich, UK) and LB broth with agar (LENNOX, 35 g/L, Sigma-Aldrich, UK) respectively. LB broth and LB agar were dissolved in dH_20, sterilised by autoclaving, and then cooled prior to the addition of antibiotics. Bacterial culture broth and agar plates were prepared to contain Kanamycin (50 µg/mL, Kanamycin Sulphate, Invitrogen, UK) or Ampicillin (50 µg/mL, Ampicillin Sodium, Sigma-Aldrich, UK).

Single bacterial colonies identified on culture plates after transformation were picked and grown overnight in broth (3 mL mini-prep or 125 mL maxi-prep) in the presence of the relevant selection antibiotic at 37 ºC with agitation (200 rpm) using a Sanyo orbital incubator (SANYO Electric Biomedical Co. Ltd, USA).

2.1.2. Bacterial cells

XL10 Gold Ultra-competent *E.coli* bacteria (Stratagene) were used to amplify DNA for the majority of cloning projects. When a cloning strategy necessitated DNA free of dam and dcm methylation at key restriction sites, JM110 *E.coli* (Stratagene) were used. These cells are deficient in methyl transferase enzymes and allow high purity methyl deficient DNA to be amplified. To prepare competent cells, aliquots of XL10 or JM110 cells were grown in 3 mL

of sterile 2xYT medium and incubated at 37 ºC until an Optical Density (OD) of 0.3 at λ 550 nm was reached. Cells were transferred to a liquid culture of 200 mL 2xYT medium and grown until OD550 = 0.480, after which cells were kept on ice for 5 minutes. Cells were spun at 3000 rpm in an Allegra X-15R centrifuge with an SX4750 rotor (Beckman Coulter, UK) at 4ºC for 20 minutes before re-suspension in 80 mL sterile transformation buffer I (TFBI) total. Tubes were kept on ice for 5 minutes before centrifugation at 3000 rpm at 4ºC for 20 minutes. Bacterial cells were re-suspended in 8 mL sterile transformation buffer II (TFBII) and left on ice for 15 minutes before being aliquoted in 100 µL volumes into pre-chilled Eppendorf tubes for storage at -80ºC.

2.1.3. Plasmid purification

Plasmids were purified from cultured bacterial cells for screening and small-scale applications using the QIAprep Spin Miniprep Kit (Qiagen, UK). For larger-scale applications, maxi-prep purifications were performed using the Qiagen High Speed Maxi-prep kit (Qiagen, UK). Plasmid identity was confirmed by diagnostic restriction digest and agarose gel electrophoresis. When plasmids were engineered, the selected colony was also further validated by DNA sequencing (Source Bioscience, UK).

2.1.4. DNA restriction digests (preparative and qualitative)

Restriction endonucleases were used to give diagnostic digestion patterns or to produce DNA molecules with ‘sticky’ overhanging ends for subsequent ligation with other DNA molecules terminated with compatible overhangs. All digests were performed according to conditions specified by the manufacturer (New England Biolabs, UK).

2.1.5 Agarose gel electrophoresis

Size fractionation of DNA on 1% (w/v) agarose (Invitrogen, UK) gels containing ethidium bromide (Sigma-Aldrich, UK) (0.5 µg/mL) in 0.5 x TAE buffer (4.84 g Tris-base, 1.09 g glacial acetic acid, 0.29 g EDTA in 1 L dH_20) enabled visualisation of DNA and size estimation, by relative comparison to the commercially available molecular weight marker HyperLadder I (Bioline Ltd, UK). DNA molecules from purified plasmids or fragments from PCR reactions or restriction digestions were subjected to gel electrophoresis (10 volts per cm gel length, 30-120 minutes) in horizontal DNA electrophoresis gel tanks (Bio-Rad Laboratories Ltd, UK). DNA bands were visualised using a gel and fluorescent imaging

system (AlphaImager, Alpha Innotech Corporation, USA) under ultraviolet light or excised under blue light using Dark Reader trans-illuminator (GRI, UK) for purification and subsequent use.

2.1.6. DNA quantification

DNA was quantified using a Nanodrop spectrophotometer (Thermo Scientific, UK). Prior to analysis, the nanodrop was blanked using distilled water and then background readings were taken using the buffer in which the DNA was dissolved (Qiagen Elution Buffer or nuclease-free H_2O). The final quantity of DNA was expressed as ng/µL.

2.1.7. PCR amplification

PCR reactions were carried out using a PTC-225 DNA Engine Tetrad thermal cycler (MJ Research, Massachusetts). Custom synthesised primers (Sigma-Aldrich, UK) and Phusion DNA polymerase Master Mix (New England Biolabs, UK) were used for PCR reactions according to the manufacturer's instructions for three-step amplifications. This involved an initial denaturation (98 ºC for 30 seconds); 30 repeated cycles of denaturation (98 ºC for 10 seconds), annealing (10 seconds at a temperature determined after estimating the annealing temperature of the reaction primers), and extension (72 ºC for 15 seconds per kilobase [kb]); followed by a final extension step (72 ºC for 10 minutes).

2.1.8. DNA ligation

Donor (insert) and recipient (vector) DNA were digested with single or double (for directional cloning) restriction enzyme(s) generating compatible overhangs for complementary base-pairing and, thus, ligation of insert and vector. Digested insert was gel-purified or cleaned up, while the vector was de-phosphorylated by treatment with 2 µL of calf intestinal alkaline phosphatase (37 ºC, 1 h) (Invitrogen, UK) to reduce the number of colonies resulting from vector re-ligation. Vectors were then purified by column clean up using the QIAprep Spin Miniprep Kit (Qiagen, UK) according to the manufacturer's protocol. The correct size of fragments for cloning – generated by Polymerase Chain Reaction (PCR) or restriction digest – was confirmed by visualisation after gel electrophoresis. Fragments were either purified from excised gel bands using the QIAquick Gel Extraction Kit (Qiagen, UK), or, where it was unnecessary to resolve fragments of different sizes, purified directly from the digestion reaction using the QIAprep Spin Miniprep Kit (Qiagen, UK).

All purified DNA was eluted in nuclease-free water. Ligation reactions were performed with T4 DNA Ligase (New England Biolabs, UK) at room temperature according to the manufacturer's protocol.

2.2. Cell culture

2.2.1. Growth of cell lines

Cell lines were cultured in the appropriate media at 37 ºC in humidified incubator with 5% CO_2 supplementation. To passage adherent cells, monolayers were washed with PBS (PAA laboratories, UK) then treated with 0.05% trypsin/0.2% EDTA (Sigma-Aldrich, UK) for several minutes and agitated until cells had lifted from the culture surface. Growth media containing 10% FCS (fetal calf serum) was then added to the trypsin/EDTA-treated cells at a ratio of five volumes to one to neutralise the proteolytic trypsin and to prepare cell suspensions for subsequent passage or analysis. When experiments required cells to be seeded into microplates (e.g. TCID50), cells were counted using a haemocytometer (Marienfeld) and adjusted to the required concentration with growth media before being applied to microplates.

Cell line	Description	Source	Culture media
Vero	Kidney epithelial cell line derived from an African green monkey	European Collection of Cell Cultures (Porton Down, UK)	DMEM + 10% FCS
HEK293A	An adherent subclone of the 293 cell line. HEK293s were derived from human embryonic kidney cells transformed with the adenoviral E1A gene.	European Collection of Cell Cultures (Porton Down, UK)	DMEM + 10% FCS
HEK293T	A subclone of the 293 cell line also containing the SV40 large T antigen.	European Collection of Cell Cultures (Porton Down, UK)	DMEM + 10% FCS
HEK-Blue-mTLR9	HEK293 cells transfected with both the murine TLR9 gene and an inducible form of secreted alkaline phosphatase under the control of the IFN-β minimal promoter fused to five NF-κB and AP-1-binding sites.	Invivogen, (France).	DMEM + 10% FCS with blasticidin (30 μg/ml) and zeocin (100 μg/ml)
293-3-46	HEK293 cells constitutively expressing T7 RNA polymerase together with MV nucleocapsid protein and phosphoprotein.	Professor Stephen Russell, Mayo Clinic, USA	DMEM + 10% FCS with 1.2mg/mL G418

Table 2.1. Characteristics and growth conditions of cell lines.

2.2.2 DNA transfection

DNA transfection of cells was performed at approximately 80% confluence using Lipofectamine 2000 (Life Technologies, UK). Briefly, DNA and lipid transfection reagent were mixed in OptiMEM media (Life Technologies, UK) at ratio of 1 μg DNA to 2.5 μL transfection reagent, scaled up or down as required for each particular experiment. This

solution was incubated at room temperature for 30 minutes before being added to wells containing target cells for transfection and media with 2% FCS.

2.2.3. Generation of cell lines by transfection

Transfected DNA elements can be readily maintained in mammalian cell culture if they contain an expression cassette that confers resistance to an antibiotic otherwise toxic to mammalian cells. 293A or 293T cell lines were transfected with plasmids with SV40 origins of replication containing genes of interest and either a blasticidin or puromycin resistance gene under a PGK promoter. In 293T cells, the large T antigen of SV40 is expected to allow replication of the plasmid through its action on the SV40 origin. 24 hours after transfection, media was replaced with DMEM containing 10% FCS and the relevant cytotoxic antibiotic (hygromycin at 150 μg/mL or puromycin at 3 μg/mL). These concentrations of antibiotics had previously been demonstrated to kill all untransfected cells within 96 hours. Resistant clones were selected and expanded to give stably transduced cell lines. These cell lines were maintained in selection antibiotic up until they were harvested for use in a given experiment.

2.2.4. Lenti-X Tet-On Advanced Inducible Expression System

The Lenti-X Tet-On Advanced Inducible Expression System (Clontech, UK) was used to facilitate inducible expression of the MV fusion and haemagglutinin genes, which would be toxic if constitutively expressed in a cell line. pLVX lentiviral plasmids were generated containing either the F and H gene under the control of the tetracycline responsive pTight promoter along with either puromycin or blasticidin resistance cassettes. The pTight promoter allows gene expression in the presence of both the Tet-On 3G transactivator protein and doxycycline. The Tet-On 3G transactivator protein was incorporated in the genome of our vaccine constructs, while doxycycline was provided in the culture medium.

2.2.5. Production of lentiviral constructs

Lentiviruses were generated by the transfection of 293T cells with lentiviral plasmids and a packaging mix containing the necessary accessory genes and a pseudotyping glycoprotein using Xfect transfection polymer (Clontech, UK). 48 hours after transfection, supernatant was collected and filtered through a 0.45 μm filter to remove cellular debris. This was then aliquoted and frozen for future use.

2.2.6. Generation of cell lines by lentiviral infection

Lentiviral infection was performed by adding serial dilutions of lentiviral aliquots added to culture medium of 293A cells seeded 24 hours earlier in a six-well plate at $2x10^5$ cells per well. To enhance infection efficiency, media containing lentiviruses was mixed with polybrene (a polycation that reduces charge repulsion between the virus and the cellular membrane) to give a final concentration in culture of 4 μg/ml. The plate was centrifuged at 1,200 x g for 60 min at 32°C then moved to a humidified incubator at 37°C. 24 hours after infection, media was replaced with DMEM containing 10% FCS and the relevant cytotoxic antibiotic (blasticidin at 10 μg/mL or puromycin at 3 μg/mL). Over 7-14 days, colonies were allowed to form. These were isolated and individual clones were grown in selection media to generate stably transduced cell lines.

2.3. Flow cytometry

2.3.1. Overview of flow cytometry methods

For cultured cells, media was removed from flasks and cells were washed with PBS before the addition of enzyme-free cell dissociation buffer (Invitrogen, UK). Cells were suspended in media and transferred to FACS tubes (Becton Dickinson, USA) for staining with appropriate antibodies in 100 μL total volumes. Staining was performed at 4°C for one hour with agitation. Excess antibody was removed by adding 3 mL of PBS; followed by centrifugation at 300g for three minutes, re-suspension of the cell pellet in a further 3 mL of PBS, repeat centrifugation, then re-suspension of cells in 100 μL of appropriate media for further staining or analysis. Staining with secondary antibodies was also performed in 100 μL volumes and at 4°C with agitation. Staining with fluorophore-conjugated antibodies was performed in the dark.

2.3.2. Antibodies used in flow cytometry

Antibody	Species	Dilution	Company and catalogue number
Anti-CSP 2A10	Mouse monoclonal	1:1000	Jenner Institute, University of Oxford, UK.
Anti-gp100	Rabbit polyclonal	1:200	Santa Cruz Biotechnology (USA) sc-38590
Anti-her2/neu	Mouse monoclonal 9G6	1:200	Santa Cruz Biotechnology (USA) sc-08
Anti-mouse IgG (Fc specific) FITC-labelled	Goat $F(ab)_2$	1:500	Sigma-Aldrich (UK) F2772
Anti-rabbit IgG (whole molecule) (FITC labelled	Goat $F(ab)_2$	1:500	Sigma-Aldrich (UK) F1262
Anti-MV Haemagglutinin	Mouse monoclonal	1:200	Genway Biotech (USA) 20-511 241553
Anti-CD4 (mouse) AlexaFluor647	Mouse monoclonal RM4-5	1:500	BD Biosciences 557681
AntiCD8a (mouse) AlexFluor488	Mouse monoclonal 53-6.7	1:500	BD Biosciences 557688

Table 2.2. An overview of antibodies used in flow cytometry

2.4. Microscopy

Bright field and fluorescent images of live cells were obtained using a Zeiss Axiovert 25 microscope and captured with a Nikon DS5M camera and Nikon Imaging Software.

2.5. Western and dot blotting

2.5.1. Cellular samples

Protein samples were obtained by treating cells with an appropriate lysis buffer followed by freeze-thawing. Samples were spun at 2000 rpm for 5 minutes at 4 °C to remove cell debris. Protein quantification was performed using APAR quantification. In Western blot assays, standardised amounts of protein were loaded 10% polyacrylamide gels. The gel was run at 160 V for one hour and then protein was transferred to a nitrocellulose membrane over two hours at 400mA. The membrane was then blocked with 5% milk before incubation with primary antibodies (in 5% milk) at 4°C overnight (or one hour at room temperature for blots against the CSP protein). The membrane was washed and then incubated with the appropriate secondary antibodies conjugated to HRP (in 5% milk) for one hour at room temperature before visualisation and film development using ECL reagent (Pierce, UK).

2.5.2. Liposomal samples

Studies using liposomes were mixed with Laemmli buffer before loading onto MiniPROTEAN 16.5% Tris Tricine gels (BioRad Laboratories, UK). Coumassie Brilliant Blue reagent (Pierce, USA) was used to stain Tris Tricine gels. After transfer to nitrocellulose, membranes were developed as described in 2.5.1.

For dot blot assays, 3 µL of untreated liposomal preparations was blotted directly onto a nitrocellulose membrane and allowed to dry before blocking with 5% milk, washing, and subsequent probing with antibodies.

Silver staining was performed using the Silver Stain Plus kit (BioRad, UK) following the manufacturer's instructions.

2.6. Function-spacer-lipid (FSL) modification of cells and viruses

FSL technology (KODE Biotech, New Zealand) is a useful tool for labelling the surface of cells, viruses, or other structures comprised of a phospholipid membrane. 293A cells or measles virus particles were mixed with FSL constructs either containing a biotin, fluorescein, or CSP moiety as the 'F' functional group. Labelling reactions were performed at the specified concentration of FSL (0.01 – 100 μg/mL) in PBS (for MV) or DMEM (for 293A cells) at 37°C for one hour. Prior to flow cytometric analysis, no purification steps were taken. When studying FSL-labelled MV or liposomal particles by flow cytometry, FSL constructs in solution were analysed to ensure they did not form micelles that resulted in a detectable signal within the MV or liposomal particle gate. For CSP labelling of MV for *in vivo* vaccination studies, labelled particles were purified using Vivaspin 500 columns with a MWCO of 100,000 Da (GE Healthcare, UK).

2.7. Production of Recombinant Measles Virus

2.7.1. Rescue of MV-RFP from cDNA

The recovery of Measles Virus (MV) from cDNA typically requires the expression of key viral proteins *in trans* and T7 to drive genome transcription. To this end, a plasmid encoding measles virus anti-genomic cDNA under a T7 promoter was transfected into Vero cells. MV large polymerase (L), Nucleocapsid protein (N) and Phosphoprotein (P) were also expressed by transient transfection of three separate CMV-driven expression plasmids (kind gift of Professor Stephen Russell, Mayo Clinic, USA). T7 expression was achieved by infecting Vero cells with either a recombinant Vaccinia Virus vector expressing T7 (VV-T7) or recombinant Modified Vaccinia Ankara (MVA-T7, kind gift of Dr Adele Fielding, University College London, UK) vector at a multiplicity of infection (MOI) of one, as described by (Schneider et al. 1997), for one hour prior to transfection. VV-T7 caused a marked cytopathic effect in VEROs which was only partially controlled with 40μg/mL of the VV inhibitor Ara-C. MVA, in contrast, does not replicate efficiently in Vero cells, removing the need for Ara-C and allowing purification of rescued MVA without concern about contamination with replicating MVA helper virus particles. 72-96 hours after transfection, RFP-positive syncytia were observed and these were isolated as a P0 stock.

2.7.2. MV-RFP propagation and production in Vero cells

The Edmonston strain of MV has been adapted to tissue culture and Vero cells allow production of high titre MV. P0 stocks were used to infect a 25cm^2 tissue culture flask which was harvested by removing supernatant, trypsin/EDTA treatment of the cellular fraction, neutralisation of the trypsin/EDTA with DMEM + 10% FCS. The cellular fraction was then isolated by centrifugation at 2000 rpm for 5 minutes at 4°C in an Allegra X-15R centrifuge with an SX4750 rotor (Beckman Coulter, UK). This was then subjected to three freeze-thaw cycles to release cell associated virus. Cellular debris was then removed by pelleting again at 2000 rpm for 5 minutes at 4°C to give a P1 stock. This was used to infect a 175cm^2 tissue culture flask to generate P2 stocks (prepared by freeze thawing the cell fraction, as described previously, in 10 mL of culture supernatant) for HyperFlask infection and production of purified virus.

Cells from a confluent T175 flask of Vero cells were harvested and diluted in 500 mL of DMEM with 10% FCS and then seeded into a Hyperflask (Corning, The Netherland). 48 hours later, when the cells were 80% confluent, 10% FCS media was removed and replaced with 500 mL 2% FCS DMEM containing the clarified crude virus P2 preparation of MV-RFP. Approximately 72 hours later, when extensive RFP-positive syncytia were visible, vigorous agitation was applied to dislodge infected cells. Cells and media were removed and spun at 2000 rpm for 10 minutes to isolate the cell pellet. 250 mL of PBS was subsequently applied to the hyperflask and agitation was used to dislodge any remaining cells. This PBS cell suspension was spun at 2000 rpm for 10 minutes to pellet the cellular fraction. Cell fractions were combined in 5 mL of culture supernatant, subjected to two freeze-thaw cycles, and stored at -80°C prior to iodixanol purification.

2.7.3. Purification of MV-RFP iodixanol banding

Banding of virus by ultracentrifugation allows the purification of viral particles on the basis of size and density. A 52% solution of iodixanol was prepared by diluting OptiPrep (Sigma, UK) solution (60% iodixanol) in 1 M MgSO4, 0.25 M sucrose, 100 mM Tris-HCl, pH 7.5. Lower density solutions were obtained by diluting this 52% solution in 100 mM MgSO4, 0.25 M sucrose, 10 mM Tris-HCl, pH 7.5 to give concentrations of 52%, 36%, and 20% w/v iodixanol. Discontinuous iodixanol gradients were prepared by layering these in Ultra-Clear Tubes (14 x 95mm, 14.0mL, Beckman Coulter, UK). Gradients were overlaid with freeze-

thawed virus stock and centrifuged at 150,000 rcf in a Beckman Coulter ultracentrifuge for 90 minutes at 4ºC. Visible bands were extracted by piercing the centrifuge tube with an 18 gauge needle and aliquots were prepared for freezing prior to titre analysis by TCID50.

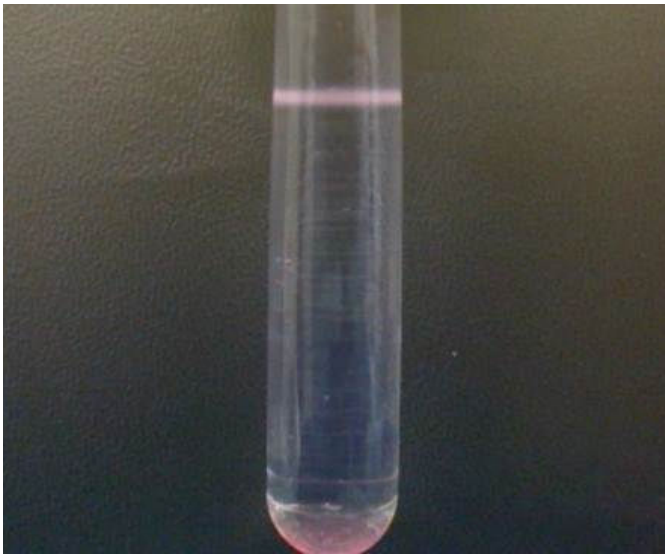


Figure 2.1. The appearance of the MV-RFP band after ultracentrifugation in an iodixanol gradient.

2.7.4. Assessment of MV titre by $TCID_{50}$

$TCID_{50}$ (50% tissue culture infectious dose) is a method for quantifying the number of infectious viral particles. Vero cells were seeded at $1x10^4$ cells per well in a 96 well flat-bottomed plate in 100µL of DMEM with 10% FCS and incubated overnight at 37 ºC, 5% CO_2. Serial, logarithmic dilutions ranging from 10^{-1} to 10^{-8} of virus stock were prepared in DMEM with 2% FCS. Plate media was replaced with these 100µL dilutions of virus or virus-free control media, with ten replicate wells for each concentration. After 72 hours, RFP-positive syncytia were assessed using a Zeiss Axiovert 25 microscope. For each dilution, the number of syncytia-positive wells was counted (with syncytia being used as the readout for cytopathic effect (CPE) and the ratio of wells with syncytia to those without syncytia was calculated. From this data, the $TCID_{50}$ was calculated using the KÄRBER statistical method. Calculation of TCID50:

$$\text{Titre } (TCID_{50}/mL) = 10^{\,1 + D\,(S - 0.5)}$$

$$D = \log(d);\ d = \text{dilution factor}$$

$$S = \text{sum of the ratios of wells with CPE to CPE-free wells}$$

2.8. Liposome production and purification

2.8.1. Lipid film methodology

Liposomal particles were produced using the lipid film hydration method originally described by Bangham (Bangham et al. 1965). Briefly, lipids as powder were individually dissolved in a (2:1 chloroform:methanol) solvent mix and then mixed in appropriate quantities in a round bottom flask, to achieve molar ratios as outlined in table 2.8.2 and total final lipid concentrations of 20-40 mg/mL. A LABOROTOR 4011 rotary evaporator and water bath (Heidolph Instruments, Germany) – set to 60 rpm, 45 °C, and 200 mmHg vacuum – was used to remove the solvent over a period of up to 30 minutes. Trace solvent was then removed from the resulting thin lipid film using a high vacuum pump for at least one hour. This film was then hydrated with a 1 mL of citrate (20 mM, pH 6.3), PBS (pH 6.2), or HEPES (20 mM, pH 8.2) buffer containing the relevant peptide or CpG DNA (both used at 1 mg/mL) where indicated using the rotary evaporator at 80 rpm and 45°C without vacuum, under argon. The resulting multi-lamellar lipid and antigen/adjuvant preparation was then extruded at 50°C with eleven passes through a 400 nm polycarbonate membrane (Avanti Polar Lipids, USA) using 1 mL glass syringes (Hamilton Company, USA) and a mini-extruder (Avanti Polar Lipids, USA). This process was repeated with eleven passes through a 200 nm polycarbonate membrane (Avanti Polar Lipids, USA) before the resulting liposomes were purified using a PBS-washed Sephadex G-25 PD10 size exclusion column (GE Healthcare, UK). Liposomal preparations, now in PBS solution, were then immediately added to 10 mg/mL CSP antigen and left to react overnight at room temperature prior to dialysis (see below). Validation of the attainment of the required size and dispersity was achieved using Dynamic Light Scattering (see section 2.9.1). Control liposomes unable to form a stable thio-ether linkage with the cysteine-terminated CSP antigen were prepared by replacing the DSPE-PEG-maleimide lipid with an equal molar amount of DSPE-PEG (Avanti Polar Lipids, USA).

2.8.2. Lipid composition of liposomal preparations

Lipid	Mass	Molar mass	Molar ratio (%)
DMPC Avanti Polar Lipids (USA)	7.45069916	677.933	43
Cholesterol Sigma-Aldrich (UK)	4.150583	386.65	42
DMPG Avanti Polar Lipids (USA)	0.88030529	688.845	5
DSPE-PEG(2000)-Maleimide Avanti Polar Lipids (USA)	7.51841255	2941.605	10
Total	20	N/A	100

Table 2.3. An overview of the lipids used for liposome formulation

2.8.3. Antigens and TLR9 agonists

Antigen or agonist	Sequence	Source	Purpose
OVA323-339	ISQAVHAAHAEINEAGR	Custom peptide synthesis (Thermo Fisher, Germany)	MHCII epitope of ovalbumin in C57Bl/6 (H2-IAb) mice and BALB/C (H2-IAd) mice. This was dissolved in citrate buffer (pH 6.3) and encapsulated in liposomal particles.
OVA323-339(FITC)	FITC-LC-ISQAVHAAHAEINEAGR	AnaSpec, USA.	Fluorescently labelled version of the OVA323-339 peptide. This was dissolved in citrate buffer (pH 6.3) and used to study the incorporation of OVA323-339 in liposomal particles.
Scrambled OVA323-339	HIAAAQAANEIRHEGVS	Custom peptide synthesis (Thermo Fisher, Germany)	Randomly generated variant of the OVA323-339 epitope. This was dissolved in citrate buffer and encapsulated in liposomal particles.
Full-length ovalbumin	Product number: A5503. Predicted sequence: Uniprot entry P01012	Sigma-Aldrich (UK)	Full-length ovalbumin protein. This was dissolved in citrate buffer (pH 6.3) and encapsulated in liposomal particles.
CSP	NANPNANPNANPNANPNANPKDKDKDC	Custom peptide synthesis (Thermo Fisher, Germany)	Five repeats of the NANP B cell epitope from *Plasmodium falciparum* CSP protein with KD for solubility and a terminal cysteine with a reactive thiol group for maleimide conjugation to the surface of liposomal vaccine particles.

M09	GYLYIYPSAGNSFDL	Custom peptide synthesis (Thermo Fisher, Germany)	MHCII epitope of MCMV in C57Bl/6 (H2-IAb) mice. This was dissolved in HEPES buffer (pH 8.2) and encapsulated in liposomal particles.
Scrambled M09	LSGFYAGYIDSNYLP	Custom peptide synthesis (Thermo Fisher, Germany)	Randomly generated scrambled variant of the M09 MCMV epitope. This was dissolved in HEPES buffer (pH 8.2) and encapsulated in liposomal particles.
CpG DNA	5'-tccatgacgttcctgacgtt-3' with a phosphodiester backbone (the commercially available ODN1826 has a nuclease resistant phosphorothioate backbone).	Custom oligo synthesis (Sigma, UK)	Synthesised version of the ODN1826 with described murine TLR9 agonism (Ballas et al. 2001). This was dissolved in peptide+buffer and encapsulated in liposomal particles.
erbb2/neu	TQVCTGTDMKLRLPASPETHLDMLRHLYQGCQVVQGNLELTYLPANASLSFLQDIQEVQGYMLIAHN RVKHVPLQRLRIVRGTQLFEDKYALAVLDNRDPLDNVTTAAPGRTPEGLRELQLRSLTEILKGGVLIR GNPQLCYQDMVLWKDVLRKNNQLAPVDMDTNRSRACPPCAPTCKDNHCWGESPEDCQILTGTICTS GCARCKGRLPTDCCHEQCAAGCTGPKHSDCLACLHFNHSGICELHCPALITYNTDTFESMLNPEGRYT FGASCVTTCPYNYLSTEVGSCTLVCPPNNQEVTAEDGTQRCEKCSKPCAGVCYGLGMEHLRGARAIT SDNIQEFAGCKKIFGSLAFLPESFDGNPSSGVAPLKPEHLQVFETLEEITGYLYISAWPESFQDLSVFQNL RVIRGRILHDGAYSLTLQGLGIHSLGLRSLRELGSGLALIHRNTHLCFVNTVPWDQLFRNPHQALLHSG NRPEEACGLEGLVCNSLCARGHCWGPGPTQCVNCSQFLRGQECVEECRVWKGLPREYVRGKHCLPC HPECQPQNSSETCYGSEADQCEACAHYKDSSSCVARCPSGVKPDLSYMPIWKYPDEEGICQPCPINCT HSCVDLDERGCPAEQRASPVTAHHHHHHHHHH	SinoBiological Inc. (China)	His-tagged purified extracellular domain of the murine erbb2/neu protein. Used to coat liposomal particles and as an antigen on ELISA plates.
MV H mosaic	Predicted sequence: MSPQRDRINAFYKDNPHPKGSRIVINREHLKFISDKIKFLNPDREYDFRDLTWCINPPERIKLDYTCFQQ ACKGKIQALCENPEWAPLKDNRIPSY	Alpha Diagnostic (USA)	MV H was used to stimulate splenocytes from MV vaccinated mice in ELISPOT studies.
MV N protein	Predicted sequence: Uniprot entry Q89933	Alpha Diagnostic (USA)	MV N was used to stimulate splenocytes from MV vaccinated mice in ELISPOT studies.
Inactivated MV	Purified Edmonston strain measles virus stock (see section 2.7) heat inactivated at 95 degrees for 10 minutes.	Produced in house.	Used for in vivo vaccination studies either mixed with TMG or modified with FSL-CSP. Heat-inactivated MV was also used to stimulate splenocytes from MV-vaccinated mice in ELISPOT studies.

Table 2.4. Characteristics of antigens and agonists used in this project

2.8.4. Dialysis

Dialysis was performed using 20,000 MWCO Slide-A-Lyzer cassettes (Pierce, USA) in 1 L of PBS at 4 °C with gentle stirring of the dialysis buffer. After two hours, the initial buffer was replaced and the dialysis proceeded overnight. The following day, the buffer was again changed and dialysis continued for another hour before the sample was isolated by piercing the cassette with a needle and syringe.

2.9. Vaccine particle characterisation

2.9.1. Dynamic light scattering (DLS) to determine particle size

Dynamic light scattering (DLS) is a useful tool for estimating the size distribution profile of particles in solution. Particles in solution undergo Brownian movement and this results in time-dependent differences in the scattering of light which can be detected and converted into information on size and polydispersity using the Stokes-Einstein relationship. The polydispersity index gives an indication of how narrow a Gaussian size distribution curve could represent the fitted DLS size distribution data. A Zetasizer Nano ZS instrument (Malvern, UK) was used to analyse samples diluted 1:50 in PBS up to a 1 mL volume in UV grade cuvettes (Fisher Scientific, UK). Data was analysed using Malvern Zetasizer software v6.32 (Malvern, UK).

2.9.2. Determination of particle zeta potential

Zeta potential measurement gives information about the surface charge of a population of particles in solution by measuring the potential difference between the media and the layer of fluid surrounding the particle. Zeta potential measurements were performed using the Zetasizer Nano ZS instrument. Samples were diluted 1:50 in HEPES buffer (20 mM, pH 7.2) and analysed in disposable folded capillary cells (Malvern, UK). Zeta potential values were calculated using the Smoluchowski method with Malvern Zetasizer software (Malvern, UK).

2.9.3. Flow cytometry to detect viruses and liposomes

Flow cytometry is a powerful tool for counting, sorting, and characterising cells. However, its utility is not limited to studying cells and there are several publications where flow cytometry

is used to characterise smaller particles (Tesfay et al. 2013). Here, a FACSCalibur flow cytometer (Becton Dickinson, San Jose, Calif.) equipped with a 15-mW 488-nm argon-ion laser was used to characterise viral particles and liposomes in solution. Measurement of PBS buffer alone defined the size region where noise was observed and it was established that both MV and liposomes gave a FSC/SSC particle distinct from their suspension buffers and that these populations could be gated to allow analysis of fluorescence.

2.9.4. Electron microscopy

Electron microscopy studies of liposomal preparations were performed in conjunction with Professor David Ferguson (University of Oxford, UK). For negative staining electron microscopy, formvar/carbon-coated grids were floated on 50 µL drops of liposome suspension, washed in distilled water, and negatively stained with 1% methyl tungstate before examination in a Jeol 1200EX electron microscope (Jeol UK Ltd, UK).

2.9.5. ssDNA oligo quantification

The presence of CpG DNA TLR9 agonists in liposomal particles was assessed using the Quant-iT OliGreen ssDNA Assay reagent (Life Technologies, UK) which fluoresces upon binding ssDNA in solution. Liposomal preparations were diluted in PBS, as were serial dilutions of CpG DNA oligos to generate standard curves. Assay reagent was diluted 200x in 10 mM Tris-HCl, 1 mM EDTA, pH 7.5. In a 96 well plate format, 50 µL this diluted reagent was incubated with 50 µL of liposomal preparation or PBS alone to give background readings. After 5 minutes in the dark at room temperature, fluorescence was detected with a Victor2 plate reader (PerkinElmer) using excitation/emission settings of 485/535nm for 1 second.

2.9.6. ELISA for quantification of particle-associated antigens

To ensure a standardise the dose of CSP antigen administered was *in vivo* in studies that compared different liposomal vaccine formulations, CSP-coated liposomes were lysed by heat treatment (95 °C for 5 minutes), serially diluted, coated onto ELISA plates in triplicate, and incubated overnight at 4 °C. Plates were then washed six times with PBS/0.05% Tween, blocked with 5% BSA, then incubated with the anti-CSP monoclonal antibody 2A10 (50 µL/well, 1:10,000 dilution) for one hour at room temperature. Plates were washed a further six times and then HRP-labelled anti-mouse IgG antibody (50 µL/well, 1:5000 dilution) was

added to each well and incubated for one hour at room temperature. Secondary antibody was removed and the plate was again washed six times with PBS/0.05% Tween. HRP substrate 1-Step UltraTMB (Fisher Scientific, UK) was added to the wells (50 µL/well) and the colour change was stopped after an appropriate time with 50 µL/well acid stop solution (Alpha Diagnostics). Absorbance was measured at 450 nm using a Wallac 1420 Victor2 plate reader (PerkinElmer). Background absorbance was calculated by measuring the OD of wells where the 2A10 antibody was replaced with PBS alone and these values were subtracted from all readings to give net OD for each well. Anti-CSP OD signals were compared between formulations, revealing statistically similar amounts of CSP (see figure 3.4.D).

To assess the release of core antigen from liposomes, OVA323-339 liposomes were subjected to heat treatment at 95°C for 10 minutes or phospholipase A2 treatment (Sigma-Aldrich, UK) for one hour at 37°C or one hour at 37°C without lipase as a negative control. For all groups, liposomes were diluted 1:100 in Hank's balanced salt solution (Sigma-Aldrich, UK). Samples were cooled to room temperature and serial dilutions were then coated onto ELISA plates. These were incubated for one hour at room temperature, washed six times with PBS (without tween), blocked, incubated with anti-OVA323-339 antibody (Innovagen, Sweden) at room temperature for one hour, washed again, then detected with HRP-labelled anti-rabbit (Dako, Denmark) before development with TMB substrate as described previously. Studies were performed in triplicate and data presented as normalised to the negative control signal.

2.9.7. Dose calculations

Lipid films were re-suspended with 1mg/mL solutions of core epitopes and/or TLR9 agonists. After encapsulation of these components and extrusion to form liposomes, liposomes were reacted overnight with an excess of CSP. The lipid composition used for each formulation contained 10% DSPE-PEG-maleimide by molarity, allowing calculations of the possible amount of CSP bound to the liposome surface. Assuming all liposomes were unilamellar and that 50% of the DSPE-PEG-maleimide reactive groups faced outwards (making them available for reaction with CSP), 100% reaction efficiency, 100% encapsulation efficiency, and taking into account dilutions performed prior to vaccination, each vaccine formulation administered in full-dose studies could contain 50 µg of CSP and 10-12.5 µg of core epitopes and/or TLR9 agonists.

2.10. Animal studies

2.10.1. General statement

All animal experiments were performed under valid United Kingdom Home Office project (PPL 30/2819) and personal (PIL 40/10329) licenses and were conducted in accordance with the terms of the United Kingdom Home Office guidelines and with the approval of the Medical Sciences Animal Ethics Committee, University of Oxford.

2.10.2. Housing conditions and diet

Mice were housed in temperature controlled conditions at Biomedical Services, John Radcliffe Hospital, Oxford. Mice had access to sterile water and formulated diets, in individually ventilated cages (IVCs).

2.10.3. Details of procedures

Mice were anaesthetised for immunisation by inhalation of oxygen and isoflurane (2 - 4%). Vaccinations were carried out with 25 gauge needle. For subcutaneous injections, 100 μL was injected into the tissue on the dorsum of the mouse, just below the neck. For vaccinations delivered by intramuscular injection, 20 μL was injected into a hind leg quadriceps muscle. When vaccinations were performed with the adjuvant TiterMax Gold, a stable emulsion of antigen in adjuvant was formed by vortexing for at least 30 minutes. The stability of the resulting emulsion was confirmed by pipetting 10 μL into ddH_2O, as described by (Koh et al. 2006). Antigen-adjuvant emulsions were stored at 4°C and used within one hour.

Blood was obtained for analysis by placing mice in a restrainer and then cutting the tail vein with a clean, sharp scalpel. 20 μL volumes were collected and allowed to clot in Eppendorf tubes before centrifuging to obtain the serum fraction. Serum was frozen at -20°C for later analysis. At the end of each study, cardiac punctures were performed under terminal anaesthesia using a 25 gauge needle. Where necessary, spleens were obtained from sacrificed mice and were transported to the laboratory in chilled RPMI media.

2.11. Assessment of cellular responses to vaccination

2.11.1. Preparation of mouse splenocytes

Spleens were harvested from sacrificed mice and crushed with a syringe plunger in wells of a 12-well microplate before filtration through a 70 μm cell strainer (Becton Dickinson, USA). 10 mL of RPMI media with 10% FCS was added and cells were spun at 1350 rpm for 5 minutes in an Eppendorf 5810R centrifuge with an Eppendorf A-4-62 rotor. Red blood cells were lysed by re-suspending pelleted cells in 5mL blood cell lysis buffer (Sigma-Aldrich, UK) for 5 minutes at room temperature. Lysis was stopped with the addition of 25 mL PBS before cell suspensions were spun again at 1350 rpm for 5 minutes. The resulting cell pellet was re-suspended in 10 mL media for cell counting and use in subsequent assays.

2.11.3. Enzyme-Linked ImmunoSpot (ELISPOT) assays

The ELISPOT is a commonly used assay to measure antigen specific cellular immune responses. It allows the visualisation and enumeration of cytokine-secreting cells in a heterogeneous population.

ELISPOT assays to detect IFNγ and IL-4 responses were performed using kits containing established antibody pairs and biotin-ALP (alkaline phosphatase) detection reagents (Mabtech, Sweden). High protein binding PVDF 96 well plates (Millipore, UK) were briefly activated with 50 μL of 70% ethanol per well, then washed five times with sterile PBS. Plates were coated with 50 μl diluted capture antibody (15 μg/mL in PBS) and incubated overnight at 4°C. Excess capture antibody was removed by washing five times with sterile PBS which was replaced with RPMI containing 10% FCS for one hour at 37°C to prevent non-specific binding. Blocking media was removed and replaced with isolated splenocytes at $1x10^5$ - $3.3x10^5$ cells per well, depending on the experiment. Antigenic stimuli were applied to cells in triplicate at a final concentration of 1μg/mL. Concanavalin A Type VI (Sigma-Aldrich, UK) at 1 μg/mL was used as a positive control.

Plates were incubated at 37°C for 24-48 hours then washed five times with PBS. 50 μl of biotinylated detection antibody (1 μg/mL with 0.5% FCS and 0.2μm filtered to reduce background) was added to each well. Plates were covered in foil and left for two hours at room temperature before washing five times with PBS. 50 μL streptavidin-ALP (1 μg/mL in PBS with 0/5% FCS) was added per well and incubated at room temperature for 45 minutes.

After washing plates five times with PBS, 50 μL of BCIP/NBT colour development buffer (Sigma-Aldrich) was added to each well. Plates were left at room temperature until spots developed (approximately 20-30 minutes) and then washed with water to stop the reaction. Plates were allowed to dry and then read in an ELISPOT plate reader. Spots were counted automatically using AID software (Autoimmun Diagnostika, Germany). For analysis, the number of background spots (PBS treated) for each sample was subtracted from the antigen-treated well values and the total number of spots was presented as per million splenocytes.

2.11.4. Tetramer staining

Tetramer staining allows enumeration of epitope-specific T cell populations. OVA323-339 MHC class II tetramers (I-(A)b-restricted) were obtained from the National Institutes of Health Tetramer Core Facility (USA). Splenocytes from vaccinated mice were prepared as described in section 2.11.1. $1x10^6$ splenocytes were stained at 37°C for one hour with PE-labelled tetramers diluted 1:50 in MACS buffer (PBS with 2 mM EDTA and 0.5% BSA). Tetramer A contained the epitope QAVHAAHAEIN whereas tetramer B contained the epitope HAAHAEINEA. Cells were simultaneously stained with anti-CD4 and anti-CD8 antibodies, both diluted 1:500 to allow analysis of CD4+CD8- splenocytes. After one hour, cells were washed twice in MACS buffer before re-suspension for analysis. Tetramers specific for the MHC class I immunodominant 'acute' and 'chronic' MCMV epitopes m45 (H-2d restricted, APC-labelled) and m38 (H-2Kb restricted, PE-labelled) were kindly provided by Paul Klenerman (University of Oxford, UK).

2.11.5. Cytokine multiplex assay

Multiplex cytokine bead array assays allow the quantification of multiple cytokines in one sample. We performed a flow cytometric multiplex cytokine assay using the LEGENDplex Th kit (Biolegend, UK) in accordance with the manufacturer's instructions. This assay uses multiple populations of beads of defined fluorescence levels with each different population conjugated to capture antibodies specific for given cytokines. Consequently, each bead has a distinct fluorescence profile that can be resolved in one dimension of a flow cytometry plot. After incubating beads with sample, biotinylated detection antibodies were added followed by streptavidin-PE. Fluorescence in the FL-2 channel can be measured and comparison to standard curves made with known cytokine concentrations allows quantification of cytokines of interest. Splenocytes were stimulated with peptides in 96 well microplates as described for

ELISPOT assays. 24 hours after stimulation with either the relevant antigenic peptide or PBS, supernatants were harvested and used for multiplex analysis in accordance with the manufacturer's instructions.

2.12. Assessment of humoral responses to vaccination

2.12.1. Enzyme-linked immunosorbant (ELISA) assay for total antigen-specific immunoglobulin response

High protein binding MaxiSorp 96 well plates (Nunc, Denmark) were coated with recombinant peptide, protein, or virus at 50 ng in 50 µL PBS per well and incubated at 4ºC overnight. Unbound antigen was removed by washing six times with PBS/0.05% Tween (Fisher Scientific, UK). Plates were then blocked with 5% Bovine Serum Albumin (BSA) (Sigma-Aldrich, UK) diluted in PBS for one hour at room temperature. Blocking solutions were removed and replaced with serum samples from vaccinated mice and, where necessary, primary antibodies as positive controls. Serum samples were diluted to 1:1000, unless otherwise indicated. Plates were then incubated at room temperature for two hours. Serum was removed and plates were washed six times with PBS/0.05% Tween. Secondary antibody (anti-mouse Ig HRP) was added to the plate (50 µL/well at a 1:5000 dilution) and incubated for one hour at room temperature. Secondary antibody was removed and the plate was again washed six times with PBS/0.05% Tween. HRP substrate 1-Step UltraTMB (Fisher Scientific, UK) was added to the wells (50 µL/well) and the reaction was stopped after an appropriate time with 50 µL/well acid stop solution (Alpha Diagnostics). Absorbance was measured at 450 nm using a Wallac 1420 Victor2 plate reader (PerkinElmer). For data analysis, background values (determined from control wells e.g. those incubated with PBS in place of serum) were subtracted from raw data, to give net OD values.

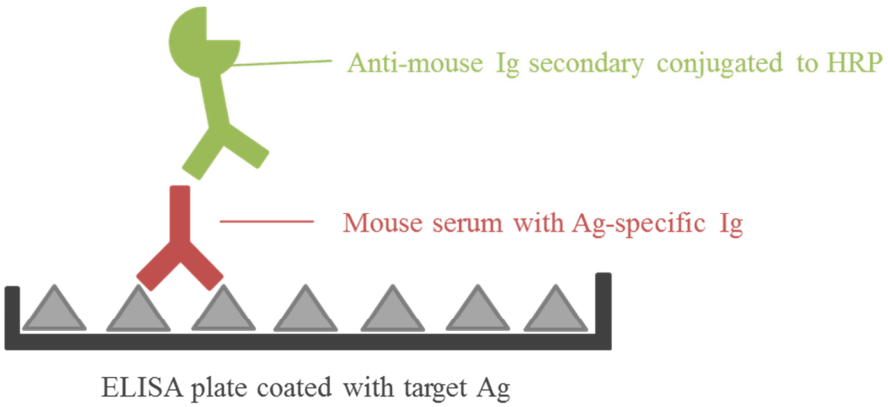


Figure 2.2. A schematic of the ELISA used to measure total antigen specific immunoglobulin responses.

2.12.2. ELISA assay for antigen-specific isotype response

To measure the isotype of antigen-specific antibody responses, plates were coated with antigen in PBS, washed, blocked with BSA, incubated with serum, and washed as described above. Biotinylated anti-isotype secondary antibodies (Biolegend, UK) were then added (50 µL per well at 1:1000 dilution) to detect the presence of specific isotypes. Plates were then washed six times with PBS/0.05% Tween and streptavidin-HRP (Invitrogen, UK) was then added (50 µL per well at 1:5000 dilution). Plates were washed six times with PBS/0.05% Tween prior to development with HRP substrate as described above.

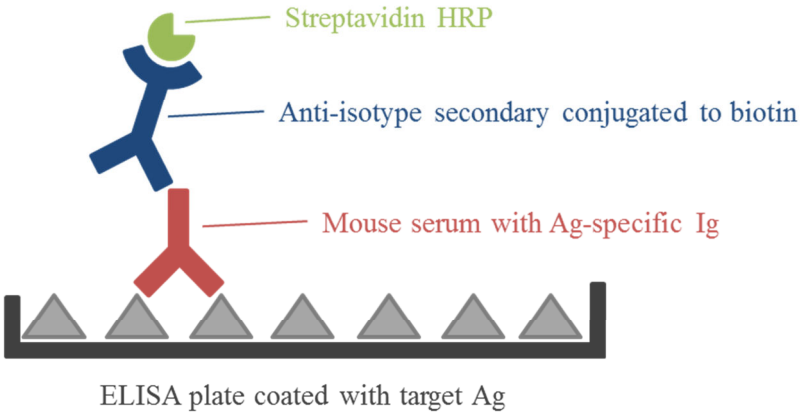


Figure 2.3. A schematic of the ELISA used to measure total antigen specific isotype antibody responses.

2.12.3. ELISA to determine endpoint titre

In vaccine studies, the magnitude of antibody response can be expressed as the endpoint titre, which is defined as the reciprocal of the highest serum dilution that gives a reading above the cut-off value. Various methods exist to define this cut-off, each with strengths and weaknesses. These studies used a statistically defined cut-off level calculated by taking the standard deviation of the negative control samples, multiplied by a factor which is based on the number of negative controls and the confidence level (1 - alpha) (Frey et al. 1998). An example cut-off level generated by this formula (for figure 4.13.B) was 5.077 standard deviations above the mean of the negative control samples. This is higher than other commonly used cut-off levels, such as three standard deviations above the mean.

To determine the endpoint titre, serial three-fold dilutions of serum (1:1000 in PBS) from vaccinated mice were prepared. These were applied in triplicate to CSP-coated ELISA plates that had been blocked with BSA, as described in 2.12.1. Following washing and detection

steps, plates were incubated with TMB substrate for one hour before stop solution was applied and the absorbance at 450nm was measured with a plate reader. Data was analysed using GraphPad Prism 5.0 software (GraphPad Software, USA).

2.12.4. Antigens used to coat ELISA plates

Target antigens used for coating ELISA plates were described earlier in table 2.8.3, with the exception of MCMV ELISA plates (Xpress Bio, USA) which come pre-coated with viral antigen.

2.12.5. Antibodies used in ELISA studies

Antibody	Source	Purpose
Rabbit anti-mouse Ig (HRP) Polyclonal. Catalogue: P0260	Dako, Denmark.	Secondary antibody in western blots and ELISAs
Goat anti-mouse IgG (HRP) Polyclonal. Catalogue: sc-2005	Santa Cruz Biotechnology, USA.	Secondary antibody to quantify IgG in ELISAs
Rat anti-mouse IgG1 (biotin) Clone: RMG1-1	Biolegend, UK.	Secondary antibody to quantify IgG1 in ELISAs
Rat anti-mouse IgG2a (biotin) Clone: RMG2a-62	Biolegend, UK.	Secondary antibody to quantify IgG2a (from Balb/c mice) in ELISAs
Rat anti-mouse IgG2b (biotin) Clone: RMG2b-1	Biolegend, UK.	Secondary antibody to quantify IgG2b in ELISAs
Goat anti-mouse IgG2c (biotin) Catalogue number 1079-08	SouthernBiotech, USA.	Secondary antibody to quantify IgG2c (from C57Bl/6 mice) in ELISAs
Rat anti-mouse IgG2c (biotin) Clone: RMG3-1	Biolegend, UK.	Secondary antibody to quantify IgG3 in ELISAs
Rat anti-mouse IgM (biotin) Clone: RMM-1	Biolegend, UK.	Secondary antibody to quantify IgM in ELISAs
Purified mouse IgG1 MOPC-21	Biolegend, UK.	To generate IgG1 standard curves for ELISAs
Purified mouse IgG2a MG2a-53	Biolegend, UK.	To generate IgG2a standard curves for ELISAs
Purified mouse IgG2b MG2b-57	Biolegend, UK.	To generate IgG2b standard curves for ELISAs
Purified mouse IgG2c Catalogue: 0122-01	SouthernBiotech, USA.	To generate IgG2c standard curves for ELISAs
Purified mouse IgG3 MG3-35	Biolegend, UK.	To generate IgG3 standard curves for ELISAs
Purified mouse IgM MM-30	Biolegend, UK.	To generate IgM standard curves for ELISAs
Mouse anti-CSP antibody 2A10 Monoclonal	Jenner Institute, University of Oxford, UK.	Positive control in anti-CSP ELISA assays.
Rabbit anti-OVA323-339 Polyclonal	Innovagen, Sweden.	Positive control in anti-OVA323-339 ELISA assays and to quantify OVA323-339 in liposome characterisation studies
Mouse anti-ovalbumin Monoclonal. Catalogue: A6075	Sigma-Aldrich, UK.	Positive control in anti-ovalbumin ELISA assays.
Goat anti-rabbit Ig (HRP) Polyclonal	Dako, Denmark. P0448	Secondary antibody in western blots and ELISAs

Table 2.5. An overview of antibodies used in ELISA assays.

2.12.6. Assessing avidity using sodium thiocyanate

Antibody avidity assays were performed using the chaotropic agent sodium thiocyanate (NaSCN) to disrupt antibody-antigen interactions (Pullen et al. 1986). This assay was performed in an ELISA plate format using increasing concentrations of NaSCN (diluted in PBS). After CSP-coated ELISA plates were washed, blocked with BSA, incubated with serum from vaccinated mice (individually diluted to a level calculated to give an OD450 of 1.0), and washed five times with PBS/0.05% Tween, NaSCN-treated wells were exposed to ascending concentrations (0-5M) of NaSCN at room temperature for 10 minutes. Negative control wells were treated with PBS only. Plates were then washed five times with PBS/0.05% Tween and the presence of CSP-specific mouse antibodies was detected as described in section 2.12.1. Resistance to thiocyanate elution was used as an indicator of avidity and the concentration of NaSCN required to reduce the ELISA signal by 50% was used to compare different vaccination strategies.

2.13. Statistical analyses

Data are expressed as the mean of replicates +/- standard deviation, unless otherwise stated. Where experiments produced two datasets, significance was evaluated using a student's two-tailed t-test. When two samples had unequal variances, Welch's t test was used. Where more than two means were compared, an analysis of variance (ANOVA) test was employed. Significances are denoted on graphs as: ns ($p > 0.05$), * ($p = 0.01$ to 0.05), ** ($p = 0.001$ to 0.01), and *** ($p < 0.001$).

3. Production and characterisation of liposomal vaccine particles with spatially separated B and T cell epitopes

3.1. Introduction

To test the core hypotheses of this thesis, it was necessary to produce vaccine particles containing encapsulated CD4+ T cell epitopes that were also coated in B cell antigens. It was important these vaccine particles were of a biologically relevant size and were negatively charged, to avoid non-specific interactions with negatively charged cell membranes following administration *in vivo*. The specific lipid composition of these liposomes was chosen to generate vaccine particles with these properties (section 2.8.2).

1,2-ditetradecanoyl-sn-glycero-3-phosphocholine (DMPC) is a zwitterionic phospholipid commonly used in liposomal formulation. 1,2-ditetradecanoyl-sn-glycero-3-phospho-[1'-rac-glycerol] (DMPG) was incorporated to give liposomal particles a net negative charge. Cholesterol has been demonstrated to improve the stability of liposomal preparations (Gregoriadis & Davis 1979)(Sułkowski et al. 2005). The inclusion of cholesterol results in a lower gel-to-liquid phase transition temperature and cholesterol-containing liposomes show improved stability both *in vitro* and *in vivo* (Gregoriadis & Davis 1979). Cholesterol has also been shown to reduce non-specific uptake of liposomes by phagocytes (Semple et al. 1996). 1,2-distearoyl-sn-glycero-3-phosphoethanolamine-N-[maleimide2000] (DSPE-PEG-maleimide) contains a PEG spacer terminated with a reactive maleimide group, allowing specific conjugation to a reactive thiol. DSPE-PEG-maleimide was used to allow coating of the vaccine particle with B cell antigens.

Lipid films were prepared by solvent evaporation using a round bottom flask (section 2.8.1). These were hydrated with buffers – compatible with *in vivo* applications – containing CD4+ T cell epitopes to achieve epitope encapsulation. Liposomes of a relevant size were formed by extrusion through 400nm and then 200nm polycarbonate membranes, to give a population largely between 100 and 300nm diameter. 10% (by molarity) of the lipid used was modified

with a PEG spacer and a reactive maleimide group to allow conjugation with a free thiol moiety of a cysteine-terminated B cell antigen.

This strategy was designed to permit spatial separation of the encapsulated CD4+ T cell epitope and the surface-bound B cell antigen, to focus developing humoral immune responses on the target antigen. The Circumsporozoite B cell epitope (CSP) from *Plasmodium falciparum* was chosen as a model B cell antigen, while ovalbumin and its immunodominant MHCII epitope (OVA323-339) were used as model CD4+ T cell antigens. Ovalbumin or OVA323-339 T cell epitopes, capable of eliciting T cell help from murine anti-OVA CD4+ T cells, were encapsulated in the core of liposomal particles where they would be unavailable for B cell binding and, consequently, could not dominate the B cell response. This cloaking strategy was designed to focus the humoral immune response on the surface-bound target antigen, CSP, while still harnessing CD4+ T cell help for isotype switching, somatic hypermutation, and affinity maturation. It was hypothesised that this particle antigen arrangement could exploit pre-existing CD4+ T cells raised against core ovalbumin epitopes to enhance antibody responses to CSP.

To allow accurate hypothesis testing *in vivo*, it was important to characterise vaccine particles in detail. The physicochemical properties of each liposomal preparation were measured. The presence of core ovalbumin peptide or protein antigen was demonstrated by a combination of flow cytometry, ELISA, and dot blotting. The presence of CSP antigen was demonstrated by Western blotting and ELISA, while its location on the surface of liposomal particles was confirmed by flow cytometry and zeta potential analysis. The activity of these vaccine particles was then characterised *in vitro* by examining the release of core peptides after particle disruption with heat or lipase. The ability of these liposomal particles to stimulate splenocytes from OVA323-339 vaccinated mice *ex vivo* was assessed. Lastly, the stability of vaccine preparations was briefly examined.

3.2. Chapter aims

1. Produce liposomal particles of ~200nm diameter with MHCII epitopes encapsulated in the particle core.

2. Produce liposomal particles of ~200nm diameter with CSP B cell antigen on the particle surface.

3. Demonstrate that surface and core antigens can act as B and CD4+ T cell antigens, respectively.

3.3. Results

3.3.1. Assessment of particle size distribution

Dynamic light scattering (DLS) was performed to determine the size and polydispersity of liposomal preparations (section 2.9.1). For *in vivo* applications, it was desirable to generate vaccine particles with a relatively low polydispersity index that approximated the size of typical viral pathogens. For this reason, extrusion through 400 nm and then 200 nm polycarbonate membranes was selected as the liposome formulation methodology (figure 3.1.A).

Initial studies examined the particle size distribution of liposomal vaccines incorporating either the full-length ovalbumin protein, or its immunodominant CD4+ T cell peptide epitope OVA323-339. Production of liposomes containing full-length ovalbumin was possible, but there was considerably more resistance when extruding these liposomes than was encountered with the shorter OVA323-339 peptide. DLS characterisation of full-length ovalbumin liposomes (figure 3.1.B) revealed a more polydisperse population of particles in the target range, alongside larger particles or aggregations. It is possible that this reflects reactivity of the DSPE-PEG-maleimide with cysteine or amine residues in the ovalbumin protein and that this results in cross-linking of ovalbumin-containing liposomes. Maleimide-free liposomes incorporating full-length ovalbumin were comparatively easy to produce and gave less polydisperse populations with a mean diameter of approximately 180nm by DLS (data not shown). Liposomes prepared with OVA323-339 also reproducibly gave less polydisperse populations with a mean diameter of approximately 180nm. Analysis of five different liposomal preparations encapsulating peptide MHCII epitopes gave the following DLS profile:

Mean diameter: 176.9 nm (sd = 12.2)
Mean polydispersity index: 0.091 (sd = 0.029)

After CSP conjugation, OVA323-339 encapsulating liposomes (denoted: CSP(OVA323-339)) were visualised by negative staining electron microscopy (figure 3.1.C), confirming a relatively monodisperse population in the 100-300 nm range.

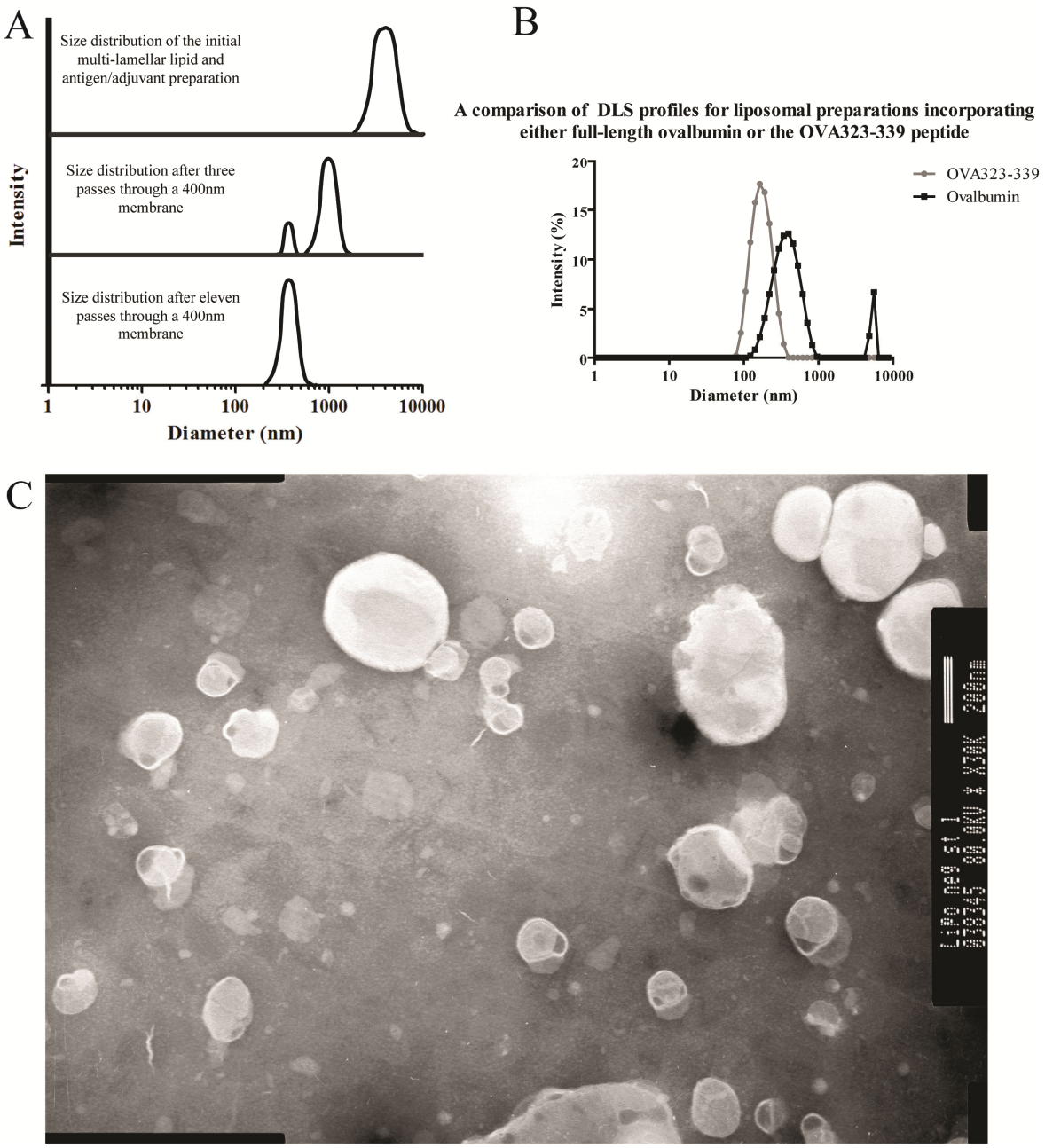


Figure 3.1. Liposome production. Liposomes were produced by extrusion through 400 nm and then 200 nm polycarbonate filters. (A) is a schematic representation of how the extrusion process forms liposomes of the desired particle diameter (adapted from Avanti Polar Lipids, USA). (B) The diameter of OVA323-339 and full-length ovalbumin liposomes diluted 1:50 in PBS was assessed by DLS. Data here are representative tracings of multiple DLS analyses. CSP(OVA323-339) liposomes were also examined by negative staining electron microscopy (section 2.9.4) and (C) is representative of other images captured.

3.3.2. Visualisation of liposomal vaccine particles by flow cytometry

Flow cytometry has traditionally been reserved for studying cells or particles in the micron diameter range. Recent studies have exploited the ability of standard flow cytometers to differentiate the forward and side scatter profiles of biological particles, such as liposomes and large viruses, from background scatter resulting from debris in dispersant or flow cytometer sheath fluid (Tesfay et al. 2013). The major limitation of this approach is a low sensitivity, as it can be difficult to distinguish signal from noise when examining the scatter profiles of particles smaller than the wavelength of the flow cytometer's laser (Steen 2004). Nonetheless, it was determined that the ability to identify vaccine particles by flow cytometry might allow this technique to be used to study the presence of core and surface antigens. Figure 3.2 demonstrates that CSP(OVA323-339) liposomes produce a forward scatter (FSC) and side scatter (SSC) profile different to that of PBS dispersant alone, validating that flow cytometry can be used to detect liposomal particles.

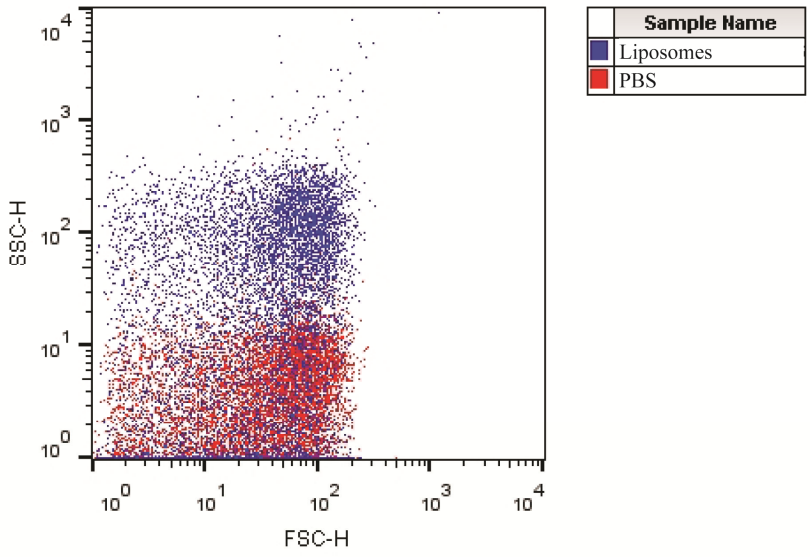


Figure 3.2. Detecting liposomal particles by flow cytometry. The FSC and SSC profiles of CSP(OVA323-339) liposomes diluted 1:10 in PBS were examined in a FACSCalibur flow cytometer (section 2.9.3) and compared with the profile generated by PBS alone.

3.3.3. Demonstration that liposomal vaccine particles contain OVA323-339

The proposed vaccine activity relies on successful incorporation of epitopes for CD4+ T cells inside liposomal vaccine particles. Using flow cytometry, the fluorescence of liposomes containing FITC-labelled OVA323-339 was assessed following PD10 purification (section 2.8.1), conjugation to CSP, and dialysis (section 2.8.4) to remove non-encapsulated and unconjugated antigen. Figure 3.3.A illustrates a representative shift in the fluorescence signal when comparing FITC-OVA323-339 liposomes with unlabelled OVA323-339 liposomes. This flow cytometry data is represented graphically in 3.3.B and indicates that FITC-OVA323-339 is incorporated in vaccine particles.

Core MHCII epitopes must also be available for release from liposomal particles upon internalisation by CSP-specific B cells. Disruption of the liposomal membrane with heat or lipase was established as an *in vitro* system to study this process. Membrane disruption allowed OVA323-339 to bind an ELISA plate where it could subsequently be detected with with anti-OVA323-339 antibodies. Figure 3.3.C demonstrates that treatment with either heat or lipase increases the anti-OVA323-339 signal.

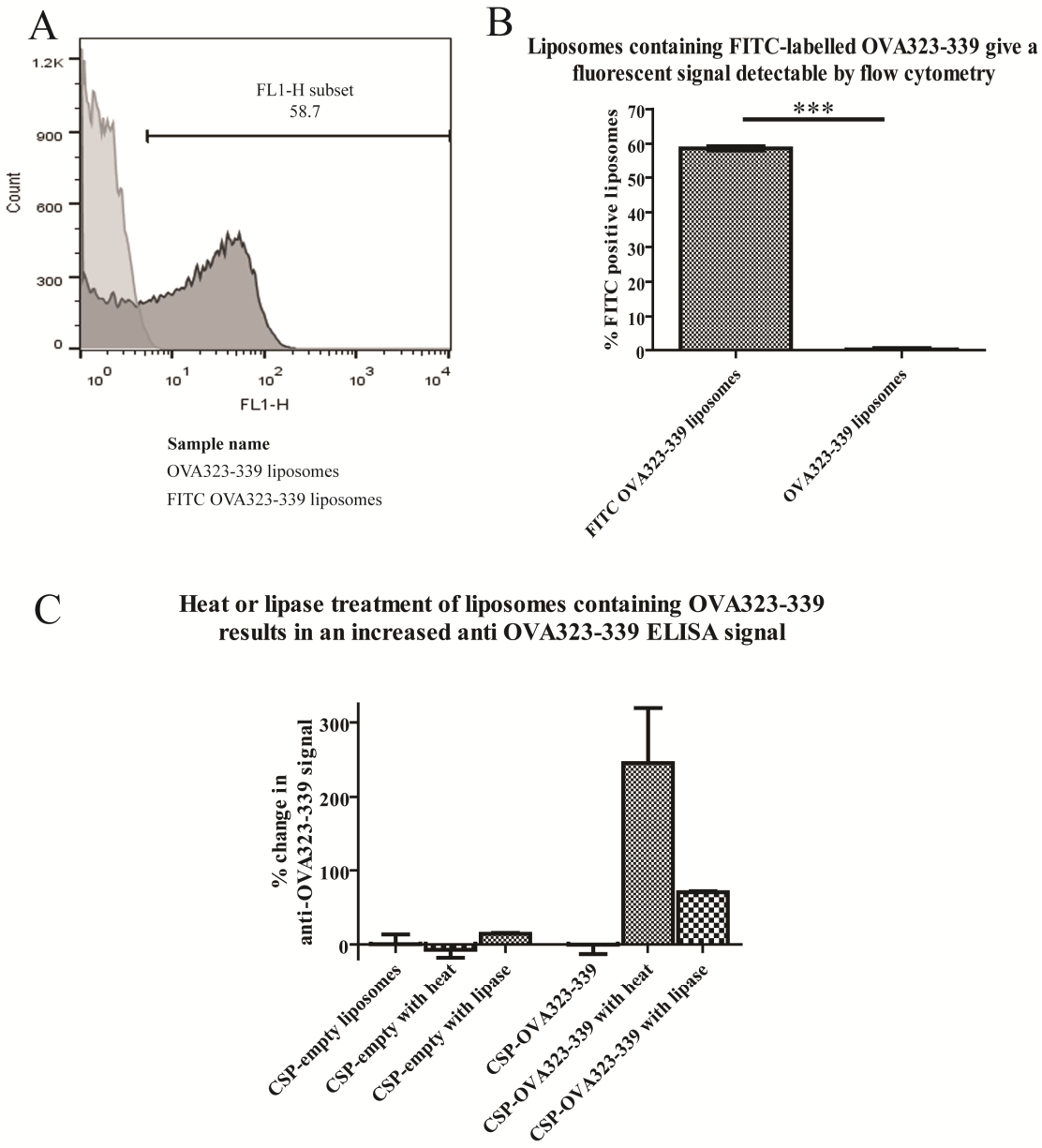


Figure 3.3. Studies demonstrating the presence of OVA323-339 in liposomal formulations. Liposomes containing either OVA323-339 or FITC-labelled OVA323-339 were analysed by flow cytometry after gating on the liposomal population, distinct from the PBS FSC/SSC background signal. (A) is a representative FL-1 fluorescence profile of the two liposomal populations while (B) shows the proportion of FL-1 positive liposomes (n=3 measurements of each liposome preparation). Means were compared with an unpaired, two-tailed t test, *** = $p<0.001$). Release of OVA323-339 from liposomes was studied using preparations containing OVA323-339 (section 2.9.6). Liposomes were heated to 95°C for 10 minutes, incubated with lipase at 37°C for one hour, or no treatment at 37°C for one hour. Samples (n=2) were then bound to an ELISA plate and detected using anti-OVA323-339 antibodies. Washes were performed without tween to minimise detergent-mediated disruption of liposomal membranes.

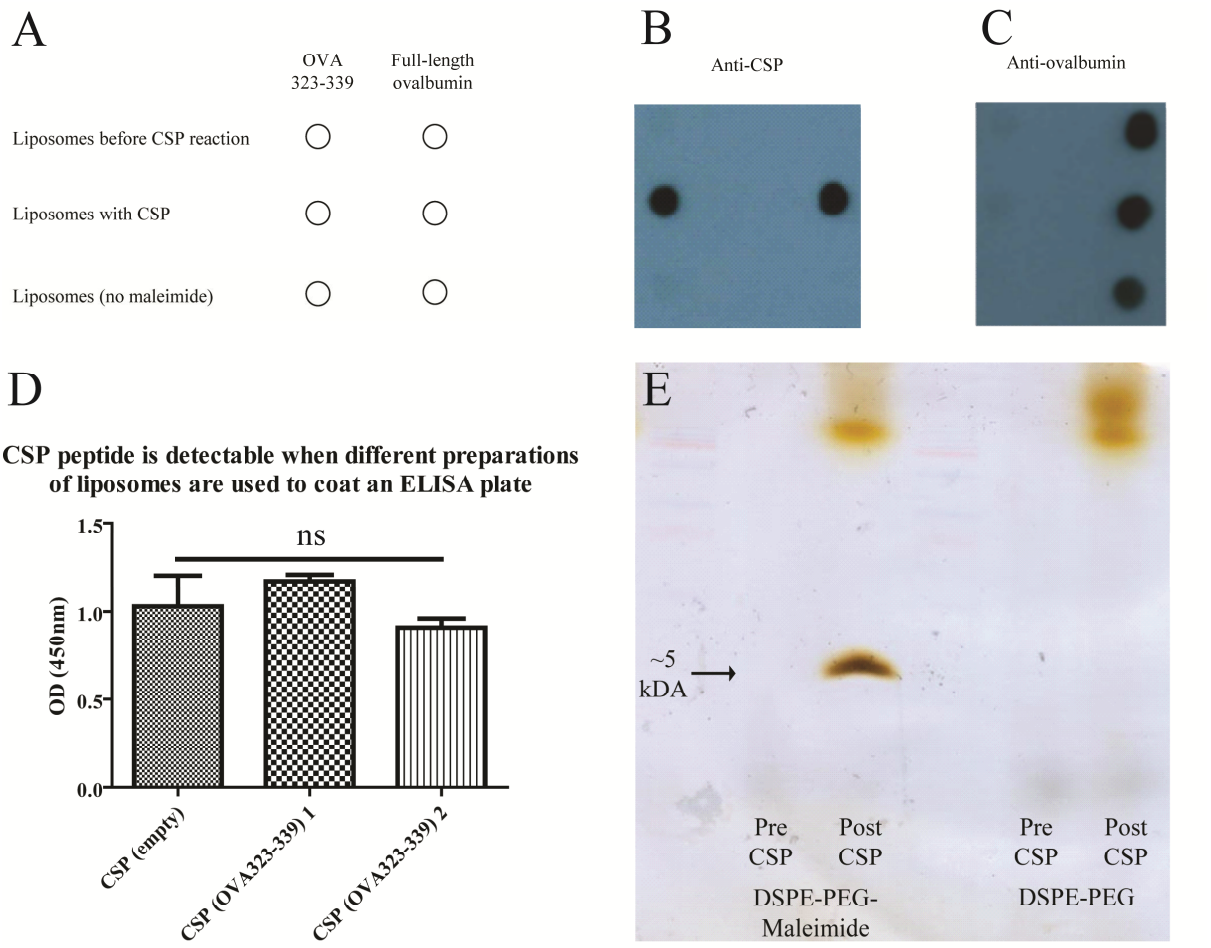
3.3.4. Demonstration of particle-bound CSP

To engage CSP-specific BCRs, vaccine particles require surface-bound CSP antigen. To achieve this, liposomes were produced with 10% of the lipid (by molarity) bearing maleimide groups, allowing conjugation to CSP via thio-ether linkages with reactive thiol groups on cysteine-terminated CSP antigens.

Liposomes containing OVA323-339 or full-length ovalbumin were reacted overnight with CSP antigen, then unconjugated antigen was removed by dialysis. CSP associated with liposomal particles was shown by dot-blotting against the CSP antigen (figures 3.4.A-B). Full-length ovalbumin in the same liposomal preparation was also detectable by dot blotting (figure 3.4.C).

To confirm this dot blot signal reflected particle-associated CSP antigen, tris tricine gel electrophoresis studies with silver staining, nitrocellulose transfer, and Western blotting (section 2.5.2) were performed. Silver staining (figure 3.4.E) revealed a 5 kDa band present only in liposomal samples after CSP conjugation and dialysis. Coomassie staining (figure 3.4.F) also revealed 5 kDa bands in CSP-conjugated samples, and when transferred to nitrocellulose these were readily stained with anti-CSP antibody (figure 3.4.G). The predicted size of free CSP is 2.7 kDa, whereas the predicted size of CSP when conjugated to DSPE-PEG-maleimide is 5.6 kDa. It is likely that this 5 kDa band represents CSP conjugated to DSPE-PEG. Preliminary studies demonstrated that free CSP peptide was not detectable by dot blot or Western blot, presumably because the free peptide does not bind nitrocellulose or PVDF membranes.

When comparing different vaccines *in vivo*, it was necessary to standardise the amount of CSP given in each vaccine dose. Anti-CSP ELISA was used to indicate the amount of CSP antigen present in each liposomal vaccine preparation. In brief, CSP-coated liposomes were heat-treated at 95°C for five minutes, serially diluted, and coated onto an ELISA plate for detection with anti-CSP antibodies. The OD at 450nm was compared across different preparations to allow standardisation prior to dosing in animal studies (figure 3.4.D).



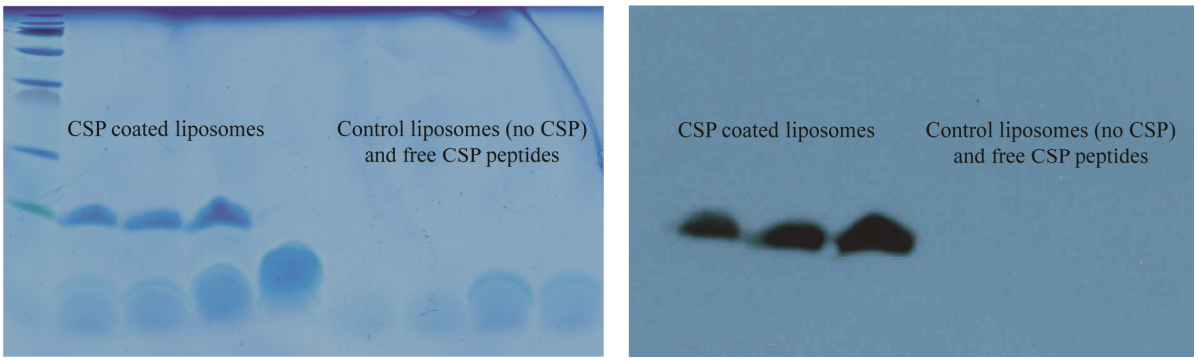


Figure 3.4. Studies demonstrating the presence of particle-associated CSP. The presence of CSP in liposomal preparations was initially confirmed by blotting onto nitrocellulose, blocking with milk, followed by detection with an anti-CSP antibody and development as described in section 2.5.2. Image (A) provides a key for dot blots (B) and (C), which indicate the presence or absence of CSP or full-length ovalbumin in a panel of three liposomal preparations. (D) CSP-coated liposomes were serially diluted and coated on ELISA plates overnight at 4°C. Plates were washed, blocked with BSA, and then probed with 1:10,000 dilution of anti-CSP mAb 2A10, before detection and development as described in section 2.9.6. Graph (D) is the data of a representative dilution (1:10,000) of liposomes and shows that comparable anti-CSP signals are generated. This assay allowed standardisation of CSP dose across different vaccine preparations. Error bars represent standard deviation (n = 3, ns = $p>0.05$). Image (D) is a silver-stained gel of liposomal preparations containing core MHCII peptides with and without CSP, which is detectable at approximately 5 kDa. Image (F) is a Coomassie stained gel and (G) is the corresponding anti-CSP Western blot demonstrating the presence of a 5 kDa band in maleimide-bearing liposome preparations probed with anti-CSP antibody.

3.3.5. Confirmation that CSP is present on the surface of vaccine particles

Previous characterisation work demonstrated that CSP antigens were present in liposomal vaccine particles and suggested these antigens were on the particle surface. To exploit the proposed mechanism of action, it was critical that B cell antigens are available on the particle surface for BCR binding. To confirm this, flow cytometry studies of CSP(OVA323-339) liposomes were performed. Staining liposomes with anti-CSP antibody and FITC-labelled secondary antibody resulted in a significant shift in FL-1 fluorescence of the gated liposome population when compared to incubation with FITC-labelled secondary alone (figures 3.5.A-B).

Zeta potential measurements provide an indication of the surface charge of particles in solution. The zeta potential of OVA323-339 liposome samples before and after conjugation to the neutral charge CSP antigen was compared (figure 3.5.C). Prior to CSP-conjugation, the mean zeta potential of a maleimide-bearing liposome preparation was -32.98; following CSP conjugation this rose to -23.6.

Taken together, these data support the presence of CSP on the vaccine particle surface and suggest that it is likely to be available for BCR binding *in vivo*.

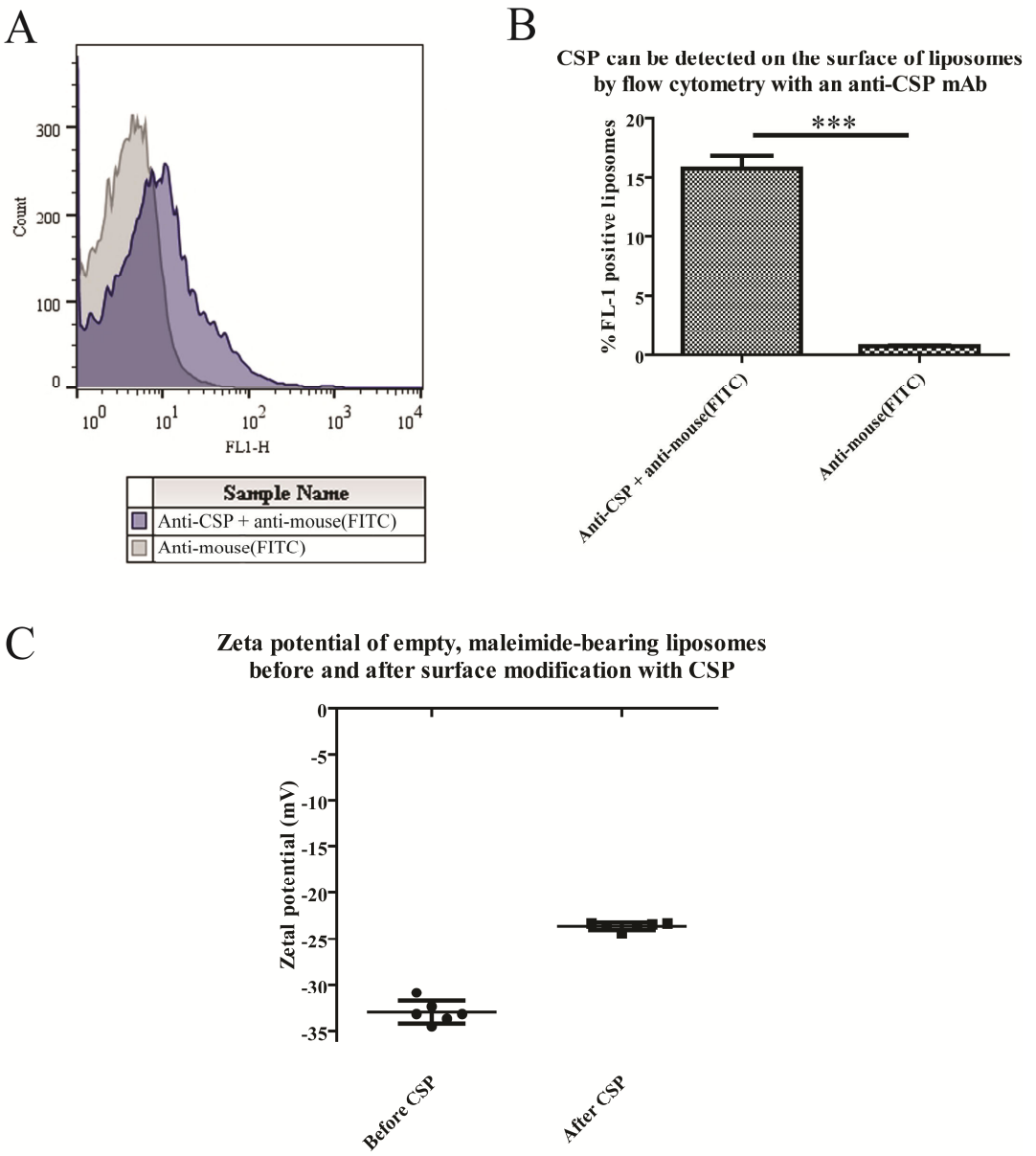


Figure 3.5. Studies demonstrating the presence of particle-bound CSP. The presence of CSP on the surface of liposomes was assessed by flow cytometry after staining CSP-coated liposomes with the anti-CSP mAb 2A10 (1:100) followed by detection with FITC-labelled anti-mouse antibody (1:500). Graph (A) is a representative histogram of the flow cytometry data whereas graph (B) presents this data as a percentage of FITC-positive liposomes (n=3 replicates of the staining procedure on one batch of CSP-coated liposomes). Means were compared with unpaired, two-way t tests. Error bars represent standard deviation, *** = $p<0.001$)). Graph (C) demonstrates the change in zeta potential (section 2.9.2) after reacting maleimide-bearing liposomes with CSP (n=6 technical replicates – repeated measures of the zeta potential of a liposomal preparation).

3.3.6. Characterising the biological activity of B cell and CD4+ T cell antigens delivered by liposomal vaccine particles

It was important to demonstrate that liposomal vaccine particles were capable of stimulating OVA323-339 specific CD4+ T cells. To demonstrate this, splenocytes from mice vaccinated with OVA323-339 in TiterMax Gold were stimulated with CSP(OVA323-339) liposomes. While not necessarily exploiting CSP-specific B cells for MHCII presentation, antigen presenting cells (APCs) in the splenocyte population should be able to phagocytose, degrade, and present antigen from liposomal particles. This should be a reasonable *ex vivo* model for B cell intracellular processing of liposomal vaccine particles *in vivo*. It was also hypothesised that CSP(OVA323-339) liposomal particles coated with serum from CSP-vaccinated mice (generated during *in vivo* studies discussed in chapter 4) would give higher anti-OVA323-339 CD4+ T cell responses, as antibody coated particles would be more readily taken up by Fc receptor-mediated phagocytosis. ELISPOT data displayed in figure 3.6 indicate that CSP(OVA323-339) liposomes can stimulate IFNγ production in splenocytes from OVA323-339 vaccinated mice. In addition, increased IFNγ production was seen when liposomes are first incubated with serum from CSP-immune mice.

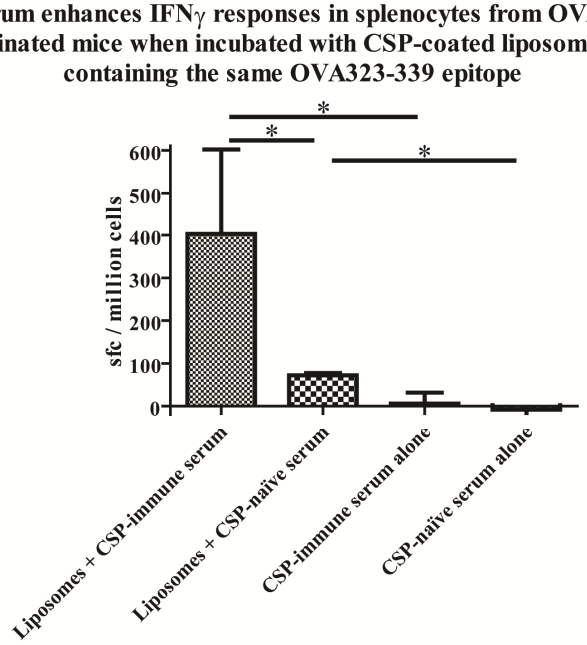


Figure 3.6. *Ex vivo* studies of liposome vaccine functionality. Splenocytes from mice (n=3) vaccinated twice with 10 µg of OVA323-339 in TMG were incubated with CSP-coated liposomes containing the OVA323-339 peptide. Liposomal preparations were pre-treated with either serum from mice vaccinated with OVA323-339 in TMG alone ('CSP naïve serum') or from mice also vaccinated with CSP-coated liposomes ('CSP-immune serum') diluted to 1:100. IFNγ responses were measured by ELISPOT after 24 hours incubation and the effect of CSP-immune serum on IFNγ production was assessed with unpaired, two-tailed t tests. Error bars represent standard deviation, * = $p<0.05$).

3.3.7. Assessment of liposomal stability

Stability is an important consideration when designing particle vaccines, while not the specific goal of this thesis. Retrospectively, the stability of liposomes prepared at different time points and stored at 4°C in glass vials was examined. Ten months after formulation, liposomal particles retained a relatively monodisperse size distribution with a mean diameter of 120-190 nm (figure 3.7.A). Liposomes prepared with maleimide for CSP conjugation still contained detectable CSP out to ten months after formulation (figure 3.7.B)

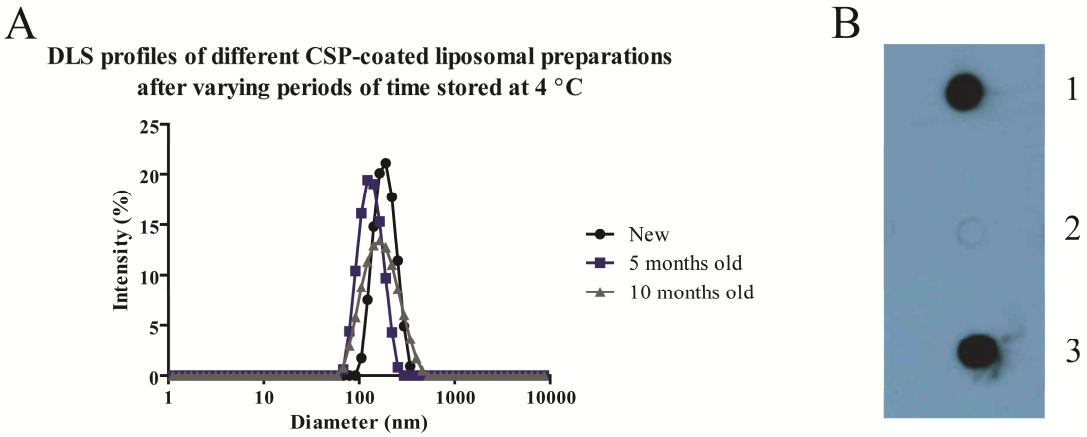


Figure 3.7. Liposome stability. (A) Three different CSP-coated liposome preparations formulated at different time points were analysed by DLS. (B) The presence of CSP on the surface of two CSP-coated liposomal preparations and one maleimide-free (and thus free of covalently-linked CSP) liposomal preparation months after they were produced was assessed by blotting onto nitrocellulose followed by detection with anti-CSP antibody. Key: 1 = CSP-coated liposomes five months after preparation; 2 = maleimide-free liposomes five months after preparation; and 3 = CSP-coated liposomes 10 months after preparation.

3.4. Chapter conclusions

1. Liposomal particles of ~200nm diameter can be produced to contain OVA323-339 MHCII epitopes in the particle core.

2. These particles can be coated with the model B cell antigen CSP.

3. Surface-bound CSP and encapsulated OVA323-339 are available to act as B cell and CD4+ T cell epitopes respectively.

3.5. Chapter discussion

3.5.1. Discussion of results

To test whether non-cognate CD4+ T cell help could be exploited to enhance antibody responses to B cell antigens, it was important to produce and characterise particles capable of first engaging BCRs and then delivering CD4+ T cell epitopes for presentation on MHCII. To ensure that only B cells specific for the target antigen were stimulated, it was critical to ensure the B cell epitope was surface bound, but the MHCII 'helper' epitopes were contained within the particle core. In this chapter, a method to produce liposomal particles fulfilling these criteria was described.

Lipid films were produced and then hydrated in physiological buffers containing MHCII epitopes. The resulting large lipid complexes with encapsulated OVA323-339 MHCII epitopes were then extruded to give particles of a size range that represented typical viral pathogens. Pendant maleimide groups on the liposome surface were then used to conjugate thiol-terminated CSP antigens. Lipids were chosen to give liposomes an overall negative charge so as to maximise the likelihood of engaging CSP-specific B cells and to reduce non-specific uptake that can be achieved with cationic liposomes.

Liposomal vaccine particles produced by this method were shown – by flow cytometry and ELISA – to contain OVA323-339. These epitopes could be liberated from liposomal particles by either heat or lipase treatment and were able to stimulate CD4+ T cells in an ELISPOT assay. Similarly, flow cytometry, ELISA, Western blotting, and zeta potential analysis confirmed that particles were coated with CSP. Flow cytometry studies where anti-CSP antibodies were used to stain the particle suggested that surface-bound CSP was available for

BCR binding. Further, ELISPOT responses in splenocytes from OVA323-339 vaccinated mice stimulated with CSP(OVA323-339) liposomes could be enhanced by the inclusion of CSP-immune – but not CSP-naïve – serum.

3.5.2. Limitations and future work

This chapter sought to produce and characterise CSP-coated liposomes that contained MHCII epitopes from the model antigen ovalbumin. While these goals were achieved, it is worth noting that it was difficult to extrude liposomes that encapsulated the full-length ovalbumin protein. Full-length ovalbumin liposomes were larger and less monodisperse than OVA323-339 liposomes. While both were able to be produced and could be tested in chapter two, it is possible that full-length ovalbumin reacts with the maleimide-modified DSPE lipid and consequently forms cross-linked particles. Importantly, this could leave full-length ovalbumin exposed on the outside of the particle, undermining the spatial segregation of B and T cell epitopes that is crucial for our proposed vaccine mechanism of action. While both full-length ovalbumin and OVA323-339 liposomes could be produced for testing in chapter two, it was clear that – at least from a manufacturing view point – encapsulating shorter MHCII epitopes was the preferred strategy.

Several methods were used to characterise liposomal particles and to confirm the presence of encapsulated OVA323-339 and surface-bound CSP. None of these methods is without its flaws. In particular, the use of flow cytometry to characterise vaccine particles in the 100-300 nm range is relatively novel and at the limit of what a flow cytometer is capable of measuring. However, when taken together the data presented in this chapter show that CSP-coated liposomal virus-like particles can be produced to contain OVA323-339. Further studies to confirm this are possible, and other techniques could include electron microscopy using gold labelled antibodies to detect the presence of CSP on the particle surface, or assays to measure OT-II CD4+ T cell proliferation upon exposure to OVA323-339 encapsulating liposomes.

This project developed a method of producing virus-like particles based on anionic liposomes. Cationic liposomes are generally more immunogenic than neutral or anionic liposomes (Christensen et al. 2007). However, this effect appears to be mediated by non-specific local cell damage (Shi & Rock 2002) or through interactions with negatively charged surface components of APCs (Foged et al. 2004). In this project, specific targeting of CSP-

specific B cells was the goal. Consequently, neither of these properties of cationic liposomes was deemed desirable. However, given that the lipid composition of the vaccine particles described here is in no way optimised for immunogenicity, future work could consider strategies to improve the intrinsic immunogenicity of the liposomal particle.

The number and spacing of B cell antigens on the surface of these liposomal particles, along with the concentration of MHCII epitopes encapsulated in its core, have not been optimised. A future direction of this project could be to study these properties of the vaccine particles and to optimise these parameters for *in vivo* immunogenicity. Further, here CSP and ovalbumin were used as model antigens. However, the methodology used to produce CSP(OVA323-339) liposomal vaccine particles should be suitable for generating vaccine particles that are coated with different B cell antigens and encapsulate other MHCII epitopes. Indeed, future work could seek to produce liposomal particles exploiting a range of different pre-existing CD4+ T cell populations to target different B cell antigens.

4. Exploiting pre-existing vaccine-induced immunity to provide non-cognate CD4+ T cell help

4.1. Introduction

This chapter seeks to test the hypothesis that pre-existing, non-cognate, CD4+ T cells that have been generated by a previous vaccination will enhance antibody responses against distinct target antigens on the surface of particulate vaccines that encapsulate relevant T cell epitopes.

In the context of human diseases, vaccination can elicit high titre antibodies together with robust CD4+ T cell responses (Hammarlund et al. 2003). Memory CD4+ T cell populations may persist for an entire lifetime (Lees & Farber 2010). Some well-studied vaccines – such as the Edmonston strain of measles virus (Naniche et al. 2004), vaccinia virus (Amara et al. 2004), or the tetanus toxoid vaccine (Diethelm-Okita et al. 2000) – can induce durable CD4+ T cell responses that can persist for years after vaccination. These CD4+ T cells represent an attractive population to exploit when designing new vaccines against target antigens, particularly those where an efficacious response may be limited by a lack of CD4+ T cell help.

An effective humoral response to a vaccine requires antigen binding to the BCR, followed by internalisation and processing of antigen for presentation on MHCII. Binding of 'cognate' CD4+T cells to this processed MHCII-presented antigen can then further stimulate B cell antibody production, affinity maturation, and isotype switching (Parker 1993). Provided two antigens are internalised by one B cell, these 'helper' signals could come from CD4+ T cells that recognise a different antigen from that which engaged the BCR (i.e. 'non cognate' T cells – see figure 1.2). This concept has been exploited in the design of conjugate vaccines (section 1.4.2) which link carbohydrate antigens with protein antigens containing strong CD4+ T cell epitopes to elicit high titre, high affinity, isotype-switched antibodies against carbohydrate targets. However, due to the structure of conjugate vaccines, the protein helper antigen is also available for B cell binding and can subsequently dominate the developing

antibody response (Peeters et al. 1991). Indeed, in different contexts, conjugation to carrier proteins has been shown to both enhance and suppress anti-target antibody responses (Schutze et al. 1985). In this project, helper epitopes were concealed within liposomal particle vaccines, to focus the antibody response on the target surface antigen.

4.2. Chapter aims

1. Establish a model of vaccine-induced, pre-existing, CD4+ T cell immunity.

2. Exploit this pre-existing immunity as a source of non-cognate CD4+ T cell help to enhance vaccine responses against CSP.

3. Evaluate whether engaging non-cognate CD4+ T cell help generates faster, higher affinity, and isotype switched antibody responses to CSP.

4. Assess whether pre-existing CD4+ T cells generated by vaccination at one injection site can be exploited by liposomal vaccination at a distant site.

5. Investigate the relative importance of liposomal vaccine dose and pre-existing, non-cognate, CD4+ T cell help.

4.3. Results

4.3.1. Development of a vaccination regime to establish CD4+ T cell immunity

To assess whether vaccine-induced CD4+ T cell immunity could support antibody responses to non-cognate antigens displayed on the surface of liposomes, it was important to establish a system for generating CD4+ T cell immunity by vaccination. From the range of commercially available agents, it was desirable to select an adjuvant capable of eliciting strong CD4+ T cell responses, preferably in the context of high-titre antibody responses. An adjuvant with a previously described and readily measurable effect on T_H cell phenotype was also preferable, as this would allow us to characterise the pool of pre-existing CD4+ T cells and then measure their effect on a developing humoral responses to liposomal particle vaccines. Given the study protocol would involve multiple administrations of different vaccines over a period of several weeks, an additional requirement of a superior toxicity

profile than seen with many potent adjuvants – such as Freund's – was desirable. TiterMax Gold (TMG) was selected as the best adjuvant to fulfil these requirements.

TMG contains microparticulate silica, squalene (a degradable oil), a block copolymer CRL8300, and the emulsifier sorbitan monooleate. The immunogenicity of block copolymers containing linear chains of hydrophilic polyoxyethylene flanked by linear chains of hydrophobic polyoxypropylene was originally described by (Hunter & Bennett 1984). The mechanism by which block copolymers exert their adjuvant effect is believed to be a combination of enhanced antigen presentation, complement activation, chemotaxis, and macrophage activation (Howerton et al. 1990). Depending on the antigen and *in vivo* model used, TMG has been shown to elicit comparable antibody titres to the more widely used Freund's adjuvant with less toxicity (Stills 2005). However, this lower toxicity has also been reported to correspond with a lower level of antibody production (Leenaars et al. 1998).

Full-length ovalbumin protein, the immunodominant MHCII peptide OVA323-339, or PBS alone was emulsified in the adjuvant TMG (section 2.10.3). These vaccine emulsions were administered to mice as two doses given subcutaneously (subcut) two weeks apart, alongside the additional control of adjuvant-free antigen. Two weeks after the second vaccination, cellular and humoral immune responses to ovalbumin or OVA323-339 were characterised. IFNγ and IL-4 ELISPOT responses to OVA323-339 or full-length protein were quantified after vaccination with full-length ovalbumin (figure 4.1) or OVA323-339 (figure 4.2) as described in section 2.11.3.

Splenocytes from mice vaccinated with full-length ovalbumin in TMG gave higher IFNγ responses to full-length protein when compared to PBS + TMG or protein alone, and these approached statistical significance (figure 4.1.B). There was no observed difference in IL-4 responses between groups (figure 4.1.D), or in IFNγ or IL-4 responses specifically against the immunodominant OVA323-339 epitope (figures 4.1.A and 4.1.C).

Vaccination with OVA323-339 in TMG was observed to give an OVA323-339 IFNγ ELISPOT response significantly higher than vaccination with either PBS+TMG or free OVA323-339 peptide (figure 4.2.A). There was a trend towards higher anti-OVA323-339 IL-4 responses in OVA323-339 + TMG vaccinated mice that approached statistical significance (figure 4.2.C). There was also an indication that stimulating splenocytes from OVA323-339 vaccinated mice with full-length ovalbumin protein could stimulate IFNγ production (figure 4.2.B), while no effect on IL-4 was observed (figure 4.2.D).

Vaccination with full-length ovalbumin or OVA323-339 in TMG was further assessed by tetramer staining. Tetramer staining allows enumeration of epitope-specific T cells by flow cytometry, using fluorescently-labelled MHC-peptide tetramers (as described in section 2.11.4). Tetramer reagents against OVA323-339 have been developed by the National Institutes of Health, but are notoriously problematic and, even at very high concentrations, may not adequately stain all OVA323-339 specific T cells (National Institutes of Health n.d.). Two anti-OVA323-339 I-(A)b-restricted tetramers were employed. Staining with these tetramers 'A' and 'B' revealed the highest number of tetramer positive splenocytes in the OVA323-339 + TMG vaccinated group (figure 4.3.). Alongside the ELISPOT data in figure 4.2, this supports OVA323-339 + TMG vaccination as capable of inducing significant anti-OVA323-339 CD4+ T cell responses.

To further appreciate the T_H cell polarisation induced by vaccination with OVA323-339 + TMG, a multiplex cytokine bead array (section 2.11.5) was performed. Stimulation of splenocytes from OVA323-339 + TMG vaccinated mice with OVA323-339 peptide for 24 hours resulted in the production of an array of T_H1, T_H2, and T_H17 cytokines (figure 4.3.C). Strikingly, the concentration of IFNγ was tenfold higher than other cytokines. Moreover, other mediators of a T_H1 response – TNFα ($p = 0.0015$) and IL-2 ($p = 0.0026$) – were readily produced in response to OVA323-339 stimulation. This is in keeping with the body of literature describing TMG as either a T_H1-biased or a balanced T_H1/T_H2 adjuvant (Cribbs et al. 2003) (Stephenson et al. 2014). IL-4, a key driver of T_H2 responses, was not detected at significant concentrations in either stimulated or unstimulated samples, although IL-5 could be detected after stimulation with OVA323-339 ($p = 0.0085$). The T_H17 cytokine IL-17F was also detectable after stimulation with OVA323-339 ($p = 0.030$). T_H17 cells are a pro-inflammatory T_H cell subset important in responses to many bacterial and fungal pathogens, but have also been implicated in a range of autoimmune conditions (Korn et al. 2009). Recently, it has been demonstrated that T_H17 can provide help to B cells and induce class-switching to IgG1, IgG2a, IgG2b, and IgG3 isotypes. IL-17 alone was sufficient to drive the production of IgG2a and IgG3 (Mitsdoerffer et al. 2010).

CD4+ T cell responses to vaccination with full-length ovalbumin in TMG

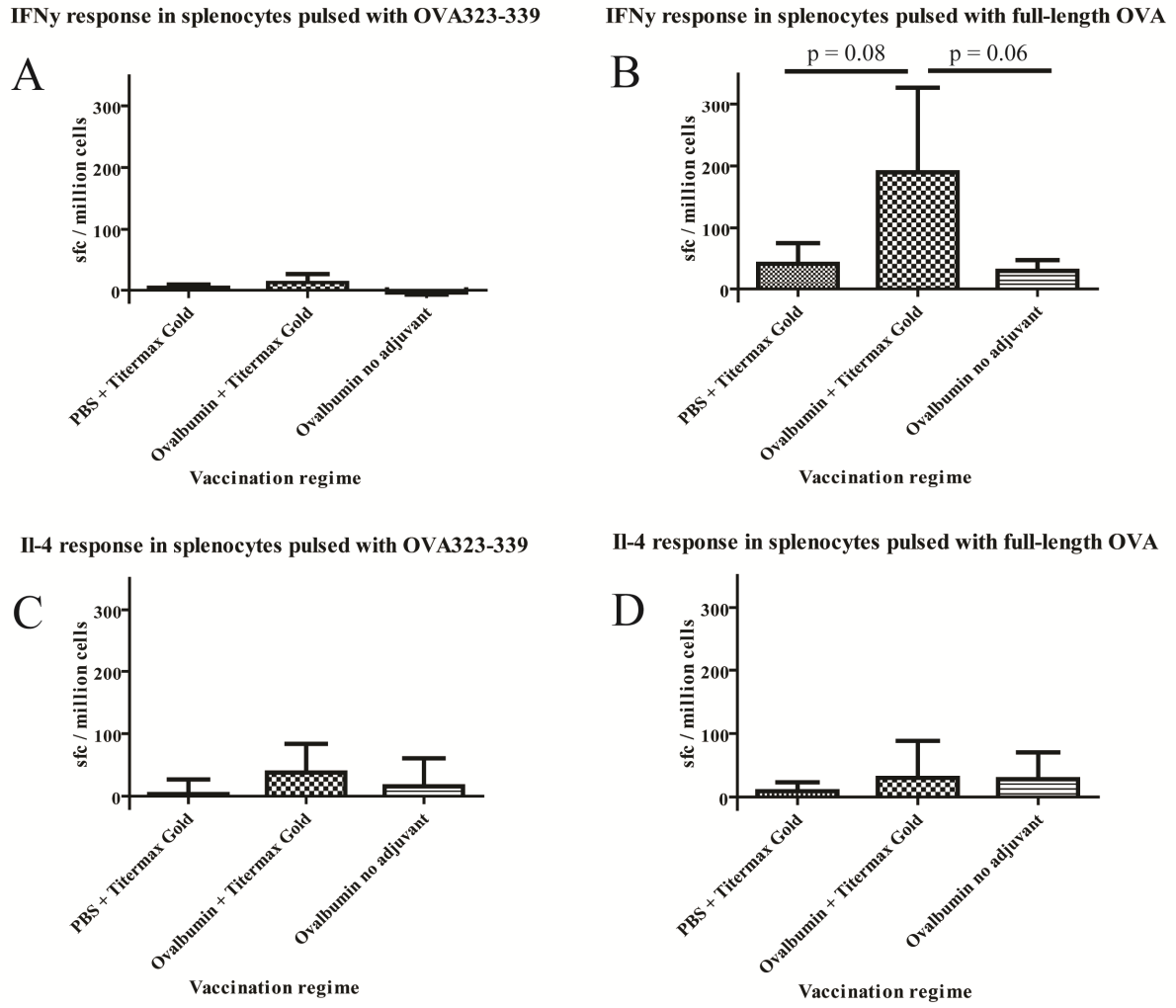


Figure 4.1. ELISPOT characterisation of the anti-OVA CD4+ T cell response in mice vaccinated with full-length ovalbumin in TMG. 6-8 week old female C57Bl/6 mice (n=3) were administered two subcutaneous vaccinations of 10 µg of full-length ovalbumin or PBS emulsified in TiterMax gold adjuvant, or ovalbumin alone, with a two week interval between doses. Two weeks after the second vaccination, splenocytes were harvested and stimulated with either full-length ovalbumin protein (A and C) or OVA323-339 peptide (B and D) at a final concentration of 1 µg/mL. 36 hours later, cellular responses to IFNγ (A and B) and IL-4 (C and D) were measured by ELISPOT assay (section 2.11.3) and the number of spot forming units (sfc) was counted for each well (n=3 wells per mouse). Technical triplicates were averaged and mean responses were calculated for each group before comparison with unpaired, two-tailed t tests.

CD4+ T cell responses to vaccination with OVA323-339 peptide in TMG

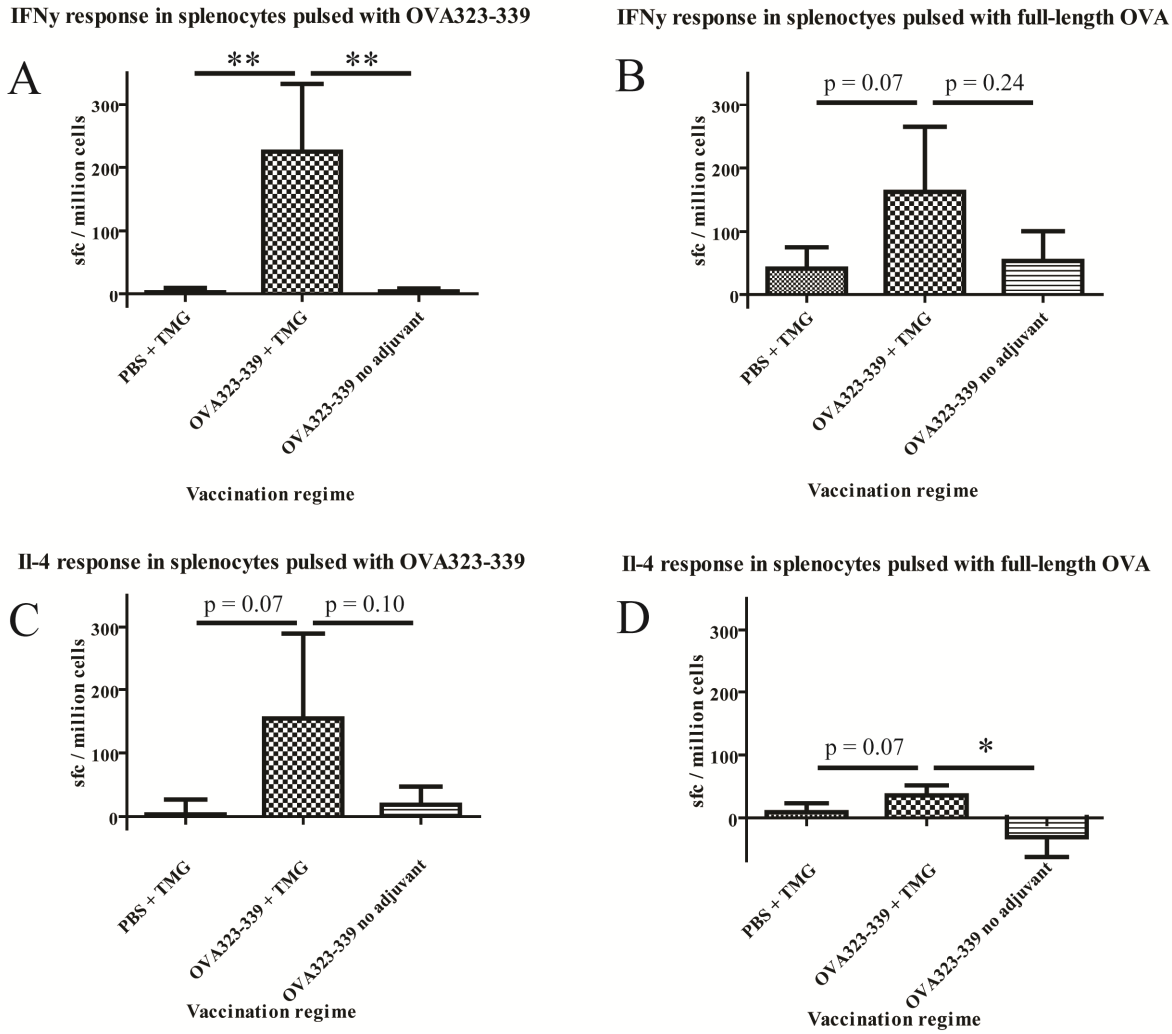


Figure 4.2. ELISPOT characterisation of the anti-OVA CD4+ T cell response in mice vaccinated with OVA323-339 peptides in TMG. 6-8 week old female C57Bl/6 mice (n=3) were administered two subcutaneous vaccinations of 10 µg of OVA323-339 peptide or PBS emulsified in TiterMax gold adjuvant, or OVA323-339 alone, with a two week interval between doses. Two weeks after the second vaccination, splenocytes were harvested and stimulated with either OVA323-339 peptide (A and C) or full-length ovalbumin protein (B and D) at a final concentration of 1 µg/mL. 36 hours later, cellular responses to IFNγ (A and B) and IL-4 (C and D) were measured by ELISPOT assay (section 2.11.3) and the number of spot forming cells (sfc) was counted for each well (n=3 wells per mouse). Technical triplicates were averaged and mean responses were calculated for each group before comparison with unpaired, two-tailed t tests.

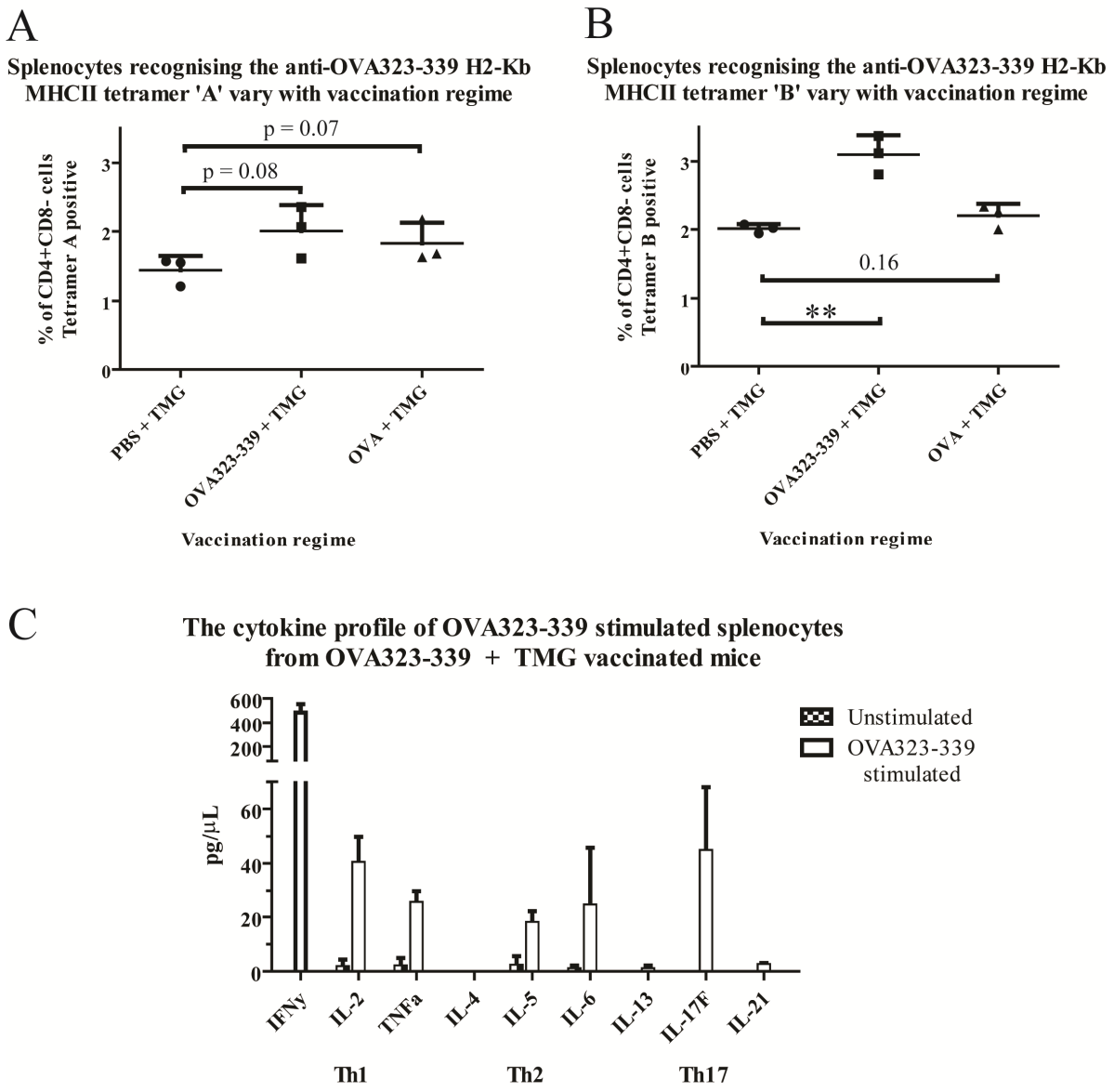


Figure 4.3. Tetramer staining and cytokine production analysis to characterise the anti-OVA323-339 CD4+ T cell response to OVA323-339 + TMG vaccination. 6-8 week old female C57Bl/6 mice (n=3) were administered two subcutaneous vaccinations of 10 µg of OVA323-339 peptide, 10 µg of full-length ovalbumin, or PBS, emulsified in TiterMax gold adjuvant with a two week interval between doses. CD4+CD8- splenocytes were stained with two different tetramers recognising the immunodominant OVA323-339 peptide in the context of the class II MHC molecule I-(A)b (graph A and graph B). Means (n=3) were compared with unpaired, two-tailed t tests. Splenocytes from OVA323-339 + TMG vaccinated mice were also stimulated with OVA323-339 and the resulting T_H1, T_H2, and T_H17 cytokine profile was measured using a multiplex cytokine bead array (C). Mean levels of each cytokine were compared between unstimulated and OVA323-339-stimulated groups using unpaired, two-tailed t tests. For clarity, significant differences are not shown in this figure. Instead, key findings are discussed in the main text.

4.3.2. Characterisation of the antibody response to OVA323-339 + TiterMax Gold vaccination

The ultimate goal of OVA323-339 + TMG vaccination was to generate CD4+ T cells that could support antibody responses to non-cognate antigens. To further characterise these cells, the antibody response to OVA323-339 itself was assessed.

In a developing immune response, CD4+ T cells are often described in terms of their T_H1 or T_H2 polarisation (section 1.2.1) and assessing the antigen-specific antibody isotype profile has emerged as a surrogate indicator of T_H cell polarisation. T_H1 responses tend to induce an antibody response where IgG2a predominates, whereas T_H2 responses drive IgG1 production (Coffman et al. 1988)(Stevens et al. 1988). Consequently, the IgG1:IgG2a ratio is often reported to characterise T_H1/T_H2 polarisation following vaccination. The allele encoding IgG2a is not present in the commonly-studied C57Bl/6 mouse strain used in these experiments, and these mice produce IgG2c instead. Anti-IgG2a antibodies cross-react with IgG2c, but do so inadequately (Martin et al. 1998). In these studies, the isotype profile (including IgG1 and IgG2c) of anti-OVA323-339 antibodies was measured (figure 4.4.B) alongside the affinity of anti-isotype secondary antibodies for purified isotype (4.4.A).

These results indicate that OVA323-339 + TMG vaccination drives the production of both IgG1 and IgG2c, but that the levels of IgG2c are significantly higher. This was indicated by the higher OD signal (figure 4.4.B) detected with an anti-IgG2c, but was more evident when calculated as the total amount of antigen specific isotype produced. Standard curves using plate bound purified isotypes (figure 4.4.A) allowed quantification of IgG1 and IgG2c and revealed that the quantity of anti-OVA323-339 IgG2c produced was significantly higher than the level of anti-OVA323-339 IgG1 (figure 4.4.C). The mean ratio of IgG1:IgG2c was 0.0311 (sd = 0.00247). Together, these data support a T_H1-dominated, anti-OVA323-339 immune response.

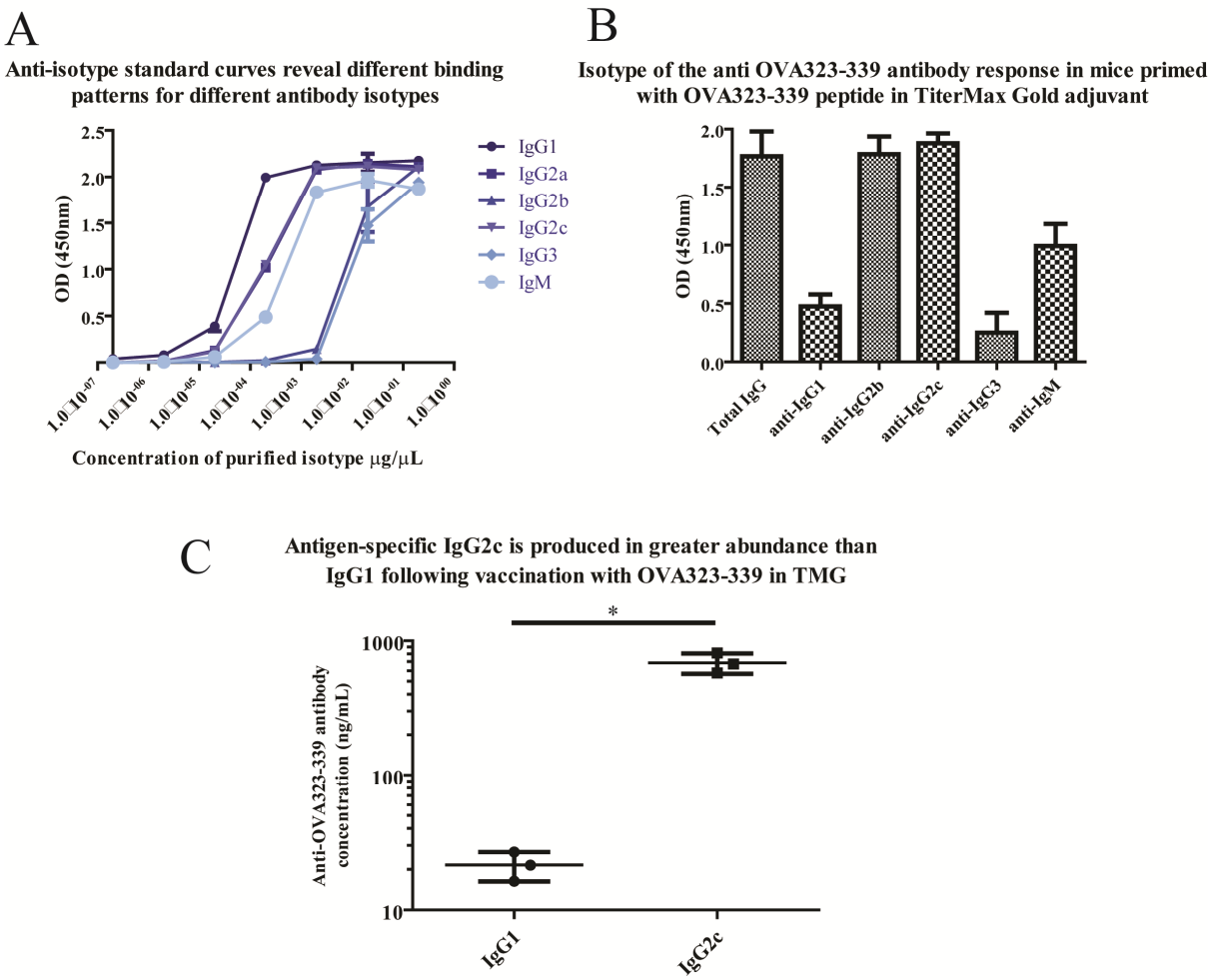


Figure 4.4. Characterisation of the antibody response to OVA323-339 + TMG vaccination. Serial dilutions of purified mouse Ig isotypes were bound to an ELISA plate and then detected with anti-isotype secondary antibodies (as described in section 2.12.2) to provide information on the relative detection abilities of these secondary antibodies. The resulting binding curves are displayed in graph (A) and the isotype profile of anti-OVA323-339 antibodies in serum from OVA323-339 + TMG vaccinated mice (two weeks after the second vaccine dose) is shown in graph (B). Standard curves allowed the quantification of each isotype using quantifications based on a line of best fit. Graph (C) shows the relative amounts of IgG1 and IgG2c elicited by OVA323-339 + TMG vaccination. Means are compared with Welch's t test.

4.3.3. Exploiting pre-existing immunity to full-length ovalbumin to enhance anti-CSP antibody responses

Initial pilot studies to test the hypothesis that pre-existing, non-cognate CD4+ T cells could enhance anti-CSP antibody responses were performed in mice pre-vaccinated with full-length ovalbumin that were subsequently administered CSP-coated liposomes encapsulating the full-length protein.

The study protocol (figure 4.5.A) involved two doses of ovalbumin in TMG, followed by two doses of liposomal vaccine particles. The anti-CSP antibody response occurred earlier and

was of a higher magnitude in ovalbumin-immune mice when compared to those pre-vaccinated with PBS + TMG (figure 4.5.B). Anti-CSP responses were not detected following the administration of 'nude' liposomes, devoid of maleimide-modified lipid and therefore incapable of covalently binding CSP. Liposomes containing full-length ovalbumin were difficult to produce (section 3.3.1) Ovalbumin contains many cysteine and amine residues, which may react with maleimide bearing lipids and result in either ovalbumin exposed on the surface of liposomes, or cross-linking of liposomal particles. Anti-ovalbumin antibody responses were measured after liposomal vaccination (figure 4.5.C). Anti-ovalbumin antibodies were detectable in mice that had previously only been vaccinated with PBS in TMG, indicating that ovalbumin was not completely encapsulated by our liposomal particles.

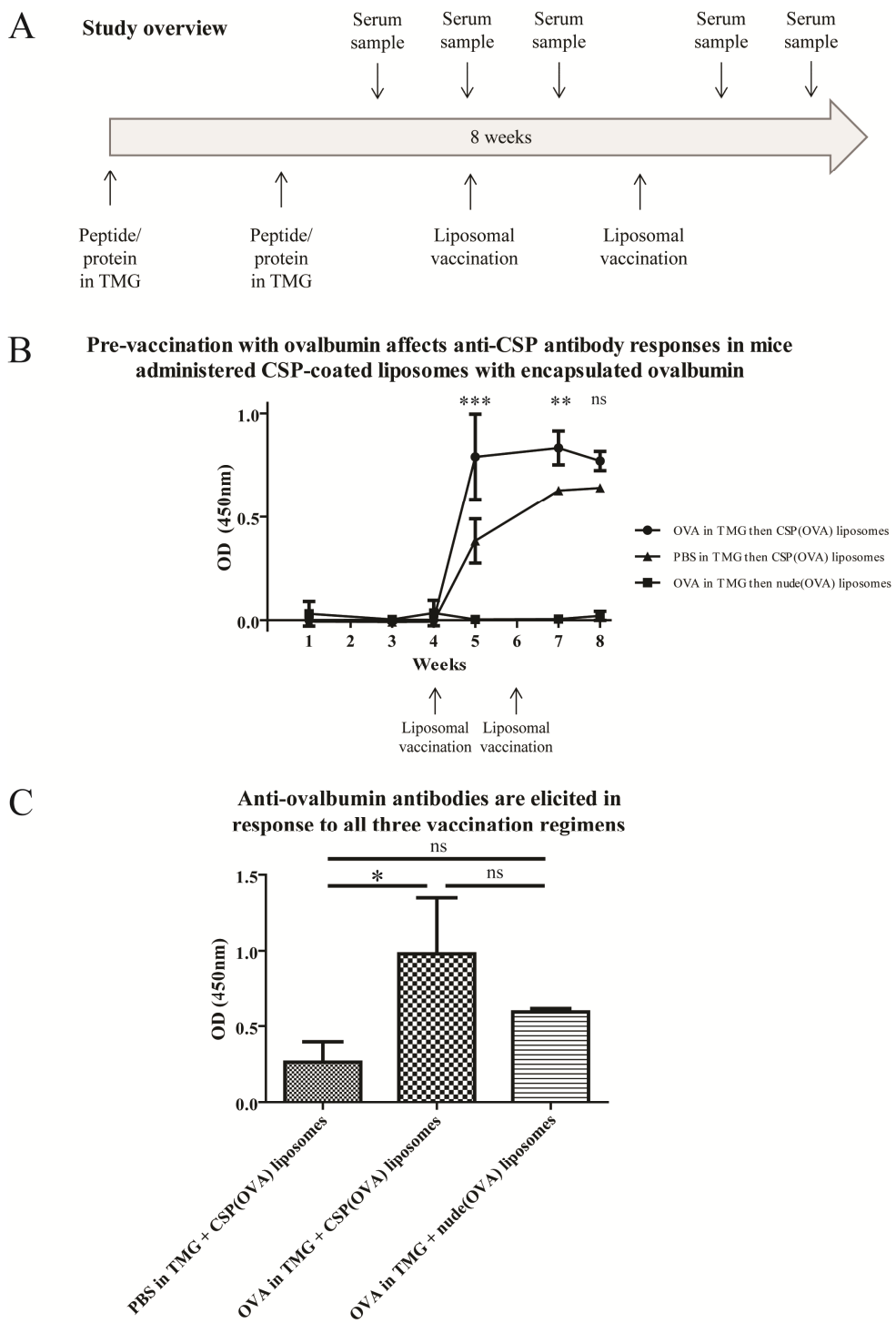


Figure 4.5. Pilot *in vivo* study to characterise humoral immune responses to CSP(OVA) liposomes in mice pre-vaccinated with full-length ovalbumin or PBS in TMG. 6-8 week old female C57Bl/6 mice (n=3) were administered two subcutaneous vaccinations of 10 µg of full-length ovalbumin protein or PBS emulsified in TiterMax Gold adjuvant, with a two week interval between doses. Two weeks later, this was followed by two doses of liposomes (two weeks apart) coated in CSP and encapsulating full-length ovalbumin protein. PBS + TMG vaccinated mice were included as a control for the presence of pre-existing anti-ovalbumin CD4+ T cell immunity, and 'nude' liposomes where DSPE-PEG replaced DSPE-PEG-maleimide were included as a negative control for non-specific coating of liposomes or contamination of preparations with free CSP antigen. Each vaccine dose contained 10 µg ovalbumin, except in nude(OVA) liposomes, 50 µg of CSP (see section 2.9.7 for dosing calculations). Graphic (A) outlines the study protocol. (B) Anti-CSP Ig responses over the course of

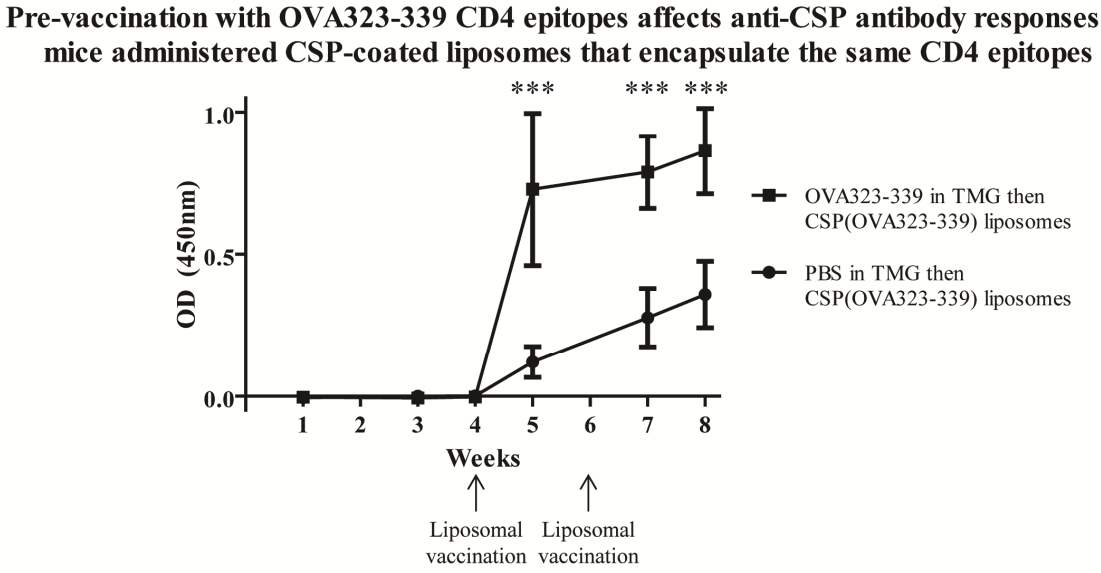
the study were measured at a serum dilution of 1:200, as described in section 2.12.1. Mean responses were compared using two-way ANOVA with Bonferroni's post-test (n=3). At the termination of the study, detectable anti-ovalbumin responses (in serum diluted 1:400) were quantified for all three study groups (C) Mean responses were compared using one-way ANOVA with Tukey's post-test for multiple comparisons.

4.3.4. Exploiting pre-existing immunity to OVA323-339 to enhance anti-CSP antibody responses

Next, the effect of vaccination with OVA323-339 in TMG on the anti-CSP immune response following vaccination with CSP-coated, ovalbumin encapsulating, liposomes was examined. Studies detailed in sections 4.3.1 and 4.3.2 had identified a protocol for establishing pre-existing anti-OVA323-339 immunity and CSP-coated liposomes that encapsulated OVA323-339 were produced and characterised in sections 3.3 and 3.4.

The study protocol (figure 4.5.A) involved two doses of OVA323-339 in TMG, followed by two doses of liposomal vaccine particles. Higher anti-CSP responses were observed in OVA323-339-immune mice than mice pre-vaccinated with PBS + TMG (figure 4.6.A). In contrast to liposomes produced with full-length ovalbumin, OVA323-339 encapsulating liposomes did not elicit a significant anti-OVA323-339 response in PBS-primed mice (figure 4.6.B), indicating that OVA323-339 was not available for BCR binding. An anti-OVA323-339 response was readily detectable in the OVA323-339 + TMG vaccinated group, and did not change appreciably following liposomal vaccination.

A



B

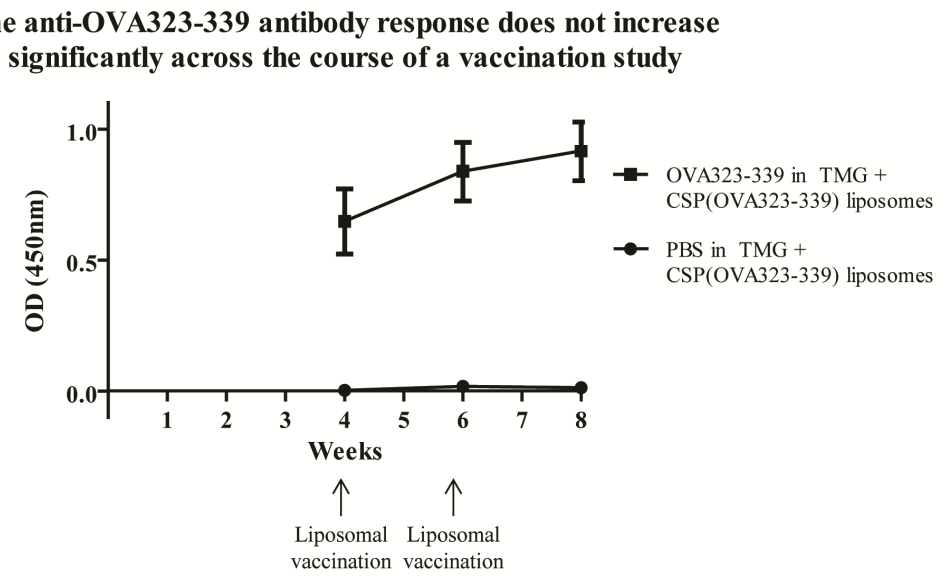


Figure 4.6. Pilot *in vivo* studies to characterise humoral immune responses to CSP(OVA323-339) liposomes in mice pre-vaccinated with OVA323-339 or PBS in TMG. 6-8 week old female C57Bl/6 mice (n=3) were administered two subcutaneous vaccinations of 10 µg of OVA323-339 peptide or PBS emulsified in TiterMax gold adjuvant, with a two week interval between doses. Two weeks later, this was followed by two doses of liposomes (two weeks apart) coated in CSP and encapsulating OVA323-339 peptides. PBS + TMG vaccinated mice were included as a control for the presence of pre-existing anti-OVA323-339 CD4+ T cell immunity. Each vaccine dose contained 50 µg of CSP and 10 µg OVA323-339 (see section 2.9.7 for dosing calculations). Graph (A) displays anti-CSP Ig responses over the course of the study, measured at a serum dilution of 1:200. Mean responses were compared using two-way ANOVA with Bonferroni's post-test (n=3). Graph (B) shows anti-OVA323-339 responses (in serum diluted 1:400) over the course of the study.

4.3.5. Confirming the proposed mechanism of action

Flexibility during particle engineering is a benefit of using a liposomal platform and it is possible to design vaccine particles to test specific hypotheses. To confirm the findings outlined in figure 4.6.A, and to demonstrate that liposome-encapsulated OVA323-339 was crucial to engage pre-existing anti-OVA323-339 CD4+ T cells, a further study was conducted where a single dose of liposomes was administered and an additional control – CSP-coated liposomes without any core peptide – was included. Again, this study demonstrated higher anti-CSP IgG responses in mice pre-vaccinated with OVA323-339 + TMG when compared with PBS + TMG pre-vaccinated mice. Anti-CSP responses were mounted rapidly in OVA323-339 pre-vaccinated mice; there was no difference in the level of anti-CSP antibody detectable at week five, seven, or nine in this group. OVA323-339 pre-vaccinated mice that were then vaccinated with CSP(empty) liposomes mounted anti-CSP responses that were lower than the other two groups. This trend was evident from week five to seven, but reached statistical significance at nine weeks.

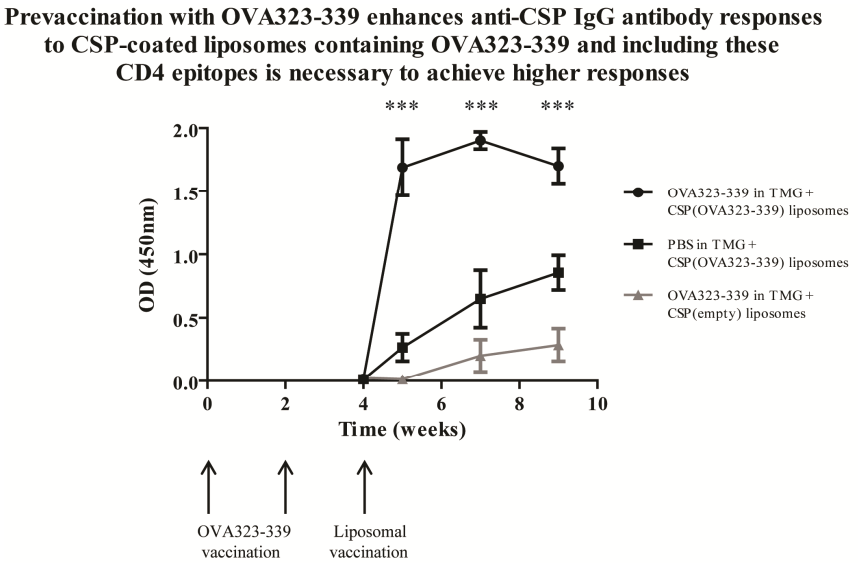


Figure 4.7. *In vivo* studies to further study the humoral immune response to CSP(OVA323-339) and CSP(empty) liposomes in mice pre-vaccinated with OVA323-339 or PBS in TMG. 6-8 week old female C57Bl/6 mice (n=4) were administered two subcutaneous vaccinations of 10 µg of OVA323-339 peptide or PBS emulsified in TiterMax gold adjuvant, with a two week interval between doses. Two weeks later, this was followed by two doses of liposomes (two weeks apart) coated in CSP and encapsulating OVA323-339 peptides. An additional control to the study detailed in figure 4.6 was included where CSP-coated liposomes contained no core OVA323-339 (denoted as 'CSP(empty)'). Each vaccine dose contained 50 µg of CSP and, except for the CSP(empty) control, 10 µg of OVA323-339. Anti-CSP Ig responses over the course of the study were quantified and mean OD levels were compared by two-way ANOVA. Statistical significance is indicated for comparisons between the two groups shown in black. Responses in OVA323-339 + TMG pre-vaccinated mice administered CSP(OVA323-339) liposomes were compared at week five, seven, and nine by one-way ANOVA with Tukey's post-test for multiple comparisons.

4.3.6. The effect of pre-existing, non-cognate, CD4+ T cell immunity on anti-CSP isotypes

CD4+ T cell help is important for B cell isotype switching. It was hypothesised that the presence of pre-existing, anti-OVA323-339 CD4+ T cells would drive an isotype-switched anti-CSP antibody response earlier and to a higher magnitude than that seen in PBS + TMG pre-vaccinated mice. To study this, a CSP-specific isotype ELISA (section 2.12.2) was developed. In addition to the total anti-CSP immunoglobulin (figure 4.10.B), anti-CSP IgG (figure 4.10.D), IgG1 (figure 4.10.E), IgG2b (figure 4.10.F), IgG2c (figure 4.10.G), IgG3 (figure 4.10.H), and IgM (figure 4.10.I) were measured. OVA323-339 + TMG pre-vaccination resulted in earlier isotype switching to all IgG subclasses. Notably, it drove the earlier production of IgG subclasses that were also raised against OVA323-339 (e.g. IgG2c). IgG2b. IgG2c, and IgG3 were significantly higher in OVA323-339 pre-vaccinated mice at all post-vaccination time points. In contrast, IgM and IgG1 were initially higher in OVA323-339 pre-vaccinated mice, but levels were comparable by four weeks post vaccination.

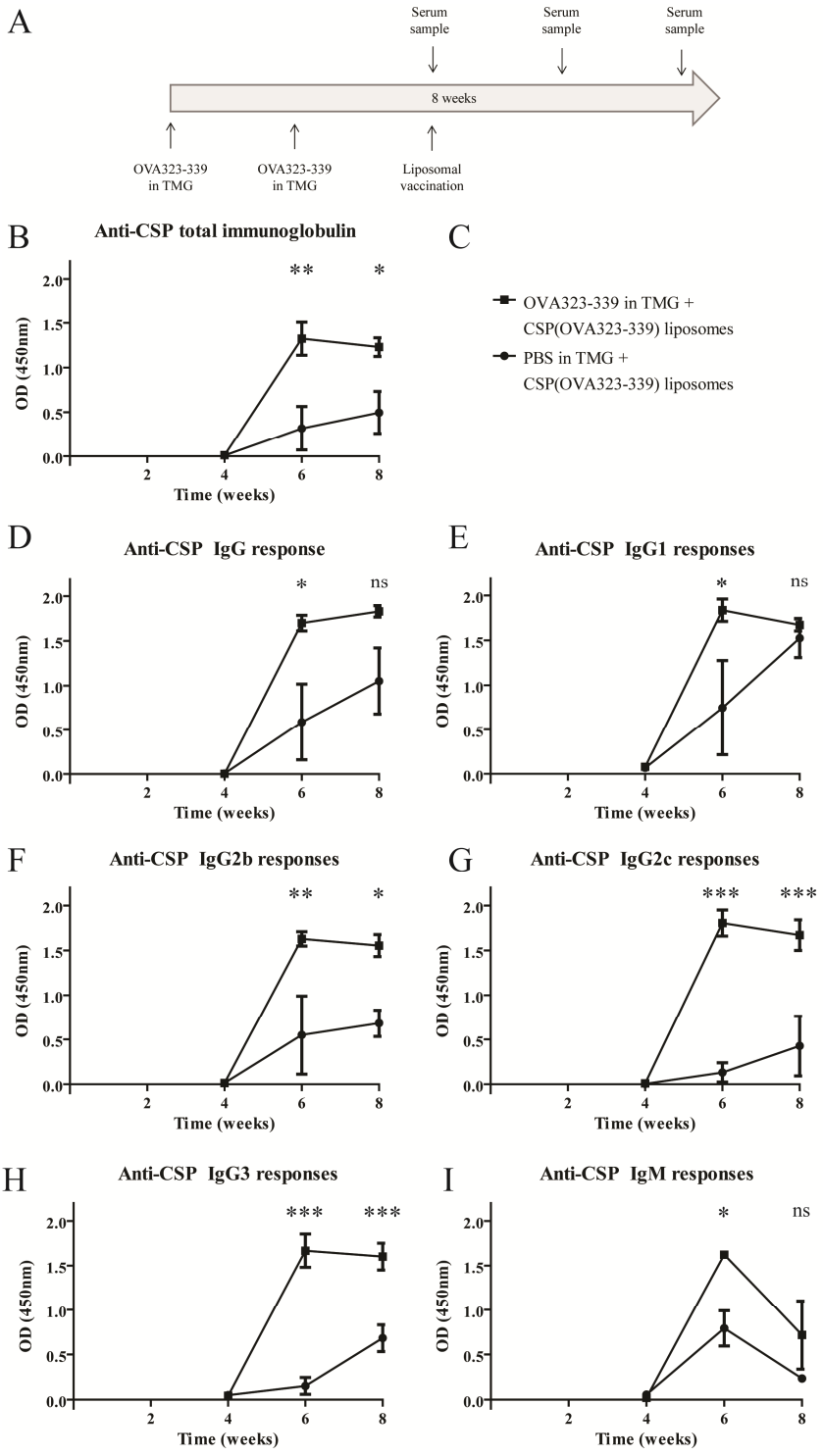
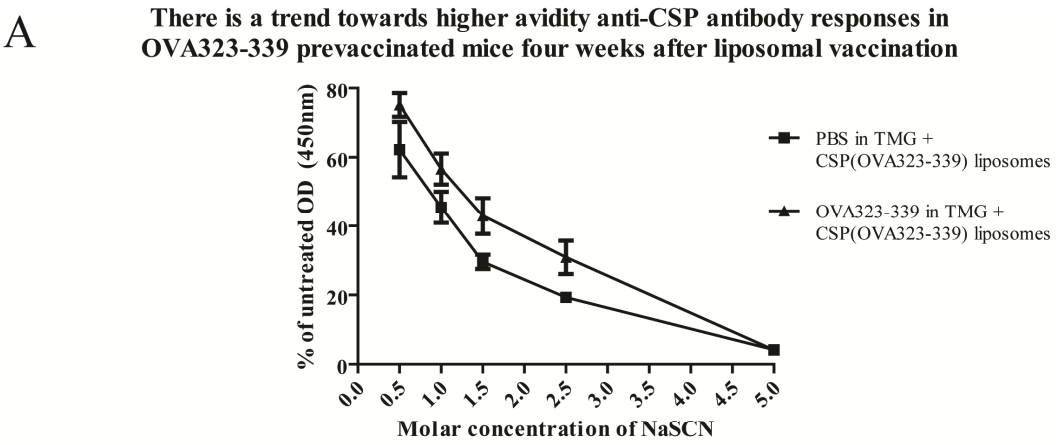


Figure 4.8. Evaluation of the isotype profile of anti-CSP responses to CSP(OVA323-339) liposomes in mice pre-vaccinated with either OVA323-339 or PBS in TMG. 6-8 week old female C57Bl/6 mice (n=3) were administered two subcutaneous vaccinations of 10 µg of OVA323-339 peptide or PBS emulsified in TiterMax gold adjuvant, with a two week interval between doses. Two weeks later, this was followed by a single dose of liposomes coated in CSP and encapsulating OVA323-339 peptides. Each vaccine dose contained 50 µg of CSP and 10 µg of OVA323-339. Graphic (A) outlines the study protocol. The effect of pre-existing CD4+ T cell immunity on the developing total anti-CSP antibody response was measured over four weeks (B) and can be interpreted with the figure legend (C). The effect of pre-existing immunity on the degree and speed of switching to different anti-CSP antibody isotypes (D-I) was also assessed by ELISA with biotinylated anti-isotype secondary antibodies (section 2.12.2). Means were compared using two-way ANOVA with Bonferroni's post-test (n=3).

4.3.7. The effect of pre-existing, non-cognate, CD4+ T cell immunity on anti-CSP antibody avidity

CD4+ T cell help is also important for B cell somatic hypermutation and affinity maturation. It was hypothesised that anti-CSP antibody responses would be of a higher avidity when supported by pre-existing anti-OVA323-339 immunity. To measure avidity, the chaotropic agent sodium thiocyanate (NaSCN) was used to disrupt weaker antibody-antigen interactions (section 2.12.6) as originally described by (Pullen et al. 1986). There was a trend towards higher avidity anti-CSP antibodies in OVA323-339 + TMG pre-vaccinated mice across a range of NaSCN concentrations (figure 4.9.A) and when the amount of NaSCN required to reduce ELISA signal by 50% was calculated, there was a statistically significant higher avidity anti-CSP response in mice with pre-vaccinated with OVA323-339 in TMG.

A



B

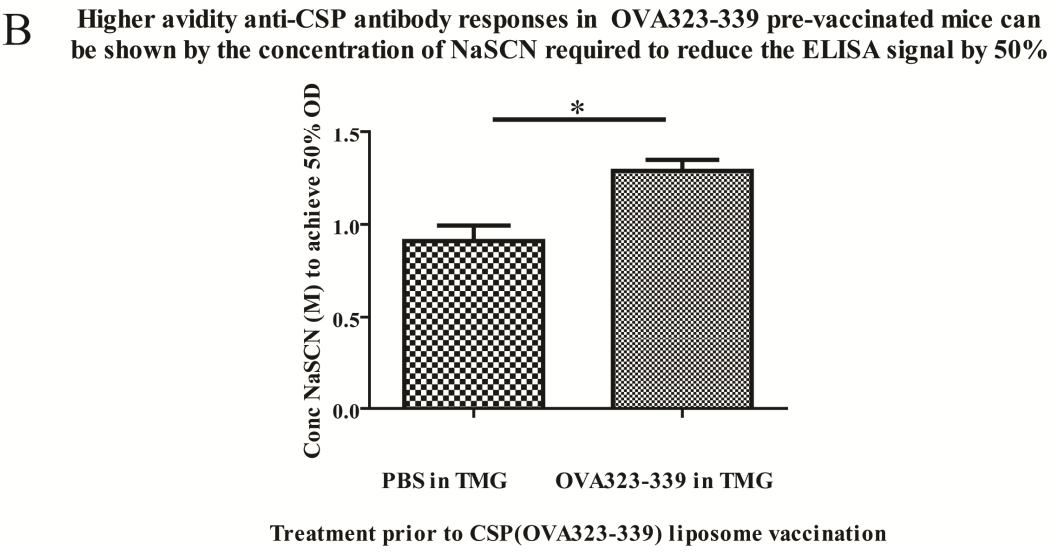


Figure 4.9. The avidity of anti-CSP antibody responses to CSP(OVA323-339) liposomes in mice pre-vaccinated with PBS or OVA323-339 in TMG. The effect of pre-existing, non-cognate, CD4+ T cell immunity on antibody avidity was assessed using a sodium thiocyanate (NaSCN)-displacement ELISA (section 2.12.6). 6-8 week old female C57Bl/6 mice were administered two subcutaneous vaccinations of 10 μg of OVA323-339 peptide or PBS emulsified in TiterMax gold adjuvant, with a two week interval between doses. Two weeks later, this was followed by a single dose of liposomes coated in CSP and encapsulating OVA323-339 peptides. Four weeks after liposomal vaccination, serum samples (n=4) were obtained and the avidity of anti-CSP antibody response was assessed. The effect of increasing concentrations of NaSCN on anti-CSP ELISA signal (A) and the concentration of NaSCN required to decrease this signal by 50% (B) were measured. Mean NaSCN concentrations were compared using unpaired, two-tailed t tests.

4.3.8. Distinguishing between the local immunostimulatory effect of TiterMax Gold and pre-existing, non-cognate, CD4+ T cell help

TiterMax Gold is known to induce persistent, local inflammatory changes following subcutaneous administration in mice (Leenaars et al. 1998). For this reason, the control group throughout previous studies in this chapter was PBS emulsified in TMG. However, it is possible that these persistent local changes enhance the antibody response to subsequent liposomal particles administered via the same route in a non-specific fashion, thus understating the true effect of pre-existing CD4+ T cell immunity to OVA323-339. The magnitude of this problem was first assessed by comparing CSP responses in mice that had not been pre-vaccinated (4.10.A) with PBS + TMG (4.10.B) and OVA323-339 + TMG (4.10.C) pre-vaccinated mice. This demonstrated that PBS + TMG gold did enhance anti-CSP responses above the level achieved if CSP(OVA323-339) liposomes were administered with no preparatory vaccination regimen ($p<0.05$). IgG1 production was higher in both PBS + TMG ($p<0.05$) and OVA323-339 + TMG ($p<0.01$) groups compared to mice that were not pre-vaccinated, but there was no difference between these two groups. IgG2c production was markedly higher in the OVA323-339 + TMG group when compared with mice that were not pre-vaccinated ($p<0.001$) or that were pre-vaccinated with PBS + TMG ($p<0.001$).

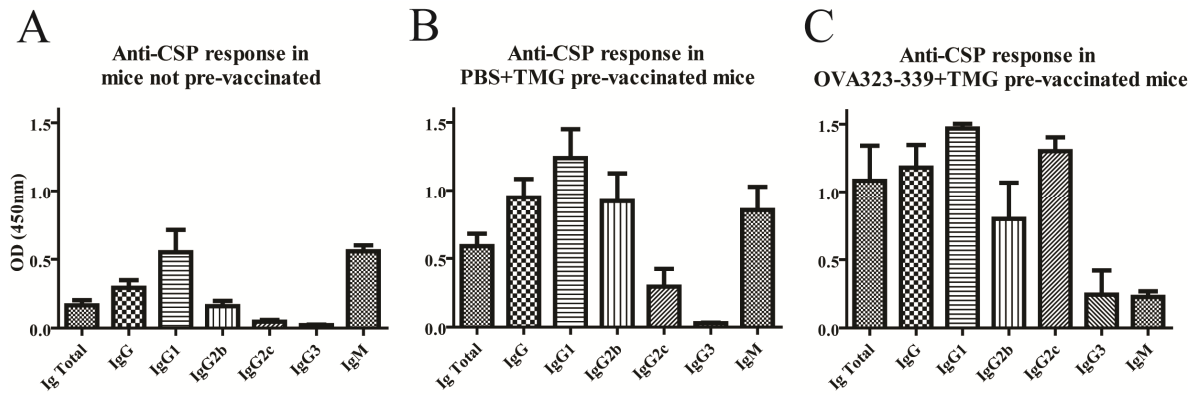


Figure 4.10. The isotype profile of anti-CSP responses to CSP(OVA323-339) liposomes in mice pre-vaccinated with PBS + TMG, OVA323-339 + TMG, or not pre-vaccinated. 6-8 week old female C57Bl/6 mice (n=3) were either pre-vaccinated with two doses of OVA323-339 in TMG (following the established regimen for generating pre-existing CD4+ T cell immunity to OVA323-339 set out in figure 4-5), PBS in TMG, or received no pre-treatment. Two weeks after the final vaccination, mice were administered a single dose of liposomes coated in CSP and encapsulating OVA323-339 peptides. Each vaccine dose contained 50 µg of CSP and 10 µg of OVA323-339. Four weeks later, serum samples were obtained and the isotype of anti-CSP antibody response was measured with biotinylated anti-isotype secondary antibodies, as described in section 2.12.2. Mean OD levels were compared using one-way ANOVA with Tukey's post-test. For clarity, significant differences are not shown in this figure. Instead, key findings are discussed in the main text.

4.3.9. Exploiting systemic CD4+ T cell immunity at anatomically distinct vaccination sites

The protocol of administering liposomes via the same route as our recent pre-vaccination protocol (which included the persistent agent TMG) is complicated by the depot-forming nature of the TMG adjuvant. It is possible that injection of liposomes at the same site as pre-vaccination with TMG could enhance responses as a result of administration of liposomes into an inflamed environment. This might elevate responses to liposomal vaccines in both PBS + TMG and in OVA323-339 + TMG pre-vaccinated mice, and could result in an underestimation of the influence of pre-existing, non-cognate, CD4+ T cell immunity on anti-CSP antibody responses. Consequently, other models were examined where these anti-OVA323-339 CD4+ T cells were generated by vaccination at a site distinct from the route of liposome administration. It could be argued that this model has more translational relevance, where a particle vaccine may be required to exploit pre-existing immunity at a location that is anatomically distinct from a vaccine that was given years earlier.

First, the established protocol of subcutaneous OVA323-339 + TMG vaccination was studied alongside intramuscular (i.m) OVA323-339 + TMG and intramuscular PBS + TMG. The effect of pre-existing anti-OVA323-339 immunity generated by either subcut or i.m. vaccination was compared to subcut PBS + TMG pre-vaccination. The total anti-CSP response following vaccination with subcut CSP(OVA323-339) liposomes was higher in both i.m and subcut OVA323-339 pre-vaccinated mice (figure 4.11.A). These two OVA323-339 pre-vaccinated groups displayed very similar anti-CSP isotype response kinetics that were notably different from PBS + TMG pre-vaccinated mice (4.11.B-G), suggesting that in both groups anti-OVA323-339 CD4+ T cells could influence the developing anti-CSP humoral response.

Similarly, when the converse study was performed and liposomes were administered subcutaneously, the groups pre-vaccinated with OVA323-339 + TMG i.m or subcut both mounted higher anti-CSP antibody responses (4.12.A) when compared with mice pre-vaccinated i.m. with PBS + TMG. Again, a similar anti-CSP isotype response profile was observed in both OVA323-339 pre-vaccinated groups and this was significantly different from that observed to PBS + TMG pre-vaccinated mice.

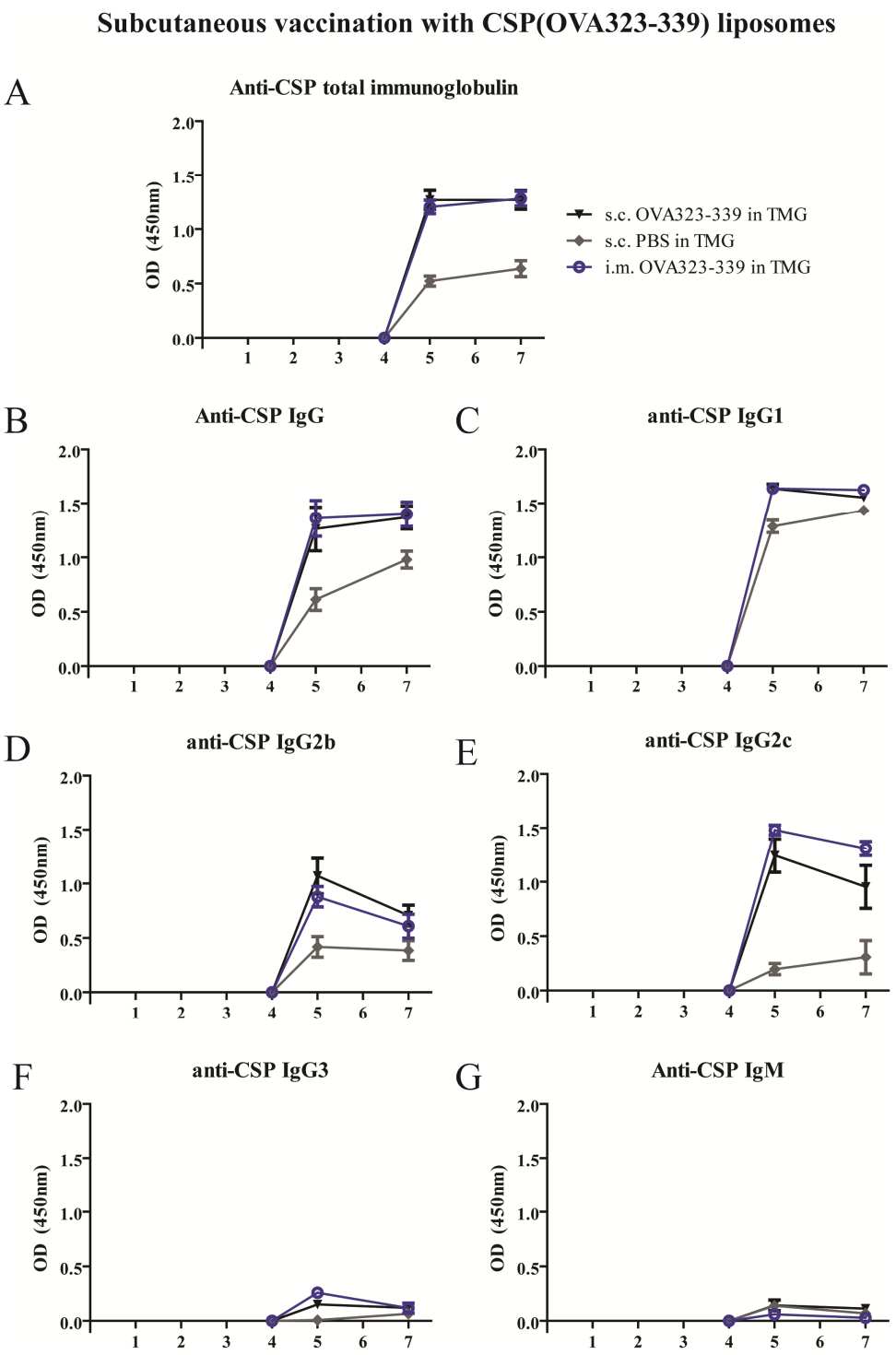


Figure 4.11. The isotype profile of anti-CSP responses to CSP(OVA323-339) liposomes administered subcutaneously following subcutaneous or intramuscular vaccination with OVA323-339 + TMG. 6-8 week old female C57Bl/6 mice (n=4) were administered two subcutaneous vaccinations of 10 µg of OVA323-339 peptide or PBS emulsified in TiterMax Gold adjuvant, or two intramuscular injections of 10 µg of OVA323-339 peptide in TiterMax Gold adjuvant, with a two week interval between doses. Two weeks later, this was followed a single subcutaneous dose of liposomes coated in CSP and encapsulating OVA323-339 peptides. Each vaccine dose contained 10 µg of CSP and 2 µg of OVA323-339. The effect of pre-existing anti-OVA323-339 CD4+ T cell immunity, generated by subcutaneous or intramuscular vaccination, on the developing total anti-CSP antibody response was measured over four weeks (A). The effect of pre-existing immunity on the degree and speed of switching to different anti-CSP antibody isotypes (B-G) was also assessed by ELISA with biotinylated anti-isotype secondary antibodies, as described in section 2.12.2.

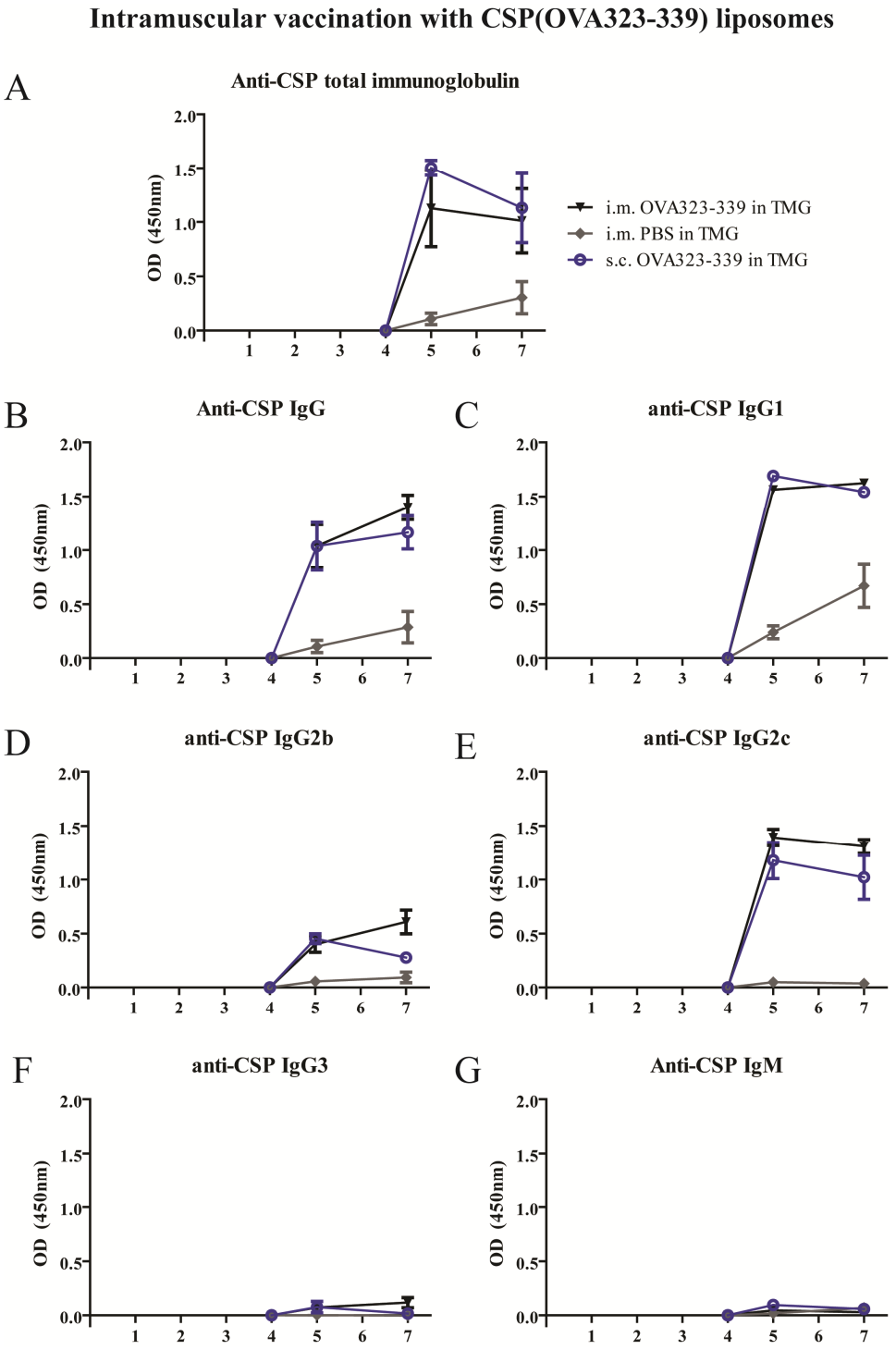


Figure 4.12. The isotype profile of anti-CSP responses to CSP(OVA323-339) liposomes administered intramuscularly following subcutaneous or intramuscular vaccination with OVA323-339 + TMG. 6-8 week old female C57Bl/6 mice (n=4) were administered two intramuscular vaccinations of 10µg of OVA323-339 peptide or PBS emulsified in TiterMax Gold adjuvant, or two subcutaneous injections of 10µg of OVA323-339 peptide in TiterMax Gold adjuvant, with a two week interval between doses. Two weeks later, this was followed a single intramuscular dose of liposomes coated in CSP and encapsulating OVA323-339 peptides. Each vaccine dose contained 10 µg of CSP and 2 µg of OVA323-339. The effect of pre-existing anti-OVA323-339 CD4+ T cell immunity, generated by subcutaneous or intramuscular vaccination, on the developing total anti-CSP antibody response was measured over four weeks (A). The effect of pre-existing immunity on the degree and speed of switching to different anti-CSP antibody isotypes (B-G) was also assessed by ELISA with biotinylated anti-isotype secondary antibodies, as described in section 2.12.2.

4.3.10. Assessing the relative importance of liposomal vaccine dose and pre-existing, non-cognate, CD4+ T cell immunity

Lastly, the relative effect of liposomal vaccine dose and the presence or absence of pre-existing anti-OVA323-339 immunity on anti-CSP antibody responses was assessed. Mice were pre-vaccinated subcutaneously with either OVA323-339 or PBS in TMG, as described previously, then administered CSP(OVA323-339) liposomes subcutaneously. OVA323-339 pre-vaccinated mice were divided into four groups, receiving either full-dose, $1/5^{th}$ dose, $1/25^{th}$ dose, or $1/125^{th}$ dose CSP(OVA323-339) liposomes.

Anti-CSP antibody responses measured by OD at 450nm revealed that even at $1/25^{th}$ the dose of liposomes, the anti-CSP response was higher in mice pre-vaccinated with OVA323-339 + TMG when compared to PBS + TMG pre-vaccinated mice that received the a dose of CSP(OVA323-339) liposomes that was 25-fold higher. When these responses were measured by an ELISA to measure endpoint titre (section 2.12.3) this trend persisted, although significance was lost at the $1/25^{th}$ dose group. The same pattern, indicating pre-vaccination with OVA323-339 + TMG drives higher anti-CSP antibody responses even at lower liposomal vaccine doses was evident across different anti-CSP IgG subclasses (figure 4.14). The T_H1 isotype IgG2c was only produced to significant levels in mice pre-vaccinated with OVA323-339 (figure 4.14.D) and was detectable at a high level even in mice administered 125-fold less CSP(OVA323-339) vaccine.

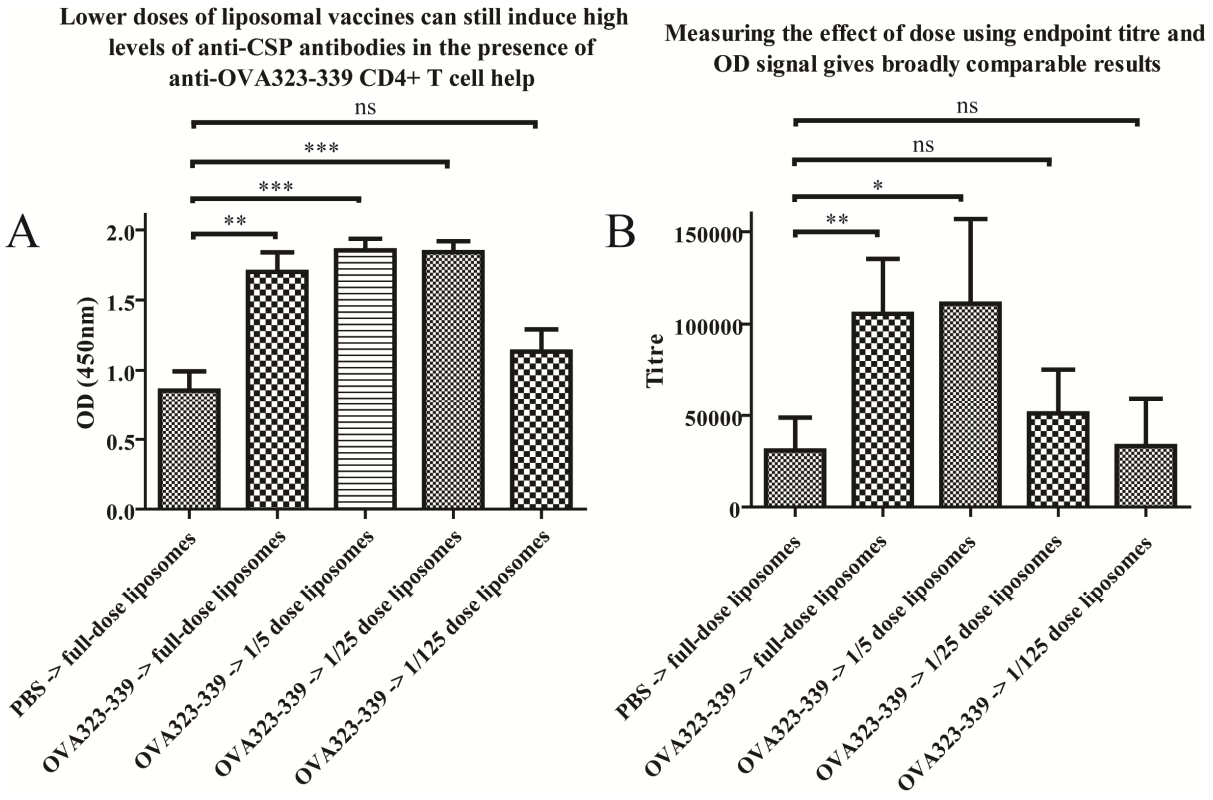


Figure 4.13. The effect of CSP(OVA323-339) liposome dose on anti-CSP responses in mice pre-vaccinated with OVA323-339 or PBS in TMG. 6-8 week old female C57Bl/6 mice (n=4) were administered two subcutaneous vaccinations of 10 μg of OVA323-339 peptide or PBS emulsified in TiterMax Gold adjuvant, with a two week interval between doses. Two and four weeks later, this was followed by varying doses of liposomes coated in CSP and encapsulating OVA323-339 peptides. Full dose vaccines contained 50 μg of CSP and 10 μg of OVA323-339, and five-fold serial dilutions were prepared to give vaccine preparations $1/5^{th}$, $1/25^{th}$, and 125^{th} this dose. Graph (A) displays the total anti-CSP Ig responses three weeks after the second liposomal vaccination as absorbance signal at 450nm. Graph (B) represents the same anti-CSP responses as endpoint titres using the methodology set out in section 2.12.3. Means were compared using a one-way ANOVA with Tukey's post-test for multiple comparisons.

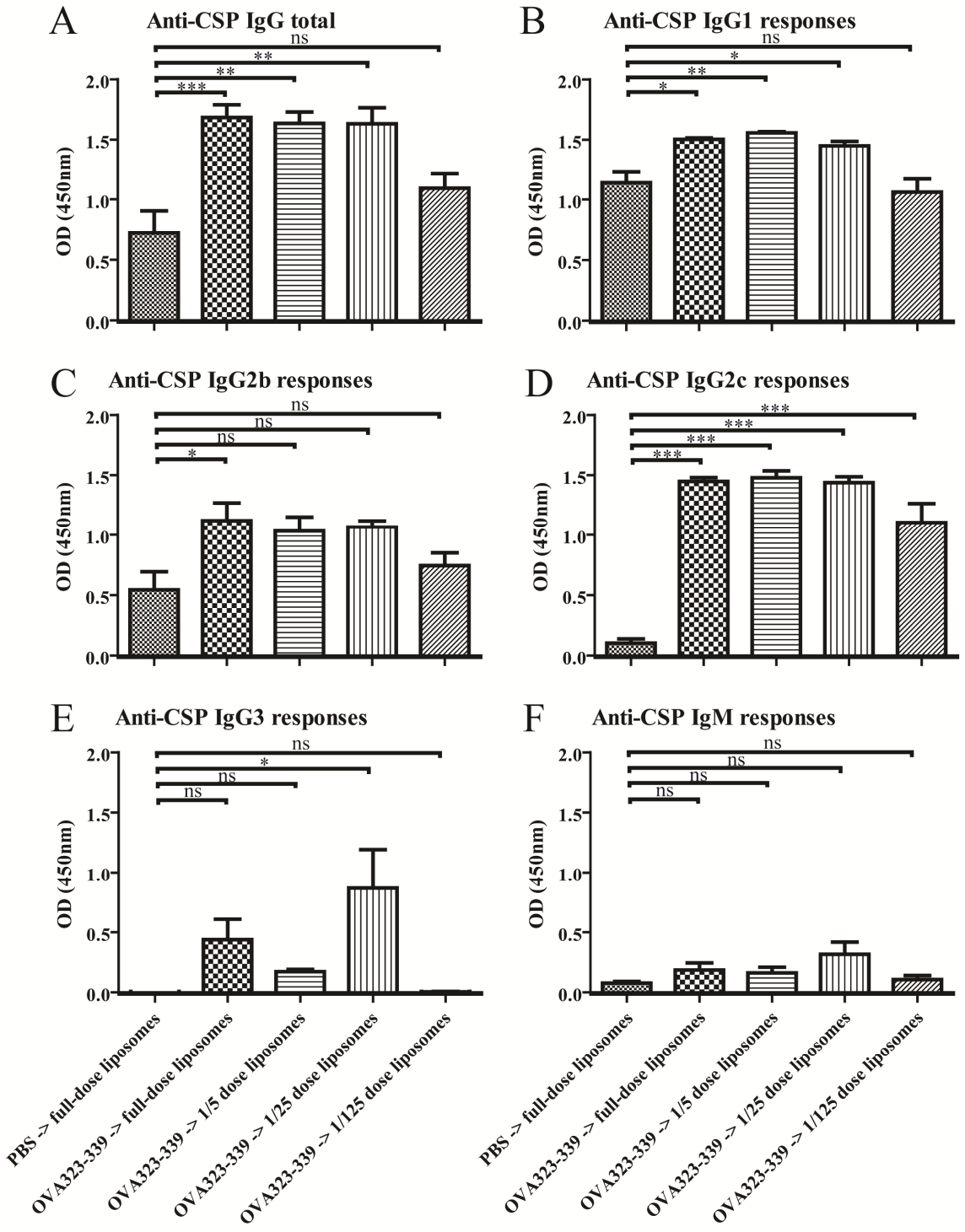


Figure 4.14. The effect of CSP(OVA323-339) liposome dose on the isotype of anti-CSP responses in mice pre-vaccinated with OVA323-339 or PBS in TMG. 6-8 week old female C57Bl/6 mice (n=4) were administered two subcutaneous vaccinations of 10 µg of OVA323-339 peptide or PBS emulsified in TiterMax Gold adjuvant, with a two week interval between doses. Two and four weeks later, this was followed by varying doses of liposomes coated in CSP and encapsulating OVA323-339 peptides. Three weeks after the second liposomal vaccination, the effect of liposomal vaccine dose and pre-existing immunity on anti-CSP antibody isotype switching (A-F) was assessed by ELISA with biotinylated anti-isotype secondary antibodies, as described in section 2.12.2. Means were compared using a one-way ANOVA with Tukey's post-test for multiple comparisons.

4.4. Chapter conclusions

1. Vaccination with two-doses of OVA323-339 in TMG is effective at inducing CD4+ T cell immunity. The resulting population of CD4+ T cells produce both IL-4 and IFNγ by ELISPOT, but a multiplex analysis of a larger panel of cytokines revealed a T_H1-bias. The isotype profile of anti-OVA323-339 antibodies produced in response to OVA323-339 + TMG vaccination also supported a T_H1-biased immune response.

2. Pre-existing anti-OVA323-339 CD4+ T cells can augment antibody responses to surface bound CSP on particles that encapsulate OVA323-339 epitopes.

3. In OVA323-339 + TMG pre-vaccinated mice, anti-CSP antibody responses to CSP(OVA323-339) were generated faster, reached higher levels, and contained more isotype switched antibody than the response seen in mice pre-vaccinated with PBS + TMG.

4. CSP(OVA323-339) liposomes could exploit pre-existing anti-OVA323-339 CD4+ T cell immunity that was generated at anatomical sites distinct from the route of liposomal administration.

5. In the presence of pre-existing anti-OVA323-339 T cells, administering lower doses of CSP(OVA323-339) liposomal vaccines can elicit similar anti-CSP antibody responses to vaccination with higher doses CSP(OVA323-339).

4.5. Chapter discussion

4.5.1. Discussion of results

In this chapter, a vaccination regime was developed to elicit CD4+ T cell immune responses against full-length ovalbumin protein or OVA323-339 peptide. It was demonstrated that two subcutaneous doses of OVA323-339 in TMG resulted in readily detectable populations of anti-OVA323-339 CD4+ T cells. Next, this anti-OVA immune response was characterised in terms of cytokine production, T_H cell polarisation, and antibody isotype. ELISPOT assays revealed that both IFNγ and IL-4 were produced. A more complex analysis of the cytokine secretion profile was undertaken using a multiplex bead array. Here, OVA323-339 stimulation of splenocytes from OVA323-339 + TMG vaccinated mice revealed a broad cytokine expression profile, with a likely T_H1 bias. Analysis of the anti-OVA323-339 antibody response also supported this conclusion. IgG1 and IgG2c production was heavily biased towards IgG2c, indicating a T_H1-dominated immune response.

After establishing that vaccination with OVA323-339 in TMG could generate non-cognate, CD4+ T cell responses, these cells were harnessed to support anti-CSP antibody responses to the liposomal vaccine particles described in chapter 1. The effect of pre-existing CD4+ T cells on the magnitude, affinity, and isotype of the anti-CSP antibody response was examined. It was demonstrated that mice pre-vaccinated with OVA323-339 in TMG produced faster and higher anti-CSP responses following vaccination with CSP(OVA323-339) liposomes. The isotype profile of these responses was also significantly altered by pre-vaccination with OVA323-339. Importantly, production of the TH1 isotype IgG2c was favoured in animals pre-vaccinated with OVA323-339 + TMG, suggesting that the T_H1-polarised anti-OVA323-339 CD4+ T cells is able to drive IgG2c production in these mice.

The flexibility of the liposomal platform was useful, as it meant *in vivo* experiments were not restricted to comparing anti-CSP responses to one vaccine formulation that was administered in the presence or absence of pre-existing anti-OVA CD4+ T cell immunity. Experiments were also conducted to assess the immunogenicity of particles with and without either CSP surface antigen or ovalbumin-derived core antigen. Anti-CSP responses to particles that did not contain the relevant OVA323-339 were significantly lower than those induced by CSP(OVA323-339) vaccination. This indicated that the enhanced anti-CSP response seen in OVA323-339 pre-vaccinated mice was a result of anti-OVA323-339 CD4+ T cells, rather

than a non-specific effect. A lack of a detectable antibody response to OVA323-339 following CSP(OVA323-339) administration was also noted in these studies. This suggests that OVA323-339 was adequately 'hidden' in the particle core and was not available for B cell binding.

TMG causes a local inflammatory response and acts as an antigen depot, slowly releasing antigen at the site of injection (Stills 2005). Consequently, it was important to demonstrate that enhanced anti-CSP responses seen after CSP(OVA323-339) administration in our model were not a result of a short-term, local phenomenon. From a translational perspective, exploiting detectable systemic immune responses at anatomical locations distinct from the original vaccination site, would be an important goal. First, we compared the anti-CSP response to CSP(OVA323-339) immunisation in OVA323-339 + TMG and PBS + TMG pre-vaccinated mice with that seen mice that received no pre-treatment. Again, anti-CSP responses were highest in OVA323-339 pre-vaccinated mice, but it was of note that PBS + TMG pre-vaccinated mice mounted higher responses than mice that were not pre-treated. This suggested that TMG does have a persistent, local, pro-inflammatory effect and that administering vaccine particles into this antigen/adjuvant-modified immune microenvironment could diminish our ability to accurately measure the benefit of pre-existing non-cognate CD4+ T cells.

To further examine this, and to ensure that we could exploit pre-existing *systemic* CD4+ T cell immunity, studies were performed where OVA323-339 + TMG and CSP(OVA323-339) liposomes were administered at anatomically distant sites. Encouragingly, these demonstrated that anti-OVA323-339 CD4+ T cells generated by vaccination at a site distinct from the route of liposome administration could still enhance anti-CSP responses.

Lastly, the relative importance of liposomal vaccine dose and the presence or absence of pre-existing, non-cognate, CD4+ T cell help was considered. Anti-CSP responses to CSP(OVA323-339) vaccination were higher in mice pre-vaccinated with OVA323-339 + TMG, compared to PBS + TMG pre-vaccinated mice, even at $1/5^{th}$, and $1/25^{th}$ the dose of liposomal vaccine. At $1/125^{th}$ of the dose, anti-CSP responses were similar to those seen in PBS + TMG pre-vaccinated mice who then received 125-fold more CSP(OVA323-339). These data emphasise the importance of pre-existing CD4+ T cell immunity in enhancing antibody responses to the CSP(OVA323-339) particle vaccine. Additionally, the data suggest that any potential reduction in immunogenicity at lower vaccine doses could be overcome by

establishing pre-existing, non-cognate, CD4+ T cell immunity. The inclusion of additional PBS + TMG control groups for each of the lower CSP(OVA323-339) vaccine dosing regimens would have provided information on the relative influence of pre-existing CD4+ T cell help and liposomal vaccine dose. The flexibility of liposomal particle engineering could allow a range of doses of OVA323-339 to be incorporated in otherwise comparable CSP-coated vaccine particles. OVA323-339 dose-dependent enhancement of anti-CSP antibody production would further define the influence of non-cognate CD4+ T cell help in this model.

4.5.2. Limitations and future work

Data in this chapter support using liposomal vaccine particles that spatially segregate B and T cell antigens to enhance antibody responses by exploiting non-cognate CD4+ T cell help. Here, it was shown that pre-existing populations of anti-ovalbumin CD4+ T cells generated by vaccination could enhance anti-CSP antibody responses. This effect was particularly apparent with OVA323-339 + TMG pre-vaccination and CSP(OVA323-339) liposomes, when compared with studies using full-length ovalbumin. Future work could re-assess encapsulating full-length proteins to provide helper MHCII epitopes, but the remaining work in this thesis used shorter peptide MHCII epitopes. Future directions for this project could also include surface-conjugated carbohydrate antigens – where T-dependent responses could be achieved thanks to non-cognate CD4+ T cell help. Other examples of immune responses to unconventional antigens that could arise in this project are antibodies raised against non-protein components of our vaccine particle. The presence of antibodies recognising lipid and PEG components of our liposomal particles could be studied using serum from existing experiments. While these are not the goal of the current project, it is interesting to consider whether anti-lipid responses would have any therapeutic utility – such as in managing hypercholesterolaemia.

The higher anti-CSP responses in OVA323-339 pre-vaccinated mice described in this chapter were deemed to occur as a result of pre-existing CD4+ T cell immunity for several reasons. First, responses were higher in mice pre-vaccinated with OVA323-339 in TMG when compared with PBS in TMG, suggesting that higher responses were not simply due to TMG. Second, responses to CSP(empty) liposomes were very low, even in mice pre-vaccinated with OVA323-339 + TMG, indicating that higher responses were dependent on the presence of the MHCII epitope in the core of the CSP-coated particle. Lastly, anti-CSP responses could be enhanced by vaccination with OVA323-339 + TMG at anatomical sites distinct from where

CSP(OVA323-339) liposomes were administered – suggesting this was an effect that could be exploited systemically and most likely resulted from CD4+ T cell circulation. However, further studies could be performed to confirm this. If the augmented CSP response truly depends on pre-existing anti-OVA323-339 CD4+ T cells, higher anti-CSP responses should also be seen in animals adoptively transferred CD4+ T cells from OVA323-339 + TMG vaccinated mice.

In this chapter, several assays were used to assess the TH1/TH2 balance of the developing immune response. ELISPOT assays demonstrated that both IL-4 and IFNγ were produced in response to OVA323-339 + TMG vaccination. However, a multiplex cytokine bead array to measure cytokine secretion from OVA323-339 pulsed splenocytes could not detect IL-4 and indicated that IFNγ secretion dominated the immune response to OVA323-339. The reason for this discrepancy could result from the 36, as opposed to 24, -hour incubation used in ELISPOT studies. Or, perhaps more likely, it results from different sensitivities of the two assays. Isotype analysis revealed a very low IgG1:IgG2c ratio, providing more evidence for a T_H1/IFNγ response to OVA323-339 + TMG vaccination. It appeared that the isotype of the anti-CSP response to CSP(OVA323-339) liposomes was influenced by the T_H1/T_H2 polarisation of pre-existing anti-OVA323-339 CD4+ T cells. An interesting future experiment could involve using a range of adjuvants to generate different balances of T_H1/T_H2 anti-OVA323-339 immunity and then gauging the effect this has on anti-CSP responses to CSP(OVA323-339) liposomes.

Studies here examined the *local* influence of TMG pre-vaccination (section 4.3.8) and the effect of *systemic* CD4+ T cell immunity (section 4.3.9) on anti-CSP responses to CSP(OVA323-339) vaccination. A critical finding was that pre-existing vaccine-induced CD4+ T cell immunity could be exploited by liposomal vaccination at distal sites, rather than elevated anti-CSP responses only resulting from a local phenomenon. This observation led to a body of work that sought to exploit other sources of pre-existing immunity – such as anti-viral CD4+ T cells – presented in chapter six.

5. Incorporating TLR9 agonists as the 'third signal' for B cell activation

5.1. Introduction

For an antigen-driven B cell response to fully mature, it was traditionally thought that two sequential antigen-dependent signals were required. In this model, BCR crosslinking by its target antigen was designated 'signal one', and resulted in efficient antigen uptake, processing, and presentation on MHCII (Parker 1993). MHCII-epitope complexes could then interact with CD4+ T cells at an immunological synapse, which results in the delivery of 'signal two' via co-stimulatory molecules and soluble mediators such as cytokines (Mills & Cambier 2003). In chapter four, these two signals were achieved by administering liposomal particles with surface-bound B cell antigen (CSP) and encapsulated MHCII epitopes (OVA323-339), in the context of pre-existing non-cognate anti-OVA323-339 CD4+ T cell immunity. This chapter examines whether TLR agonists could further enhance the immunogenicity of these liposomal particle vaccines.

It has long been known that TLR agonists can induce transient antigen-independent proliferation in naïve B cells (Krieg et al. 1995). More recently, the two-signal model has been reassessed to include TLR agonism as an important 'third signal' driving naïve B cell responses to antigen. It was observed that TLR agonism can synergise with BCR triggering and CD4+ T cell help for full differentiation of naïve human B cells into long-lived, class-switched, antibody-secreting plasma cells (Ruprecht & Lanzavecchia 2006)(Liu et al. 2003). Further, it was shown that these enhanced responses resulted from the direct action of TLR agonists on B cells, rather than through an indirect effect on other APCs or CD4+ T cells (Ruprecht & Lanzavecchia 2006).

TLR9 is widely expressed in different murine B cell subsets and TLR9 agonism can stimulate proliferation and immunoglobulin secretion (Gururajan et al. 2007)(Krieg et al. 1995). TLR9 agonists have emerged as important adjuvants that stimulate a T_H1-biased immune response (Vollmer & Krieg 2009)(Lin et al. 2004). In this chapter, CSP-coated liposomes containing OVA323-339 and a CpG DNA TLR9 agonist were produced, characterised, and used for *in vivo* vaccination studies. The effect of TLR9 agonism on B cell responses – either in the

presence or absence of pre-existing anti-OVA323-339 immunity – was studied by evaluating the magnitude and isotype of the developing anti-CSP antibody response.

5.2. Chapter aims

1. Produce CSP-coated, OVA323-339 encapsulating liposomes that also contain unmethylated CpG DNA in the particle core

2. Measure the effect of particle-encapsulated TLR9 agonists on the magnitude of the anti-CSP antibody response

3. Assess the effect of particle-encapsulated TLR9 agonists on the isotype of the anti-CSP antibody response

5.3. Results

5.3.1. Incorporation of unmethylated CpG DNA oligonucleotides in liposomal vaccine constructs

To test the hypothesis that TLR9 agonism would augment anti-CSP antibody responses, it was necessary to establish a protocol for encapsulation of TLR9 agonists in liposomal vaccine particles. First, water soluble, CpG-containing DNA oligonucleotides were synthesised and dissolved with CD4+ T cell helper epitopes for liposomal formulation. These oligonucleotides were synthesised to have the same nucleotide sequence as the commercially available murine TLR9 agonist ODN1826 (5'-tccatga**cg**ttcctga**cg**tt-3'). Of note, ODN1826 is prepared with a phosphorothioate backbone – conferring nuclease resistance – whereas the oligonucleotides used in this project have conventional phosphodiester linkages.

To detect the presence of CpG DNA oligonucleotides (hereafter referred to as 'CpG') in liposomal particles during formulation and after purification, the OliGreen ssDNA detection reagent was employed. This is a membrane permeable agent that provides a fluorescent signal after binding ssDNA, allowing quantification. The highest concentrations of oligonucleotides were detected in the liposomal fractions after PD10 purification and were retained in liposomal particles following dialysis (figure 5.1).

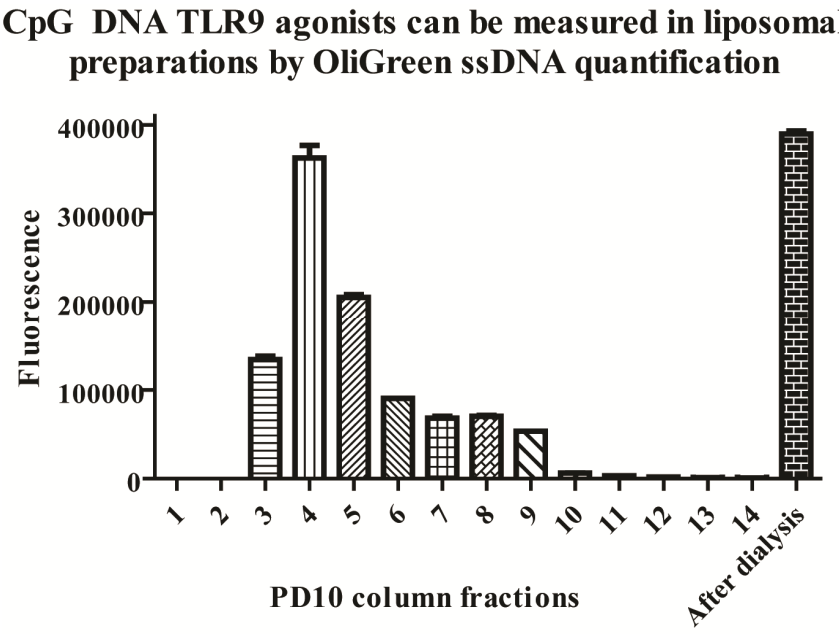


Figure 5.1. Measurement of CpG DNA in liposomal vaccine formulations. The presence of CpG DNA TLR9 agonists was measured in the PD10 column fractions during purification of liposomes encapsulating CpG and the peptide OVA323-339. PD10 fractions 3, 4, and 5 and were grossly opaque, suggesting they contained liposomes. PD10 fraction 4 was reacted overnight with CSP antigen and then dialysed overnight before CpG content was measured by OliGreen assay.

5.3.2. *In vitro* characterisation of liposomal vaccine particle TLR9 agonism

To confirm that TLR9 agonists encapsulated in liposomal vaccine particles were biologically active, *in vitro* assays using the commercially available reporter cell line HEK-Blue-mTLR9 were performed. TLR9 signalling involves the adapter molecule MyD88 and results in transcription of genes under the control of factors such as AP-1 and NF-κB (Takeda & Akira 2004). This cell line was produced by co-transfection of the murine TLR9 gene and an inducible, secreted form of embryonic alkaline phosphatase (SEAP). SEAP expression is under the control of the IFN-β minimal promoter fused to five AP-1 and NF-κB binding sites. Treatment of reporter cells with either liposomes encapsulating CpG or free oligonucleotides (figure 5.2.A and 5.2.B) was able to induce SEAP expression. In contrast, SEAP could not be induced by empty liposomal particles or particles containing only OVA323-339.

To assess if OVA323-339 processing was affected by the presence of TLR9 agonists, the ability of liposomal particles to induce IFNγ secretion from splenocytes of OVA323-339 immune mice was assessed. Liposomes containing OVA323-339 with and without CpG DNA oligonucleotides were able to induce comparable levels of IFNγ secretion, however this did not reach statistical significance when compared with IFNγ secretion from splenocytes pulsed with a control peptide (figure 5.2.C).

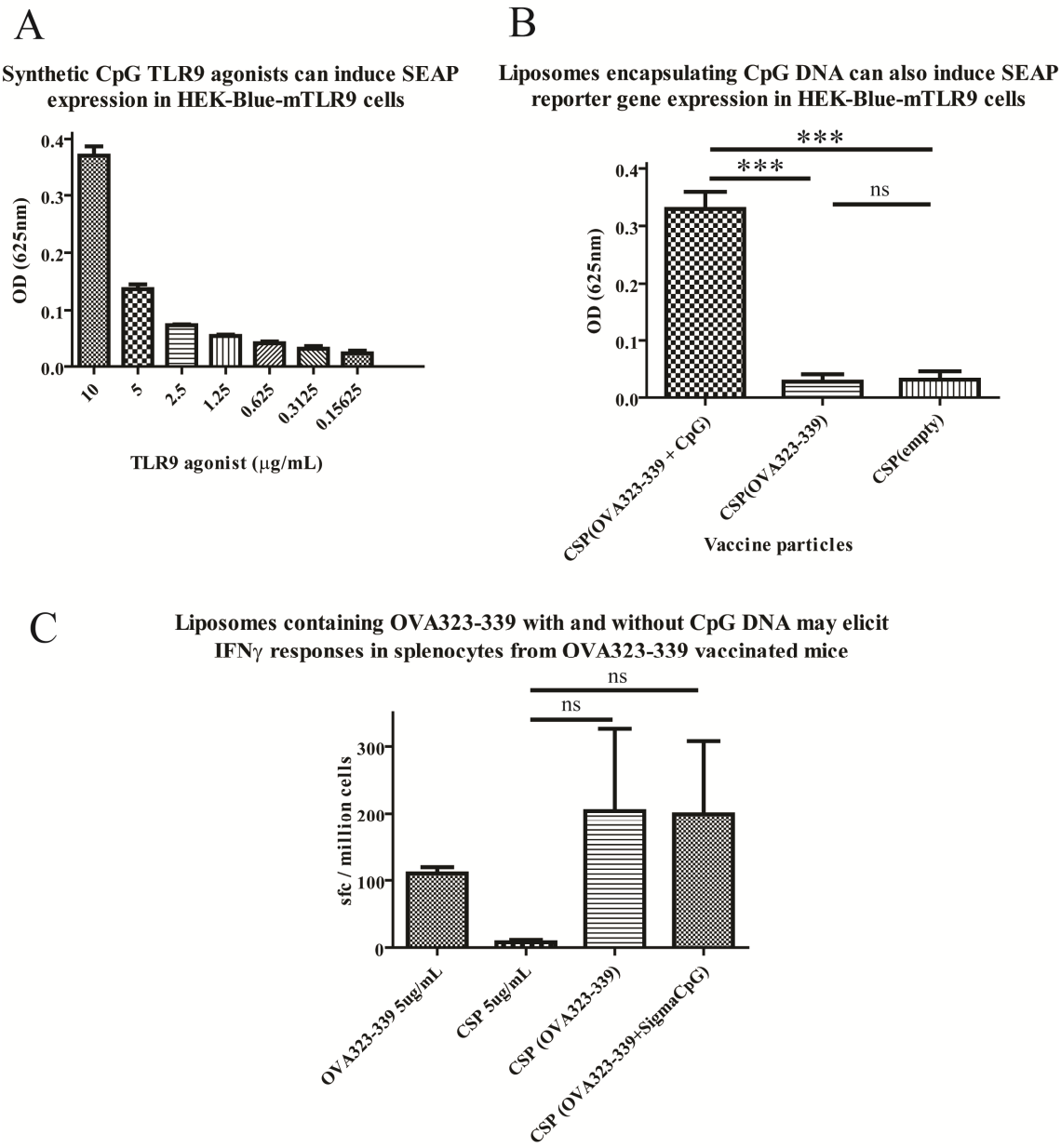


Figure 5.2. Assessment of the functionality of liposomal particles that contain CpG DNA. HEK-Blue-mTLR9 reporter cells were incubated for 24 hours with increasing concentrations of TLR9 agonist (figure 5.2.A) or with CSP(OVA323-339 + CpG) liposomes, CSP(OVA323-339) liposomes, or CSP(empty) liposomes (figure 5.2.B). SEAP expression levels were measured by detection of a colorimetric product from SEAP substrate-containing HEK-blue detection media. Splenocytes from OVA323-339 + TMG vaccinated mice were incubated with either OVA323-339, the control antigen CSP, CSP(OVA323-339) liposomes, or CSP(OVA323-339 + CpG) liposomes. IFNγ production was measured by ELISPOT after 24 hours. Means were compared by one-way ANOVA with Tukey's post-test (n=3).

5.3.3. *In vivo* safety studies of TLR9-incorporating liposomes

CpG DNA oligonucleotides have been shown to cause TLR9-dependent toxicity in mice at high doses (Campbell et al. 2009)(Behrens et al. 2011). Considerable weight loss was observed following the first dose of liposomes containing CpG DNA (figure 5.3.B), but this was not apparent after the second dose of liposomal vaccine.

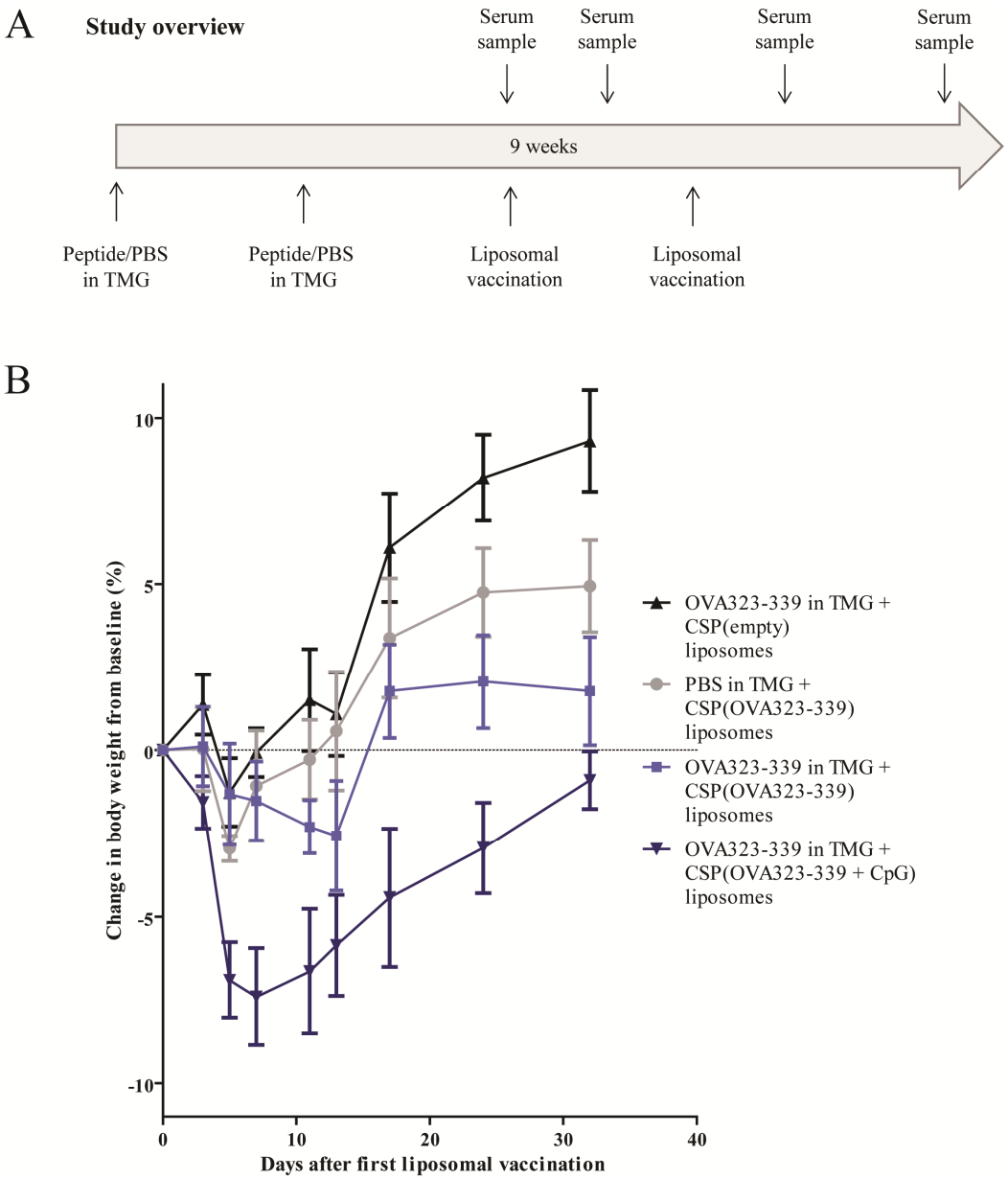


Figure 5.3. Study overview and toxicity profile of CpG DNA encapsulating liposomes *in vivo*. 6-8 week old female C57Bl/6 mice were vaccinated twice with either PBS or OVA323-339 in TMG as previously described in section 4.3.1. They were then administered two subcutaneous doses of CSP(empty), CSP(OVA323-339), or CSP(OVA323-339 + CpG) liposomes in 100 µL. Each vaccine dose contained 50 µg of CSP and, where indicated, 10 µg OVA323-339 and 10 µg CpG DNA (see section 2.9.7 for dosing calculations). The weight of each mouse was monitored from week four to week nine of the study and is plotted for each group as a percentage change from baseline in figure 5.3.B.

5.3.4. Pilot *in vivo* studies assessing the effect of TLR9 agonism on anti-CSP antibody responses

It was hypothesised that the inclusion of CpG DNA in liposomal particles would enhance anti-CSP antibody production and alter the isotype profile of the anti-CSP response. To study this, mice pre-vaccinated with two doses of OVA323-339 in TMG were subsequently administered two doses of either CSP(OVA323-339 + CpG) liposomes, CSP(OVA323-339) liposomes, or CSP(empty) liposomes. Developing anti-CSP responses were compared with mice administered PBS in TMG and then CSP(OVA323-339) liposomes (figure 5.4.A). Anti-CSP total IgG responses were highest following vaccination with CSP(OVA323-339) liposomes or CSP(OVA323-339 + CpG) liposomes, but differences between these two groups did not reach statistical significance.

The anti-CSP isotype profile was compared between treatment groups and the effect of TLR9 agonists was considered. Mice vaccinated with CSP(OVA323-339) liposomes made IgG1 faster than those administered CSP(OVA323-339 + CpG), demonstrated by significantly different mean anti-CSP IgG1 at the five week time point (figure 5.3.B, $p<0.001$). Conversely, TLR9 agonism drove the production of more IgM at the five week time point ($p<0.001$) and more IgG2c at each time point post-vaccination ($p<0.001$).

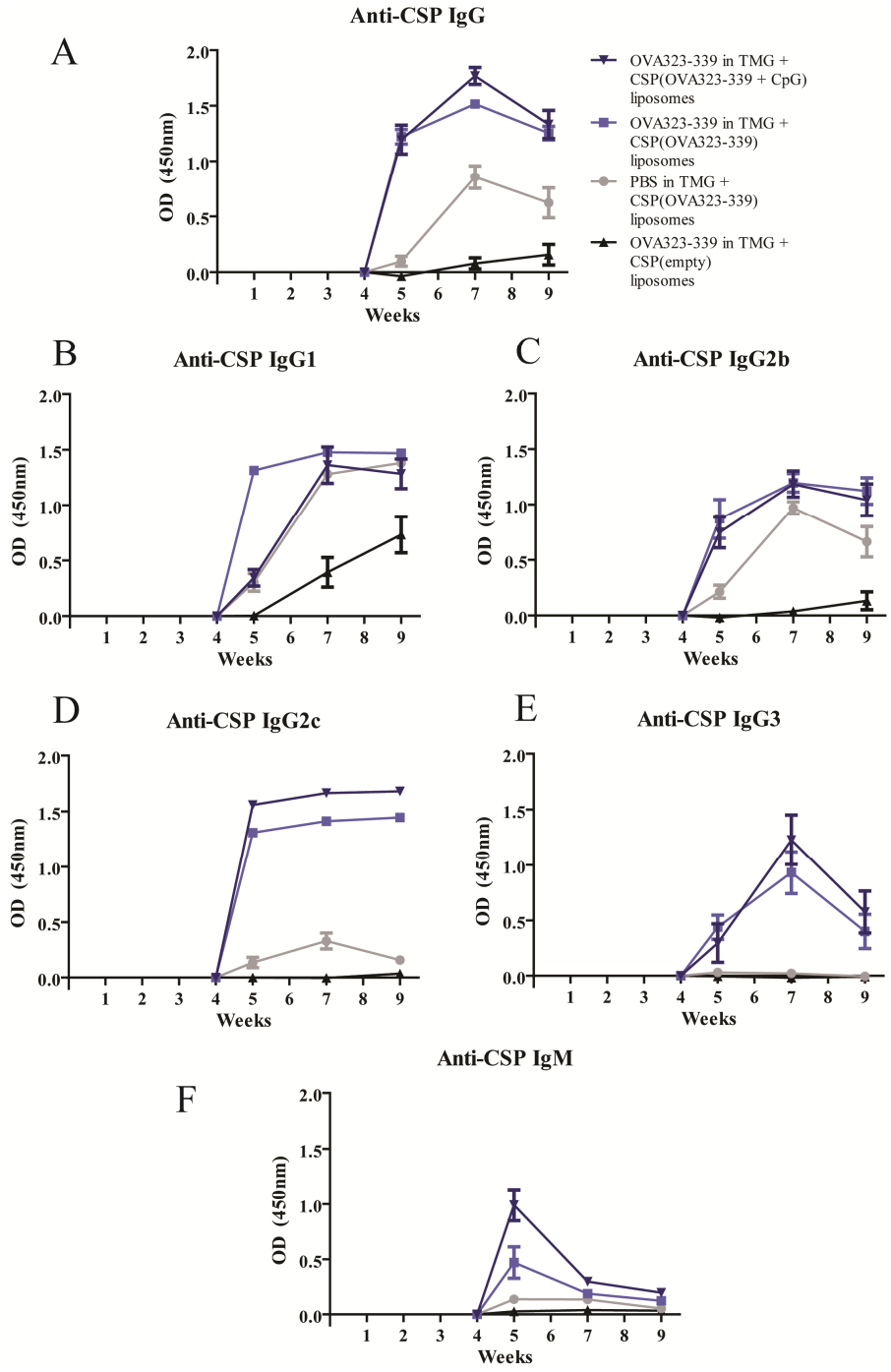


Figure 5.4. Evaluation of anti-CSP responses to CSP(OVA323-339), CSP(empty) and CSP(OVA323-339 + CpG) liposomes in mice pre-vaccinated with either OVA323-339 or PBS in TMG. 6-8 week old female C57Bl/6 mice were administered two subcutaneous vaccinations of 10 µg of OVA323-339 peptide or PBS emulsified in TMG adjuvant, with a two week interval between doses. Mice were then given two subcutaneous doses of CSP(empty), CSP(OVA323-339), or CSP(OVA323-339 + CpG) liposomes in 100 µL as described in figure 5.3.A. Each vaccine dose contained 50 µg of CSP and, where indicated, 10 µg OVA323-339 and 10 µg CpG DNA (see section 2.9.7 for dosing calculations). The effect of pre-existing CD4+ T cell immunity and liposome-encapsulated TLR9 agonists on the developing total anti-CSP IgG antibody response was measured by ELISA over six weeks (A). The effect of pre-existing immunity and TLR9 agonists on the degree and speed of switching to different anti-CSP antibody isotypes (B-F) was also assessed by ELISA with biotinylated anti-isotype secondary antibodies (section 2.12.2). Mean responses were compared with two-way ANOVA and Bonferroni's post-test. For clarity, significant differences are not shown in this figure. Instead, key differences are discussed in the main text.

5.3.5. *In vivo* studies with a single lower dose of vaccine for further characterisation of the effect of TLR9 agonism on anti-CSP responses

To further investigate whether CpG altered the anti-CSP antibody response quantitatively or qualitatively, a repeat study was performed at a lower dose and with different control groups. Data presented in chapter two (figures 4.13 and 4.14) indicated that liposomal vaccine dose could be reduced without dramatically affecting anti-CSP responses in OVA323-339 pre-vaccinated mice. Consequently, each liposomal vaccine preparation was used at a hundred-fold lower dose than in the pilot study. Additionally, each liposomal vaccine was only administered once. Lastly, the CSP(empty) group was omitted. This modified vaccination protocol resulted in complete abrogation of the toxicity seen in section 5.3.3, with no significant weight loss in any study group (data not shown).

The anti-CSP response was highest in mice pre-vaccinated with OVA323-339 + TMG and then administered CSP(OVA323-339 + CpG) liposomes, with the increase due to TLR9 agonism reaching statistical significance at the six and nine week time points (figure 5.5.C, $p < 0.05$ and $p < 0.01$, respectively).

Anti-CSP IgG1 was produced earlier and in greater quantities in mice pre-vaccinated with OVA323-339, independent of the inclusion of CpG (figure 5.5.D). In OVA323-339 pre-vaccinated mice, the inclusion of TLR9 agonists drove a higher IgG2b response which reached statistical significance by week nine (figure 5.5.E, $p < 0.001$). Similarly, TLR9 agonism resulted in a higher anti-CSP IgG2c response that reached statistical significance at week six (figure 5.5.F, $p < 0.05$). In mice pre-vaccinated with PBS, the inclusion of TLR9 agonists lifted the IgG2c response to levels comparable with OVA323-339 pre-vaccinated mice that were subsequently administered CSP(OVA323-339) liposomes. IgG3 and IgM responses were broadly comparable in all groups (figures 5.5.G and 5.5.H).

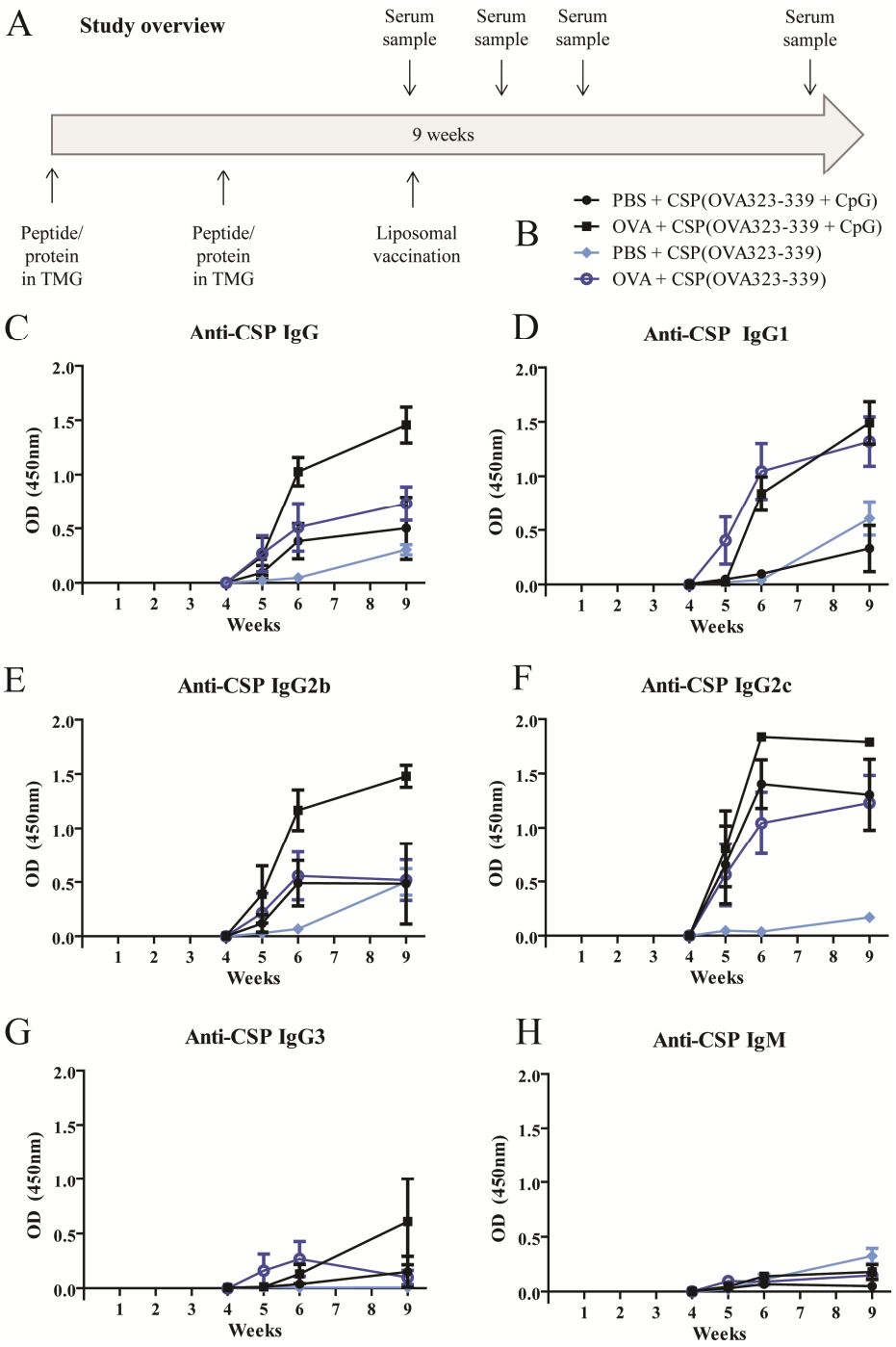


Figure 5.5. Anti-CSP responses to CSP(OVA323-339) and CSP(OVA323-339 + CpG) liposomes in mice pre-vaccinated with OVA323-339 or PBS in TMG. 6-8 week old female C57Bl/6 mice were administered two subcutaneous vaccinations of 10µg of OVA323-339 peptide or PBS emulsified in TMG adjuvant, with a two week interval between doses. Mice were then given a single subcutaneous dose of CSP(OVA323-339), or CSP(OVA323-339 + CpG) liposomes in 100µL as described in figure 5.3.A. Each vaccine dose contained 0.5 µg of CSP and, where indicated, 0.1 µg OVA323-339 +/- 0.1 µg CpG DNA (see section 2.9.7 for dosing calculations). Graphic (B) can be used for interpretation of all figures in this panel. The effect of pre-existing CD4+ T cell immunity and liposome-encapsulated TLR9 agonists on the developing total anti-CSP IgG antibody response was measured by ELISA over six weeks (C). The effect of pre-existing immunity and TLR9 agonists on the degree and speed of switching to different anti-CSP antibody isotypes (D-H) was also assessed by ELISA with biotinylated anti-isotype secondary antibodies (section 2.12.2). Mean responses were compared with two-way ANOVA and Bonferroni's post-test (n=4). For clarity, significant differences are not shown in this figure. Instead, key differences are discussed in the main text.

5.4. Chapter conclusions

1. It is possible to produce CSP-coated liposomal vaccine particles that contain both TLR9 agonists and MHCII epitopes. These encapsulated components are available for TLR9 binding and presentation to CD4+ T cells, respectively.

2. The inclusion of TLR9 agonists increases the magnitude of the anti-CSP antibody response.

3. TLR9 agonists drive the isotype of the developing anti-CSP antibody response towards the production of IgG2c, both in the presence and absence of pre-existing non-cognate CD4+ T cell immunity. This observation is in keeping with the literature that describes CpG DNA as driver of a T_H1-biased immune response.

4. The highest total anti-CSP responses, and responses with the greatest T_H1 bias, were seen in mice with pre-existing anti-OVA323-339 CD4+ T cell immunity subsequently vaccinated with CSP(OVA323-339 + CpG) liposomes.

5.5. Chapter discussion

5.5.1. Discussion of results

This chapter sought to build on previous work that had described a liposomal vaccine platform capable of delivering B cell activation signals one and two (BCR binding and CD4+ T cell help), but not signal three (TLR agonism). It was shown that pre-existing non-cognate CD4+ T cells could provide helper signals that enhanced B cell responses, but the effect of TLR agonism in this context was not known.

In this chapter, the TLR9 agonist CpG DNA was encapsulated with OVA323-339 MHCII epitopes in CSP-coated liposomal particles. First, a TLR9 reporter cell system was used to confirm that the synthesised CpG DNA oligonucleotide was capable of signalling through the murine TLR9 receptor. Next, encapsulated CpG DNA was shown to be active in this TLR9 reporter system and its inclusion did not adversely affect MHCII antigen processing in an ELISPOT assay. Stimulation of reporter cells with CpG-encapsulating liposomes was an important assay to confirm that CpG contained in liposomal preparations remained biologically active. However, in this context it is not clear whether reporter gene expression

in this assay system indicated leakage from the liposome and subsequent uptake by HEK-Blue-mTLR9 cells, or uptake and processing of CpG inside liposomal particles. As the parental HEK293 cell line is not derived from a professional phagocyte lineage, its processing of extracellular particles is unlikely to reflect the biology of immune cells *in vivo*.

Consequently, an *in vivo* pilot study was needed to determine whether particle-encapsulated CpG could signal through B cell TLR9 to meaningfully alter the anti-CSP response quantitatively and/or qualitatively. The data generated in this study supported the hypothesis that incorporating CpG DNA as a third signal in our vaccine regimen could augment antibody production to CSP. However, problems with this initial vaccination regimen were also evident. First, toxicity was encountered in the group administered two high doses of CSP(OVA323-339 + CpG) liposomal vaccine. A mean weight loss of 7% was apparent in the week following the first administration of liposomes that encapsulated CpG DNA. This adverse effect was not seen in other study groups and was not encountered in any group following the second vaccine dose. With this result in mind, it is interesting to consider how CSP-coated liposomal particles would be processed differently at the first and second vaccination time points. At the time mice receive a second dose, data show they have mounted a significant anti-CSP response. It is possible that particles administered at this time may be rapidly coated in antibody and that these opsonised particles are processed differently by the phagocytic cells of the immune system.

Data from this pilot study once again confirmed that pre-existing anti-OVA323-339 CD4+ T cell immunity could enhance anti-CSP responses following vaccination with CSP(OVA323-339). Additionally, there was preliminary evidence that the level of anti-CSP antibody produced was enhanced by encapsulating CpG DNA in the liposomal vaccine particle. This was not apparent at all time points, but the effect was significant at week 7. It was clear, however, that the inclusion of CpG DNA altered the isotype profile of the anti-CSP response. Incorporating CpG resulted in reduced production of the 'T_H2 isotype' IgG1 one week after the first liposomal vaccination; but levels were comparable at other time points. Simultaneously, CpG drove the production of more of the 'T_H1 isotype' IgG2c at all post-vaccination time points.

These preliminary findings were considered to be encouraging, but they also raised questions about whether the vaccine regimen used was optimally designed to detect TLR9-mediated effects. The high dose and the repeat administration of liposomal vaccines were considered to

be problematic both in terms toxicity and accurately quantifying CpG-mediated effects. For example, the second liposomal vaccination is likely to exploit both pre-existing CD4+ T cells raised by OVA323-339 + TMG vaccination, but also CD4+ T cell responses elicited by liposomal vaccination – particularly when the adjuvant CpG was included. These concerns, combined with data discussed in chapter four – where the liposomal dose was significantly reduced (section 4.3.10) – led to a repeat study with a single administration of a lower vaccine dose.

Using a hundred-fold lower vaccine dose, there was no appreciable weight loss or other toxicity. Clear evidence emerged that CpG could increase the magnitude of the anti-CSP antibody response. Additionally, the inclusion of CpG increased the production of anti-CSP antibodies with a T_H1-biased isotype profile, both in the presence and absence of pre-existing CD4+ T cell immunity. Significantly more IgG2c was produced in mice pre-vaccinated with OVA323-339 in TMG and then administered CSP(OVA323-339), but the level was highest when CSP(OVA323-339 + CpG) liposomes were administered. At this lower dose, the amount of IgG1 produced was determined by the presence or absence of pre-existing anti-OVA323-339 CD4+ T cell immunity, but was not affected by the inclusion of CpG in the liposomal particle. While CpG is known to drive IgG2a production (or its equivalent in C57Bl/6 mice, IgG2c), its effect on IgG2b is less well-established. In fact, it is not clear how IgG2b production fits with the simple T_H1/T_H2 isotype profile paradigm (Visciano et al. 2012). We found that the inclusion of CpG significantly increased IgG2b production, in keeping with previous studies of CpG-loaded VLPs (Visciano et al. 2012).

It is not clear from these data whether a T_H1 bias occurs because CpG is detected by the B cell itself, or indirectly through altered CD4+ T cell polarisation. It has been demonstrated that, in the presence of IFNγ, CpG DNA can act directly on B cells to drive isotype switching to IgG2a (Davis et al. 1998). It has also been shown that CpG DNA loaded into VLPs (Jegerlehner et al. 2007) can drive production of the T_H1 isotype IgG2a. Consequently, it is appealing to conclude that the TLR agonist cargo delivered to B cells by CSP-coated liposomal particles is able to directly alter the isotype profile of the developing anti-CSP response. Further, it is interesting to consider whether this approach could be used to reshape the antigen-specific humoral immune response in allergy. Allergen-coated vaccine particles that encapsulate CpG could act directly on allergen-specific B cells to drive production away from a T_H2-polarised response, with its associated IgE production, and towards isotypes that are not associated with allergy.

5.5.2. Limitations and future work

This chapter demonstrates that B cell activation signals one, two, and three can be delivered by a particle vaccine designed to exploit pre-existing, non-cognate CD4+ T cells. Particles designed to deliver all three signals elicit higher anti-CSP antibody responses with a T_H1 isotype profile. Future directions for this project could include more detailed analysis of the antibody response to CSP. This could be investigated with:

- Avidity studies, such as NaSCN dissociation or BiaCore surface plasmon resonance assays (Shi et al. 1999).
- Functional studies, such as *in vitro* inhibition of sporozoite invasion (Hollingdale et al. 1984).
- Or efficacy models, such as *in vivo* challenge with *Plasmodium bergheii* transgenic for the *Plasmodium falciparum* CSP (Persson et al. 2002).

Further, there is scope for a significant amount of work to optimise the immunogenicity of this platform. The CpG DNA oligonucleotide used in this project was synthesised with a phosphodiester backbone, whereas the commercially available oligonucleotide with the same sequence – ODN1826 – has a phosphorothioate backbone. This change confers nuclease resistance and increases the immunogenicity ten-fold (Krieg et al. 1995). This approach employed CpG DNA as a TLR9 agonist, but there are multiple TLRs expressed in B cells and the flexibility of this liposomal platform would allow the incorporation of multiple different TLR agonists. In particular, TLR2/6 and TLR7/8 agonists could all potentially enhance responses and agonists could either be incorporated in the lipid bilayer or the fluid-phase core of the liposomal particle (Bekeredjian-Ding & Jego 2009).

An optimised platform could be taken forward to target more challenging vaccine targets, such as cancer antigens (see chapter seven). Other approaches would be to produce multiple liposomal vaccine constructs each with same MHCII epitope and TLR agonist core components, but with different B cell epitopes on their surface. These could then be mixed and administered where they may be able to stimulate different B cells to respond in germinal centres, while exploiting the same CD4+ T_{FH} cell signals. This would allow one powerful, pre-existing, non-cognate CD4+ T cell population to support antibody responses to multiple target antigens.

6. Exploiting pre-existing anti-viral immunity to provide non-cognate T cell help

6.1. Introduction

In chapters four and five, CD4+ T cell immunity produced by vaccination against ovalbumin epitopes was exploited to enhance responses to the model B cell antigen, CSP. Here, TCR transgenic and murine cytomegalovirus (MCMV)-infected mice were examined as other sources of pre-existing, non-cognate CD4+ immunity.

This chapter first studied the utility of non-cognate CD4+ T cell help in the context of a TCR transgenic mouse model. The OT-II mouse strain expresses murine alpha and beta chains of a TCR that is specific for OVA323-339 in the context of H2-IAb and the majority of CD4+ T cells bear this transgenic TCR (Barnden et al. 1998). CSP-coated liposomes incorporating OVA323-339 were used to vaccinate OT-II mice and the developing anti-CSP response was measured.

Next, cytomegalovirus infection was evaluated as a model of pre-existing, non-cognate CD4+ T cell help with more translational relevance. The majority of the human population are chronically infected with HCMV, though rates vary with geography and detection methodology. Seroprevalence increases with age from 36% in 6–11-year-olds to 90.8% in those over 80 years old (Staras et al. 2006).

In chronic HCMV infection, a significant proportion of the CD8+ and CD4+ T cell pools recognise viral antigen. Approximately one third of infected adults have HCMV-specific cell populations comprising >20% of their circulating CD4+ and/or CD8+ memory T cell repertoire. Memory CD8+ responses can be oligoclonal and inflationary; up to 23% of CD8+ T cells from a healthy seropositive donor have been reported to recognise just one viral epitope (Khan et al. 2002). Approximately 5% of the CD4+ T cell pool is directed against HCMV epitopes in healthy seropositive individuals, but this can be as high as 40% (H. S. Dunn et al. 2002)(Harcourt et al. 2006)(Sester et al. 2002). Individual clones can represent 0.3-1.5% of the total peripheral CD4+ T cell population (Weekes et al. 2004). The number of HCMV-specific CD4+ T cells increases markedly in the elderly (H. S. Dunn et al. 2002).

These cells have a memory phenotype and secrete the T_H1 cytokines IFNγ and TNFα (Vescovini et al. 2007)(Sester et al. 2002).

MCMV is a widely used murine model for HCMV and infection with MCMV leads to lifelong latency with sporadic, low level replication (Simon et al. 2006). This viral replication is controlled by CD8+ and CD4+ T cell responses (Simon et al. 2006)(Walton et al. 2013)(Sims & Klenerman 2014). In chronic MCMV infection, CD4+ and CD8+ T cell responses are also inflationary, with up to 20% of CD8+ T cells recognising one MCMV epitope one year after infection (Karrer et al. 2003). Clonal inflationary CD4+ T cell responses of the same magnitude seen with anti-viral CD8+ T cells have not been identified for MCMV (Walton et al. 2008), but the CD4+ T cell response to the $m09_{133-147}$ epitope (here referred to as m09) was described as inflationary (Arens et al. 2008). While responses to m09 immediately after infection were undetectable, by day 40, 0.21% of the peripheral CD4+ T cell population produced IFNγ in response to m09 stimulation. At 100 days, this had fallen to 0.11%, but many of these cells were polyfunctional, also producing TNFα or IL-2.

In this chapter, anti-MCMV immunity was studied – with a focus on CD4+ T cell responses to the m09 epitope. CSP-coated liposomes containing this m09 epitope were produced, characterised, and then used to vaccinate MCMV-infected mice. The effect of MCMV-infection on the magnitude and isotype on the developing anti-CSP antibody response was evaluated. The ability of the TLR9 agonist CpG DNA to enhance the anti-CSP antibody response in the context of pre-existing anti-viral CD4+ T cells was also examined.

6.2. Chapter aims

1. Evaluate TCR transgenic and murine cytomegalovirus (MCMV) infected mice as sources of non-cognate, CD4+ T cell help to support anti-CSP antibody responses

2. Measure the effect of anti-viral CD4+ T cells on the magnitude of the anti-CSP antibody response

3. Measure the effect of anti-viral CD4+ T cells on the isotype of the anti-CSP antibody response

4. Assess the effect of particle-encapsulated TLR9 agonists on the magnitude and isotype of the anti-CSP antibody response in the context of pre-existing anti-MCMV CD4+ T cell help.

6.3. Results

6.3.1. Evaluating OT-II transgenic mice as a source of anti-OVA323-339 CD4+ T cells to support anti-CSP antibody responses

OT-II transgenic mice were evaluated as a source of non-cognate CD4+ T cell help that could support anti-CSP responses following the administration of liposomal vaccines described in chapters four and five. OT-II transgenic mice were pre-vaccinated with PBS or OVA323-339 peptide in TMG prior to liposomal vaccination. Higher anti-CSP responses to CSP(OVA323-339) liposomes were only observed in mice pre-vaccinated with OVA323-339 (figure 6.1).

Higher anti-CSP responses to liposomal particle vaccination in OTII transgenic mice are dependent on pre-vaccination with OVA323-339 epitopes in TMG

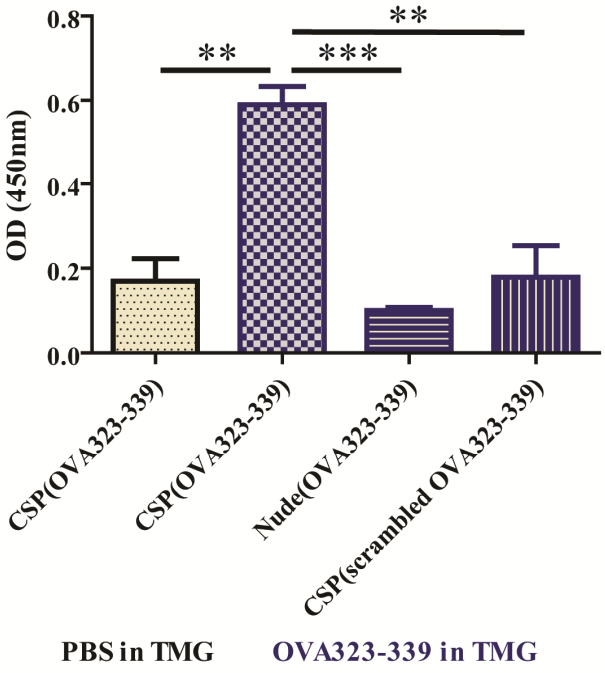


Figure 6.1. Vaccine responses in OT-II mice. Anti-CSP responses to CSP(OVA323-339), Nude(OVA323-339), or CSP(scrambled OVA323-339) liposomes in OT-II mice pre-vaccinated with either OVA323-339 or PBS in TMG. 6-8 week old female OT-II mice were administered two subcutaneous vaccinations of 10 µg of OVA323-339 peptide (blue bars) or PBS (black bars) emulsified in TMG adjuvant, with a two week interval between doses. Mice were then given one 100 µL subcutaneous dose of CSP(OVA323-339) liposomes or CSP(scrambled OVA323-339) liposomes, each containing 50 µg of CSP and 10µg of OVA323-339 or scrambled OVA323-339 (for dose calculations, see section 2.9.7). An additional control group were vaccinated with maleimide-free that do not have surface conjugated CSP denoted as 'nude(OVA323-339)'. Two weeks after liposomal vaccination, serum was taken and anti-CSP antibody response was measured by ELISA at a serum dilution of 1:200. Means were compared by one-way ANOVA with Tukey's post-test (n=3).

6.3.2. Production of liposomes containing the immunodominant murine cytomegalovirus MHCII epitope

To test whether anti-viral CD4+ T cells could be co-opted to support responses against non-cognate antigens, CSP-coated liposomal vaccine particles containing the immunodominant MHCII epitope of MCMV were produced. The solubility of m09 demanded that a HEPES buffer (pH 8.2) was used during the production of these liposomes. Analysis by DLS confirmed that liposomal particles of comparable size to those used in chapters three and four could be produced by this method (figure 6.2.A), and dot blot studies demonstrated that CSP could be conjugated to the surface of these particles (figure 6.2.B).

DLS profile and anti-CSP dot blot of liposomal preparations for exploiting pre-existing anti-viral immunity

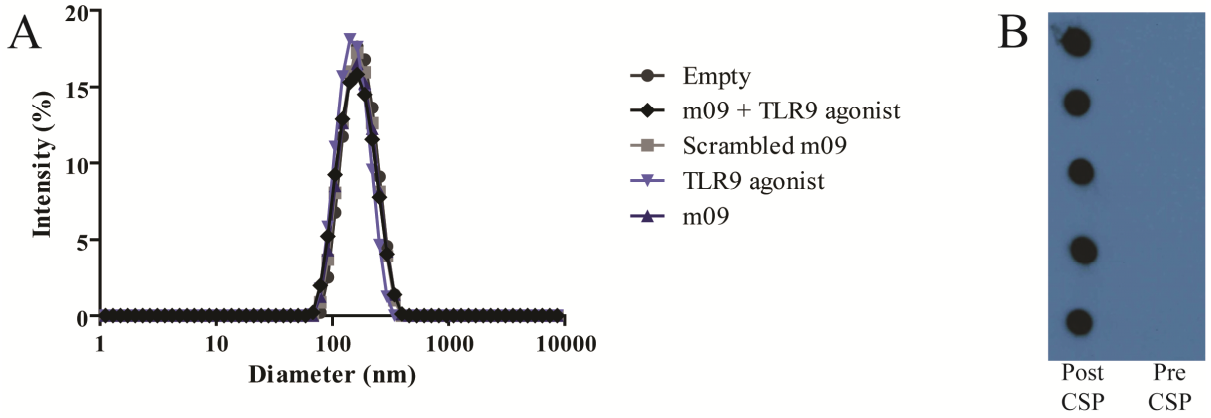


Figure 6.2. Characterisation of liposomal particles containing MCMV epitopes. The diameter of five preparations of liposomes diluted 1:50 in PBS was assessed by DLS (A). Liposome preparations were either empty or encapsulated m09, scrambled m09, CpG, or m09 and CpG. The presence of surface-conjugated CSP was then confirmed by dot blot against the CSP antigen (B).

6.3.3. Characterising the immune response of MCMV-infected mice

Prior to liposomal vaccination studies, it was important to further characterise the existing immune response to MCMV – with a particular focus on CD4+ T cell immunity and the m09 epitope.

MHC class I tetramers have been established to study the evolving anti-MCMV immune response and here these were employed to confirm that all mice were infected by i.v. injection of MCMV. Two tetramers were used – one recognising the acutely elevated m45 epitope and another recognising the inflationary m38 epitope. Blood was taken three weeks after infection (see figure 6.6.A) and m45 and m38-positive CD8+ T cells were enumerated. Considerably higher numbers of m45 and m38-positive cells were evident in MCMV-

infected mice (figure 6.3.A and 6.3.B). Representative gates for uninfected (figure 6.3.C and 6.3.D) and infected mice (figure 6.3.E and 6.3.F) are shown. The magnitude of the response to the inflationary m38 epitope was significantly higher than the m45 epitope (mean 9.67 vs 1.34, $p < 0.0001$ [unpaired, two-tailed t test]). This is in keeping with published data describing a rapid expansion and contraction of m45 CD8 T cells post-infection (Walton et al. 2011).

IFNγ and IL-4 ELISPOT assays were used to characterise the T_H1 and T_H2 profile of the CD4+ T cell response to MCMV. IFNγ responses to MCMV lysate and the m09 epitope were readily detectable in MCMV eight weeks after infection (figure 6.4.A). In contrast, IL-4 responses were detected when splenocytes were pulsed with the m09 epitope, but not MCMV lysate (figure 6.4.B). Comparing data on splenocytes stimulation with the m09 epitope presented in figures 6.4.A and 6.4.B revealed that IFNγ responses to were higher than IL-4 responses in MCMV infected mice ($p<0.05$).

To characterise anti-MCMV immunity in our model further, the anti-MCMV antibody response was studied 10 and 50 days after infection. Anti-MCMV antibody responses of all isotypes measured were higher in infected mice when compared with uninfected controls. Higher IgM responses were detected at 10 days (figure 6.5.A), but not at 50 days post infection, where IgG responses dominated (figure 6.5.B). The individual IgG isotypes produced against MCMV were also measured (figure 6.5.C and 6.5.D) and increased with time. To better allow comparison between isotypes detected using different anti-isotype antibodies, standard curves similar to those shown previously (figure 4.4.A) were generated to allow quantification and comparison of IgG1 and IgG2c responses (figure 6.5.E). The quantity of anti-MCMV IgG2c produced was significantly higher than the level of anti-MCMV IgG1 at both day 10 and day 50 post-infection (figure 6.5.E). The mean ratio of IgG1:IgG2c was 0.00634 (sd = 0.00283) at 10 days post-infection and 0.0150 (sd = 0.000466) 50 days post-infection. Together, these data support heavily TH1-dominated anti-MCMV immune response.

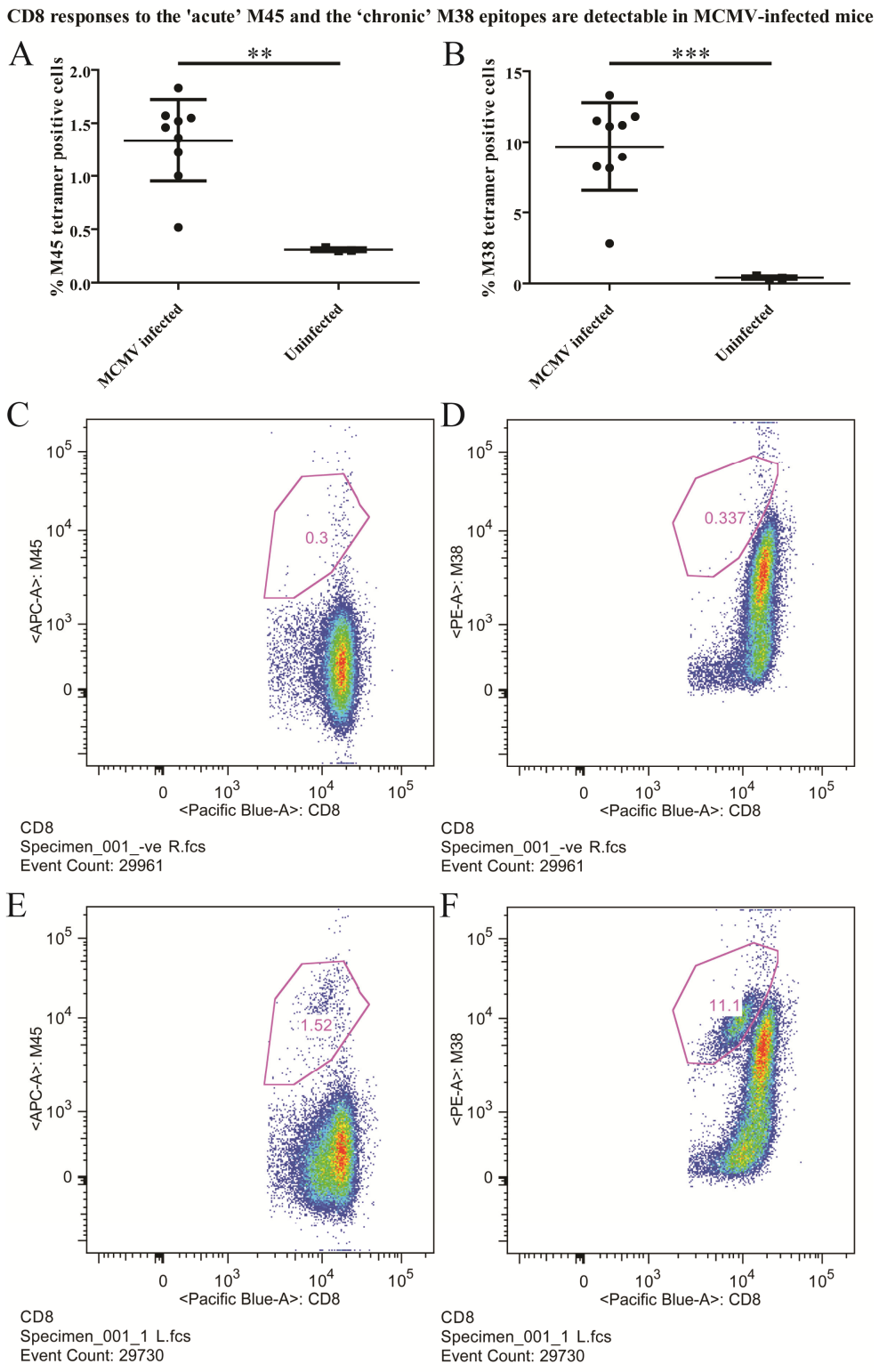
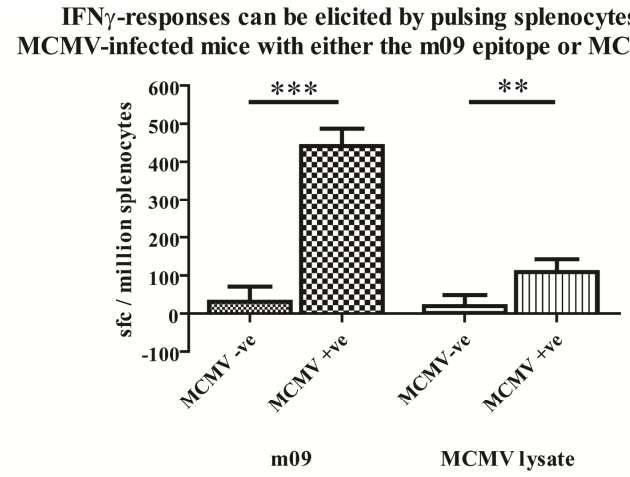


Figure 6.3. Flow cytometric analysis of CD8 T cell responses to MCMV three weeks post-infection. 6-8 week old female C57Bl/6 mice were administered $1x10^5$ pfu of MCMV i.v. Three weeks later, peripheral blood samples were taken and numbers of M38 and m45 tetramer-positive CD8+ T cells were counted by flow cytometry (section 2.11.4). All mice administered MCMV mounted a readily detectable response to either M38 or m45. The points indicating the lowest number of tetramer-positive cells in the MCMV-infected group shown on graphs (A) and (B) do not represent the same animal. The proportion of CD8+ cells that were gated as tetramer-positive is indicated for m45 (C) and M38 (D) in uninfected mice, and for m45 (E) and m38 (F) in infected mice.

A



B

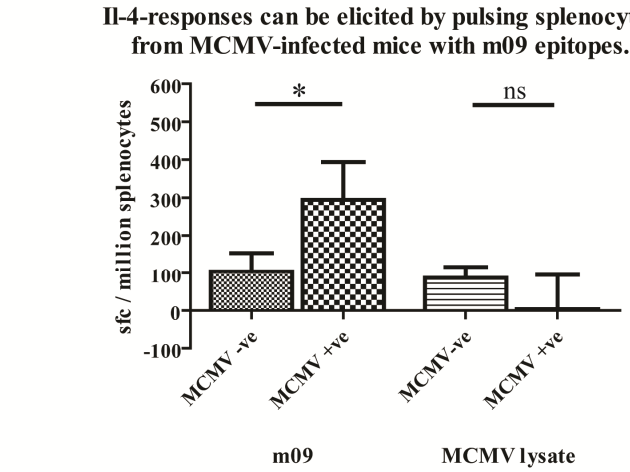


Figure 6.4. ELISPOT analysis of anti-MCMV CD4+ T cell responses. Eight weeks after female 6-8 week old C57Bl/6 mice were infected with $1x10^5$ pfu of MCMV i.v. (n=9), splenocytes were harvested and stimulated with either the m09 epitope or MCMV lysate at a final concentration of 1 µg/mL and 10 µg/mL, respectively. Splenocytes from uninfected controls (n=3) were also harvested and subjected to the same stimulation. 36 hours later, cellular responses to IFNγ and IL-4 were measured by ELISPOT and are represented here as spot forming colonies per million splenocytes. Mean responses in infected and uninfected mice were compared with unpaired, two-tailed t tests. Additionally, the IFNγ and IL-4 responses to m09 in infected mice – displayed here in graph (A) and graph (B) were compared with unpaired, two-tailed t tests.

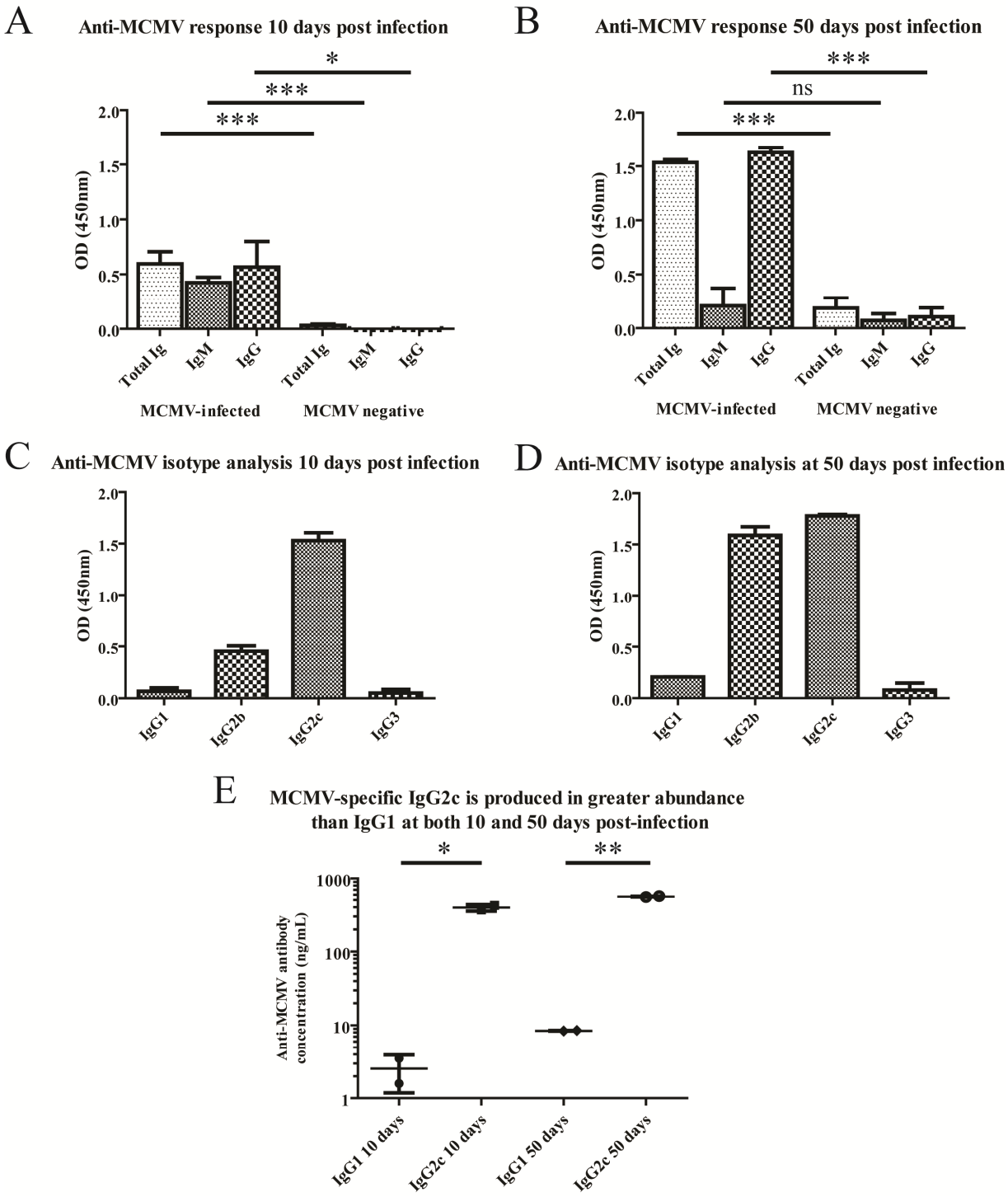


Figure 6.5. Characterisation of the antibody response to MCMV infection. The anti-MCMV antibody response was assessed by ELISA (sections 2.12.1 and 2.12.2). 10 days and 50 days post infection, serum samples were obtained from infected mice and uninfected controls. Anti-MCMV total Ig, IgM, and IgG was measured at day 10 (A) and day 50 (B). The individual IgG isotypes IgG1, IgG2b, IgG2c, and IgG3 were also measured at day 10 (C) and day 50 (D). Mean responses in infected and uninfected mice (n=2 per group) were compared with unpaired, two-tailed t tests where variances were equal (graphs A and B) and Welch's t test where variances were unequal (graph E).

6.3.4. Pilot *in vivo* studies exploiting anti-MCMV CD4+ T cell help to enhance anti-CSP responses

After establishing a protocol for generating pre-existing anti-MCMV immunity, mice were vaccinated with CSP-coated liposomes containing the m09 epitope. Eight weeks after infection, mice were administered a single dose of subcutaneous liposomal vaccine containing 50µg of CSP and 10µg m09 (figure 6.6.A). The developing anti-CSP antibody response was compared in MCMV-infected and uninfected mice. MCMV-infected mice mounted significantly higher anti-CSP antibody responses at the nine ($p<0.001$), 10 ($p<0.001$), and 12 ($p<0.001$) week time points (figure 6.6.B).

The isotype of anti-CSP antibodies produced in infected and uninfected mice following vaccination with CSP(m09) liposomes was then compared. Anti-CSP IgG (figure 6.7.A) followed a similar pattern to total anti-CSP immunoglobulin, with significant differences between infected and uninfected groups at all time points ($p<0.001$). Anti-CSP IgG1 was higher in infected mice at week nine of the study ($p<0.001$) but there was no difference at later time points (figure 6.7.B). In contrast, anti-CSP IgG2c levels (figure 6.7.D) were only seen at high levels in infected mice, and significant differences were noted at nine ($p<0.05$), 10 ($p<0.001$), and 12 ($p<0.001$) week time points. Anti-CSP IgG2b and IgG3 levels were not different between groups (figures 6.7.C and 6.7.E). In contrast, anti-CSP IgM levels were higher in MCMV infected mice at early time points ($p<0.001$), but were similar by week 12 of the study (figure 6.7.F).

This pilot *in vivo* study included two additional control groups: infected and uninfected mice vaccinated with liposomes encapsulating a scrambled variant of the m09 epitope. The anti-CSP response to CSP-coated liposomes containing this scrambled m09 epitope were measured across the course of the study and are superimposed on the responses to liposomes containing the wild-type m09 epitope in figure 6.8. MCMV-infected mice initially mounted comparable anti-CSP responses to liposomes containing either the scrambled or wild-type variant of m09 ($p>0.05$ at week 9). However, as the study progressed, higher responses were evident in the group vaccinated with CSP(m09) at week 10 ($p<0.05$) and week 12 ($p<0.001$). There was a trend for uninfected mice administered CSP(scr m09) liposomes to mount the lowest anti-CSP responses, when compared with uninfected mice administered CSP(m09) liposomes. This reached statistical significance at week 12 ($p<0.05$).



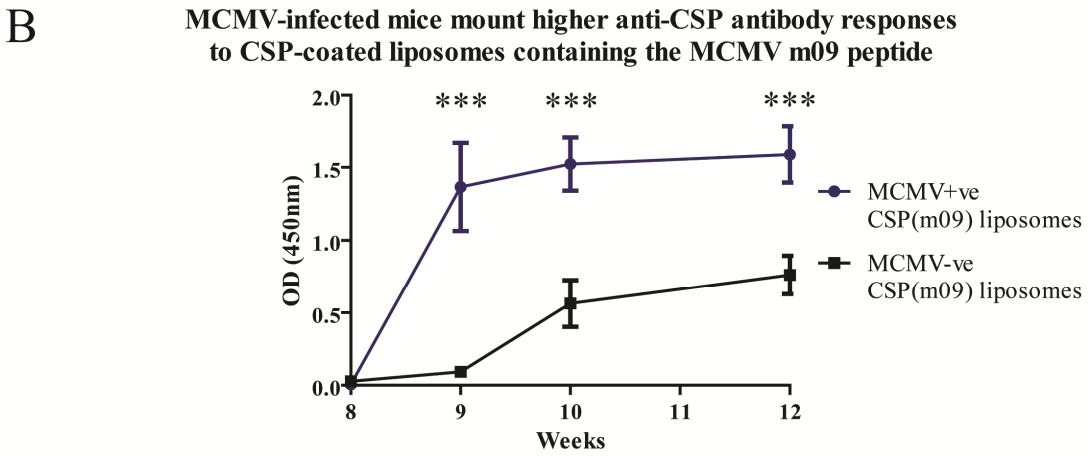


Figure 6.6. Pilot *in vivo* study to characterise the anti-CSP response to CSP(m09) liposomes in uninfected and MCMV-infected mice. Female 6-8 week old C57Bl/6 mice were infected with MCMV or housed as uninfected controls. Eight weeks later, both groups were vaccinated subcutaneously with CSP(m09) liposomes containing 50 µg of CSP and 10µg m09 (see section 2.9.7 for dosing calculations) in 100 µL volumes (A). Serum was collected at weeks 9, 10, and 12. The anti-CSP antibody response was measured by ELISA (B). Mean OD levels (+/- SEM) are displayed. Means were compared using two-way ANOVA with Bonferroni's post-test (n=4).

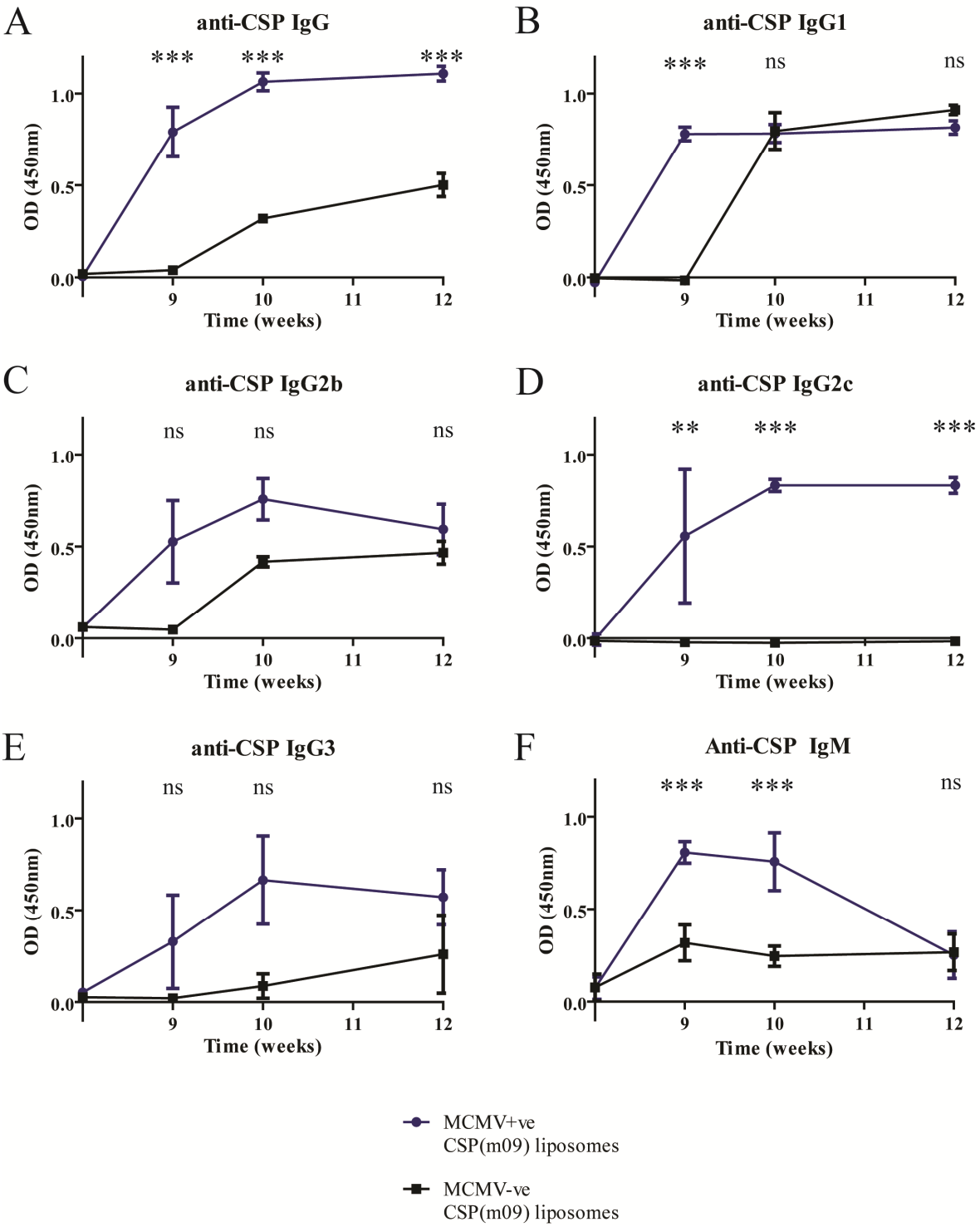


Figure 6.7. Analysis of the isotype profile of anti-CSP antibodies elicited by CSP(m09) liposome vaccination in uninfected and MCMV-infected mice. Female 6-8 week old C57Bl/6 mice were infected with MCMV or housed as uninfected controls. Eight weeks later, both groups were vaccinated subcutaneously with CSP(m09) liposomes containing 50 µg of CSP and 10 µg m09 (see section 2.9.7 for dosing calculations) in 100 µL volumes (as set out in figure 6.6.A). Serum was collected at weeks 9, 10, and 12. The effect of MCMV infection on the degree and speed of switching to IgG was measured (A). Additionally, the effect of MCMV infection on different anti-CSP antibody isotypes (B-F) was assessed by ELISA with biotinylated anti-isotype secondary antibodies, as described in section 2.12.2. Mean OD levels (+/- SEM) are displayed. Means were compared using two-way ANOVA with Bonferroni's post-test (n=4).

Anti-CSP response in MCMV-infected and uninfected mice vaccinated with CSP-coated liposomes containing either the MCMV m09 peptide or a scrambled control peptide

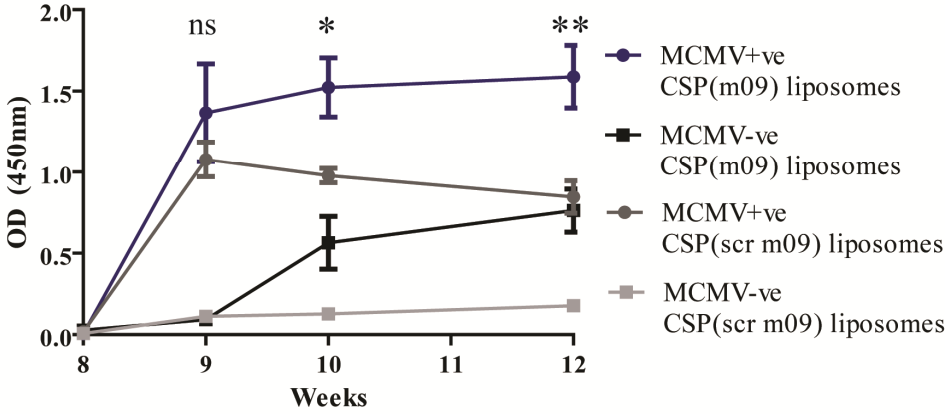


Figure 6.8. Comparison of anti-CSP responses to CSP(m09) and CSP(scr m09) liposomes in uninfected and MCMV-infected mice. Female 6-8 week old C57Bl/6 mice were infected with MCMV or housed as uninfected controls. Eight weeks later, both groups were vaccinated subcutaneously with CSP(m09) liposomes or CSP(scr m09) liposomes containing 50 µg of CSP and 10 µg m09 or scrambled m09 (see section 2.9.7 for dosing calculations) in 100 µL volumes (as set out in figure 6.6.A). Serum was collected at weeks 9, 10, and 12. The anti-CSP antibody response was measured by ELISA (B). Datasets in blue and black represent the infected and uninfected groups vaccinated with CSP(m09) liposomes that are also detailed in figure 6.6.B. In this figure, anti-CSP ELISA data from MCMV-infected and uninfected mice vaccinated with CSP(scr m09) liposomes are superimposed for comparison. Mean OD levels (+/- SEM) are displayed. Means were compared using two-way ANOVA with Bonferroni's post-test (n=4). For clarity, statistical significance is only shown for the comparison between mean responses in the MCMV+ve CSP(m09) liposome vaccinated group (shown in blue) and the MCMV+ve CSP(scr m09) liposome vaccinated group (shown in dark grey).

6.3.5. *In vivo* studies to characterise the effect of anti-MCMV CD4+ T cell immunity and TLR9 agonism on anti-CSP responses

Pilot studies performed in section 6.3.4 suggested that pre-existing CD4+ T cells raised against the m09 epitope by chronic infection with MCMV could support higher anti-CSP responses than seen in uninfected mice. To confirm this finding, a repeat study with a lower vaccine dose and additional control groups was performed.

Information garnered from figure 4.13 indicated that, in the context of pre-existing anti-OVA323-339 immunity, lower doses of CSP-coated liposomal vaccine particles could be used without a significant reduction in anti-CSP response. Guided by this dosing information from the OVA323-339 pre-vaccination model, a 100-fold lower dose of liposomal vaccine than was used in section 6.3.4 was administered to mice. An additional formulation of CSP(empty) liposomes was included to assess if the scrambled m09 epitope – despite containing no predicted H2-IAb epitopes – could harness CD4+ T cell help in MCMV-infected mice. To evaluate whether anti-CSP responses were affected by the inclusion of TLR9 agonists, two additional liposomal preparations were generated: CSP(m09 + CpG) liposomes and CSP(CpG) liposomes.

Responses to CSP were higher in MCMV-infected compared to uninfected mice when liposomal particles contained the m09 epitope – CSP(m09) liposomes and CSP(m09 + CpG) liposomes – figure 6.9.A and 6.9.C. Total anti-CSP responses were low and comparable in infected and uninfected mice for each of the remaining control groups – CSP(scr m09), CSP(empty), and CSP(CpG) liposomes – figures 6.9.B, 6.9.D, and 6.9.E.

The isotype of anti-CSP antibodies produced in infected and uninfected mice following vaccination with CSP(m09) liposomes was then compared. Anti-CSP IgG (figure 6.10.A) followed a similar pattern to total anti-CSP immunoglobulin, with significant differences between infected and uninfected groups at both the 10 day ($p<0.001$) and 20 day ($p<0.001$) time points. Anti-CSP IgG1 was higher in infected mice at 10 days ($p<0.001$) and 20 days ($p<0.001$) post-vaccination ($p<0.01$) (figure 6.10.B). Anti-CSP IgG2b (figure 6.10.C) and IgG2c levels (figure 6.10.D) were higher in infected mice, with significant differences noted at 10 days ($p<0.001$) and 20 days ($p<0.001$) post vaccination. Anti-CSP IgG3 and IgM levels were higher in MCMV infected mice at the earlier time point ($p<0.05$), but were similar by day 20 (figure 6.10.E and 6.10.F).

The role of CpG DNA incorporated alongside m09 in CSP(m09 + CpG) liposomes was evaluated in MCMV-infected and uninfected mice. Both MCMV-infected and uninfected mice mounted high IgG2c responses (figure 6.11.D) and relatively low IgG1 responses (figure 6.11.B) when vaccinated with CSP(m09 + CpG) liposomes. By 20 days post-vaccination, IgG2c responses were higher in MCMV-infected mice when compared with uninfected controls ($p<0.05$), but levels were comparable at the earlier day 10 time point. This finding is in contrast to the low IgG2c responses seen in the absence of CpG (figure 6.10.D). In keeping with data generated using CSP(m09) liposomes, MCMV-infected mice mounted higher anti-CSP IgG2b responses at all post-vaccination time points (figure 6.11.C). IgG3 and IgM responses were also higher in MCMV-infected mice (figures 6.11.E and 6.11.F).

To evaluate the ability of CpG to enhance responses in MCMV-infected mice, data from MCMV-infected groups in figures 6.10 and 6.11 were compared. The inclusion of CpG DNA enhanced the anti-CSP IgG response at day 20 post-vaccination ($p<0.05$). Anti-CSP IgG2b responses were increased by the inclusion of CpG DNA 10 days ($p<0.05$) and 20 days ($p<0.01$) post-vaccination. However, anti-CSP IgG2c responses were not affected by the inclusion of CpG. Anti-CSP IgG1 levels were lower in MCMV-infected mice vaccinated with CSP(m09 + CpG) at day 10 ($p<0.01$) and day 20 ($p<0.01$) post-vaccination.

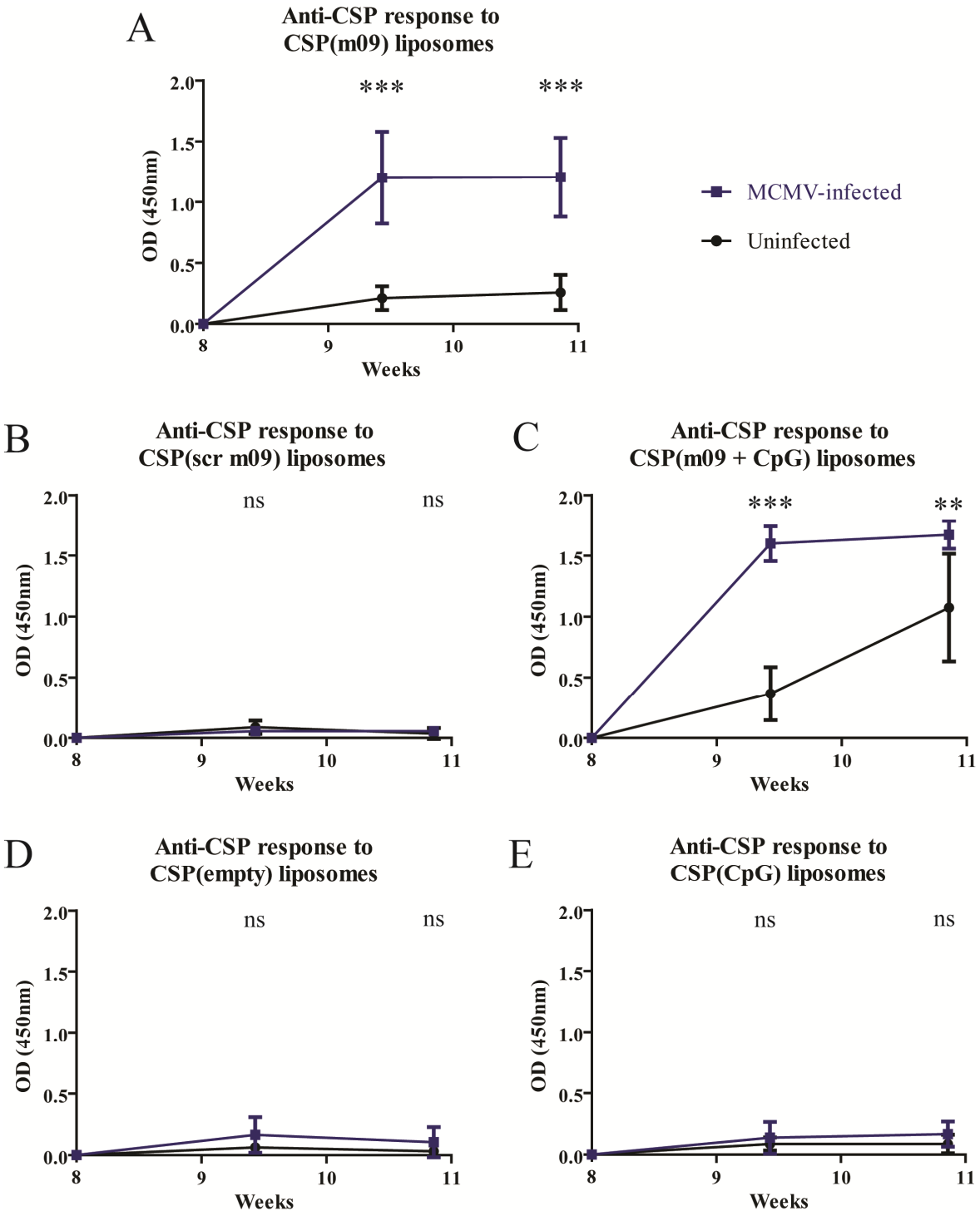


Figure 6.9. Anti-CSP responses to lower dose vaccination with CSP(m09), CSP(scr m09), CSP9(m09 + CpG), CSP(empty), and CSP(CpG) liposomes in uninfected and MCMV-infected mice. Female 6-8 week old C57Bl/6 mice were infected with MCMV or housed as uninfected controls. Eight weeks later, infected and uninfected groups were vaccinated subcutaneously with CSP(m09), CSP(scr m09), CSP(m09 + CpG), CSP(empty), or CSP(CpG) liposomes containing 0.5 µg of CSP and, where indicated, 0.1 µg m09 or scrambled m09 and/or 0.1 µg CpG DNA (see section 2.9.7 for dosing calculations) in 100 µL volumes. Serum was collected at before liposomal vaccination and at days 10 and 20 after it. The effect of MCMV-infection on the production of anti-CSP immunoglobulin was measured by ELISA for each vaccine formulation (A-E). For each formulation, mean OD levels (+/- SEM) are displayed. Means were compared between MCMV-infected and uninfected groups using two-way ANOVA with Bonferroni's post-test (n=4).

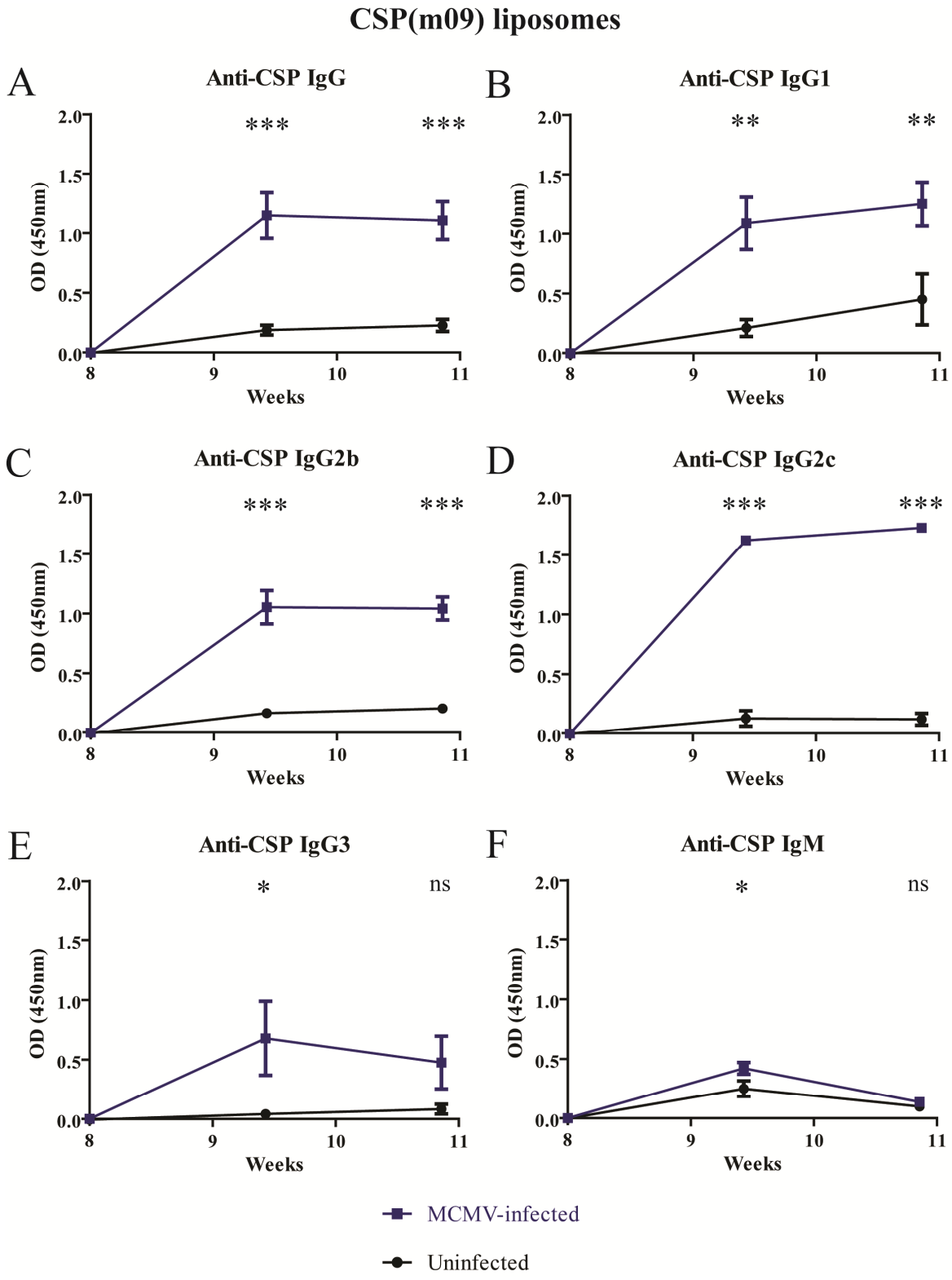


Figure 6.10. Analysis of the isotype profile of anti-CSP antibodies elicited by low dose CSP(m09) liposome vaccination in uninfected and MCMV-infected mice. Female 6-8 week old C57Bl/6 mice were infected with MCMV or housed as uninfected controls. Eight weeks later, both groups were vaccinated subcutaneously with CSP(m09) liposomes containing 0.5 µg of CSP and 0.1 µg m09 (see section 2.9.7 for dosing calculations) in 100 µL volumes. The effect of MCMV infection on the degree and speed of switching to IgG was measured (A). Additionally, the effect of MCMV infection on different anti-CSP antibody isotypes was assessed (B-F). Mean OD levels (+/- SEM) are displayed. Means were compared using two-way ANOVA with Bonferroni's post-test (n=4).

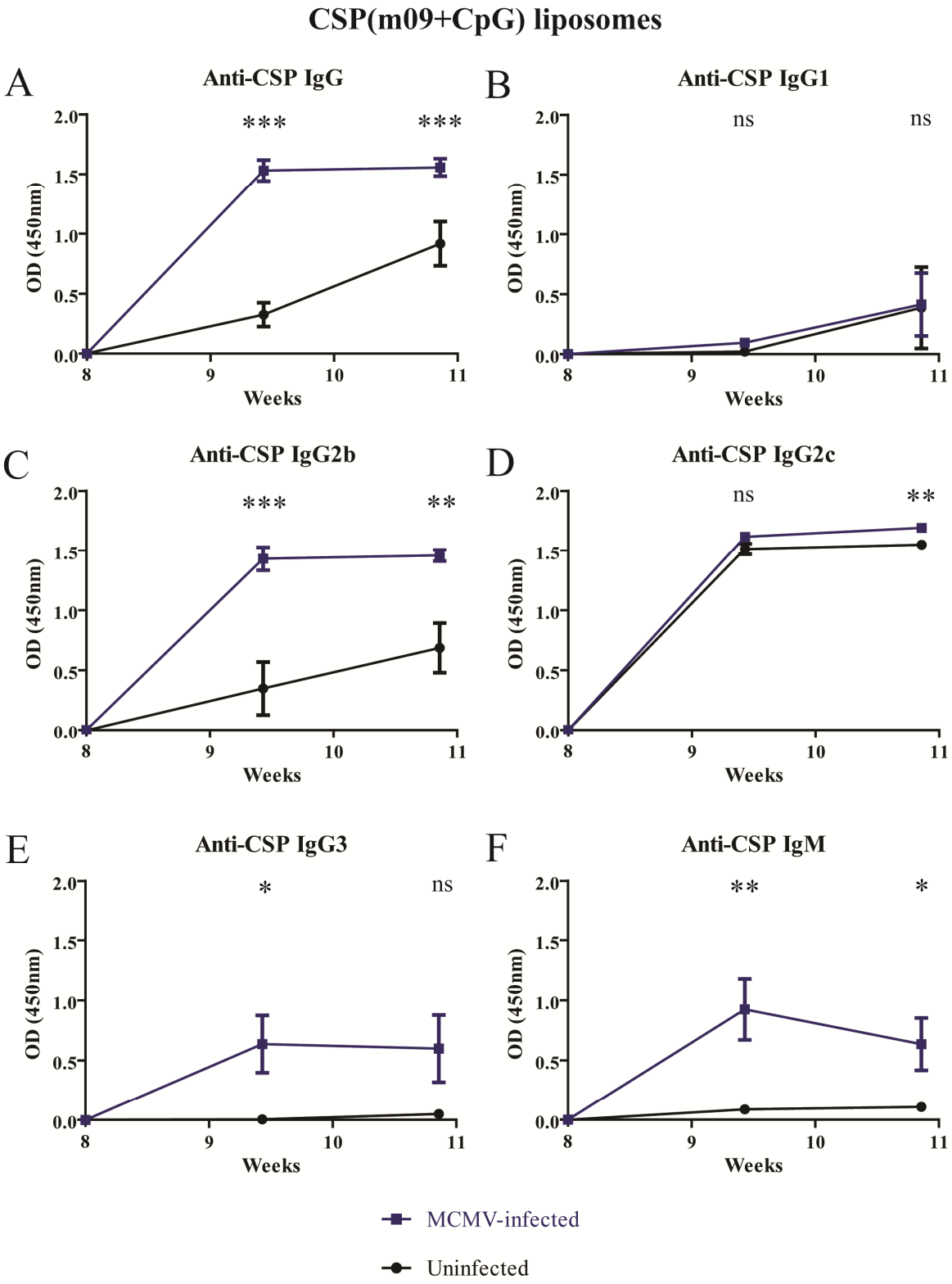


Figure 6.11. Analysis of the isotype profile of anti-CSP antibodies elicited by low dose CSP(m09 + CpG) liposome vaccination in uninfected and MCMV-infected mice. Female 6-8 week old C57Bl/6 mice were infected with MCMV or housed as uninfected controls. Eight weeks later, both groups were vaccinated subcutaneously with CSP(m09 + CpG) liposomes containing 0.5 µg of CSP, 0.1 µg m09, and 0.1 µg of CpG DNA (see section 2.9.7 for dosing calculations) in 100 µL volumes. The effect of MCMV infection on the degree and speed of switching to IgG was measured (A). Additionally, the effect of MCMV infection on different anti-CSP antibody isotypes was assessed (B-F). Mean OD levels (+/- SEM) are displayed. Means were compared using two-way ANOVA with Bonferroni's post-test (n=4).

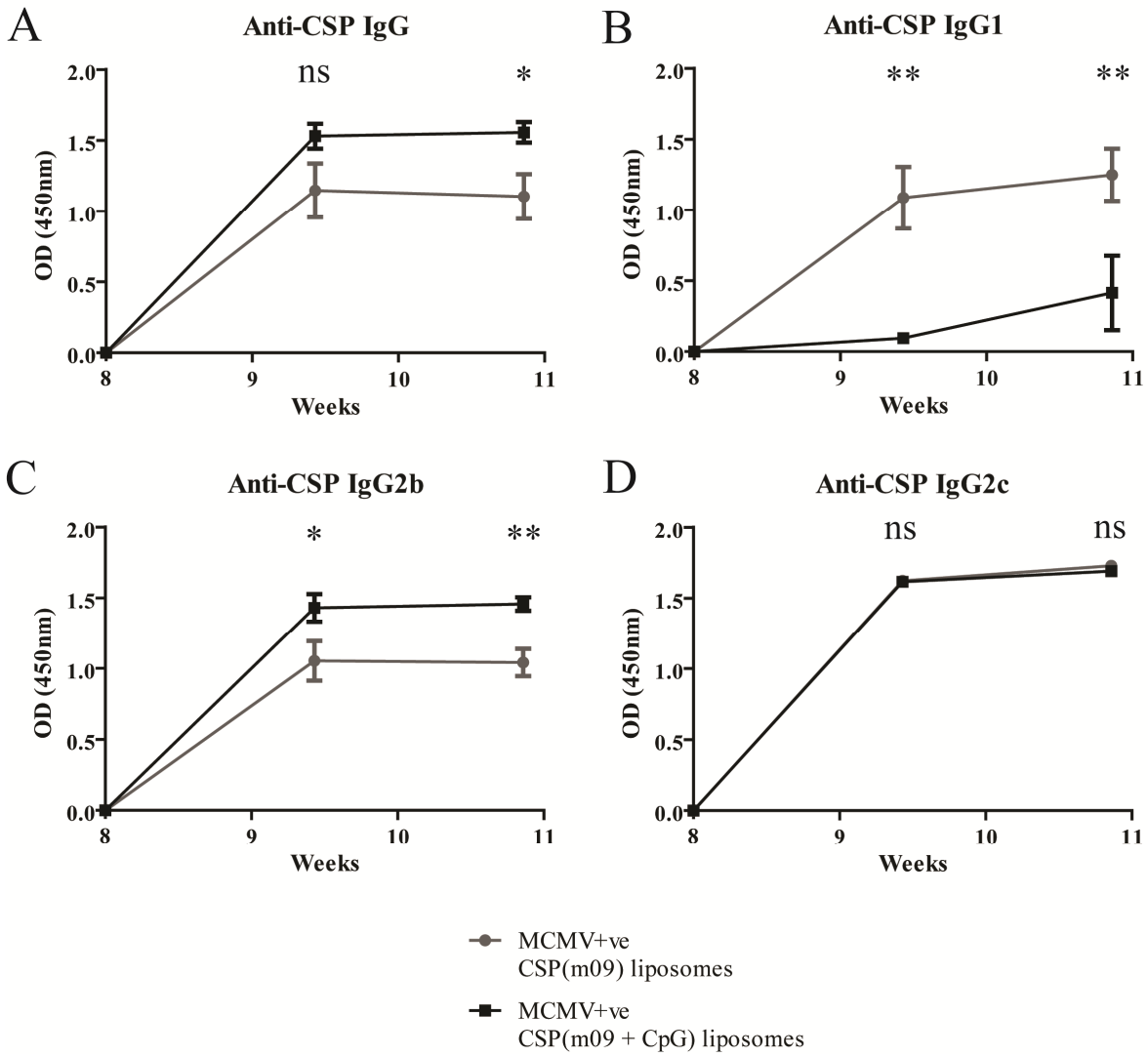


Figure 6.12. Comparison of anti-CSP responses elicited by low dose vaccination with CSP(m09) or CSP(m09 + CpG) liposomes in MCMV-infected mice. Female 6-8 week old C57Bl/6 mice were infected with MCMV. Eight weeks later, infected mice were vaccinated subcutaneously with either CSP(m09) or CSP(m09 + CpG) liposomes containing 0.5 µg of CSP, 0.1 µg m09, and where indicated 0.1 µg of CpG DNA (see section 2.9.7 for dosing calculations) in 100 µL volumes. The effect of CpG DNA on the production of anti-CSP IgG (A), IgG1 (B), IgG2b (C) and IgG2c (D) was assessed. Mean OD levels (+/- SEM) are displayed. Means were compared using two-way ANOVA with Bonferroni's post-test (n=4).

6.4. Chapter conclusions

1. OT-II TCR transgenic mice and C57Bl/6 mice infected with MCMV were studied as other models of pre-existing non-cognate CD4+ T cell help. In both models, pre-existing activated CD4+ T cells could enhance anti-CSP responses to CSP-coated liposomal particle vaccines containing the relevant CD4+ epitope.

2. Mice chronically infected with MCMV mounted higher antibody responses to CSP(m09) liposomes than uninfected controls, indicating that anti-viral immunity could be co-opted to enhance vaccine responses.

3. In MCMV-infected mice, the anti-CSP antibody response to CSP(m09) was generated faster, reached higher levels, and contained more isotype switched antibody than in uninfected controls. IgG2c isotypes were more prevalent than IgG1, indicating a T_H1-biased response to CSP(m09) particles in MCMV-infected mice.

4. In MCMV-uninfected mice, particle-encapsulated TLR9 agonists increased the magnitude of the overall anti-CSP antibody response and drove this towards a T_H1 isotype profile. When combined with the MHCII epitope m09 to exploit T_H1-biased anti-viral CD4+ T cells, the inclusion of CpG enhanced total anti-CSP responses. However, CpG did not increase the already high levels of the 'T_H1 isotype' IgG2c. Instead, CpG drove the production of more IgG2b.

6.5. Chapter discussion

6.5.1. Discussion of results

Previous work had established that non-cognate CD4+ T cell help generated by vaccination against OVA323-339 could be used to enhance anti-CSP responses to CSP(OVA323-339) liposomes. This chapter assessed whether other sources of non-cognate CD4+ T cell help to could also be exploited to enhance anti-CSP responses.

Initially, OT-II mice transgenic for a TCR recognising the OVA323-339 epitope in the context of H2-IAb were studied. Interestingly, these mice did make higher anti-CSP antibody responses to CSP(OVA323-339) liposomes, but only if they had been pre-vaccinated with OVA323-339 in TMG. This suggests that there may be a defect in either T or B cell

activation in these mice that can only be overcome in the presence of antigen and adjuvant, as responses were not enhanced in PBS + TMG mice. CD4+ T cells from OT-II mice are typically used for *ex vivo* or adoptive transfer studies. Recent data has highlighted issues with using OT-II mice to study antibody responses. In the context of ovalbumin vaccination with a helper antigen/adjuvant – cholera toxin – OT-II mice were unable to produce significant anti-ovalbumin antibody responses (Leung et al. 2013). The reason for this failure was not clear, although it was noted that B cells from OT-II mice could present ovalbumin epitopes *in vitro*. It was also demonstrated that T_H2 cytokine production in response to ovalbumin stimulation in CD4+ T cells from vaccinated OT-II mice was markedly reduced when compared with C57Bl/6 mice. It was hypothesised that this impaired T_H2 phenotype may limit the ability of OT-II mice to mount effective antibody responses. Anti-cholera toxin responses were not measured, rendering it impossible to determine if this defect is limited to responses to ovalbumin. Nonetheless, it is possible that anti-CSP responses were achieved in our vaccine model because OVA323-339 + TMG vaccination could overcome the issues with OT-II CD4+ T cell polarisation and activation proposed by Leung et al.

Subsequent studies were performed using murine cytomegalovirus as a model of pre-existing CD4+ T cell immunity. This has significantly more translational relevance, and is considered a good model for human cytomegalovirus infection. The CD4+ T cell epitope m09 was incorporated in CSP-coated liposomes to exploit anti-MCMV CD4+ T cell help. This epitope had been described by Arens et al to be the focus of a persistently elevated, IFNγ-secreting CD4+ T cell response in mice chronically infected with MCMV (Arens et al. 2008). The anti-MCMV response in chronically infected mice – as measured by the isotype profile of antibodies raised against a surface glycoprotein – indicated a strong T_H1 bias, with a very low IgG1:IgG2c ratio. This T_H1 bias was confirmed by ELISPOT studies assessing responses against viral lysate. The response to the m09 epitope itself was also T_H1-biased, with more IFNγ than IL-4 secreted in response to m09 stimulation.

Anti-CSP responses to CSP(m09) liposomes were higher in MCMV-infected mice, suggesting that anti-MCMV CD4+ T cells could support B cell responses to CSP. These responses in MCMV-infected mice occurred faster, reached higher levels, and contained more isotype switched antibody. High levels of anti-CSP IgG2c production in response to CSP(m09) were dependent on MCMV infection, in keeping with the involvement of T_H1-polarised anti-MCMV CD4+ T cell help. Initially, responses to CSP(scr m09) liposomes - which contain a scrambled variant of the m09 peptide – were also elevated, although this

effect was transient and responses were lower than those elicited by CSP(m09) liposomes two and four weeks after vaccination.

Further studies were performed with a 100-fold lower dose of liposomes and additional control groups. Responses were highest in MCMV-infected mice administered CSP(m09) or CSP(m09 + CpG) liposomes. In contrast, CSP(empty), CSP(scr m09), and CSP(CpG) vaccination elicited minimal anti-CSP antibody responses in MCMV-infected or uninfected mice. In studies with CSP(m09) liposomes, pre-existing anti-MCMV immunity increased the production of all isotypes of anti-CSP antibody. The most marked effect was an increase in the production of the 'T_H1 isotype' IgG2c, in keeping with the T_H1 bias of the anti-MCMV immune response. Interestingly, in studies where the TLR9 agonist CpG DNA was incorporated alongside m09 in vaccine particles, both pre-existing anti-MCMV immunity and CpG drove the production of IgG2c. CpG has been described as driving a T_H1 polarised immune response and can act on B cells to enhance isotype switching to IgG2a/IgG2c (Ruprecht & Lanzavecchia 2006).

6.5.2. Limitations and future directions

The anti-m09 immune response in MCMV-infected mice was characterised in this chapter, but data generated on the functional phenotype anti-m09 CD4+ T cells was limited. IFNγ and IL-4 ELISPOT assays were performed and data on the isotype profile of the anti-MCMV response was generated using ELISA plates coated with a MCMV surface glycoprotein. While it is possible to infer that the isotype profile of the humoral response to MCMV surface glycoproteins would have been influenced by anti-m09 CD4+ T cells, it would be more accurate to study these T cells directly. There is now a tetramer available that recognises anti-m09 CD4+ T cells in this mouse model of MCMV infection (National Institutes of Health Tetramer Core Facility, Emery University, USA). These would allow the tracking of anti-m09 responses over time and, if combined with intracellular cytokine staining, could give more detailed information of the phenotype of anti-m09 CD4+ T cells.

A logical next step for this work would be to assess whether non-cognate anti-viral CD4+ T cell help could be exploited to generate antibody responses to cancer antigens. CD4+ T cell responses to HCMV infection increase with age, so it is logical to look to exploit this immunity to generate immune responses to diseases that disproportionately affect the elderly, such as cancer or pneumonia. Studies could be performed using m09-encapsulating

liposomes coated with relevant target antigens for the elderly population – such as tumour antigens, influenza antigens, or capsular polysaccharides from *Streptococcus pneumoniae* – in mice chronically infected with MCMV.

Future work could also seek to identify other dominant MHCII epitopes in MCMV infection and then assess whether these CD4+ T cell populations could be exploited as sources of non-cognate CD4+ T cell help. Additionally, it is interesting to consider the effect of including immunodominant MHC class I (MHCI) epitopes in the liposomal particle core, either in place or alongside MHCII epitopes. Encapsulating MHCI epitopes from MCMV would allow experiments to assess whether anti-MCMV CD8+ T cells could provide helper signals to B cells in the context of this vaccine platform. It has been established that B cells can present antigens to activate CD8+ T cells (Castiglioni et al. 2005), but whether CD8+ T cells can provide helper signals to B cells *in vivo* remains contentious (Mosmann & Sad 1996)(Mosmann et al. 1997). CD8+ T cells – particularly those that secrete T_H2 cytokines (sometimes termed T_C2 CD8+ T cells) – may be able to provide either 'bystander' helper signals or direct cognate help to B cells (Mohr et al. 2010)(Maggi et al. 1994). However, in other settings, a CD8+ T cell interaction with a cognate B cell could result in B cell destruction (Mosmann et al. 1997)(Sad et al. 1997). Despite these uncertainties, it is interesting to consider whether the extremely high frequency anti-CMV CD8+ T cells, capable of secreting pro-inflammatory cytokines in response to stimulation with their cognate antigen, could be exploited alongside CD4+ T cell help to enhance humoral vaccine responses to our vaccine particles.

7. Pilot studies targeting the self-antigen ErbB2/neu

7.1. Introduction

Previous chapters developed a liposomal vaccine platform that could engage B cell receptors and then deliver MHCII epitopes to exploit pre-existing CD4+ T cell help. The 'third signal' for B cell activation could also be provided by incorporating TLR9 agonists in liposomal vaccine particles. In this chapter, the utility of this platform as a cancer vaccine was evaluated.

Many cancer antigens are 'self' or 'modified self' proteins that are either expressed or overexpressed on cancer cells (Cheever et al. 2009)(Reuschenbach et al. 2009). Accordingly, the immune system may be 'tolerised' to cancer antigens and cancer vaccines face the hurdle of overcoming or 'breaking' this tolerance. A key aspect of immune tolerance may be deletion of T cells that recognise cancer antigens during thymic development. When considering a B cell vaccine strategy, this could mean a lack of cognate CD4+ T cells capable of supporting humoral responses against cancer antigens. The vaccine platform described in the previous four chapters has the potential to overcome this challenge by co-opting pre-existing non-cognate CD4+ T cells to provide the requisite helper signals.

The initial goal of this chapter was to coat liposomal vaccine particles with long peptide B cell epitopes representing the binding site of efficacious therapeutic antibodies. The mAb Pertuzumab binds the dimerization loop of Her2, preventing proliferative signalling through heterodimerization with other members of the ErbB/Her family (Olayioye et al. 2000). Long peptide antigenic sequences from this domain have been described (Allen et al. 2007) and these are conserved in the murine ErbB2/neu sequence. This strategy would have been a direct extension of the previous liposomal production chemistry. Unfortunately, problems with synthesis of these peptide constructs meant that this approach could not be pursued. Instead, the larger, commercially available, recombinant extracellular domain of murine ErbB2/neu was used.

Murine ErbB2/neu was conjugated to the surface of liposomes that contained OVA323-339 +/- CpG DNA. The immunogenicity of these particles was then evaluated in C57Bl/6 and BALB/C mice with and without pre-existing anti-OVA323-339 CD4+ T cell immunity.

7.2. Chapter aims

1. Produce liposomes coated in the cancer antigen murine ErbB2/neu that encapsulate OVA323-339 and CpG DNA to deliver the three signals necessary for B cell activation.

2. Exploit pre-existing, non-cognate CD4+ T cell help – raised by vaccination against OVA323-339 – to support anti-ErbB2/neu antibody responses.

3. Evaluate the vaccine strategy in another strain of mice where ErbB2/neu over-expressing tumour models exist.

7.3. Results

7.3.1. Production of liposomes with surface ErbB2/neu

To test whether the liposomal vaccine platform detailed in previous chapters could 'break tolerance' to cancer antigens, liposomes were produced to contain the OVA323-339 MHCII epitope and CpG DNA, then coated in recombinant murine ErbB2/neu protein. Maleimide-modified liposomes were produced as described in chapter three. Rather than utilising the specific maleimide-thiol reaction that occurs at lower pH levels, the reactivity of maleimide groups were amine residues at higher pH levels was exploited. Different concentrations of full-length ErbB2/neu were reacted overnight at pH 8.0 with maleimide bearing liposomes.

In the absence of available antibodies to accurately characterise these particles, physicochemical studies were performed. The DLS profile before and after conjugation were compared (figure 7.1.A). The negative zeta potential of these liposomes was reduced in a dose dependent fashion after conjugation with ErbB/2neu (figure 7.1.B).

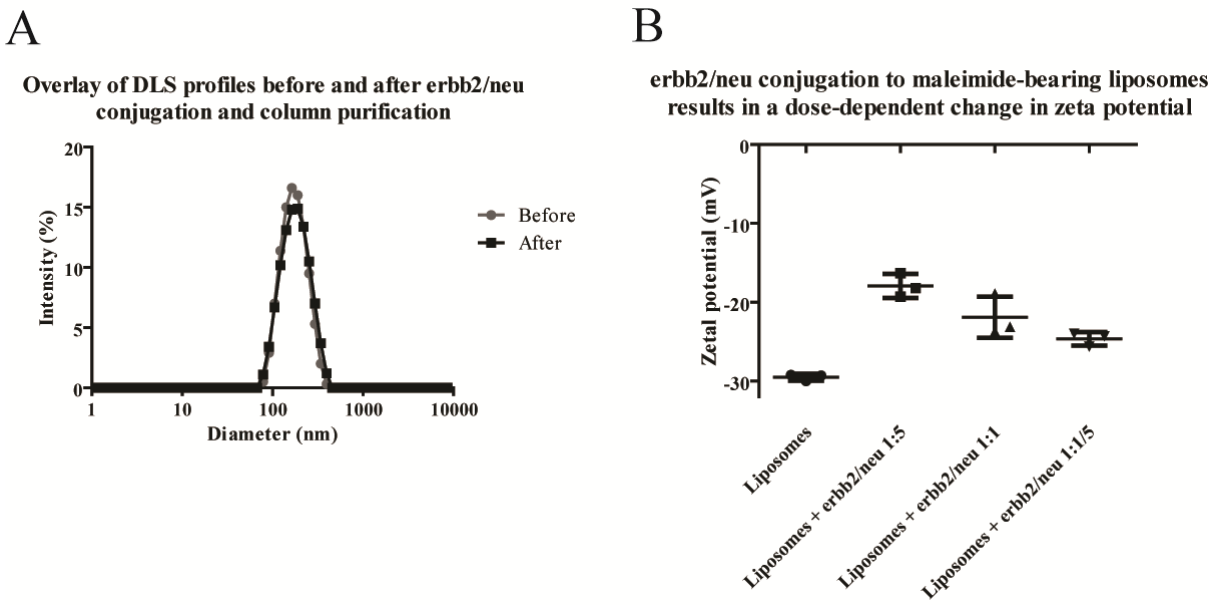


Figure 7.1. Physicochemical characterisation of liposomes before and after conjugation to Erbb2/neu. The diameter of liposomal preparations before and after overnight reaction with 5mg/mL ErbB2/neu protein was measured by DLS (A). Graph (B) shows the change in zeta potential (section 2.9.2) after reacting maleimide-bearing liposomes with decreasing concentrations (5 mg/mL, 1 mg/mL, and 0.2 mg/mL) of ErbB2/neu protein overnight at pH 8.0 (n=3 technical triplicates – repeated measures of the zeta potential of each liposomal preparation).

7.3.2. A pilot *in vivo* study targeting ErbB2/neu in C57Bl/6 mice

A pilot study was performed to assess the immunogenicity of ErbB2/neu(OVA323-339) and ErbB2/neu(OVA323-339 + CpG) vaccines in the established OVA323-339 pre-vaccination C57Bl/6 model of pre-existing non-cognate CD4+ T cell immunity. Two weeks following vaccination with these two liposomal vaccine constructs, the effect of OVA323-339 pre-vaccination was examined. Higher anti-ErbB2/neu responses were detected in the OVA323-339 pre-vaccinated group when compared with PBS + TMG pre-vaccinated mice ($p<0.01$). The inclusion of CpG DNA as a TLR9 agonist did not enhance responses in this pilot study (figure 7.2.).

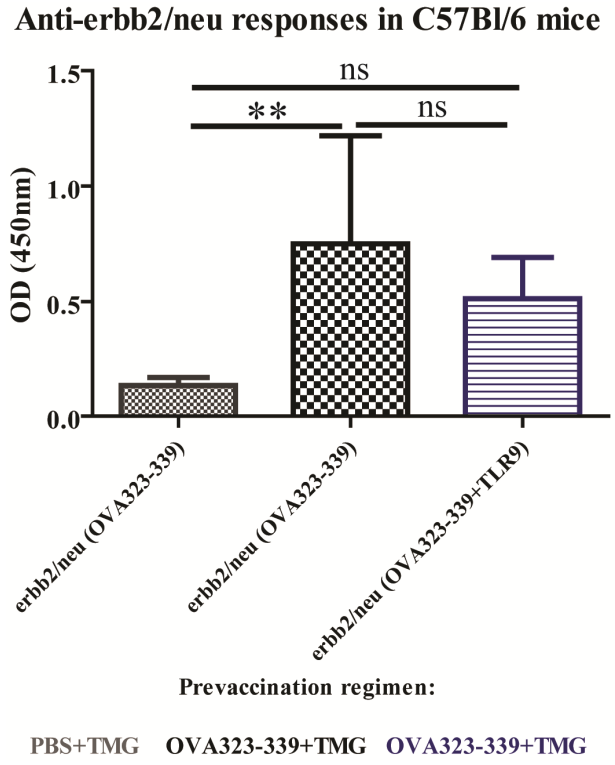


Figure 7.2. Antibody responses to Erbb2/neu-coated liposomes in C57Bl/6 mice pre-vaccinated with PBS or OVA323-339 in TMG. 6-8 week old female C57Bl/6 mice were administered two subcutaneous vaccinations of 10 µg of OVA323-339 peptide or PBS emulsified in TMG adjuvant, with a two week interval between doses. Two weeks later, mice were given one 100 µL subcutaneous dose of ErbB2/neu(OVA323-339) liposomes or ErbB2/neu(OVA323-339 + CpG DNA) liposomes, containing 0.1 µg of OVA323-339 +/- 0.1 µg CpG DNA. Two weeks post-liposomal vaccination, serum was taken and anti-ErbB2/neu antibody response was measured by ELISA at a serum dilution of 1:50. Means were compared by one-way ANOVA with Tukey's post-test (n=4).

7.3.3. Evaluating this vaccine strategy in BALB/C mice

In vivo models of murine ErbB2/neu over-expressing tumours are readily available in BALB/C mice, but do not exist on a C57Bl/6 background. Consequently, studies were performed to assess whether this vaccine platform was effective in BALB/C mice.

First, it was demonstrated that the OVA323-339 + TMG vaccination protocol used in previous chapters was also effective at generating CD4+ T cell immunity in BALB/C mice. ELISPOT data demonstrated both IFNγ and IL-4 responses were elicited by this protocol (figure 7.3.A and 7.3.B). There was a trend towards higher numbers of IL-4-secreting splenocytes compared with IFNγ-secreting splenocytes in OVA323-339 + TMG vaccinated BALB/C mice, although this did not reach statistical significance ($p = 0.203$). Analysis of the anti-OVA323-339 isotype profile (figure 7.3.C and 7.3.D) revealed an IgG1:IgG2a isotype ratio of 0.498 (sd = 0.0164).

Next, the immunogenicity of liposomes coated with the model antigen CSP that were either empty or encapsulated OVA323-339 was assessed in BALB/C mice. Significant antibody responses to low doses of CSP(empty) liposomes were not detected. Anti-CSP responses to CSP(OVA323-339) liposomes were higher in the OVA323-339 + TMG pre-vaccinated group when compared with PBS + TMG pre-vaccinated mice (figure 4.4.B, $p<0.01$). Mean anti-CSP responses were higher in OVA323-339 pre-vaccinated mice for IgG ($p = 0.021$), IgG1 ($p = 0.057$), and IgG2a ($p = 0.0001$) isotypes (figure 7.4.E and 7.4.F). Calculation of the relative amount of IgG1 and IgG2a produced using standard curves generated with purified isotypes revealed that IgG2a (161.3 ng/mL, sd = 25.8) was produced to higher levels than IgG1 (72.09 ng/mL, sd = 49.8, $p = 0.0512$ by two tailed, unpaired, t-test). In OVA323-339 pre-vaccinated mice, the anti-CSP IgG1:IgG2a ratio was 0.478 (sd = 0.340), resembling the anti-OVA323-339 ratio of 0.498.

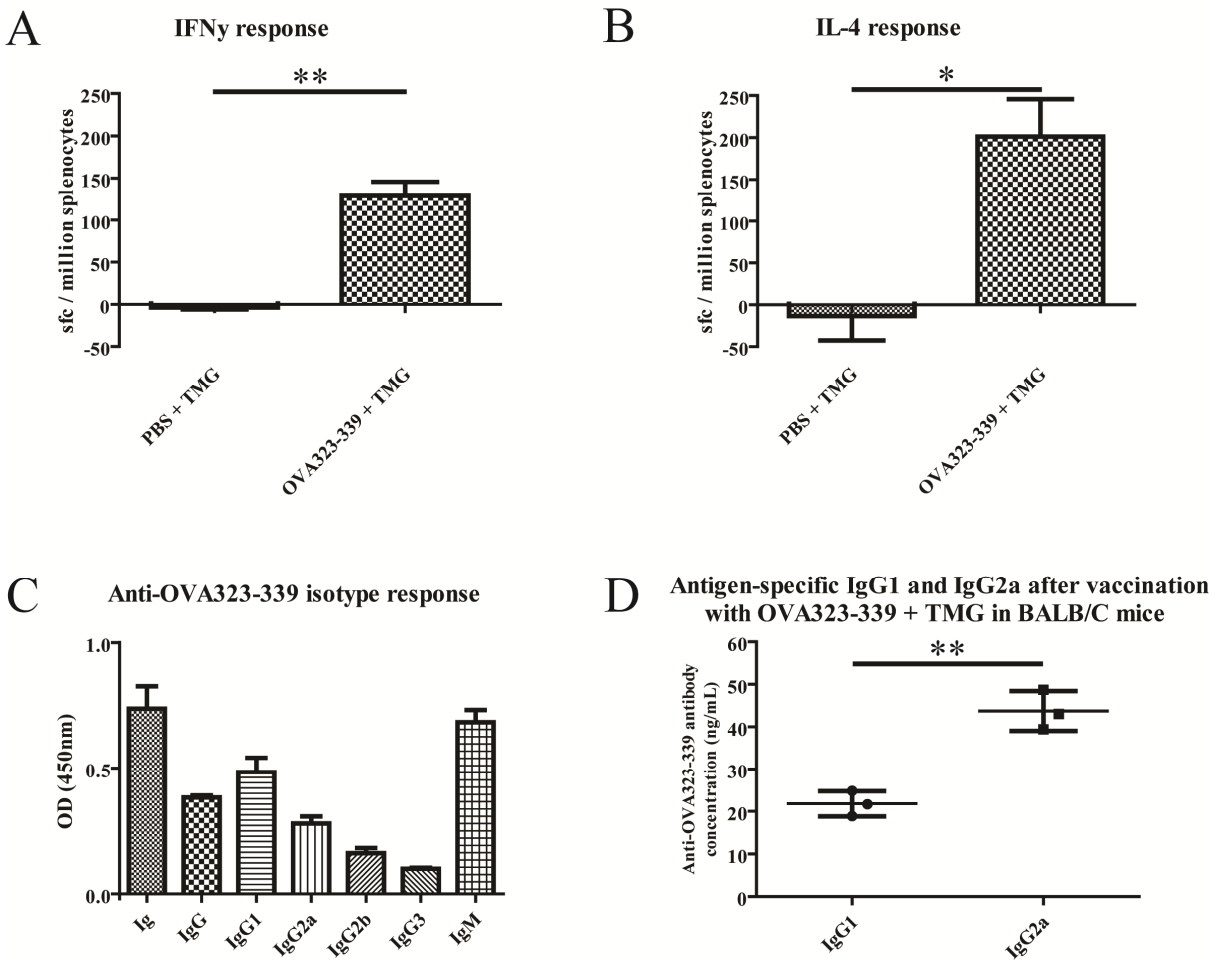


Figure 7.3. Characterisation of the anti-OVA323-339 immune response after OVA323-339 + TMG vaccination in BALB/C mice. 6-8 week old female BALB/C mice (n=3) were administered two subcutaneous vaccinations of 10 µg of full-length ovalbumin or PBS emulsified in TiterMax gold adjuvant, or ovalbumin alone, with a two week interval between doses. Two weeks after the second vaccination, splenocytes were harvested and stimulated with OVA323-339 peptide at a final concentration of 1 µg/mL. 36 hours later, cellular responses to IFNγ (A) and IL-4 (B) were measured by ELISPOT assay (section 2.11.3) and the number of spot forming units (sfc) was counted for each well. The isotype profile of anti-OVA323-339 antibodies in serum from OVA323-339 + TMG vaccinated mice (two weeks after the second vaccine dose) is shown in graph (B). Standard curves allowed the quantification of each isotype using quantifications based on a line of best fit. Graph (D) shows the relative amounts of IgG1 and IgG2a elicited by OVA323-339 + TMG vaccination. Means are compared with unpaired, two-tailed, t tests (n=3).

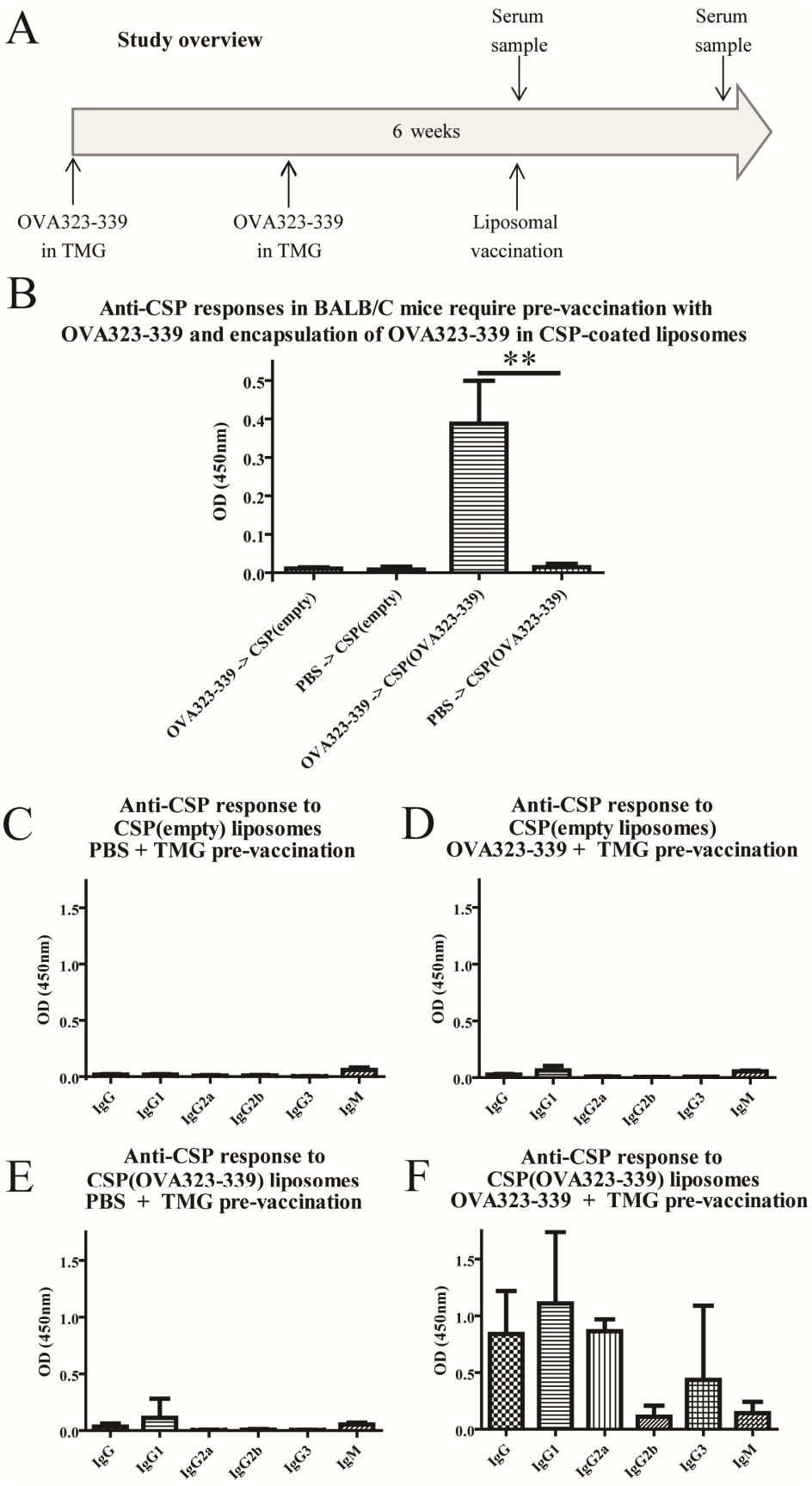


Figure 7.4. Antibody responses to CSP-coated liposomes in BALB/C mice pre-vaccinated with PBS or OVA323-339 in TMG. 6-8 week old female BALB/C mice (n=3) were administered two subcutaneous vaccinations of 10 µg of OVA323-339 peptide or PBS emulsified in TiterMax gold

adjuvant, with a two week interval between doses. Two weeks later, this was followed by a single dose of liposomes coated in CSP either containing citrate buffer only or encapsulating OVA323-339 peptides in a citrate buffer. Each vaccine dose contained 0.5 µg of CSP +/- 0.1 µg of OVA323-339. Graphic (A) outlines the study protocol. The effect of pre-existing CD4+ T cell immunity on the total anti-CSP antibody response was measured two weeks after liposomal vaccination (B). The effect of pre-existing immunity on the production of different anti-CSP antibody isotypes (C-F) was also assessed by ELISA with biotinylated anti-isotype secondary antibodies (section 2.12.2). Mean responses to CSP(OVA323-339) liposomes were compared between PBS + TMG (E) and OVA323-339 + TMG (F) pre-vaccination groups using unpaired, two-tailed, t tests and key differences are discussed in the main text.

7.3.4. Targeting ErbB2/neu in BALB/C mice

Next, the immunogenicity of ErbB2/neu(OVA323-339) and ErbB2/neu (OVA323-339 + CpG) liposomes assessed in BALB/C mice. When compared with the control group of PBS + TMG and CSP(OVA323-339) vaccinated mice, there was a trend towards higher anti-ErbB2/neu responses in OVA323-339 + TMG pre-vaccinated mice administered ErbB2/neu(OVA323-339) and ErbB2/neu(OVA323-339 + CpG) vaccinated mice, which reached statistical significance in the ErbB2/neu(OVA323-339 + CpG) group.

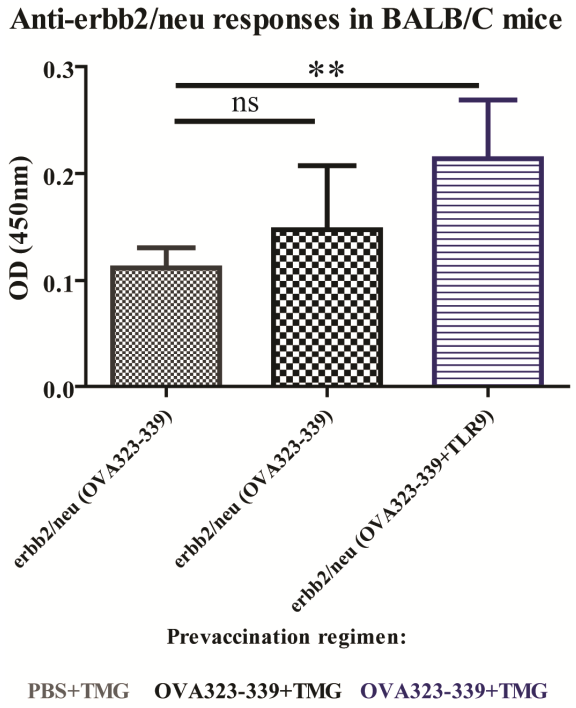


Figure 7.5. Antibody responses to Erbb2/neu-coated liposomes in BALB/C mice pre-vaccinated with PBS or OVA323-339 in TMG. 6-8 week old female BALB/C mice were administered two subcutaneous vaccinations of 10 µg of OVA323-339 peptide or PBS emulsified in TMG adjuvant, with a two week interval between doses. Two weeks later, mice were given one 100 µL subcutaneous dose of ErbB2/neu(OVA323-339) liposomes or ErbB2/neu(OVA323-339 + CpG DNA) liposomes, containing 0.1 µg of OVA323-339 +/- 0.1 µg CpG DNA. Two weeks post-liposomal vaccination, serum was taken and anti-ErbB2/neu antibody response was measured by ELISA at a serum dilution of 1:50. Means were compared by one-way ANOVA with Tukey's post-test (n=6).

7.4. Chapter conclusions

1. Preliminary data suggest that OVA323-339 and CpG DNA encapsulating liposomes can be coated with murine ErbB2/neu.

2. ErbB2/neu(OVA323-339)) liposomes elicit anti-ErbB2/neu antibody responses in the presence of pre-existing anti-OVA323-339 CD4+ T cell immunity.

3. In BALB/C mice, pre-existing non-cognate CD4+ T cell immunity can be exploited to enhance anti-CSP responses to CSP(OVA323-339) liposomes. In studies with the cancer antigen ErbB2/neu, ErbB2/neu(OVA323-339 + CpG DNA) liposomes were capable of eliciting anti-ErbB2/neu antibody responses in BALB/C mice pre-vaccinated with OVA323-339 + TMG.

7.5. Chapter discussion

7.5.1. Discussion of results

This chapter provides preliminary evidence that this liposomal vaccine platform can exploit pre-existing non-cognate CD4+ T cell immunity to generate antibody responses to cancer antigens..

In C57Bl/6 mice, a statistically significant increase in anti-ErbB2/neu antibody responses was seen in OVA323-339 pre-vaccinated mice, providing support for the overarching hypothesis of non-cognate CD4+ T cell help overcoming tolerance to 'self' antigens. However, in BALB/C mice, this effect was only statistically significant if the TLR9 agonist CpG DNA was also incorporated in the vaccine particle. Of note, the magnitude of the anti-ErbB2/neu response in BALB/C mice was lower than in C57Bl/6 mice. To assess vaccine efficacy, it is possible to challenge BALB/C mice with the ErbB2/neu over-expressing TUBO tumour cell line. However, it was determined that the immunogenicity of the platform in BALB/C mice needed to be optimised before mice were subjected to tumour challenge.

The balance of the T_H1/T_H2 immune response to OVA323-339 + TMG in BALB/C mice was noted to be different to that observed in C57Bl/6 mice (sections 4.3.1 and 4.3.2). In BALB/C mice, the IgG1:IgG2a ratio was 0.498 whereas in C57Bl/6 mice the IgG1:IgG2c ratio was 0.0311. This is in keeping with the literature which described C57Bl/6 as T_H1-biased and

BALB/C mice as T_H2-biased (Watanabe et al. 2004)(De Vooght et al. 2010). Even so, studies with the model B cell antigen CSP in BALB/C mice demonstrated that pre-existing anti-OVA323-339 CD4+ T cells could be exploited to enhance humoral immune responses to non-cognate antigens.

7.5.2. Limitations and future directions

Anti-cancer vaccine studies in this chapter were performed using liposomes coated in the extracellular domain of murine ErbB2/neu. This was not the initial strategy that was devised to test the utility of this liposomal vaccine platform as a cancer vaccine. Consequently, the liposomal particles that were produced were inadequately characterised. Ideally, the presence of surface bound ErbB2/neu protein would have been demonstrated by Western blotting and flow cytometry, not only a change in particle zeta potential.

Particles were produced using a suboptimal linkage strategy – where the reactivity of maleimide with amine groups at higher pH levels was used to conjugate ErbB2/neu to the liposome surface. It is difficult to know how efficient this process is and, consequently, what amount of ErbB2/neu is contained in each vaccine dose. Further, due to a restricted supply of recombinant ErbB2/neu protein, a low dose of ErbB2/neu(OVA323-339) and erb2/neu(OVA323-339 + CpG) vaccines were used. While this lower dose had worked in previous chapters in the context of CSP, it may have been insufficient to elicit robust responses to ErbB2/neu. This linkage chemistry will also mean that ErbB2/neu protein is bound to the particle in a range of different orientations. While this theoretically could lead to an increased breadth of the anti-ErbB2/neu response, with multiple B cell epitopes exposed for B cell binding, another possibility is that the variable orientation of ErbB2/neu could mean an insufficient density of B cell epitopes arranged in the orientation needed to cross-link BCRs on the surface of anti-ErbB2/neu B cells.

Ideally, these studies would be performed again with shorter B cell antigens that could be reliably conjugated to the liposome particle surface to ensure the availability of antigen for BCR binding and cross-linking. There are a broad range of possible targets. A peptide sequence (LHCPALVTYNTDTFESMHNPEGRYTFGASCV) has been described which represents the ErbB2/neu dimerization loop (Allen et al. 2007). These longer peptide antigens could be conjugated to liposome surfaces using maleimide-thiol or DBCO-azide linkages. Targeting this antigen using with this liposomal vaccine platform would be a logical next step

for this project. Responses against the ErbB2/neu dimerization loop epitope could be studied in both the OVA323-339 pre-vaccination model and in MCMV-infected mice, perhaps while incorporating a range of different TLR agonists to assess their effect on immunogenicity. If high-titre responses could be generated against this peptide or the ErbB2/neu protein, the ability of serum from vaccinated mice to bind TUBO cells and its effect on cell growth could be studied *in vitro*, before prophylactic or therapeutic vaccination studies are considered in BALB/C mice.

8. Modifying measles virus particles with B cell target antigens as a strategy to exploit pre-existing anti-measles CD4+ T cells

8.1. Introduction

Measles Virus (MV) is a negative sense RNA virus of the Paramyxovirus family. It has two surface glycoproteins – Fusion (F) and Haemagglutinin (H) (Moss & Griffin 2012).The Edmonston strain of MV has been used as a vaccine in humans for over four decades. It has an excellent safety profile and induces long lasting CD4+ T cell responses (Naniche et al. 2004). A reverse genetics system, allowing rescue of MV from cDNA, was developed in 1995 (Radecke et al. 1995) and this gave rise to new applications for MV as a gene therapy vector, vaccine vector, and oncolytic agent.

To rescue the virus, the negative sense genome transcribed from the plasmid encoding MV (pMV) by T7 RNA polymerase must bind to the Phospho- (P) and Nucleocapsid (N) proteins. Therefore, these must be provided *in trans*. Once the resultant ribonucleoprotein (RNP) complex has formed, the encapsidated genome can be transcribed by the Large polymerase (L) protein, which must also be supplied *in trans* during rescue, but is cytotoxic (Radecke et al. 1995). Interestingly, the nucleotide length of the MV genome must be a multiple of six and a deviation of even a single base pair deviation from this 'rule of six' results in unsuccessful rescue of a genetically modified virus (Kolakofsky et al. 1998). Thus, successful rescue of MV relies on the presence of T7 RNA polymerase, the N protein, P protein, L polymerase protein, and the correct-length MV genome, in a producer cell.

This chapter seeks to modify the surface of the Edmonston vaccine strain of MV so it exclusively displays target B cell antigens (and no residual measles antigens) on the viral particle surface. To achieve this, the genes encoding the MV envelope glycoproteins Haemagglutinin (H) and Fusion (F) were replaced with a chimeric gene encoding the extracellular domain of a target antigen with the transmembrane and cytoplasmic domains of F. The MV H glycoprotein is the primary determinant of viral tropism and H from the Edmonston vaccine strain of MV preferentially binds CD46 whereas wild-type strains use

CD150 as a receptor (Yanagi et al. 2006). Binding of the attachment protein H to its cellular receptor induces re-folding of the F gene, resulting in membrane fusion (Wild et al. 1991)(Brindley et al. 2012). The cytoplasmic tail of the MV F glycoprotein interacts with matrix proteins and this is important in MV particle formation (Cathomen et al. 1998). Consequently, the H gene was removed and the extracellular domains of each target antigen was fused with the transmembrane and cytoplasmic domains of F. Target antigens studied in this chapter were the *Plasmodium falciparum* circumsporozoite protein (CSP) and the human tumour antigens Her2 and gp100.

Antigen	Function	Justification as a target antigen	Therapeutic relevance
CSP (P. falciparum)	Malaria sporozoite stage surface protein	Neutralising antibody to CSP could prevent malaria sporozoites from initiating hepatocyte infection, and thus provide protective immunity.	Targeted in several antibody and cell-mediated vaccine strategies, including RTS,S (Casares et al. 2010)(Ballou 2009).
Her2 (Erbb2/neu)	Epidermal growth factor receptor	Up-regulated in 20-30% of breast cancers and overexpressed in some other malignancies (Ménard et al. 2000). Very high homology with murine Erbb2/neu.	Target of the monoclonal antibodies Trastuzumab and Pertuzumab (Mir et al. 2007)(Murphy & Modi 2009).
gp100	Pre-melanosome and melanosome formation	Overexpressed in many cases of melanoma (Marincola et al. 1996). Significant homology with murine gp100.	Targeted in several antibody and cell-mediated cancer vaccine strategies (Cassaday et al. 2007)(Phan et al. 2003).

Table 8.1. Overview of target antigens used in modifying MV particles

By removing F and H and replacing them with a target antigen, viral particles are no longer endowed with their usual tropism. Accordingly, rescue and propagation of tropism-ablated MV-CSP, MV-Her2, and MV-gp100 is a significant challenge. In an attempt to overcome this, cell lines were generated to provide F and H *in trans* during rescue and propagation of vaccine constructs. Because co-expression of F and H mediates cell membrane fusion and syncytia formation, these could not be constitutively co-expressed in a cell line. Consequently, cell lines were developed where F and H expression could be induced in the presence of a rescued MV vaccine construct. Viral particles produced from these cell lines could be passaged once on normal cells (i.e. those without inducible F and H expression), to produce non-infectious viral particles with target antigen on the particle surface. An additional strategy was also explored where the vaccine strain of MV was produced with F and H glycoproteins *in situ* and then the surface of these viral particles was then chemically

modified to display target antigens. This approach did not face the same challenge of rescue and propagation of a tropism-ablated virus. Function-spacer-lipid (FSL) constructs were used to label the surface of MV particles with CSP (Deborah A et al. 2011). Pre-existing anti-MV immunity was then generated by vaccination of mice with MV and adjuvant. The effect of MV pre-vaccination on the immune response to CSP-coated MV particles was then measured.

8.2. Chapter aims

1. Modify the Edmonston strain of measles virus (MV) so its surface glycoproteins are replaced with one of the target antigens CSP, gp100, or Her2.

2. Generate pre-existing immunity to the Edmonston strain of measles virus by vaccination.

3. Exploit this pre-existing anti-measles virus immunity as a source of non-cognate CD4+ T cell help to enhance vaccine responses against target B cell antigens.

8.3. Results

8.3.1. Genetic modification of MV to replace the surface glycoproteins with fusion proteins containing the extracellular domains of target antigens

To produce MV particles coated in CSP, gp100, or Her2, a plasmid containing the full-length measles genome (pMV-GFP) was first digested with BsiWI and re-circularised to increase the number of unique restriction sites. F and H genes were removed by digestion with PspOMI and SpeI and replaced with a previously synthesised construct containing, in order: the intergenic region preceding F, the F signal peptide, the extracellular domain of gp100, the F transmembrane and cytoplasmic domains, followed by the F-H intergenic region, then the TetR gene, followed by the H-L intergenic region to give a pMV-GFP-(BsiWI)gp100-TetR construct. The pMV-GFP backbone was reconstructed by digesting pMV-GFP with BsiWI, extracting the 4.1kb fragment and ligating this into a BsiWI linearised pMV-GFP-(BsiWI)gp100-TetR plasmid.

The gp100TetR insert was designed to allow the target antigen to be replaced with an alternative antigen sequence flanked by BstBI and AscI. PCR amplification of the CSP extracellular domain with primers that added BstBI and AscI sites generated fragments that could be ligated into the BstBI + AscI digested MV-GFP vector. The correctness of all engineering steps was confirmed by diagnostic restriction digest and then sequence verified (section 2.1.1 – 2.1.8).

The resulting plasmids contained a T7-driven modified MV-GFP genome where the F and H glycoprotein genes had been replaced with genes encoding for chimeric F-target antigen glycoproteins and the TetR protein. These were denoted ‘MV-CSP-TetR’, ‘MV-gp100-TetR’, and ‘MV-Her2-TetR’.

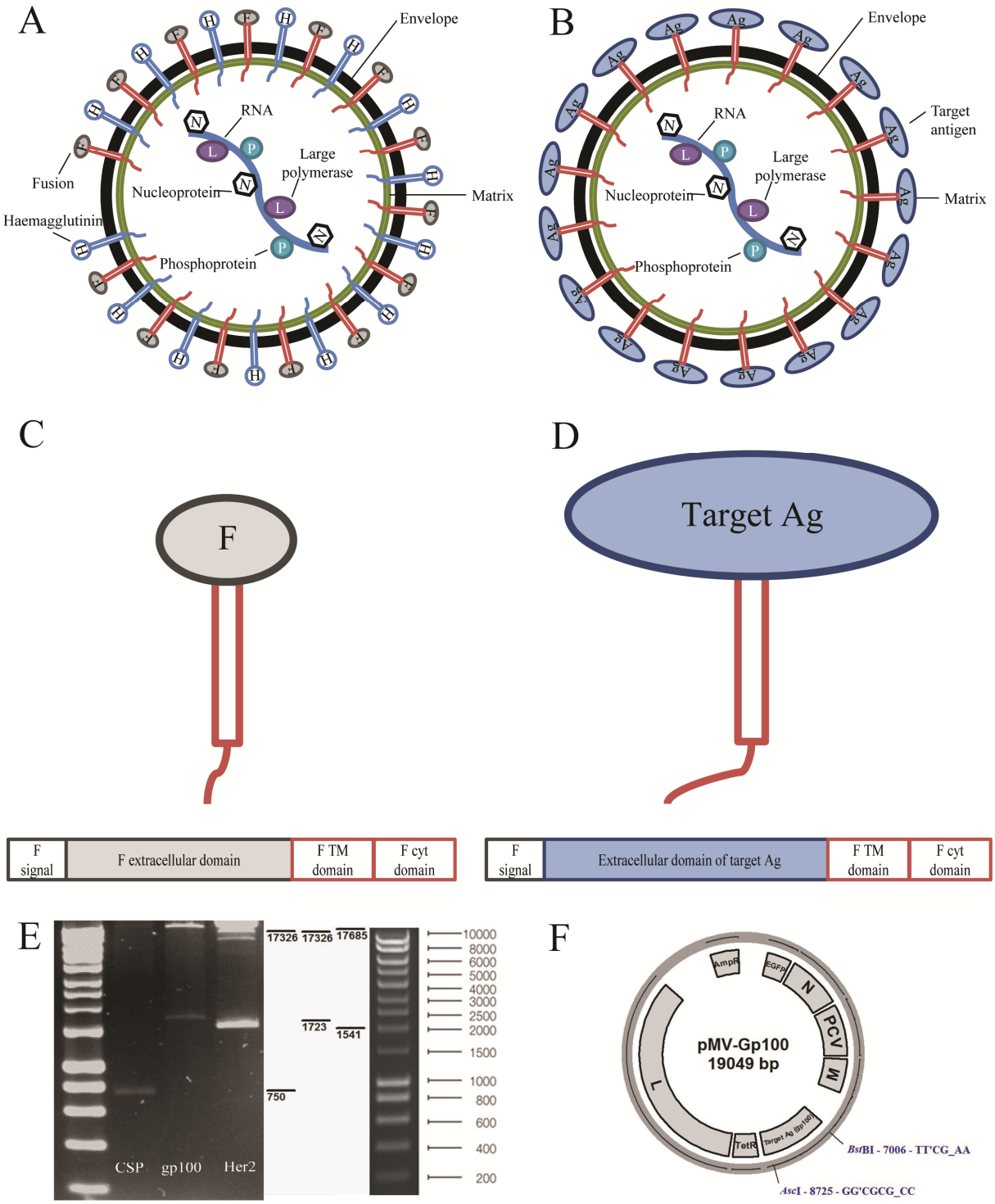


Figure 8.1. Genetic modification of MV to encode target antigen as the sole surface glycoprotein, in place of F and H. Edmonston strain MV-GFP was modified to remove the H gene, and replace the extracellular domain of F with the extracellular domain of target antigens. The genome was also modified to encode TetR or Cre recombinase (see sections 8.3.3 and 8.3.5). The structure of the Edmonston strain of MV (A) and a genetically modified variant described in this chapter (B) are shown, alongside the F glycoprotein structure in the vaccine strain (C) and a genetically modified variant (D). Plasmids encoding the MV-GFP anti-genomic cDNA under a T7 promoter were engineered to contain F chimeric target antigens CSP, gp100, and Her2 in place of MV surface glycoproteins. The resulting clones were screened by BstBI + AscI digest, giving the expected band sizes (E) and (F).

8.3.2. Confirming the functionality of target Ag-F chimeric proteins

To assess whether chimeric F-antigen proteins could be transcribed, translated, and expressed on the cell surface, CMV expression vectors were engineered. The chimeric gene was PCR amplified from its respective MV vector and ligated into a CMV expression vector pSF-CMV (figure 8.2.A-B). The resulting plasmids were denoted pSF-CMV-CSP(Ftm+Fcyt), pSF-CMV-gp100(Ftm+Fcyt), and pSF-CMV-Her2(Ftm+Fcyt). Expression of each chimeric gene was detectable by flow cytometry on the surface of transfected 293A cells (figure 8.2.C-G).

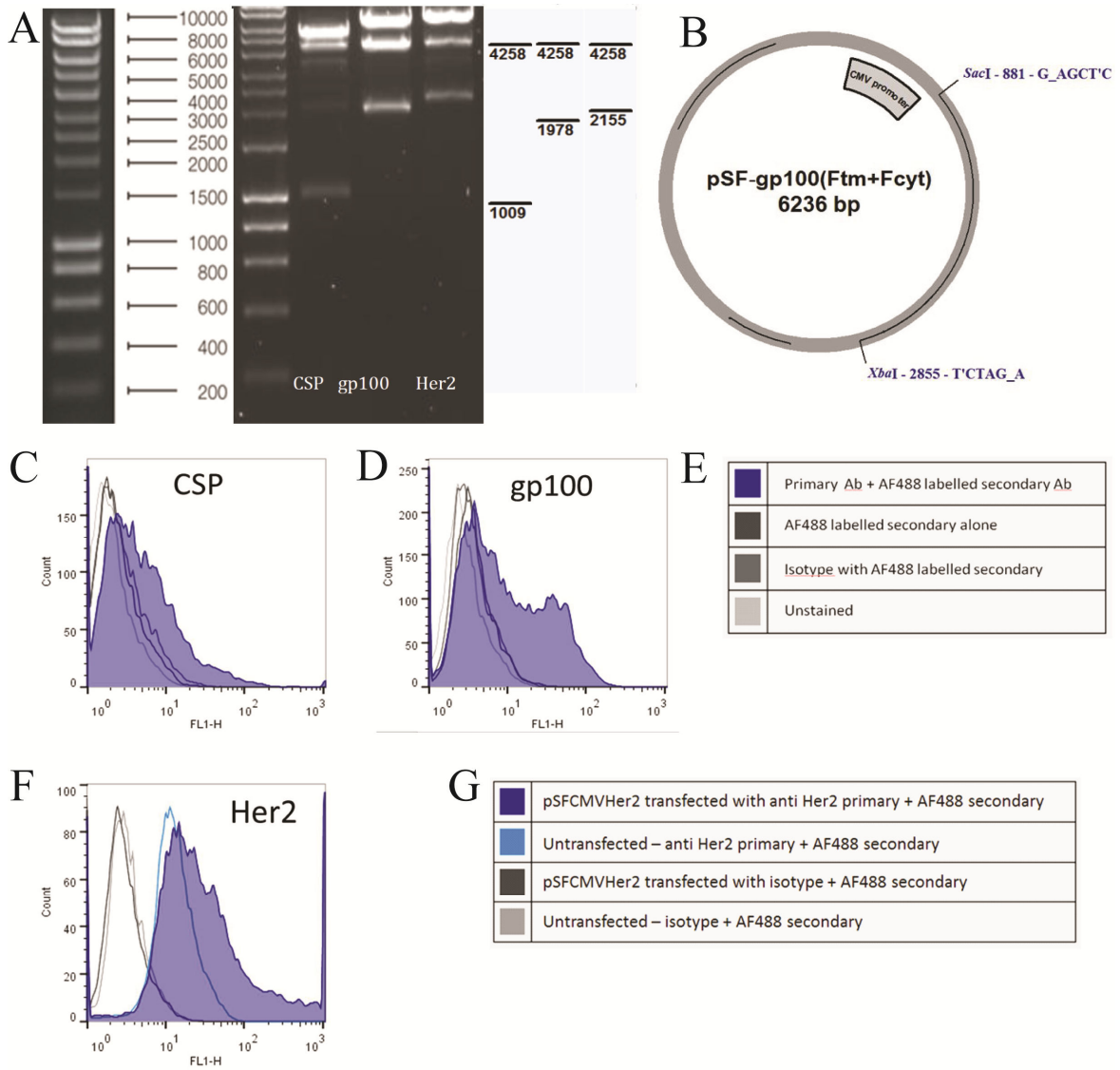


Figure 8.2. Generation and characterisation of CMV-driven expression vectors for each of the F-antigen chimeric genes. pSF-CMV-CSP(Ftm+Fcyt), pSF-CMV-gp100(Ftm+Fcyt), and pSF-CMV-Her2(Ftm+Fcyt) were digested with SacI and XbaI, which flank the chimeric antigen gene and gave the expected pattern of bands on gel electrophoresis (A) and (B). 293A cells were transiently transfected with vectors containing CMV-driven chimeric proteins. The expression of each chimeric protein (C), (D), and (F), was measured on the cell surface by flow cytometry at 24 hours post-transfection. The legend (E) acts as a key for histograms (C) and (D), whereas (G) is the legend for histogram (F).

8.3.3. Development and characterisation of a tetracycline-responsive rescue system to provide the MV glycoproteins *in trans* during rescue and propagation of genetically modified vaccine constructs

The rescue of MV from cDNA is often achieved using the 293-3-46 cell line that is stably transduced with T7, N, and P (Cathomen et al. 1998)(Radecke et al. 1995). The goal of this project was to produce a cell line where the F and H genes of MV could be supplied *in trans* during the rescue and propagation of tropism-ablated MV vaccine constructs. Consequently, it was desirable to develop a system that could be used beyond the 293-3-46 cell line.

Rescue systems have been described where the T7 polymerase is expressed from a viral vector, and other components are delivered by transient transfection (Schneider et al. 1997). A comparable system was developed where VERO cells were infected with vaccinia virus expressing T7 (VV-T7) and then transfected with separate CMV-driven plasmids encoding N, P, L, and the MV-GFP genome. MV virus could be rescued using this system, but VV-T7 infection resulted in significant cytopathic effect (CPE) (8.3.A-B). An inhibitor of VV-T7 replication AraC was included in the tissue culture media and this reduced the CPE while allowing rescued MV-GFP to spread throughout the monolayer (8.3.D-E).

Next, cell lines with inducible expression of F and H were produced and characterised to allow the rescue and propagation of tropism-ablated MV vaccine constructs (figure 8.4). This strategy involved using the tetracycline responsive pLVX-TetOn system to generate lentiviruses expressing either F or H under the pTight promoter along with puromycin or blasticidin resistance cassettes. In this system, a tetracycline-sensitive transactivator protein (TetR) controls transcription from the pTight promoter. Thus, transcription is limited to cells where the TetR protein is expressed and doxycycline is present. In this rescue system, the TetR protein was encoded in the genome of MV-CSP-TetR, MV-gp100-TetR, or MV-Her2-TetR constructs and doxycycline was supplied in the tissue culture media. It was proposed that – in this system – F and H expression would be limited to cells where MV genome is transcribed and translated.

The F and H genes were amplified from MV-GFP cDNA and cloned into the pLVX vector downstream of the pTight promoter (data not shown). This gave the lentiviral plasmids pLVX-F and pLVX-H (figure 8.5.A). The pLVX vector also contains a puromycin resistance cassette, allowing selection of stably transduced cells. The puromycin resistance gene in

pLVX-H was then exchanged for blasticidin resistance (data not shown). Lentiviruses were then generated for each of these plasmids and used to sequentially infect 293A cells to give double-transduced cell lines resistant to both puromycin and blasticidin. This was first done with the pLVX-F-Puro construct. Selection was performed with puromycin (see Appendix 4) and resistant colonies were picked and expanded. To test the functionality of these pLVX-F-Puro transduced colonies, a plasmid containing H under a CMV promoter was transfected alongside pCMV-TetR in the presence of doxycycline. Syncytia formation was evident (data not shown). Two of these colonies were then infected with the pLVX-H-Blast lentivirus particles, and colonies resistant to blasticidin were selected, expanded, and designated '293A-pTightF-pTightH'.

The presence of the F and H genes in these cell lines after ten passages was confirmed by PCR on cellular DNA (figure 8.5.B). The ability of pLVX-F and pLVX-H to mediate syncytia formation was confirmed by transient transfection of 293A cells with these constructs and a CMV-driven TetR expression plasmid, in the presence of doxycycline (figure 8.5.C). 293A-pLVX-F+H cell lines were also transfected with TetR in the presence of doxycycline and the formation of small syncytia was observed.

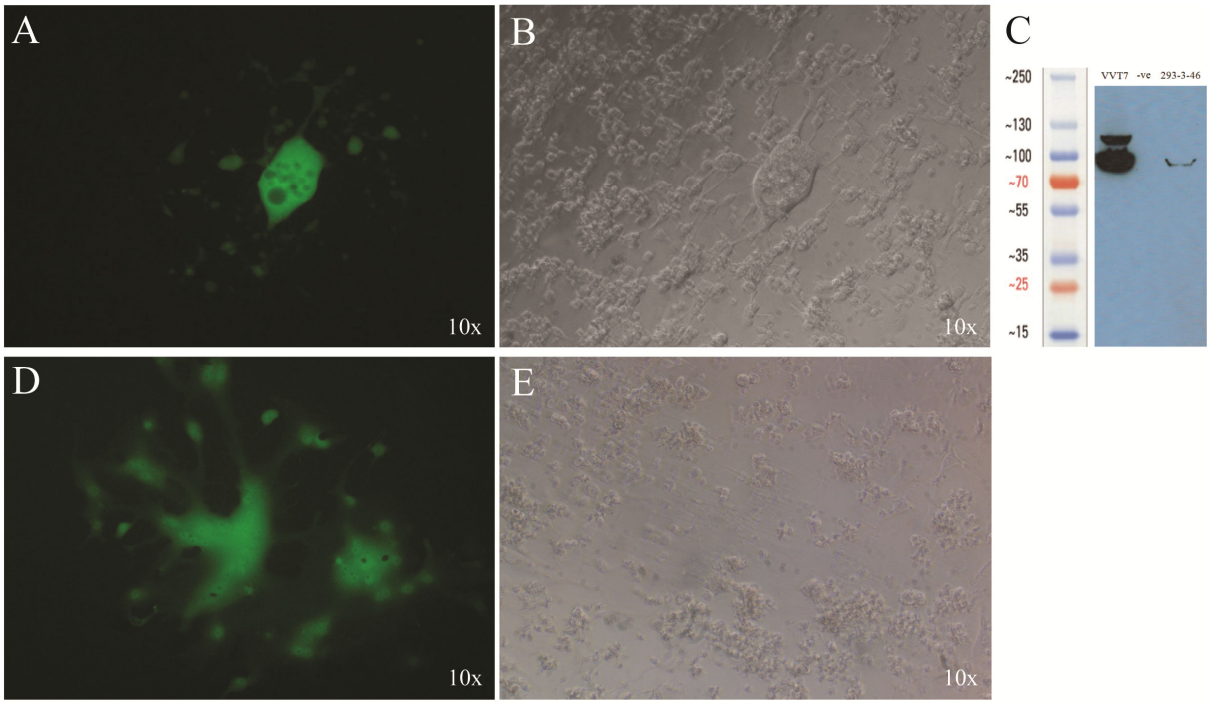


Figure 8.3. Successful rescue of a GFP-expressing Edmonston strain of MV using a VVT7 helper system. GFP positive syncytia (A) were evident in six-well plates of VERO cells infected with VV-T7 (MOI = 5), then transfected with N, P, and L, CMV-driven expression vectors and a plasmid encoding measles virus anti-genomic cDNA under a T7 promoter. Initial rescue attempts were notable for marked VV-T7 cytopathic effect (CPE) – (B). Optimization of the VV-T7 MOI (MOI = 1) and the addition of the VV inhibitor Ara-C reduced VV CPE, coupled with the addition of further VERO cells to give a 90% confluent monolayer at 96 hours, increased rescue efficiency (D) and (E). Expression of T7 from the VV-T7 vector 24 hours after infection of VERO cells (MOI = 1) was confirmed by Western blotting and compared to the level in the same number of 293-3-46 cells (C).

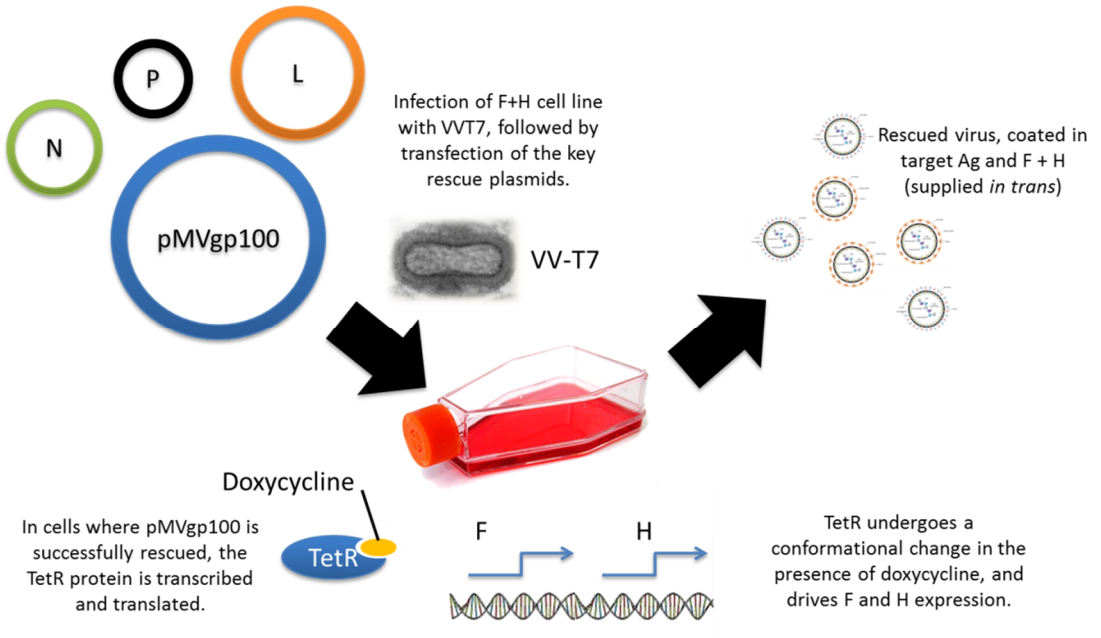


Figure 8.4. Overview of the rescue of tropism-ablated vaccine constructs in a cell line that provides F and H *in trans*, under the control of an TetR inducible promoter. In the presence of doxycycline, the expression of TetR from rescued MV RNA results in transcription and translation of F and H from the genome of the packaging cell line (293A-pTightF-pTightH). Temporarily infectious virus is produced by coating with F and H, allowing propagation *in vitro*. When passaged once on normal cells (i.e. those without the lentiviral TetR-responsive glycoproteins), only non-infectious virus with target antigen on its surface will be produced.

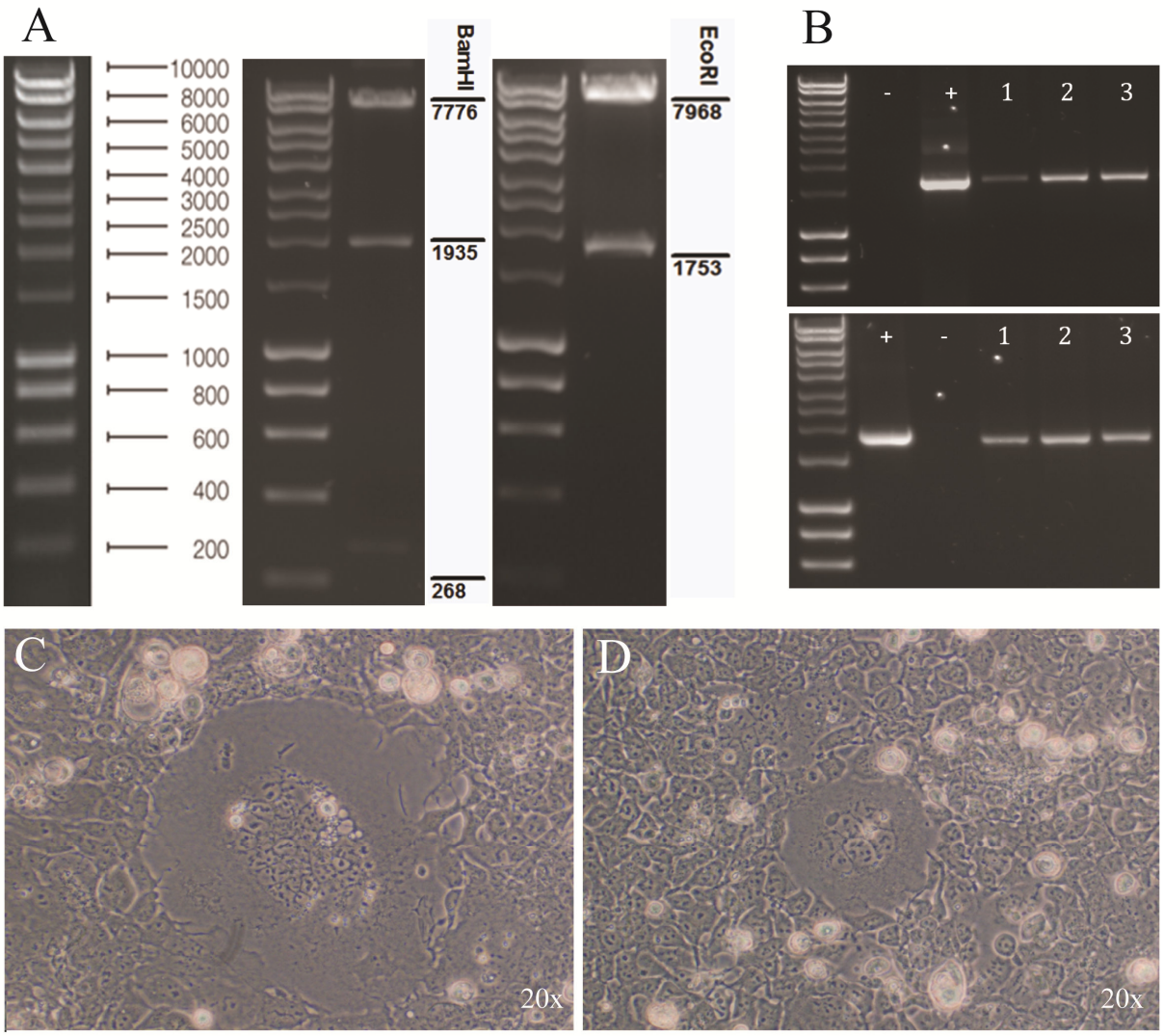


Figure 8.5. – Engineering and characterising lentiviral constructs and stably transduced cell lines where the expression of the F and H genes is controlled by a tetracycline-response promoter. Separate lentiviral plasmids were engineered to contain the surface glycoproteins F and H under the control of a TetR-responsive promoter. F and H genes were cloned into a parental pLVX vector with either puromycin (for pLVX-F) or blasticidin (for pLVX-H) resistance and this was confirmed by restriction digest with BamHI for F and EcoRI for H (A). Lentiviruses were produced and then used sequentially to infect 293A cells. The resulting 293A-pTightF-pTightH stable cell lines could be grown in the presence of both puromycin and blasticidin. PCR amplification (B) was performed to ensure the presence of the F and H transgenes these cell lines (three representative cell lines are labelled 1-3). Transient transfection of pLVX-F and pLVX-H, and CMV-TetR plasmids in 293A cells gave syncytia in the presence of 2500 ng/µL doxycycline (C). 293A-pTightF-pTightH cell lines produced smaller syncytia when transfected with CMV-TetR in the presence of 2500 ng/µL of doxycycline (D).

8.3.4. Attempts at MV-CSP, MV-gp100, and MV-Her2 rescue in a tetracycline inducible MV glycoprotein expression cell line

To examine whether these cell lines with F and H expression under the control of a TetR promoter could be used to rescue MV-CSP-TetR, MV-gp100-TetR, and MV-Her2-TetR, cell lines were infected with VV-T7 and then transfected with each MV construct alongside CMV-driven N, P, and L plasmids. GFP positive cells were observed from 24 hours post-transfection (figure 8.6.A-D), indicating that positive-sense MV RNA was being transcribed from plasmids by T7. GFP-positive cells were observed at a similar frequency to rescue of the unmodified MV-GFP using the same VV-T7 system in 293A cells. However, with MV-GFP – which retains its own F and H glycoproteins – GFP-positive cells rapidly developed into GFP-positive syncytia (figure 8.3.D-E). When GFP-positive cells were harvested from MV-CSP-TetR, MV-gp100-TetR, and MV-Her2-TetR -transfected wells and added to fresh confluent monolayers, no further GFP positive cells were seen (data not shown). Taken together, these data show a functional rescue system for viruses that retain their tropism-endowing F and H glycoproteins, but not for tropism-ablated MV-CSP-TetR, MV-gp100-TetR, and MV-Her2-TetR which rely on the expression of F and H *in* trans from an inducible system to form syncytia and spread.

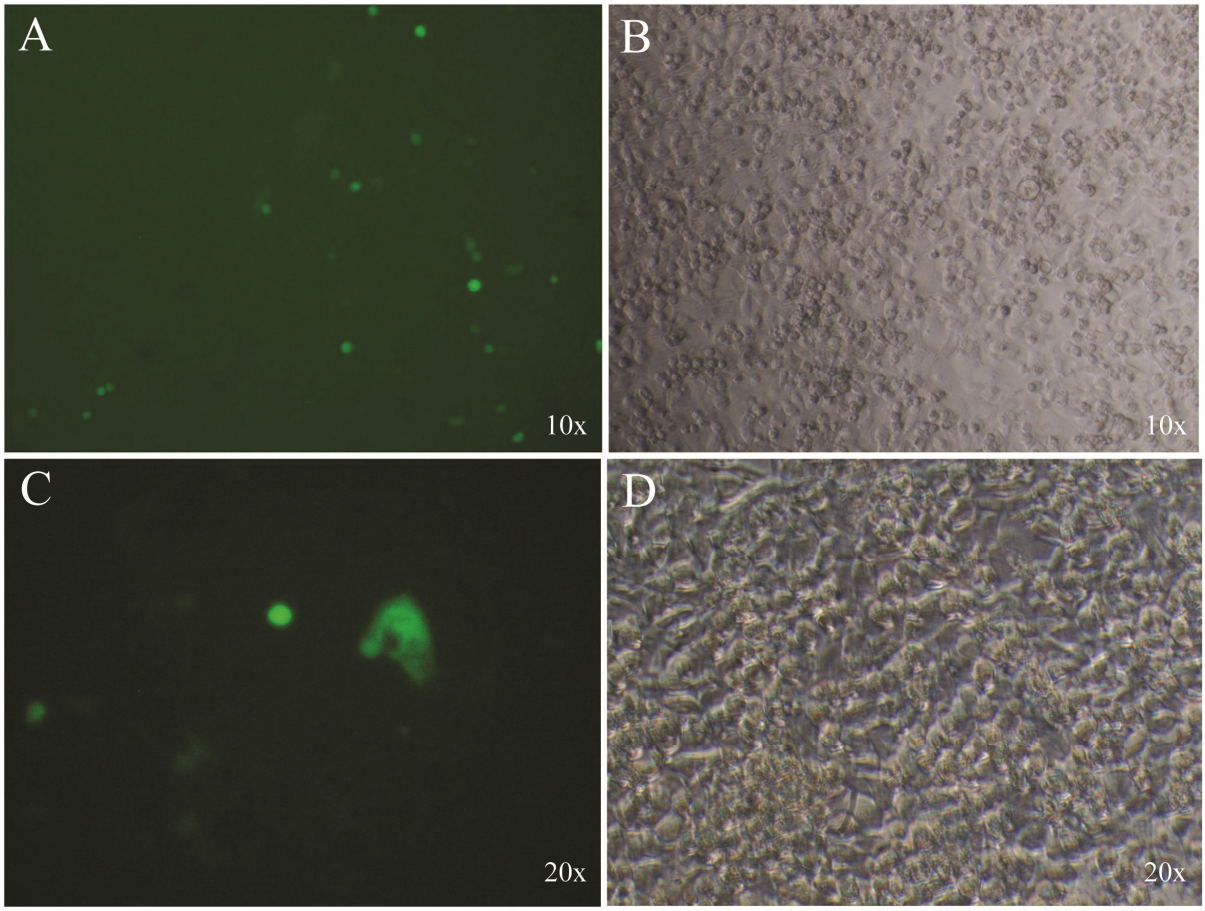


Figure 8.6. Overview of rescue attempts of MV-CSP-TetR, MV-gp100-TetR, and MV-Her2-TetR in TetR inducible F and H expression cell lines. Six-well plates containing 293A cell lines stably transduced with LVX-F and LVX-H were infected with VV-T7 (MOI = 1) and then transfected with expression plasmids for N, P, and L, alongside the full length pMV-gp100-TetR (A) and (B) or pMV-CSP-TetR (C) and (D). The media included 2500ng/mL of doxycycline, along with 40µg/mL AraC to inhibit VVT7 growth. Images were taken 120 hours post-infection/transfection.

8.3.5. Development and characterisation of an alternative rescue cell line based on the Cre-loxP system

An alternative rescue and propagation cell line was devised based on Cre-loxP technology (figure 8.7). Here, F was constitutively expressed under a CMV-promoter. H, however, would only be expressed after the excision of a loxP-flanked RFP-PolyA insulator sequence found between the CMV promoter and the H gene (figure 8.8.A). MV-CSP-TetR, MV-gp100-TetR, and MV-Her2-TetR were modified to replace TetR with the gene encoding Cre recombinase (data not shown). The resulting constructs were denoted 'MV-CSP-Cre', 'MV-gp100-Cre', and 'MV-Her2-Cre'.

The ability of Cre recombinase to excise the loxP-flanked RFP-PolyA sequence was confirmed by co-transfection of 293A cells with a CMV-loxPRFP-PolyAloxP plasmid and

either a CMV-empty vector or CMV-Cre (figure 8.8.B-D). In the presence of Cre, the RFP fluorescence was markedly reduced. Next, a construct was produced where the gene for GFP was encoded downstream of the loxP-flanked RFP where the MV H gene would ultimately be encoded. GFP and RFP expression were measured 24 hours after co-transfection of this construct with either a CMV-empty vector or CMV-Cre plasmid (figure 8.8.E). Again, a Cre-mediated reduction in RFP expression was observed. GFP expression increased in the presence of Cre.

Plasmid constructs with SV40 origins of replication and puromycin or hygromycin resistance cassettes were engineered to contain the F gene under a CMV promoter or the H gene following a CMV-driven loxPRFP-PolyAloxP insulator sequence. The ability of Cre to excise this loxP-flanked insulator sequence was again confirmed by assessing RFP expression after transient co-transfection of 293A cells with CMV-loxPRFP-PolyAloxP-H-BlastR and CMV-F-PuroR plasmids along with either a CMV-empty vector or CMV-Cre plasmid (figure 8.9.A). Sequential transfection of 293A or 293T cells with these constructs and passage with the appropriate selection antibiotic gave dual-transduced cell lines resistant to both puromycin and hygromycin designated ‘CMVF-loxPH’. These cells were transfected with CMV-empty, CMV-Cre, or CMV-H plasmids. Syncytia formation was monitored by microscopy over the next 72 hours. Small syncytia were visible in CMV-Cre transfected wells (8.9.B-C), but noticeably more syncytia were visible in CMV-H transfected cells (8.9.D-E).

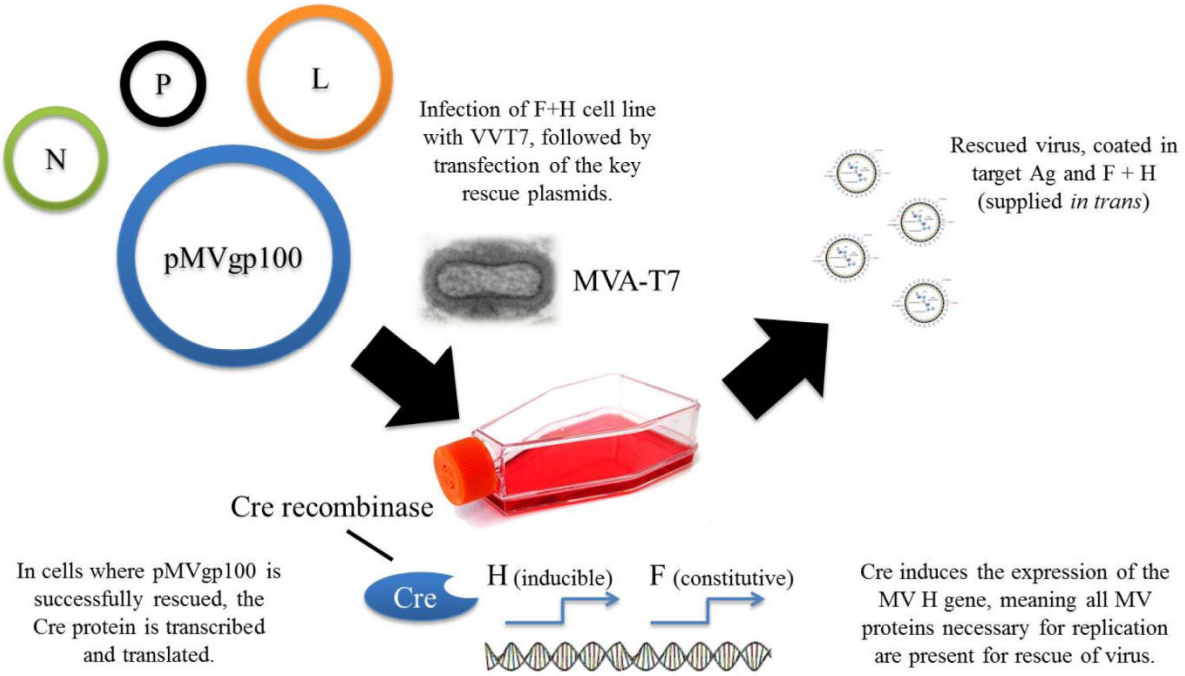


Figure 8.7. Overview of the rescue of tropism-ablated vaccine constructs in a cell line that provides F and H *in trans* using Cre-loxP technology. F is constitutively expressed, while H is only expressed following Cre-mediated excision of a loxP-flanked insulator RFP sequence. Cre is encoded in the measles virus anti-genomic cDNA. Modified Vaccinia Ankara expressing T7 (MVA-T7), which cannot replicate efficiently in mammalian cells, was used to deliver T7. Translation of viral genes following T7-driven transcription will result in the production of Cre recombinase, which can act to induce H expression from the genome of the cell line. Temporarily infectious virus is produced by coating with F and H, allowing propagation *in vitro*. When passaged once on normal cells, only non-infectious virus with target antigen on its surface will be produced.

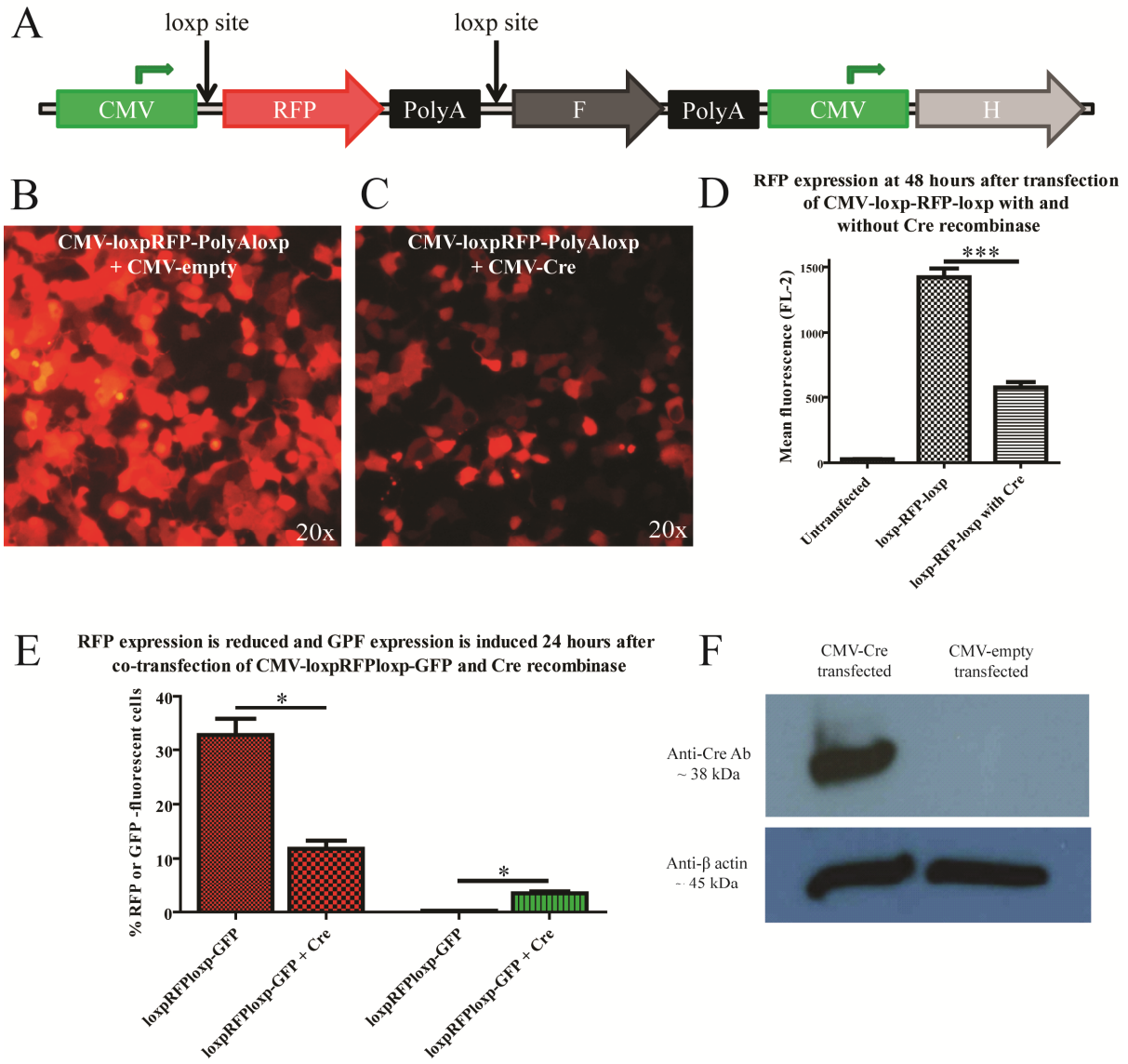


Figure 8.8. Characterisation of Cre-loxP inducible systems with reporter genes. A system where F was constitutively expressed and H could be induced by the excision of a loxP-flanked RFP-PolyA gene was devised (A). RFP-expression was assessed by microscopy (B) and (C) and flow cytometry (D) 24 hours after transfection of 293A cells with a CMV-loxPRFP-PolyAloxP plasmid and either a CMV-empty vector (B) or CMV-Cre (C). A plasmid was engineered with the gene for GFP downstream of the CMV-loxPRFP-PolyA-loxP cassette. 24 hours after transfection of 293A cells with this plasmid, flow cytometry was performed to measure the effect of co-transfecting CMV-Cre or CMV-empty on RFP and GFP expression (E). Cre expression was confirmed by Western blotting using 293A cell lysate 24 hours after transient transfection of CMV-Cre (F).

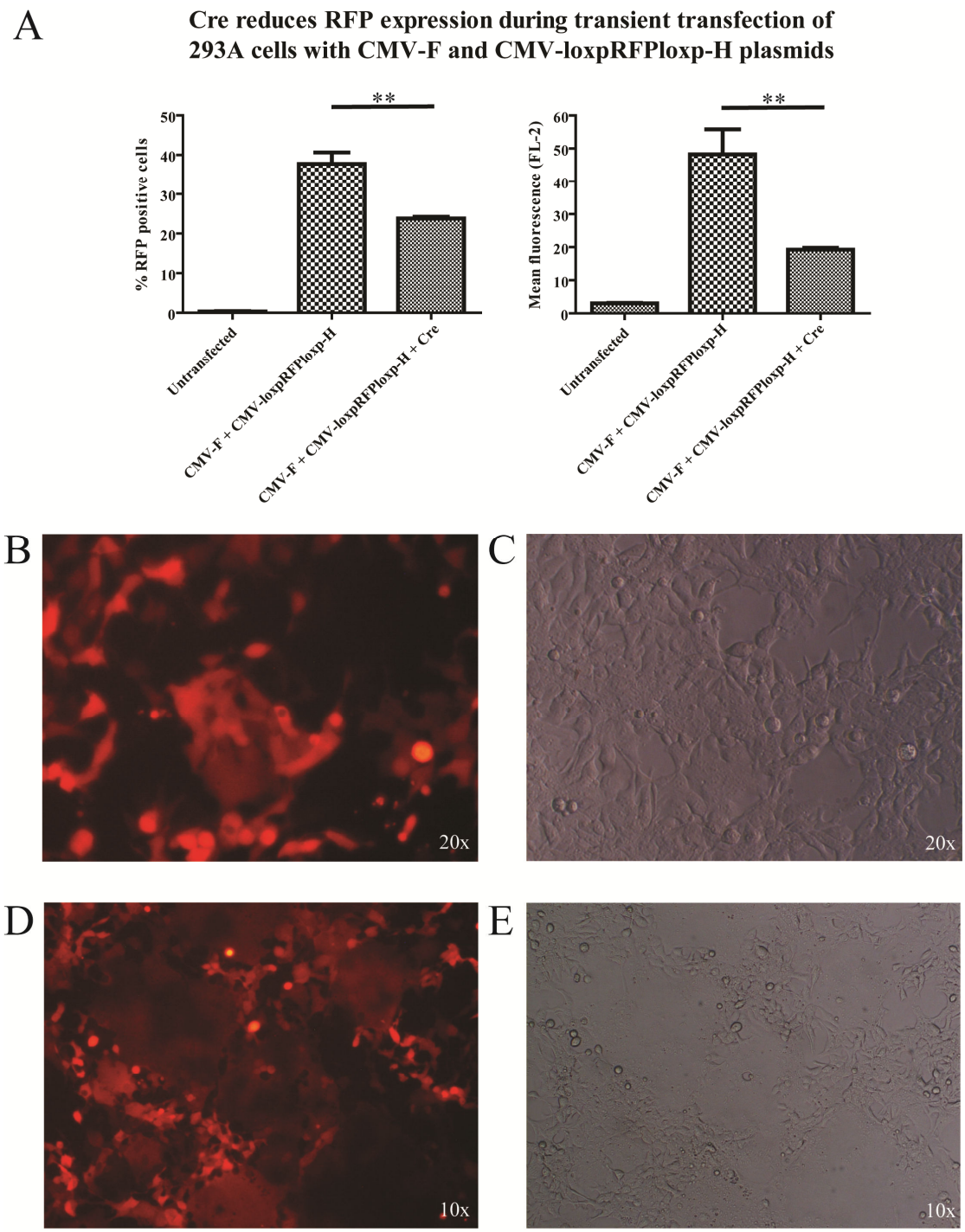


Figure 8.9 Characterisation of cell lines with constitute F expression and Cre-loxP inducible H expression. Six-well plates containing plasmid construct was engineered with a CMV promoter followed by loxP-flanked RFP-PolyA, then the gene encoding MV H and then a blasticidin resistance cassette (CMV-loxPRFP-PolyAloxP-H-BlastR). A separate plasmid encoding the MV F gene under a CMV promoter with a puromycin resistance cassette was also produced (CMV-F-PuroR). 293A cells were transiently transfected with these plasmids alongside CMV-Cre or CMV-empty vectors. RFP expression was assessed at 48 hours by flow cytometry and the percentage of FL-2 positive cells and the mean fluorescence intensity of cells were recorded (A). 293A and 293T cells were sequentially transfected with these F and H plasmids and stably transduced cells were selected with puromycin and blasticidin. The resulting cell lines (data shown from 293A cell lines) were transfected with CMV-Cre (B) and (C) and a CMV-H expression construct (D) and (E). Syncytia formation was monitored of the next 72 hours and representative images shown here are from 48 hours post-transfection.

8.3.6. Attempts at MV-CSP, MV-gp100, and MV-Her2 rescue in an inducible MV glycoprotein expression cell line based on a Cre-loxP system

Next, the usefulness of cell lines with constitutive F expression and H only in the presence of Cre recombinase promoter in rescuing MV-CSP-Cre, MV-gp100-Cre, and MV-Her2-Cre was assessed. 293A-CMVF-loxPH and 293T-CMVF-loxPH cell lines were infected with MVA-T7 and then transfected with each MV construct alongside CMV-driven N, P, and L plasmids. Small GFP-positive syncytia were observed from 48 hours post-transfection (figure 8.10) but these did not spread throughout the monolayer. GFP-positive syncytia were harvested and added to fresh confluent monolayers but no new GFP-positive cells were seen (data not shown). These studies suggest that this Cre-loxP cell line is inadequate for the rescue and propagation of MV-CSP-Cre, MV-gp100-Cre, and MV-Her2-Cre.

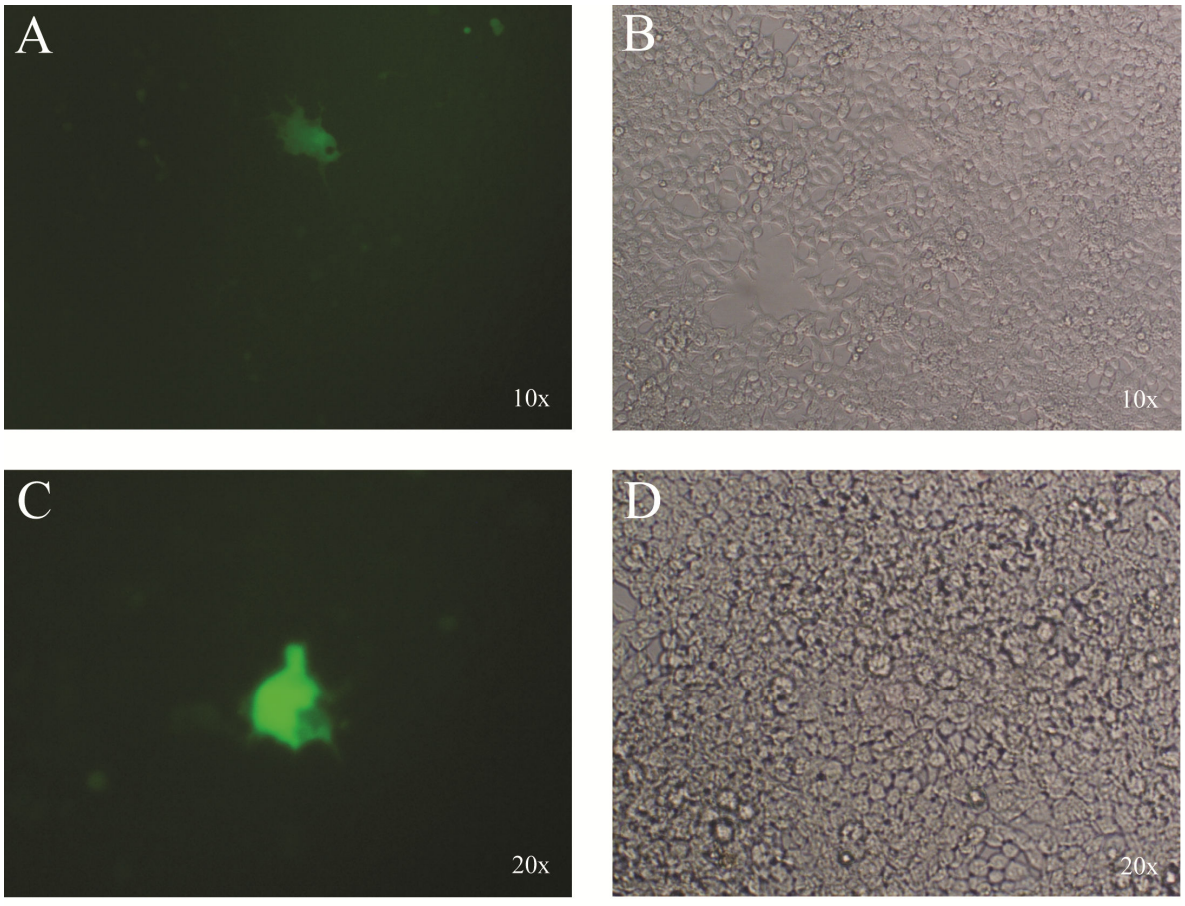


Figure 8.10. Overview of rescue attempts in cell lines with constitute F expression and Cre-loxP inducible H expression. Six-well plates containing 293A-CMVF-loxPH cells were infected with MVA-T7 (MOI = 1) and then transfected with CMV-driven expression plasmids encoding N, P, and L, alongside the full length pMV-CSP-Cre (A) and (B) or pMV-gp100-Cre (C) and (D). Images (A) and (B) were acquired 24 hours post-transfection, whereas (C) and (D) were acquired 72 hours post-transfection.

8.3.7. Production of MV-RFP as a modified version of the Edmonston vaccine strain of MV

An alternative strategy where MV particles were produced with F and H glycoproteins intact and then subsequently modified to attach a target antigen was considered. A strain of MV where the GFP reporter gene was replaced with RFP was engineered (data not shown). MV-RFP was rescued in VERO cells by infection with MVA-T7 and transfection of MV-RFP alongside CMV-driven N, P, and L expression plasmids. RFP syncytia were readily observable and a single syncytium was picked and propagated on VERO cells before harvest and purification with an iodixanol gradient (section 2.7.3).

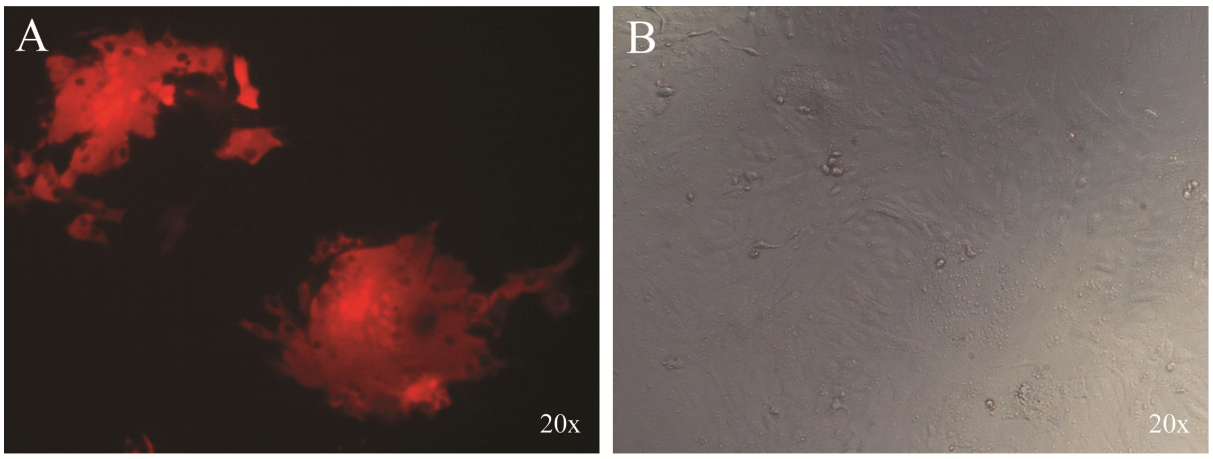


Figure 8.11. Rescue of MV-RFP from cDNA. Six-well plates containing VERO cells were infected with MVA-T7 (MOI = 1) and then transfected with CMV-driven expression plasmids encoding N, P, and L, alongside the full length pMV-RFP. Images were 48 hours after transfer of an isolated MV-RFP colony onto uninfected VERO cells.

8.3.8. Labelling the surface of MV-RFP with FSL technology

Function-spacer-lipid (FSL) technology is a versatile tool for labelling the surface of cells and virus particles. Here, a FSL construct where the 'functional' group is a fluorescein molecule was shown to efficiently label 293A cells after incubation at 37°C for one hour (figure 8.12.A-B). Previously, flow cytometry had been used to characterise liposomal vaccine particles in the 100-300 nm range. Flow cytometry has been used by others to detect and count other viruses (Steen 2004)(Tesfay et al. 2013). The ability to detect the FSC/SSC profile of MV particles by flow cytometry was assessed. MV diluted in PBS gave a FSC/SSC pattern readily distinguishable from the background signal seen with PBS alone (figure 8.12.C). This population could be gated and the fluorescence of MV particles was measured after incubation with increasing concentrations of FSL-fluorescein constructs (figure 8.12.D).

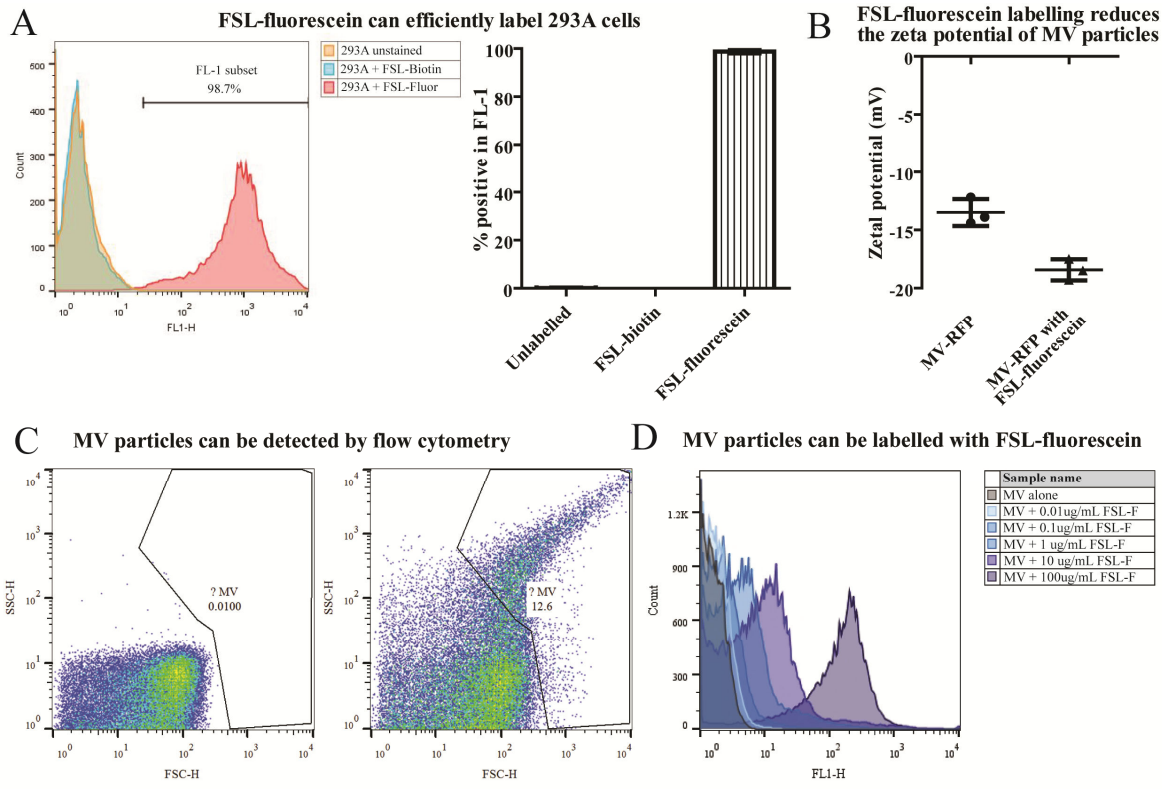


Figure 8.12. Modifying the surface of MV with FSL technology. 293A cells were incubated with 100 µg/mL FSL-fluorescein (FSL-F) or FSL-Biotin at 37°C for one hour. The fluorescence of cells was then measured by flow cytometry (A) and (B). The FSC and SSC profile of purified MV-RFP particles was assessed by flow cytometry (C). MV-RFP particles were incubated with increasing concentrations (0.01 – 100 µg/mL) of FSL-Fluorescein at 37°C for one hour. The fluorescence of viral particles was then measured by flow cytometry and the FL-1 signal in the MV-gated population is displayed in (D). FSL-Fluorescein constructs alone were studied by flow cytometry and did not give a signal detectable within the MV gate.

8.3.9. Modifying the surface of MV-RFP with CSP antigen

The labelling of 293A cells with a FSL construct where the 'functional' group was the CSP antigen was assessed. The presence of CSP on the surface of 293A cells labelled with FSL-CSP was readily detectable by flow cytometry following staining with anti-CSP antibody (figure 8.13.A-B). Next, MV-RFP particles were also labelled with FSL-CSP. After staining with anti-CSP antibody, CSP was also detectable on the surface of FSL-CSP labelled MV particles (figure 8.13.C-D). Unlabelled MV particles were also stained with anti-H antibody to confirm that MV surface proteins could be detected using this technique (figure 8.13.E). Lastly, the titre of MV-RFP viruses with and without FSL-labelling was assessed by TCID50 assay. There was no difference in titre between unlabelled, FSL-Fluorescein labelled, and FSL-CSP labelled MV-RFP viruses (figure 8.13.F).

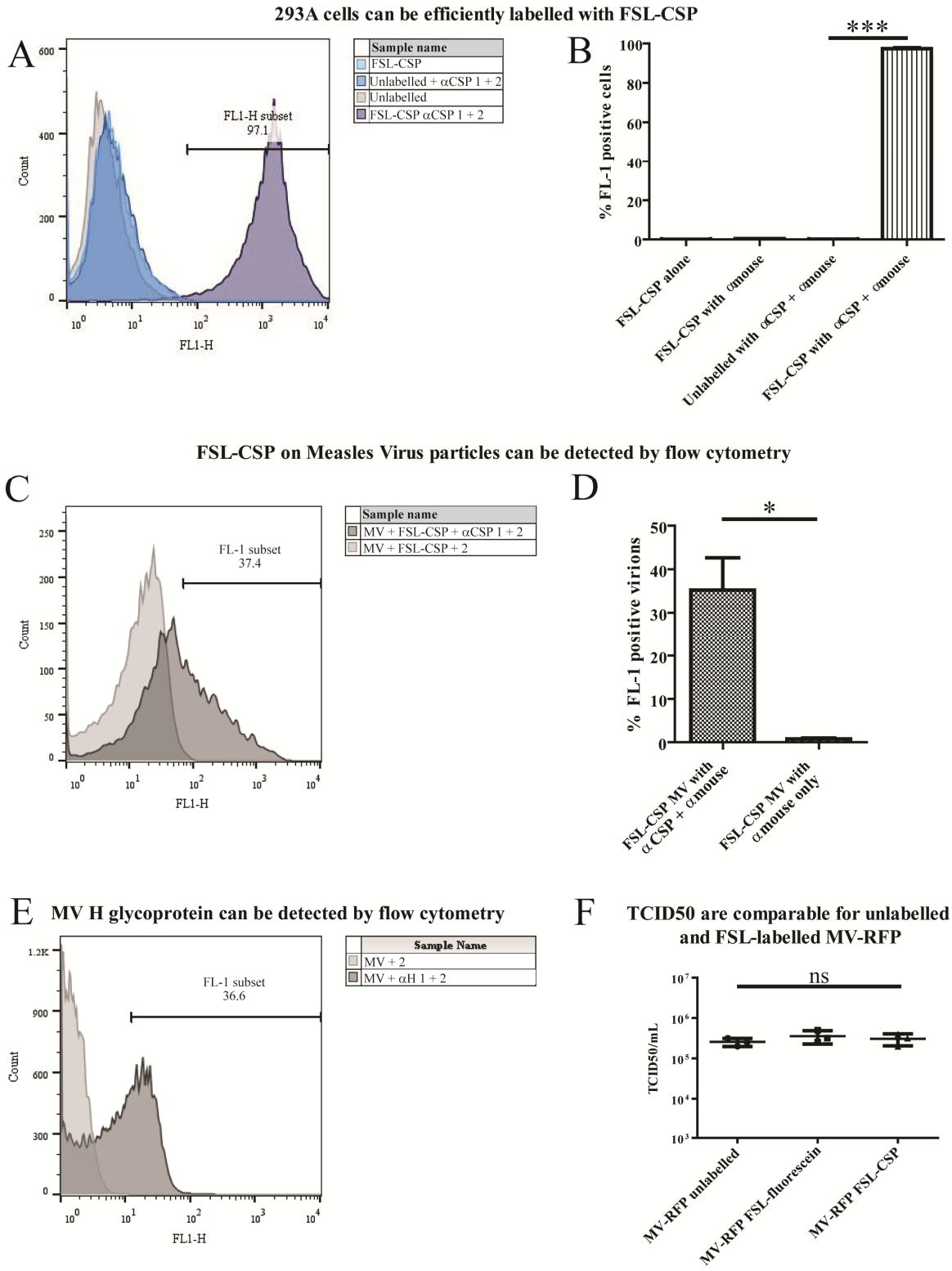


Figure 8.13. Modifying the surface of MV with FSL-CSP. 293A cells and MV-RFP viral particles were incubated with 100 µg/mL of FSL-CSP for one hour at 37°C. Cells or viral particles were then stained with the anti-CSP mAb 2A10 and a FITC-labelled anti-mouse secondary antibody. The fluorescence of FSL-CSP labelled cells (A) and (B) and MV particles (C) and (D) was measured by flow cytometry. The fluorescence of MV-RFP stained with anti-H mAb and a FITC-labelled anti-mouse secondary antibody was also measured (E). The infectivity of MV-RFP labelled with FSL-Fluorescein and FSL-CSP was measured by TCID50 (F).

8.3.10. Pilot in vivo studies exploiting pre-existing anti-MV immunity to enhance responses to CSP

The immune response to MV-RFP-CSP was assessed in mice pre-vaccinated with MV-RFP or PBS in TMG. First, the immune response to MV-RFP + TMG vaccination was characterised. CD4+ responses were measured by ELISPOT to three different MV antigens – a mosaic H protein, purified N protein, or MV-RFP lysate. IFNγ responses to all three antigens were readily detectable in MV-RFP + TMG vaccinated mice (figure 8.14.B). In contrast, IL-4 responses were only detectable in splenocytes from MV-RFP + TMG vaccinated mice that were stimulated with purified N protein or MV-RFP lysate (figure 8.14.C). IFNγ responses were of a significantly higher magnitude than IL-4 responses for mosaic H protein ($p = 0.0001$), purified N protein ($p = 0.0046$), and MV lysate ($p = 0.0035$).

Finally, mice pre-vaccinated with PBS or MV-RFP in TMG were administered MV-RFP-CSP (figure 8.14.A). To test the over-arching hypothesis of exploiting non-cognate CD4+ T cell help in the context of vaccine particles based on measles virus, the anti-CSP and anti-MV antibody responses were measured two weeks after vaccination. Both anti-CSP and anti-MV responses were higher in mice pre-vaccinated with MV-RFP + TMG (figure 8.14.D-E).

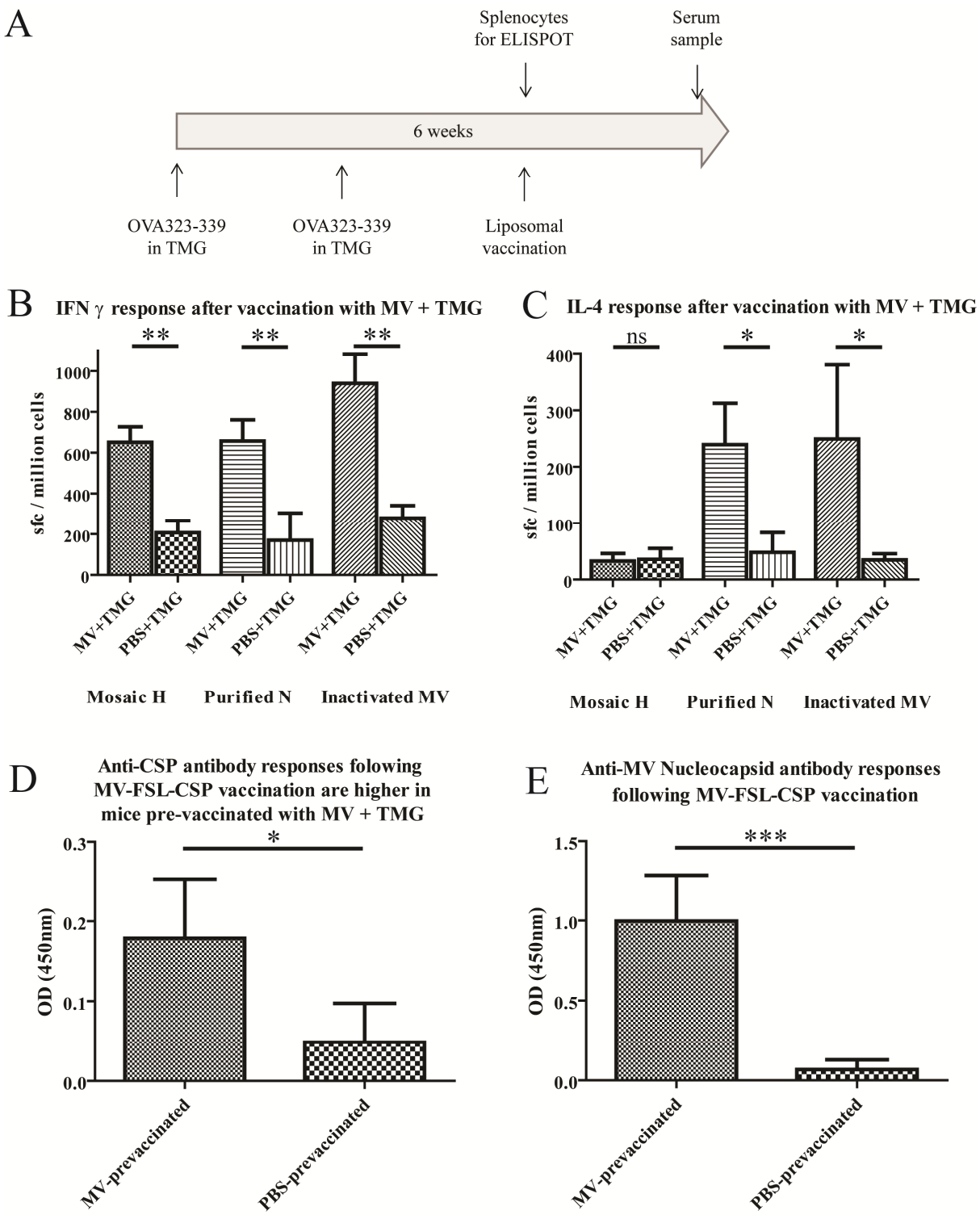


Figure 8.14. *In vivo* studies assessing the effect of pre-existing anti-MV immunity on the immunogenicity of MV-RFP-CSP. 6-8 week old female C57Bl/6 mice were vaccinated twice with either PBS or MV-RFP ($1x10^4$ TCID50 units) in TMG subcutaneously, with two weeks between doses. Two weeks after the second vaccination, splenocytes were harvested from vaccinated mice (n=3) and pulsed with either mosaic H antigen, (1 µg/mL), purified N antigen (1 µg/mL), or MV lysate (10 µg/mL). IFNγ (B) and IL-4 (C) responses were measured by ELISPOT and are displayed as spot forming colonies per million splenocytes. Two weeks after their second vaccination, mice (n=4) were administered 100 µL (approximately $2 x10^4$ TCID50 units) of MV-RFP labelled with FSL-CSP subcutaneously. Antibody responses to CSP (D) and purified N protein (E) were measured by ELISA. Means were compared with unpaired, two-tailed, t tests.

8.4. Chapter conclusions

1. Genetically modified MV plasmids where the F and H glycoproteins were replaced with a single chimeric F protein displaying the extracellular domain of CSP, gp100, or Her2 were produced. Two different inducible cell lines were trialled to provide the F and H glycoproteins *in trans* during virus rescue. It was not possible to rescue and propagate these tropism-ablated MV particles in either cell line.

2. Vaccine strains of MV expressing either GFP or RFP reporter genes were able to be rescued and propagated.

3. Purified MV-RFP particles could be used for vaccination to elicit anti-MV immune responses in mice.

4. Purified MV-RFP particles could be modified with FSL-CSP to display CSP on the particle surface.

5. Pre-existing anti-MV immunity could be exploited to enhance anti-CSP antibody responses following the administration of MV-FSL-CSP.

8.5. Discussion

8.5.1. Discussion of results

This chapter sought to modify the surface of MV particles to replace the native F and H glycoproteins with target B cell antigens CSP, gp100, and Her2. By genetically modifying MV, this strategy necessarily ablated the natural tropism of the virus. Consequently, two different strategies were employed to provide the tropism-endowing glycoproteins – F and H – *in trans* during viral rescue and propagation. Neither a tetracycline-responsive nor a Cre-recombinase-inducible expression system could facilitate viral rescue and propagation. This was despite the observation that small syncytia could be formed in both systems when gene expression was appropriately induced.

The reasons for these failures are not clear. It is possible that gene expression in both systems is not of sufficient magnitude to provide the number of glycoproteins necessary for viral packaging. Both systems use the ‘strong’ CMV promoter or a CMV variant. However, in

both cell line systems it is evident that induction of F and H expression is not optimal. Higher numbers of larger syncytia were observed by transient transfection using the pLVX tetracycline inducible system when compared with stably transduced cells (section 8.3.3, figure 8.5.C-D). Similarly, supplying the H gene from a CMV-H plasmid cell line gave markedly more syncytia than the level achieved by CMV-Cre transfection (section 8.3.5, figure 8.9.B-E). This may reflect the copy number of glycoprotein expression cassettes per cell, which could be lower for cell lines stably transduced with lentiviral vectors or plasmids. Studies using fluorescent reporter genes demonstrated that Cre-mediated induction of gene expression only reached low levels 24 hours post-transfection (figure 8.8.E), although it is possible that at later time points this expression level may have risen. Problems with F and H expression may be temporal. MV infection would ordinarily result in replication of the viral genome and then extensive production of structural on non-structural proteins from the positive-sense RNA strand. The timing of these events in a wild-type infection – or even *in vitro* rescue from plasmid DNA – may be significantly different from a rescue system where F and H are provided *in trans* from an inducible cell line.

Genetically modified particles could not be produced to test the hypothesis that pre-existing anti-MV immunity would enhance antibody responses to non-cognate surface antigens. Consequently, a strategy of chemically modifying purified particles of MV was adopted. Molecules with a CSP antigen, a spacer, and a lipid tail (FSL-CSP) were used to label the surface of purified MV-RFP without changing the expression of F and H glycoproteins. The anti-CSP response to these particles was higher in MV-RFP + TMG pre-vaccinated mice when compared with PBS + TMG mice, supporting the hypothesis that pre-existing anti-MV CD4+ T cells could enhance antibody responses to MV surface-bound CSP.

8.5.2. Limitations and future directions

Chemical modification of the surface of MV-RFP particles carries significant limitations. Crucially, it does not remove the native F and H glycoproteins. Therefore, these glycoproteins may dominate the humoral immune response to MV-RFP-CSP particles. One strategy could be to remove the F and H glycoproteins by trypsin digestion of viral particles before purification and subsequent labelling with FSL-CSP. Another strategy would be to coat viral particles with a protective polymer coat to shield surface glycoproteins and then to conjugate target antigens to this protective layer. Both of these approaches may allow the

production of large numbers of viral particles, but minimise the number of non-target antigens that are available for B cell binding on the particle surface.

In this chapter, the rescue and propagation of a tropism-ablated negative sense RNA virus was not possible, despite efforts to provide tropism-endowing glycoproteins *in trans*. Other viral vectors could be exploited to develop vaccines that exploit pre-existing non-cognate CD4+ T cell help. Positive sense RNA virus vaccines (e.g. rubella virus, yellow fever virus, etc) could be modified to replace surface glycoproteins with chimeric proteins displaying target antigens on the particle surface. In contrast to negative sense RNA viruses like MV, positive sense RNA viruses do not face the same barriers to rescue from cDNA (Racaniello & Baltimore 1981). Plasmid DNA encoding the full-length positive sense viral genome or RNA produced by *in vitro* transcription can be transfected into cells where it is readily translated and replicated to produce viral particles (Neumann et al. 2002).

Retroviral vectors could also be modified to produce immunogenic viral particles. Retroviruses could be engineered to replace surface glycoproteins with chimeric constructs to display target antigens on the particle surface. These genetically modified retroviruses could then be pseudotyped to permit the infection of producer cell lines. Once integrated in the producer cell line genome, the viral genome would be transcribed and translated to give constant production of viral particles with target antigen on their surface. To improve the immunogenicity of these particles, core proteins could be fused to immunodominant CD4+ epitopes (e.g. OVA323-339, MCMV m09, universal helper epitopes from tetanus toxoid, etc) to exploit powerful pre-existing CD4+ T cell responses.

9. Discussion:

9.1. Summary and discussion of results

9.1.1. Exploiting pre-existing non-cognate CD4+ T cells

This thesis describes particle vaccine platforms designed to exploit pre-existing non-cognate CD4+ T cell help to enhance antibody responses to target antigens. First, liposomal particles were produced with spatially segregated B and CD4+ T cell antigens from CSP and ovalbumin, respectively. These CSP(OVA323-339) liposomes were engineered to display B cell antigens on the particle surface and to encapsulate epitopes for presentation on B cell MHCII in the particle core. Mice pre-vaccinated with OVA323-339 mounted higher and faster anti-CSP antibody responses after vaccination with CSP(OVA323-339) liposomes, indicating that pre-existing CD4+ T cells recognising OVA323-339 could support anti-CSP B cells to produce antibody. It was also demonstrated that this pre-existing immunity did not need to be induced at the same anatomical site where the liposomal vaccine would subsequently be administered. This is important observation from a translational perspective, where it would be more desirable to exploit pre-existing systemic immunity than to vaccinate patients to specifically to elicit local CD4+ T cell responses.

Pre-existing non-cognate CD4+ T cells did not only affect the anti-CSP antibody response quantitatively, but also had a qualitative effect. OVA323-339 pre-vaccinated mice mounted higher affinity anti-CSP antibody responses that were isotype-switched more rapidly, with the profile of this response dominated by the 'T_H1 isotype' IgG2c. This observation is in keeping with data demonstrating a T_H1-polarised immune response to OVA323-339. It is appealing to consider that, by electing to exploit specific pre-existing CD4+ T cell populations, it might be possible to use this vaccine platform to generate responses of a desired isotype to target antigens.

Responses to OVA323-339 were not readily detectable after CSP(OVA323-339) administration to PBS + TMG pre-vaccinated mice. This is an important finding as it suggests that, in contrast to the situation with conjugate vaccines or RTS,S, these liposomal vaccine particles successfully sheltered the helper antigen in the particle core, focusing the humoral immune response on the target antigen CSP. Another interesting observation was

that – in the presence of CD4+ T cell immunity – the liposomal vaccine dose could be reduced 125-fold before anti-CSP responses were comparable to those seen in PBS pre-vaccinated mice administered a standard CSP(OVA323-339) vaccine dose (i.e. 125 times more CSP-coated vaccine). This may indicate that, in the context of this vaccine approach, CD4+ T cell responses are limiting. Consequently, particle vaccines engineered to exploit pre-existing CD4+ T cell responses may be able to be used at lower doses without a reduction in immunogenicity, which could relieve pressures that result from the need to manufacture high titre vaccines.

9.1.2. Modifying the vaccine platform to make particles 'self-adjuvanting'

These liposomes provided signal one (BCR binding) and signal two (CD4+ T cell help) to B cells to elicit a humoral antibody response. TLR agonism is now recognised as an important third signal in fully-developed antigen specific B cell responses (Ruprecht & Lanzavecchia 2006). With this in mind, vaccine particles were modified to include the TLR9 agonist CpG DNA. It was demonstrated that the inclusion of CpG DNA increased the magnitude of anti-CSP antibody responses. Combining TLR9 agonism with pre-existing non-cognate CD4+ T cell immunity resulted in additive enhancement of anti-CSP responses. The inclusion of CpG also altered the isotype profile of the anti-CSP antibody response, favouring the production of IgG2c. The highest total antibody response and the isotype profile with the greatest T_H1 bias were both seen in mice with pre-existing anti-OVA323-339 CD4+ T cell immunity that were subsequently vaccinated with CSP(OVA323-339 + CpG) liposomes.

The initial liposomal particle composition used in this thesis was selected for stability and safety *in vivo*, rather than for immunogenicity. In fact, lipids used to formulate these liposomes are often used for the delivery of drugs intravenously, where immunologically inert lipids are needed (Ming-Kung 2012). Given that immunogenicity was not prioritised in the design of these liposomes, and that liposomal engineering affords much flexibility, it is likely that far more immunogenic liposomes retaining desirable properties such as stability, size, and charge could be produced. Strategies to achieve this could include screening potential lipids for immunogenicity or incorporating additional TLR agonists in the lipid bilayer or liposome core.

9.1.3. Exploiting pre-existing anti-viral immunity

Chronic viral infection can elicit extremely high frequency T cell responses. One third of HCMV-infected adults have HCMV-specific T cells comprising >20% of their circulating CD4+ and/or CD8+ memory T cell repertoire. Cells that recognise one HCMV epitope can represent 0.3-1.5% of the total peripheral CD4+ T cell population (Weekes et al. 2004). Accordingly, this is an extremely attractive T_H cell response to exploit in vaccine design. . MCMV infection in mice is a good model for HCMV and animals infected with MCMV have similarly large numbers of CD4+ and CD8+ T cells directed against viral epitopes. A CD4+ T cell epitope – m09 – that dominates the response in chronic MCMV infection has recently been described (Arens et al. 2008). In MCMV-infected mice, CD4+ T cells recognising the immunodominant m09 epitope could drive faster and higher anti-CSP antibody responses to CSP(m09) liposomes when compared with uninfected controls. Additionally, in keeping with the T_H1-biased immune response to the viral m09 epitope, a large amount of anti-CSP IgG2c was produced in MCMV-infected mice. These results are the first demonstration that pre-existing CD4+ T cell responses to CMV can be specifically harnessed to enhance antibody responses to non-cognate target antigens. This could have important implications for the design of vaccines with optimal immunogenicity in populations with a high HCMV seroprevalence (section 9.2.2).

9.1.4. Breaking tolerance to self-antigens

Cancer vaccines face considerably different challenges to vaccines for infectious diseases. Cancer antigens are often protected by immunological self-tolerance mechanisms and vaccine strategies must overcome or bypass these. Pilot studies with liposomes coated with the full-length murine Erbb2/neu cancer antigen revealed that the vaccine platform developed in this thesis was capable of eliciting antibody responses to Erbb2/neu. While these results are promising from a proof-of-principle perspective, there is much room for improvement. Future work should seek to coat particles with specific B cell antigens from cancer antigens that are recognised by efficacious mAb therapies (section 9.2.1) and *in vivo* studies should be performed with particles that are better characterised with regards to cancer antigen display on the particle surface.

9.1.5. Modifying viral vectors to display target antigens

Given that many current vaccines elicit significant CD4+ T cell responses, an appealing strategy would be to modify the surface of a currently licensed vaccine to exclusively display target antigens. In this thesis, considerable efforts were made to genetically modify and then grow the Edmonston strain of MV with target antigens in place of its native glycoproteins. Despite efforts to provide these glycoproteins *in trans* from inducible cell lines, attempts to rescue and propagate these genetically modified viruses were unsuccessful. Consequently, an inferior strategy where the surface of vaccine strain particles – with F and H glycoproteins *in situ* – were modified with CSP antigen using lipid labelling technology was adopted. This allowed a brief study demonstrating that mice pre-vaccinated with MV-RFP mounted higher anti-CSP antibody responses to vaccination with MV-RFP-CSP. However, this approach is far from optimal as it does not remove the MV surface glycoproteins, rendering it unable to focus the immune response on the target antigen. Future – and potentially far more elegant – work on modifying viral vectors to test the hypothesis of this thesis could be undertaken with viruses more amenable to surface glycoprotein modification, rescue, and propagation, such as yellow fever or rubella virus.

9.2. Final discussion and future directions

9.2.1. Future directions for this vaccine platform

A logical initial extension of this work would be to further study the efficacy of the CSP(OVA323-339 + CpG) and CSP(m09 + CpG) vaccine approaches. Existing serum samples from immunised mice could be used for functional studies such as the *in vitro* inhibition of sporozoite invasion assay (Hollingdale et al. 1984). Rodent models of malaria using parasites transgenic for *Plasmodium falciparum* CSP could be used to assess protective efficacy *in vivo* (Persson et al. 2002). Existing serum samples could also be used to measure antibody responses to non-protein vaccine components such as cholesterol and PEG. While these responses were not the goal of the current project, it is interesting to consider whether anti-lipid responses might be generated by this platform and whether they could have therapeutic utility – such as in the management of hypercholesterolaemia. However, the most fruitful direction to take this research may be away from the studies conducted with model antigens in this thesis towards targets chosen in light of the data presented here. There are areas of unmet vaccine need where an optimised form of this vaccine platform could be useful. Possible targets include protein, peptide, and carbohydrate antigens.

This thesis demonstrates that, by exploiting pre-existing non-cognate CD4+ T cells, rapid antibody responses can be generated to target antigens. In fact anti-CSP IgG antibody levels generated in the context of OVA323-339 immunity reached their peak at the earliest time point (one week) after vaccination (figure 4.7). While the response kinetics vary for different vaccines, IgM responses typically peak around one week post-vaccination whereas IgG responses take two to three weeks to reach their peak (Hovden et al. 2005). Any future studies should consider taking earlier serum samples to better characterise antibody response kinetics. It would be interesting to consider antigens from specific infectious disease threats that might be attractive targets for a rapid response vaccine and to test the immunogenicity of liposomal vaccine particles coated with relevant target antigens.

Broadly neutralising antibodies are a key goal of vaccine design in diseases such as influenza and HIV infection (Hedestam et al. 2008). In addition to testing this vaccine platform's usefulness in generating responses to conventional influenza glycoproteins, it would be interesting to assess whether it could generate responses to epitopes recognised by broadly neutralising anti-influenza antibodies. Broadly neutralising antibodies (bNAb) that bind the

conserved influenza haemagglutinin stem region or, less frequently, epitopes in the globular head of haemagglutinin have been described. Immunogens have now been reported that either represent bNAb binding sites or that are capable of eliciting bNAb responses *in vivo* (Krause et al. 2011)(Mallajosyula et al. 2014). Vaccine particles could be engineered to exploit pre-existing CD4+ T cell immunity to generate rapid immune responses to these antigens. This would require antigens to be displayed in the appropriate conformation on the vaccine particle surface for BCR binding, but a flexible platform such as a liposomal particle could be well-placed to achieve this. If successful, there are numerous other diseases, such as Dengue and HIV, where broadly neutralising mAbs have been identified but more work is needed to translate these findings into effective vaccines.

Lastly, this vaccine platform exploits an immunological mechanism of action which could bypass one aspect of immune-tolerance to cancer antigens; by co-opting non-cognate CD4+ T cells it may be able to elicit anti-cancer antibody responses. Preliminary data generated in this thesis using the entire extracellular domain of murine Erbb2/neu support this hypothesis. However, there is much room for optimisation. It is possible that displaying smaller B cell epitopes from cancer antigens – such as the dimerization domain of Erbb2/neu that is the target of the mAb Pertuzumab – could elicit efficacious antibody responses. Investigating this possibility should be a priority for future work.

9.2.2. Broader applications of this thesis

The vaccine particles used in this platform were engineered to allow the testing of a hypothesis, rather than to be optimal vaccine constructs in terms of vital parameters like B cell antigen spacing, antigen dose, and innate immune stimulation. Therefore, while one approach to progressing this project would be optimisation of the current vaccine platform (section 9.2.1), another approach is to look at how the work in this thesis could influence other approaches to vaccine design.

Modifying existing viral vaccine technologies that have established immunogenicity and safety profiles is an attractive strategy. It has long been know that CD4+ T cell responses to core viral epitopes can enhance antibody responses to envelope glycoproteins in the context of influenza infection (Russell & Liew 1979)(Scherle & Gerhard 1986). Indeed, it was demonstrated that priming with core influenza components protected against lethal challenge – either suggesting a direct protective role for antibody or cellular responses to these core

components or perhaps the rapid generation of a protective antibody response in primed mice (Russell & Liew 1980). Nonetheless, prior to the work in this thesis, vaccine particles have not been rationally designed to exploit pre-existing non-cognate CD4+ T cells to enhance antibody responses to target antigens. There are, however, observations from vaccine trials which suggest this strategy would work well in the clinic.

Dengue vaccine development has been hampered by the requirement for an effective multivalent vaccine due to concerns about antibody dependent enhancement of infection if a vaccine failed to elicit protective responses to all four serotypes (Webster et al. 2009). A tetravalent vaccine (TDV) based on a vector from the related flavivirus yellow fever virus (YFV) is the most advanced agent undergoing evaluation. It comprises four different vaccine strains – each based on a YFV 17D vaccine particle pseudotyped with glycoproteins from one of the four Dengue virus (DENV) serotypes. In populations with high levels of immunity to the YFV vaccine, or YFV itself, this thesis would argue that pre-existing anti-YFV CD4+ T cell immunity should enhance antibody responses DENV glycoproteins. Encouragingly, this is exactly what has been observed in small immunogenicity studies (Qiao et al. 2011) and larger field trials (Guirakhoo et al. 2006)(Poo et al. 2011)(Capeding et al. 2014). Baseline immunity to YFV correlated with better antibody responses to DENV – even after one vaccine dose (Qiao et al. 2011). An important practical consequence of this observation is that, by exploiting pre-existing anti-YFV responses, protective anti-DENV antibody responses could be achieved with fewer doses of TDV vaccine.

As an alternative to liposomal vaccines, this thesis also attempted to replace the surface glycoproteins of the negative sense RNA measles virus with target antigens to exploit this phenomenon in the context of the widely used, immunogenic, and safe MV vaccine. However, the target antigens chosen did not endow the genetically modified MV with tropism for cells in tissue culture and it was not possible to rescue and propagate these vaccine constructs, despite attempts to provide MV glycoproteins *in trans*. The TDV vaccine discussed above does not suffer from these limitations as it is pseudotyped with glycoproteins that endow tropism and, as a positive sense RNA virus, is simpler to rescue *in vitro*. If this thesis was to stimulate further work modifying viral vaccine particles to display novel target antigens, careful consideration should be taken regarding the complexity of rescue systems required for genetically modified constructs and the influence of chosen target antigens on viral tropism.

Previously, this discussion has focused on altering a novel liposomal vaccine particle to refocus the immune response target B cell antigens. It is, however, worth considering what utility exploiting pre-existing non-cognate CD4+ T cell help could have in enhancing the immunogenicity and efficacy of existing technologies that target a range of different antigens. Viral vaccines, virus-like particles, and even more basic approaches such as recombinant protein vaccines, could be modified to incorporate strong CD4+ epitopes to co-opt pre-existing CD4+ T cells into providing helper signals. For example, there are numerous reports of internal viral proteins that can be tagged with fluorescent proteins to study their role during infection and this can be achieved without dramatically affecting viral titre (Lux et al. 2005). It follows, therefore, that core viral vaccine components could be tagged with immunodominant CD4+ T cell epitopes to exploit pre-existing immunity. In situations where vaccine responses are currently suboptimal – particularly if CD4+ T cell help might be a limiting factor – or where rapid responses are needed, this could be a powerful approach.

Technologies designed to exploit pre-existing CD4+ T cells also provide the alluring prospect of controlling vaccine-induced antibody responses by targeting a population of CD4+ T cells with a distinct phenotype. For example, strong IgG2a/IgG2c responses could be elicited by exploiting a pre-existing CD4+ T cell population with T_H1-polarisation. Further, consideration of what pre-existing CD4+ T cells dominate the lymphocyte pool in a given demographic could allow powerful vaccine responses to be induced. Perhaps the most obvious application of this principle would be in the design of immunogenic vaccines for elderly patients. While the precise immune defects are not characterised, vaccine responses are blunted in old age (Chen et al. 2009). Conversely, astonishingly large effector CD4+ responses to CMV are noted in healthy elderly adults (Vescovini et al. 2007). Vaccine technologies that exploit these anti-CMV CD4+ T cells to enhance responses could be uniquely well-equipped to elicit immune responses in elderly patients. Lastly, although quite distant from the work presented in this thesis, the utility of exploiting the cellular response to cytomegalovirus infection in elderly patients may not be limited to enhancing vaccine immunogenicity using strategies presented in this thesis. Anti-CMV immunotherapy approaches have been proposed for the treatment of cancers, but their usefulness has only been proposed in malignancies that express CMV epitopes (Schuessler et al. 2014). Theoretically, the specific delivery of immunodominant CD8 T cell epitopes to tumour cells – for example through liposomal targeting or gene therapy with viral vectors – could re-purpose anti-CMV CD8+ T cells for anti-cancer responses.

Lastly, it may be possible to improve cell-mediated immune responses using related strategies to those employed in this thesis. Here, work focused exclusively on generating humoral vaccine responses. However, it is possible that strategies to exploit non-cognate CD4+ T cell help could also be developed for to improve cell-mediated vaccines. The co-delivery of target CD8+ T cell epitopes and epitopes to co-opt pre-existing non-cognate CD4+ T cell help – perhaps conjugated to immune stimulatory polymers with other TLR agonists – could be a powerful approach to enhancing cell-mediated immunity.

9.2.3. Final conclusions

This thesis describes a novel particle-based vaccine platform that exploits pre-existing non-cognate CD4+ T cell help to enhance antibody responses to target antigens. In doing so, it validates the intermolecular help model, which states that CD4+ T cells recognising distinct antigens from those that bound the BCR can provide helper signals so long as the two antigens are linked by uptake into the same B cell. Of note, this is the first description of a rationally designed vaccine that exploits pre-existing non-cognate CD4+ T cells by incorporating CD4+ T cell epitopes in the vaccine particle core. In doing so, antibody responses to target antigens could be produced faster, to a higher titre, with greater affinity, and with more isotype-switching. Further, pre-existing T_H1-biased non-cognate helper populations could drive the production of antibody responses that were dominated by 'T_H1 isotypes'. The pre-existing CD4+ T cells that drove these phenomena could either be established by previous vaccination or by infection with a chronic viral pathogen. Notably, this is the first demonstration that the strikingly large T cell response induced by CMV infection can be harnessed to improve vaccine immunogenicity. Incorporating TLR9 agonists resulted in vaccine particles able to deliver a third signal – alongside BCR engagement and CD4+ T cell help – to antigen-specific B cells. This approach was shown to further augment antibody responses to target antigens, although there remains much that could be done to improve the immunogenicity of these liposomal vaccine particles. In conclusion, this thesis describes a promising novel vaccine strategy capable of exploiting pre-existing non-cognate CD4+ T cell help to enhance humoral vaccine responses. The principles underpinning the immunogenicity of this vaccine strategy, such as re-purposing pre-existing anti-viral CD4+ T cells to provide helper signals, could significantly improve the design of other vaccine technologies.

References

Abdulla, S. et al., 2013. Randomized, controlled trial of the long term safety, immunogenicity and efficacy of RTS, S/AS02 (D) malaria vaccine in infants living in a malaria-endemic region. *Malaria journal*, 12(1), p.11.

Agnandji, S.T. et al., 2012. A phase 3 trial of RTS, S/AS01 malaria vaccine in African infants. *The New England journal of medicine*, 367(24), pp.2284–2295.

Agnandji, S.T. et al., 2011. First results of phase 3 trial of RTS, S/AS01 malaria vaccine in African children. *The New England journal of medicine*, 365(20), pp.1863–1875.

Alam, S. et al., 2014. CD4 T Cell Help Is Limiting and Selective during the Primary B Cell Response to Influenza Virus Infection. *Journal of virology*, 88(1), pp.314–324.

Allen, S.D. et al., 2007. Peptide vaccines of the HER-2/neu dimerization loop are effective in inhibiting mammary tumor growth in vivo. *Journal of immunology (Baltimore, Md. : 1950)*, 179, pp.472–482.

Amara, R.R. et al., 2004. Long-lived poxvirus immunity, robust CD4 help, and better persistence of CD4 than CD8 T cells. *Journal of virology*, 78(8), pp.3811–3816.

Amato, R.J. et al., 2008. Vaccination of prostate cancer patients with modified vaccinia ankara delivering the tumor antigen 5T4 (TroVax): a phase 2 trial. *Journal of Immunotherapy*, 31(6), pp.577–585.

Andtbacka, R.H.I. et al., 2013. OPTiM: a randomized phase III trial of talimogene laherparepvec (T-VEC) versus subcutaneous (SC) granulocyte-macrophage colony-stimulating factor (GM-CSF) for the treatment (tx) of unresected stage IIIB/C and IV melanoma. *J Clin Oncol*, 31(Suppl).

Aoki, M. et al., 2009. Antibody responses against NY-ESO-1 and HER2 antigens in patients vaccinated with combinations of cholesteryl pullulan (CHP)-NY-ESO-1 and CHP-HER2 with OK-432. *Vaccine*, 27(49), pp.6854–6861.

Arama, C. & Troye-Blomberg, M., 2014. The path of malaria vaccine development: challenges and perspectives. *Journal of internal medicine*, 275(5), pp.456–466.

Arens, R. et al., 2008. Cutting edge: murine cytomegalovirus induces a polyfunctional CD4 T cell response. *Journal of immunology (Baltimore, Md. : 1950)*, 180, pp.6472–6476.

Arlen, P.M. et al., 2007. Clinical safety of a viral vector based prostate cancer vaccine strategy. *The Journal of urology*, 178, pp.1515–1520.

Aruga, A. et al., 2013. Long-term vaccination with multiple peptides derived from cancer-testis antigens can maintain a specific T-cell response and achieve disease stability in advanced biliary tract cancer. *Clinical Cancer Research*, 19(8), pp.2224–2231.

Avery, O.T. & Goebel, W.F., 1931. CHEMO-IMMUNOLOGICAL STUDIES ON CONJUGATED CARBOHYDRATE-PROTEINS : V. THE IMMUNOLOGICAL SPECIFITY OF AN ANTIGEN PREPARED BY COMBINING THE CAPSULAR POLYSACCHARIDE OF TYPE III PNEUMOCOCCUS WITH FOREIGN PROTEIN. *The Journal of experimental medicine*, 54, pp.437–447.

Avery, O.T. & Goebel, W.F., 1929. Chemo-Immunological studies on conjugated carbohydrate-proteins: II Immunological specificity of synthetic sugar-protein antigens. *The Journal of experimental medicine*, 50, pp.533–550.

Avigan, D.E. et al., 2007. Phase I/II study of vaccination with electrofused allogeneic dendritic cells/autologous tumor-derived cells in patients with stage IV renal cell carcinoma. *Journal of Immunotherapy*, 30(7), pp.749–761.

Babatz, J. et al., 2006. Induction of cellular immune responses against carcinoembryonic antigen in patients with metastatic tumors after vaccination with altered peptide ligand-loaded dendritic cells. *Cancer Immunology, Immunotherapy*, 55, pp.268–276.

Bachleitner, T. et al., 2009. Pilot trial of autologous dendritic cells loaded with tumor lysate(s) from allogeneic tumor cell lines in patients with metastatic medullary thyroid carcinoma. *Oncology Reports*, 21, pp.1585–1592.

Bachmann, M.F. & Zinkernagel, R.M., 1997. Neutralizing antiviral B cell responses. *Annual review of immunology*, 15, pp.235–270.

Ballas, Z.K. et al., 2001. Divergent therapeutic and immunologic effects of oligodeoxynucleotides with distinct CpG motifs. *Journal of immunology (Baltimore, Md. : 1950)*, 167, pp.4878–4886.

Ballou, W.R., 2009. The development of the RTS,S malaria vaccine candidate: Challenges and lessons. *Parasite Immunology*, 31, pp.492–500.

Banerjee, K. et al., 2010. IgG subclass profiles in infected HIV type 1 controllers and chronic progressors and in uninfected recipients of Env vaccines. *AIDS research and human retroviruses*, 26, pp.445–458.

Bangham, A.D., Standish, M.M. & Watkins, J.C., 1965. Diffusion of univalent ions across the lamellae of swollen phospholipids. *Journal of molecular biology*, 13, pp.238–252.

Barnden, M.J. et al., 1998. Defective TCR expression in transgenic mice constructed using cDNA-based alpha- and beta-chain genes under the control of heterologous regulatory elements. *Immunology and cell biology*, 76, pp.34–40.

Barve, M. et al., 2008. Induction of immune responses and clinical efficacy in a phase II trial of IDM-2101, a 10-epitope cytotoxic T-lymphocyte vaccine, in metastatic non-small-cell lung cancer. *Journal of Clinical Oncology*, 26, pp.4418–4425.

Batista, F. & Harwood, N., 2009. The who, how and where of antigen presentation to B cells. *Nature Reviews Immunology*, 9, pp.15–27.

Batista, F.D., Iber, D. & Neuberger, M.S., 2001. B cells acquire antigen from target cells after synapse formation. *Nature*, 411, pp.489–494.

Baxby, D., 1999. Edward Jenner's inquiry; a bicentenary analysis. *Vaccine*, 17, pp.301–307.

Behrens, E.M. et al., 2011. Repeated TLR9 stimulation results in macrophage activation syndrome: Like disease in mice. *Journal of Clinical Investigation*, 121, pp.2264–2277.

Bekeredjian-Ding, I. & Jego, G., 2009. Toll-like receptors--sentries in the B-cell response. *Immunology*, 128, pp.311–323.

Berntsen, A. et al., 2008. Therapeutic dendritic cell vaccination of patients with metastatic renal cell carcinoma: a clinical phase 1/2 trial. *Journal of Immunotherapy*, 31(8), pp.771–780.

Bolonaki, I. et al., 2007. Vaccination of patients with advanced non-small-cell lung cancer with an optimized cryptic human telomerase reverse transcriptase peptide. *Journal of clinical oncology : official journal of the American Society of Clinical Oncology*, 25, pp.2727–2734.

Brindley, M.A. et al., 2012. Triggering the measles virus membrane fusion machinery. *Proceedings of the National Academy of Sciences*, 109, pp.E3018–E3027.

Bundle, D.R., 2007. A carbohydrate vaccine exceeds the sum of its parts. *Nature chemical biology*, 3(10), pp.605–606.

Burnet, M., 1957. Cancer—A Biological Approach: III. Viruses Associated with Neoplastic Conditions. IV. Practical Applications. *British medical journal*, 1(5023), p.841.

Burton, D.R. et al., 2004. HIV vaccine design and the neutralizing antibody problem. *Nature immunology*, 5, pp.233–236.

Buskas, T., Ingale, S. & Boons, G.-J., 2005. Towards a Fully Synthetic Carbohydrate-Based Anticancer Vaccine: Synthesis and Immunological Evaluation of a Lipidated Glycopeptide Containing the Tumor-Associated Tn Antigen. *Angewandte Chemie International Edition*, 44(37), pp.5985–5988.

Buskas, T., Li, Y. & Boons, G.-J., 2004. The Immunogenicity of the Tumor-Associated Antigen Lewisy May Be Suppressed by a Bifunctional Cross-Linker Required for Coupling to a Carrier Protein. *Chemistry-A European Journal*, 10(14), pp.3517–3524.

Buskas, T., Thompson, P. & Boons, G.-J., 2009. Immunotherapy for cancer: synthetic carbohydrate-based vaccines. *Chemical communications (Cambridge, England)*, pp.5335–5349.

Butterfield, L.H. et al., 2008. Adenovirus MART-1-engineered autologous dendritic cell vaccine for metastatic melanoma. *Journal of immunotherapy*, 31, pp.294–309.

Campbell, J.D. et al., 2009. CpG-containing immunostimulatory DNA sequences elicit TNF-α-dependent toxicity in rodents but not in humans. *Journal of Clinical Investigation*, 119, pp.2564–2576.

Capeding, M.R. et al., 2014. Clinical efficacy and safety of a novel tetravalent dengue vaccine in healthy children in Asia: a phase 3, randomised, observer-masked, placebo-controlled trial. *The Lancet*, 384(9951), pp.1358–1365.

Carrasco, Y.R. & Batista, F.D., 2006. B cell recognition of membrane-bound antigen: an exquisite way of sensing ligands. *Current Opinion in Immunology*, 18, pp.286–291.

Carrasco, Y.R. & Batista, F.D., 2007. B Cells Acquire Particulate Antigen in a Macrophage-Rich Area at the Boundary between the Follicle and the Subcapsular Sinus of the Lymph Node. *Immunity*, 27, pp.160–171.

Casares, S., Brumeanu, T.D. & Richie, T.L., 2010. The RTS,S malaria vaccine. *Vaccine*, 28, pp.4880–4894.

Cassaday, R.D. et al., 2007. A phase I study of immunization using particle-mediated epidermal delivery of genes for gp100 and GM-CSF into uninvolved skin of melanoma patients. *Clinical Cancer Research*, 13, pp.540–549.

Castiglioni, P. et al., 2005. CD8 T cell priming by B lymphocytes is CD4 help dependent. *European Journal of Immunology*, 35, pp.1360–1370.

Cathomen, T., Naim, H.Y. & Cattaneo, R., 1998. Measles viruses with altered envelope protein cytoplasmic tails gain cell fusion competence. *Journal of virology*, 72, pp.1224–1234.

Celis, E., 2007. Overlapping human leukocyte antigen class I/II binding peptide vaccine for the treatment of patients with stage IV melanoma. *Cancer*, 110(1), pp.203–214.

Centers for Disease Control and Prevention, 2009. *Morbidity and Mortality Weekly Report*,

Cheever, M.A. et al., 2009. The prioritization of cancer antigens: A National Cancer Institute pilot project for the acceleration of translational research. *Clinical Cancer Research*, 15, pp.5323–5337.

Chen, W.H. et al., 2009. Vaccination in the elderly: an immunological perspective. *Trends in Immunology*, 30, pp.351–359.

Christensen, D. et al., 2007. Cationic liposomes as vaccine adjuvants. *Expert review of vaccines*, 6, pp.785–796.

Coffman, R.L. et al., 1988. The role of helper T cell products in mouse B cell differentiation and isotype regulation. *Immunological reviews*, 102(1), pp.5–28.

Coley, W.B., 1893. The treatment of malignant tumors by repeated inoculations of erysipelas: with a report of ten original cases. *The American Journal of the Medical Sciences*, 105(5), pp.487–510.

Crawford, A. et al., 2014. Molecular and Transcriptional Basis of CD4+ T Cell Dysfunction during Chronic Infection. *Immunity*, 40, pp.289–302.

Cribbs, D.H. et al., 2003. Adjuvant-dependent modulation of Th1 and Th2 responses to immunization with Beta-amyloid. *International Immunology*, 15, pp.505–514.

Crompton, P.D., Pierce, S.K. & Miller, L.H., 2010. Advances and challenges in malaria vaccine development. *J. Clin. Invest.*, 120, pp.4168–4178.

CRUK, 2012. *Cancer mortality statistics*, Available at: http://www.cancerresearchuk.org/cancer-info/cancerstats/mortality/.

Danishefsky, S. & Allen, J., 2000. From the Laboratory to the Clinic: A Retrospective on Fully Synthetic Carbohydrate-Based Anticancer Vaccines Frequently used abbreviations are listed in the appendix. *Angewandte Chemie (International ed. in English)*, 39, pp.836–863.

Davidson, A. & Diamond, B., 2001. Autoimmune Diseases. *New England Journal of Medicine*, 345, pp.340–350.

Davis, H.L. et al., 1998. CpG DNA is a potent enhancer of specific immunity in mice immunized with recombinant hepatitis B surface antigen. *Journal of immunology (Baltimore, Md. : 1950)*, 160, pp.870–876.

Deborah A, B. et al., 2011. FSL Constructs: A simple method for modifying cell/virion surfaces with a range of biological markers without affecting their viability. *Journal of Visualized Experiments*, (54).

Dedeoglu, F. et al., 2004. Induction of activation-induced cytidine deaminase gene expression by IL-4 and CD40 ligation is dependent on STAT6 and NFκB. *International immunology*, 16(3), pp.395–404.

Diethelm-Okita, B.M. et al., 1997. Epitope repertoire of human CD4+ T cells on tetanus toxin: identification of immunodominant sequence segments. *The Journal of infectious diseases*, 175, pp.382–391.

Diethelm-Okita, B.M. et al., 2000. Universal epitopes for human CD4+ cells on tetanus and diphtheria toxins. *The Journal of infectious diseases*, 181, pp.1001–1009.

Dube, D.H. & Bertozzi, C.R., 2005. Glycans in cancer and inflammation--potential for therapeutics and diagnostics. *Nature reviews. Drug discovery*, 4, pp.477–488.

Dunn, G.P. et al., 2002. Cancer immunoediting: from immunosurveillance to tumor escape. *Nature immunology*, 3, pp.991–998.

Dunn, H.S. et al., 2002. Dynamics of CD4 and CD8 T cell responses to cytomegalovirus in healthy human donors. *The Journal of infectious diseases*, 186, pp.15–22.

Einhorn, L.H., 1997. Testicular cancer: An oncological success story. In *Clinical Cancer Research*. pp. 2630–2632.

Von Euw, E.M. et al., 2008. A phase I clinical study of vaccination of melanoma patients with dendritic cells loaded with allogeneic apoptotic/necrotic melanoma cells. Analysis of toxicity and immune response to the vaccine and of IL-10-1082 promoter genotype as predictor of disease. *Journal of translational medicine*, 6(1), p.6.

Fenner, F. et al., 1988. Early efforts at control: variolation, vaccination, and isolation and quarantine. *History of International Public Health*, 6, pp.245–276.

Finn, O.J., 2003. Cancer vaccines: between the idea and the reality. *Nature reviews. Immunology*, 3, pp.630–641.

Foged, C. et al., 2004. Interaction of dendritic cells with antigen-containing liposomes: Effect of bilayer composition. *Vaccine*, 22, pp.1903–1913.

Fourcade, J. et al., 2008. Immunization with analog peptide in combination with CpG and montanide expands tumor antigen-specific CD8+ T cells in melanoma patients. *Journal of immunotherapy (Hagerstown, Md. : 1997)*, 31, pp.781–791.

Frey, A., Di Canzio, J. & Zurakowski, D., 1998. A statistically defined endpoint titer determination method for immunoassays. *Journal of Immunological Methods*, 221, pp.35–41.

Galon, J. et al., 2006. Type, density, and location of immune cells within human colorectal tumors predict clinical outcome. *Science (New York, N.Y.)*, 313, pp.1960–1964.

Garside, P. et al., 1998. Visualization of specific B and T lymphocyte interactions in the lymph node. *Science (New York, N.Y.)*, 281, pp.96–99.

Gaschen, B. et al., 2002. Diversity considerations in HIV-1 vaccine selection. *Science (New York, N.Y.)*, 296, pp.2354–2360.

Del Giudice, G., 1992. New carriers and adjuvants in the development of vaccines. *Current opinion in immunology*, 4, pp.454–459.

Goldblatt, D., 2000. Conjugate vaccines. *Clinical and Experimental Immunology*, 119, pp.1–3.

Gordon, D.M. et al., 1995. Safety, immunogenicity, and efficacy of a recombinantly produced Plasmodium falciparum circumsporozoite protein-hepatitis B surface antigen subunit vaccine. *Journal of Infectious Diseases*, 171(6), pp.1576–1585.

Greenberg, D.P. et al., 2000. Immunogenicity of a Haemophilus influenzae type b-tetanus toxoid conjugate vaccine when mixed with a diphtheria-tetanus-acellular pertussis-hepatitis B combination vaccine. *The Pediatric infectious disease journal*, 19, pp.1135–1140.

Gregoriadis, G. & Davis, C., 1979. Stability of liposomes invivo and invitro is promoted by their cholesterol content and the presence of blood cells. *Biochemical and Biophysical Research Communications*, 89, pp.1287–1293.

Guirakhoo, F. et al., 2006. Live Attenuated Chimeric Yellow Fever Dengue Type 2 (ChimeriVax^{TM}-DEN2) Vaccine: Phase I Clinical Trial for Safety and Immunogenicity: Effect of Yellow Fever Pre-immunity in Induction of Cross Neutralizing Antibody Responses to All. *Human vaccines*, 2(2), pp.60–67.

Gururajan, M., Jacob, J. & Pulendran, B., 2007. Toll-like receptor expression and responsiveness of distinct murine splenic and mucosal B-cell subsets. *PLoS ONE*, 2.

Hammarlund, E. et al., 2003. Duration of antiviral immunity after smallpox vaccination. *Nature medicine*, 9, pp.1131–1137.

Hanahan, D. & Weinberg, R.A., 2011. Hallmarks of cancer: The next generation. *Cell*, 144, pp.646–674.

Harcourt, G.C. et al., 2006. Identification of key peptide-specific CD4+ T cell responses to human cytomegalovirus: Implications for tracking antiviral populations. *Clinical and Experimental Immunology*, 146, pp.203–210.

Harrop, R. et al., 2006. Vaccination of colorectal cancer patients with modified vaccinia Ankara delivering the tumor antigen 5T4 (TroVax) induces immune responses which correlate with disease control: a phase I/II trial. *Clinical Cancer Research*, 12(11), pp.3416–3424.

Hedestam, G.B.K. et al., 2008. The challenges of eliciting neutralizing antibodies to HIV-1 and to influenza virus. *Nature Reviews Microbiology*, 6(2), pp.143–155.

Hinrichs, C.S. & Rosenberg, S.A., 2014. Exploiting the curative potential of adoptive T-cell therapy for cancer. *Immunological Reviews*, 257, pp.56–71.

Hollingdale, M.R. et al., 1984. Inhibition of entry of Plasmodium falciparum and P. vivax sporozoites into cultured cells; an in vitro assay of protective antibodies. *Journal of immunology (Baltimore, Md. : 1950)*, 132, pp.909–913.

Honma, I. et al., 2009. Phase I clinical study of anti-apoptosis protein survivin-derived peptide vaccination for patients with advanced or recurrent urothelial cancer. *Cancer immunology, immunotherapy*, 58(11), pp.1801–1807.

Horstmann, E. et al., 2005. Risks and benefits of phase 1 oncology trials, 1991 through 2002. *The New England journal of medicine*, 352, pp.895–904.

Hovden, A.-O., Cox, R.J. & Haaheim, L.R., 2005. Whole influenza virus vaccine is more immunogenic than split influenza virus vaccine and induces primarily an IgG2a response in BALB/c mice. *Scandinavian journal of immunology*, 62(1), pp.36–44.

Howerton, D.A. et al., 1990. Induction of macrophage Ia expression in vivo by a synthetic block copolymer, L81. *The Journal of Immunology*, 144(5), pp.1578–1584.

Hunter, R.L. & Bennett, B., 1984. The adjuvant activity of nonionic block polymer surfactants. II. Antibody formation and inflammation related to the structure of triblock and octablock copolymers. *The Journal of Immunology*, 133(6), pp.3167–3175.

Ingale, S. et al., 2007. Robust immune responses elicited by a fully synthetic three-component vaccine. *Nature chemical biology*, 3, pp.663–667.

Iwasaki, A. & Medzhitov, R., 2004. Toll-like receptor control of the adaptive immune responses. *Nature immunology*, 5, pp.987–995.

Izumoto, S. et al., 2008. *Phase II clinical trial of Wilms tumor 1 peptide vaccination for patients with recurrent glioblastoma multiforme.*,

Janeway, C.A. et al., 2001. Immunobiology.

Jegerlehner, A. et al., 2007. TLR9 signaling in B cells determines class switch recombination to IgG2a. *Journal of immunology*, 178, pp.2415–2420.

Kantoff, P.W., Schuetz, T.J., et al., 2010. *Overall survival analysis of a phase II randomized controlled trial of a Poxviral-based PSA-targeted immunotherapy in metastatic castration-resistant prostate cancer.*,

Kantoff, P.W., Higano, C.S., et al., 2010. *Sipuleucel-T immunotherapy for castration-resistant prostate cancer.*,

Karrer, U. et al., 2003. Memory inflation: continuous accumulation of antiviral CD8+ T cells over time. *Journal of immunology (Baltimore, Md. : 1950)*, 170, pp.2022–2029.

Kaufman, H.L. et al., 2014. Primary overall survival (OS) from OPTiM, a randomized phase III trial of talimogene laherparepvec (T-VEC) versus subcutaneous (SC) granulocyte-macrophage colony-stimulating factor (GM-CSF) for the treatment (tx) of unresected stage IIIB/C and IV melanoma. In *ASCO Annual Meeting Proceedings*. p. 9008a.

Kaumaya, P.T.P. et al., 2009. Phase I active immunotherapy with combination of two chimeric, human epidermal growth factor receptor 2, B-cell epitopes fused to a promiscuous T-cell epitope in patients with metastatic and/or recurrent solid tumors. *Journal of Clinical Oncology*, 27(31), pp.5270–5277.

Kawabe, T. et al., 1994. The immune responses in CD40-deficient mice: impaired immunoglobulin class switching and germinal center formation. *Immunity*, 1, pp.167–178.

Käyhty, H. et al., 1984. Serum antibodies after vaccination with Haemophilus influenzae type b capsular polysaccharide and responses to reimmunization: no evidence of immunologic tolerance or memory. *Pediatrics*, 74(5), pp.857–865.

Kelsoe, G., 1995. In Situ Studies of the Germinal Center Reaction. *Advances in immunology*, 60, pp.267–288.

Khan, N. et al., 2002. Cytomegalovirus seropositivity drives the CD8 T cell repertoire toward greater clonality in healthy elderly individuals. *Journal of immunology*, 169, pp.1984–1992.

Khong, H. et al., 2004. Immunization of HLA-A*0201 and/or HLA-DPbeta1*04 patients with metastatic melanoma using epitopes from the NY-ESO-1 antigen. *Journal of immunotherapy*, 27(6), pp.472–7.

Kim, M.-G. et al., 2014. Nanotechnology and vaccine development. *Asian Journal of Pharmaceutical Sciences*.

King, C., Tangye, S.G. & Mackay, C.R., 2008. T follicular helper (TFH) cells in normal and dysregulated immune responses. *Annual review of immunology*, 26, pp.741–766.

Kitano, S. et al., 2006. HER2-specific T-cell immune responses in patients vaccinated with truncated HER2 protein complexed with nanogels of cholesteryl pullulan. *Clinical Cancer Research*, 12, pp.7397–7405.

Klebanoff, C.A. et al., 2011. Therapeutic cancer vaccines: Are we there yet? *Immunological Reviews*, 239, pp.27–44.

Koh, Y.T. et al., 2006. Immunological consequences of using three different clinical/laboratory techniques of emulsifying peptide-based vaccines in incomplete Freund's adjuvant. *Journal of translational medicine*, 4(1), p.42.

Kolakofsky, D. et al., 1998. Paramyxovirus RNA synthesis and the requirement for hexamer genome length: the rule of six revisited. *Journal of virology*, 72, pp.891–899.

Kono, K. et al., 2009. Vaccination with multiple peptides derived from novel cancer-testis antigens can induce specific T-cell responses and clinical responses in advanced esophageal cancer. *Cancer Science*, 100, pp.1502–1509.

Korn, T. et al., 2009. IL-17 and Th17 Cells. *Annual review of immunology*, 27, pp.485–517.

Krause, J.C. et al., 2011. A Broadly Neutralizing Human Monoclonal Antibody That Recognizes a Conserved, Novel Epitope on the Globular Head of the Influenza H1N1 Virus Hemagglutinin. *Journal of Virology*, 85, pp.10905–10908.

Krieg, A.M. et al., 1995. CpG motifs in bacterial DNA trigger direct B-cell activation. *Nature*, 374, pp.546–549.

Kruit, W.H.J. et al., 2013. Selection of immunostimulant AS15 for active immunization with MAGE-A3 protein: results of a randomized phase II study of the European Organisation for Research and Treatment of Cancer Melanoma Group in Metastatic Melanoma. *Journal of Clinical Oncology*, 31(19), pp.2413–2420.

Kyte, J.A. et al., 2006. Phase I/II trial of melanoma therapy with dendritic cells transfected with autologous tumor-mRNA. *Cancer gene therapy*, 13(10), pp.905–918.

Lambert, P.-H., Liu, M. & Siegrist, C.-A., 2005. Can successful vaccines teach us how to induce efficient protective immune responses? *Nature medicine*, 11, pp.S54–S62.

Leenaars, P. et al., 1998. Assessment of side effects induced by injection of different adjuvant/antigen combinations in rabbits and mice. *Laboratory animals*, 32(4), pp.387–406.

Lees, J.R. & Farber, D.L., 2010. Generation, persistence and plasticity of CD4 T-cell memories. *Immunology*, 130, pp.463–470.

Lesimple, T. et al., 2006. Immunologic and clinical effects of injecting mature peptide-loaded dendritic cells by intralymphatic and intranodal routes in metastatic melanoma patients. *Clinical Cancer Research*, 12, pp.7380–7388.

Lesterhuis, W.J. et al., 2011. Wild-type and modified gp100 peptide-pulsed dendritic cell vaccination of advanced melanoma patients can lead to long-term clinical responses independent of the peptide used. *Cancer Immunology, Immunotherapy*, 60, pp.249–260.

Leung, S. et al., 2013. OT-II TCR transgenic mice fail to produce anti-ovalbumin antibodies upon vaccination. *Cellular Immunology*, 282, pp.79–84.

Levêque, D., Wisniewski, S. & Jehl, F., 2005. Pharmacokinetics of therapeutic monoclonal antibodies used in oncology. *Anticancer Research*, 25, pp.2327–2343.

Lin, L., Gerth, A.J. & Peng, S.L., 2004. CpG DNA redirects class-switching towards "Th1-like" Ig isotype production via TLR9 and MyD88. *European Journal of Immunology*, 34, pp.1483–1487.

Lindsey, K.R. et al., 2006. Evaluation of prime/boost regimens using recombinant poxvirus/tyrosinase vaccines for the treatment of patients with metastatic melanoma. *Clinical Cancer Research*, 12, pp.2526–2527.

Liu, N. et al., 2003. CpG directly induces T-bet expression and inhibits IgG1 and IgE switching in B cells. *Nature immunology*, 4, pp.687–693.

Liu, Y.J. et al., 1996. Within germinal centers, isotype switching of immunoglobulin genes occurs after the onset of somatic mutation. *Immunity*, 4, pp.241–250.

Loveland, B.E. et al., 2006. *Mannan-MUC1-pulsed dendritic cell immunotherapy: a phase I trial in patients with adenocarcinoma.*,

Luca, S. & Mihaescu, T., 2013. History of BCG Vaccine. *Mædica*, 8, pp.53–8.

Lux, K. et al., 2005. Green fluorescent protein-tagged adeno-associated virus particles allow the study of cytosolic and nuclear trafficking. *Journal of virology*, 79, pp.11776–11787.

Maggi, E. et al., 1994. Th2-like CD8+ T cells showing B cell helper function and reduced cytolytic activity in human immunodeficiency virus type 1 infection. *J Exp Med*, 180, pp.489–495.

Maisonneuve, C. et al., 2014. Unleashing the potential of NOD-and Toll-like agonists as vaccine adjuvants. *Proceedings of the National Academy of Sciences*, 111(34), pp.12294–12299.

Mallajosyula, V.V. a. et al., 2014. Influenza hemagglutinin stem-fragment immunogen elicits broadly neutralizing antibodies and confers heterologous protection. *Proceedings of the National Academy of Sciences*, pp.1–10.

Mandler, R. et al., 1993. IL-4 induction of IgE class switching by lipopolysaccharide-activated murine B cells occurs predominantly through sequential switching. *Journal of immunology (Baltimore, Md. : 1950)*, 150, pp.407–418.

Manz, R. et al., 2005. Maintenance of serum antibody levels. *Annual Review of Immunology*, 23, pp.367–386. Available at: papers://2f48f2a5-d7fa-4c28-a7e3-406f1cad5688/Paper/p253.

Marincola, F.M. et al., 1996. Analysis of Expression of the Melanoma-Associated Antigens MART-1 and gp lOO in Metastatic Melanoma Cell Lines and in In Situ Lesions. *Journal of Immunotherapy*, 19(3), pp.192–205.

Marshall, J.L. et al., 2005. Phase I Study of Sequential Vaccinations With Fowlpox-CEA (6D)-TRICOM Alone and Sequentially With Vaccinia-CEA (6D)-TRICOM, With and Without Granulocyte-Macrophage Colony-Stimulating Factor, in Patients With Carcinoembryonic Antigen--Expressing Carcinomas. *Journal of Clinical Oncology*, 23(4), pp.720–731.

Martin, R.M., Brady, J.L. & Lew, A.M., 1998. The need for IgG2c specific antiserum when isotyping antibodies from C57BL/6 and NOD mice. *Journal of Immunological Methods*, 212, pp.187–192.

Mavroudis, D. et al., 2006. *A phase I study of the optimized cryptic peptide TERT(572y) in patients with advanced malignancies.*,

McHeyzer-Williams, M. et al., 2011. Molecular programming of B cell memory. *Nature Reviews Immunology*.

Ménard, S. et al., 2000. Role of HER2 gene overexpression in breast carcinoma. *Journal of Cellular Physiology*, 182, pp.150–162.

Mills, D.M. & Cambier, J.C., 2003. B lymphocyte activation during cognate interactions with CD4+ T lymphocytes: Molecular dynamics and immunologic consequences. *Seminars in Immunology*, 15, pp.325–329.

Ming-Kung, Y., 2012. Clinically-Proven Liposome-Based Drug Delivery: Formulation, Characterization and Therapeutic Efficacy.

Mir, O., Berveiller, P. & Pons, G., 2007. Trastuzumab--mechanism of action and use. *The New England journal of medicine*, 357, pp.1664–1665; author reply 1665–1666.

Mitsdoerffer, M. et al., 2010. Proinflammatory T helper type 17 cells are effective B-cell helpers. *Proceedings of the National Academy of Sciences of the United States of America*, 107, pp.14292–14297.

Mohebtash, M. et al., 2011. A pilot study of MUC-1/CEA/TRICOM poxviral-based vaccine in patients with metastatic breast and ovarian cancer. *Clinical cancer research : an official journal of the American Association for Cancer Research*, 17, pp.7164–73.

Mohr, E. et al., 2010. IFN-{gamma} produced by CD8 T cells induces T-bet-dependent and -independent class switching in B cells in responses to alum-precipitated protein vaccine. *Proceedings of the National Academy of Sciences of the United States of America*, 107, pp.17292–17297.

Mond, J.J., Lees, A. & Snapper, C.M., 1995. T cell-independent antigens type 2. *Annual review of immunology*, 13, pp.655–692.

Morita, S. et al., 2006. A phase I/II trial of a WT1 (Wilms' tumor gene) peptide vaccine in patients with solid malignancy: safety assessment based on the phase I data. *Japanese journal of clinical oncology*, 36(4), pp.231–236.

Morse, M.A. et al., 2005. Phase I study of immunization with dendritic cells modified with fowlpox encoding carcinoembryonic antigen and costimulatory molecules. *Clinical Cancer Research*, 11, pp.3017–3024.

Mosmann, T.R. et al., 1986. Two types of murine helper T cell clone. I. Definition according to profiles of lymphokine activities and secreted proteins. *Journal of immunology (Baltimore, Md. : 1950)*, 136, pp.2348–2357.

Mosmann, T.R., Li, L. & Sad, S., 1997. Functions of CD8 T-cell subsets secreting different cytokine patterns. *Seminars in immunology*, 9, pp.87–92.

Mosmann, T.R. & Sad, S., 1996. The expanding universe of T-cell subsets: Th1, Th2 and more. *Immunology today*, 17, pp.138–146.

Moss, W.J. & Griffin, D.E., 2012. Measles. *Lancet*, 379, pp.153–64.

Muramatsu, M. et al., 2000. Class switch recombination and hypermutation require activation-induced cytidine deaminase (AID), a potential RNA editing enzyme. *Cell*, 102, pp.553–563.

Murphy, C.G. & Modi, S., 2009. HER2 breast cancer therapies: A review. *Biologics: Targets and Therapy*, 3, pp.289–301.

Naldini, L. et al., 1996. In vivo gene delivery and stable transduction of nondividing cells by a lentiviral vector. *Science*, 272, pp.263–267.

Naniche, D. et al., 2004. Decrease in measles virus-specific CD4 T cell memory in vaccinated subjects. *The Journal of infectious diseases*, 190, pp.1387–1395.

National Health Service, 2014. National Health Service Immunisation Schedule. Available at: http://www.nhs.uk/conditions/vaccinations/pages/vaccination-schedule-age-checklist.aspx [Accessed November 30, 2014].

National Institutes of Health, I-A(b) chicken Ova 323-339. *http://tetramer.yerkes.emory.edu/reagents/3831*.

Nemunaitis, J. et al., 2006. Phase 1/2 trial of autologous tumor mixed with an allogeneic GVAX vaccine in advanced-stage non-small-cell lung cancer. *Cancer gene therapy*, 13(6), pp.555–562.

Neuberger, M.S. & Milstein, C., 1995. Somatic hypermutation. *Current opinion in immunology*, 7, pp.248–254.

Neumann, G., Whitt, M.A. & Kawaoka, Y., 2002. A decade after the generation of a negative-sense RNA virus from cloned cDNA--what have we learned? *Journal of General Virology*, 83(11), pp.2635–2662.

Ni, J. et al., 2006. Toward a carbohydrate-based HIV-1 vaccine: Synthesis and immunological studies of oligomannose-containing glycoconjugates. *Bioconjugate Chemistry*, 17, pp.493–500.

Nicholaou, T. et al., 2009. Regulatory T-cell--mediated attenuation of T-cell responses to the NY-ESO-1 ISCOMATRIX vaccine in patients with advanced malignant melanoma. *Clinical Cancer Research*, 15(6), pp.2166–2173.

Nimmerjahn, F. & Ravetch, J. V, 2005. Divergent immunoglobulin g subclass activity through selective Fc receptor binding. *Science (New York, N.Y.)*, 310, pp.1510–1512.

Nimmerjahn, F. & Ravetch, J. V., 2007. Antibodies, Fc receptors and cancer. *Current Opinion in Immunology*, 19, pp.239–245.

Di Noia, J.M. & Neuberger, M.S., 2007. Molecular mechanisms of antibody somatic hypermutation. *Annual review of biochemistry*, 76, pp.1–22.

O'Rourke, M.G.E. et al., 2007. *Dendritic cell immunotherapy for stage IV melanoma.*,

Odunsi, K. et al., 2012. Efficacy of vaccination with recombinant vaccinia and fowlpox vectors expressing NY-ESO-1 antigen in ovarian cancer and melanoma patients. *Proceedings of the National Academy of Sciences*, 109, pp.5797–5802.

Ohno, S. et al., 2009. Wilms' tumor 1 (WTl) peptide immunotherapy for gynecological malignancy. *Anticancer Research*, 29, pp.4779–4784.

Olayioye, M.A. et al., 2000. The ErbB signaling network: receptor heterodimerization in development and cancer. *The EMBO journal*, 19, pp.3159–3167.

Old, L.J. & Boyse, E.A., 1964. Immunology of experimental tumors. *Annual review of medicine*, 15(1), pp.167–186.

Oldham, R.K. & Dillman, R.O., 2008. Monoclonal antibodies in cancer therapy: 25 years of progress. *Journal of Clinical Oncology*, 26(11), pp.1774–1777.

Osorio, M. et al., 2008. Heterophilic NeuGcGM3 ganglioside cancer vaccine in advanced melanoma patients. *Cancer biology & therapy*, 7(4), pp.488–495.

Overwijk, W.W. et al., 1999. Vaccination with a recombinant vaccinia virus encoding a "self" antigen induces autoimmune vitiligo and tumor cell destruction in mice: requirement for CD4(+) T lymphocytes. *Proceedings of the National Academy of Sciences of the United States of America*, 96, pp.2982–2987.

Palucka, A.K. et al., 2006. Dendritic cells loaded with killed allogeneic melanoma cells can induce objective clinical responses and MART-1 specific CD8+ T-cell immunity. *Journal of Immunotherapy*, 29(5), pp.545–557.

Palucka, K. & Banchereau, J., 2012. Cancer immunotherapy via dendritic cells. *Nature Reviews Cancer*, 12, pp.265–277.

Pape, K.A. et al., 2007. The Humoral Immune Response Is Initiated in Lymph Nodes by B Cells that Acquire Soluble Antigen Directly in the Follicles. *Immunity*, 26, pp.491–502.

Pardoll, D., 2003. Does the immune system see tumors as foreign or self? *Annual review of immunology*, 21, pp.807–839.

Pardoll, D.M., 1998. Cancer vaccines. *Nature medicine*, 4, pp.525–531.

Parida, S.K. & Kaufmann, S.H.E., 2010. Novel tuberculosis vaccines on the horizon. *Current Opinion in Immunology*, 22, pp.374–384.

Parker, D.C., 1993. T cell-dependent B cell activation. *Annual review of immunology*, 11, pp.331–360.

Pasteur, L., 1880. De l'attenuation du virus du cholera des poules. *CR Acad. Sci. Paris*, 91, pp.673–680.

Peek, L.J., Middaugh, C.R. & Berkland, C., 2008. Nanotechnology in vaccine delivery. *Advanced Drug Delivery Reviews*, 60, pp.915–928.

Peeters, C.C.A.M. et al., 1991. Effect of carrier priming on immunogenicity of saccharide-protein conjugate vaccines. *Infection and Immunity*, 59, pp.3504–3510.

Persson, C. et al., 2002. Cutting edge: a new tool to evaluate human pre-erythrocytic malaria vaccines: rodent parasites bearing a hybrid Plasmodium falciparum circumsporozoite protein. *Journal of immunology*, 169, pp.6681–6685.

Phan, G.Q. et al., 2003. Immunization of patients with metastatic melanoma using both class I-and class II-restricted peptides from melanoma-associated antigens. *Journal of immunotherapy*, 26(4), p.349.

Plotkin, S.A., 2010. Correlates of protection induced by vaccination. *Clinical and Vaccine Immunology*, 17, pp.1055–1065.

Plotkin, S.A., 2005. Vaccines: past, present and future. *Nature medicine*, 11, pp.S5–S11.

Plotkin, S.A., 2009. Vaccines: The fourth century. *Clinical and Vaccine Immunology*, 16, pp.1709–1719.

Pobre, K. et al., 2014. Carrier priming or suppression: Understanding carrier priming enhancement of anti-polysaccharide antibody response to conjugate vaccines. *Vaccine*, 32, pp.1423–1430.

Poo, J. et al., 2011. Live-attenuated tetravalent dengue vaccine in dengue-naive children, adolescents, and adults in Mexico City: randomized controlled phase 1 trial of safety and immunogenicity. *The Pediatric infectious disease journal*, 30(1), pp.e9–e17.

Powell, A. et al., 2006. Recombinant GM-CSF plus autologous tumor cells as a vaccine for patients with mesothelioma. *Lung Cancer*, 52(2), pp.189–197.

Pullen, G.R., Fitzgerald, M.G. & Hosking, C.S., 1986. Antibody avidity determination by ELISA using thiocyanate elution. *Journal of immunological methods*, 86, pp.83–87.

Qiao, M. et al., 2011. Priming effect of dengue and yellow fever vaccination on the immunogenicity, infectivity, and safety of a tetravalent dengue vaccine in humans. *American Journal of Tropical Medicine and Hygiene*, 85, pp.724–731.

Racaniello, V.R. & Baltimore, D., 1981. Cloned poliovirus complementary DNA is infectious in mammalian cells. *Science (New York, N.Y.)*, 214, pp.916–919.

Radecke, F. et al., 1995. Rescue of measles viruses from cloned DNA. *The EMBO journal*, 14, pp.5773–5784.

Reuschenbach, M., von Knebel Doeberitz, M. & Wentzensen, N., 2009. A systematic review of humoral immune responses against tumor antigens. *Cancer immunology, immunotherapy : CII*, 58, pp.1535–1544.

Roberts, T.G. et al., 2004. Trends in the risks and benefits to patients with cancer participating in phase 1 clinical trials. *JAMA : the journal of the American Medical Association*, 292, pp.2130–2140.

Ruprecht, C.R. & Lanzavecchia, A., 2006. Toll-like receptor stimulation as a third signal required for activation of human naive B cells. *European Journal of Immunology*, 36, pp.810–816.

Russell, S.M. & Liew, F.Y., 1980. Cell cooperation in antibody responses to influenza virus. I. priming of helper t cells by internal components of virion. *European journal of immunology*, 10, pp.791–796.

Russell, S.M. & Liew, F.Y., 1979. T cells primed by influenza virion internal components can cooperate in the antibody response to haemagglutinin. *Nature*, 280, pp.147–148.

Sad, S. et al., 1997. Cytotoxicity and weak CD40 ligand expression of CD8+ type 2 cytotoxic T cells restricts their potential B cell helper activity. *European Journal of Immunology*, 27, pp.914–922.

Sasieni, P.D. et al., 2011. What is the lifetime risk of developing cancer: the effect of adjusting for multiple primaries. *British journal of cancer*, 105(3), pp.460–465.

Sawada, Y. et al., 2012. Phase I Trial of a Glypican-3--Derived Peptide Vaccine for Advanced Hepatocellular Carcinoma: Immunologic Evidence and Potential for Improving Overall Survival. *Clinical Cancer Research*, 18(13), pp.3686–3696.

Scherle, P.A. & Gerhard, W., 1986. Functional analysis of influenza-specific helper T cell clones in vivo. T cells specific for internal viral proteins provide cognate help for B cell responses to hemagglutinin. *The Journal of experimental medicine*, 164, pp.1114–1128.

Schlom, J., 2012. Therapeutic cancer vaccines: Current status and moving forward. *Journal of the National Cancer Institute*, 104, pp.599–613.

Schneider, H. et al., 1997. Rescue of measles virus using a replication-deficient vaccinia-T7 vector. *Journal of Virological Methods*, 64, pp.57–64.

Schroeder Jr, H.W. & Cavacini, L., 2010. Structure and function of immunoglobulins. *Journal of Allergy and Clinical Immunology*, 125(2), pp.S41–S52.

Schuessler, A., Walker, D.G. & Khanna, R., 2014. Cytomegalovirus as a novel target for immunotherapy of glioblastoma multiforme. *Frontiers in oncology*, 4.

Schutze, M.P. et al., 1985. Carrier-induced epitopic suppression, a major issue for future synthetic vaccines. *Journal of immunology (Baltimore, Md. : 1950)*, 135, pp.2319–2322.

Scott, A.M., Wolchok, J.D. & Old, L.J., 2012. Antibody therapy of cancer. *Nature Reviews Cancer*, 12, pp.278–287.

Semple, S.C., Chonn, A. & Cullis, P.R., 1996. Influence of cholesterol on the association of plasma proteins with liposomes. *Biochemistry*, 35, pp.2521–2525.

Sester, M. et al., 2002. Sustained high frequencies of specific CD4 T cells restricted to a single persistent virus. *Journal of virology*, 76, pp.3748–3755.

Shi, Y. & Rock, K.L., 2002. Cell death releases endogenous adjuvants that selectively enhance immune surveillance of particulate antigens. *European Journal of Immunology*, 32, pp.155–162.

Shi, Y.P. et al., 1999. Immunogenicity and in vitro protective efficacy of a recombinant multistage Plasmodium falciparum candidate vaccine. *Proceedings of the National Academy of Sciences of the United States of America*, 96, pp.1615–1620.

Shih, T. & Lindley, C., 2006. Bevacizumab: An angiogenesis inhibitor for the treatment of solid malignancies. *Clinical Therapeutics*, 28, pp.1779–1802.

Siegel, R., Naishadham, D. & Jemal, A., 2013. Cancer statistics, 2013. *CA: a cancer journal for clinicians*, 63, pp.11–30.

Simon, C.O. et al., 2006. CD8 T cells control cytomegalovirus latency by epitope-specific sensing of transcriptional reactivation. *Journal of virology*, 80, pp.10436–10456.

Simpson, T.R. et al., 2013. Fc-dependent depletion of tumor-infiltrating regulatory T cells co-defines the efficacy of anti-CTLA-4 therapy against melanoma. *The Journal of experimental medicine*, 210, pp.1695–710.

Sims, S. & Klenerman, P., 2014. Increasing inflationary T-cell responses following transient depletion of MCMV-specific memory T cells. *European journal of immunology*.

Slingluff, C.L. et al., 2008. Helper T-cell responses and clinical activity of a melanoma vaccine with multiple peptides from MAGE and melanocytic differentiation antigens. *Journal of Clinical Oncology*, 26, pp.4973–4980.

Smith, J., Lipsitch, M. & Almond, J.W., 2011. Vaccine production, distribution, access, and uptake. *The Lancet*, 378, pp.428–438.

Staras, S.A.S. et al., 2006. Seroprevalence of cytomegalovirus infection in the United States, 1988-1994. *Clinical infectious diseases : an official publication of the Infectious Diseases Society of America*, 43, pp.1143–1151.

Stavnezer, J., Guikema, J.E.J. & Schrader, C.E., 2008. Mechanism and regulation of class switch recombination. *Annual review of immunology*, 26, pp.261–292.

Steen, H.B., 2004. Flow cytometer for measurement of the light scattering of viral and other submicroscopic particles. *Cytometry. Part A : the journal of the International Society for Analytical Cytology*, 57, pp.94–99.

Stephenson, R. et al., 2014. Schistosome Vaccine Adjuvants in Preclinical and Clinical Research. *Vaccines*, 2(3), pp.654–685.

Stevens, T.L. et al., 1988. Regulation of antibody isotype secretion by subsets of antigen-specific helper T cells. *Nature*, 334, pp.255–258.

Stills, H.F., 2005. Adjuvants and antibody production: dispelling the myths associated with Freund's complete and other adjuvants. *ILAR journal / National Research Council, Institute of Laboratory Animal Resources*, 46, pp.280–293.

Suekane, S. et al., 2007. Phase I trial of personalized peptide vaccination for cytokine-refractory metastatic renal cell carcinoma patients. *Cancer Science*, 98, pp.1965–1968.

Sułkowski, W.W. et al., 2005. The influence of temperature, cholesterol content and pH on liposome stability. *Journal of Molecular Structure*, 744-747, pp.737–747.

Suzuki, H. et al., 2013. Multiple therapeutic peptide vaccines consisting of combined novel cancer testis antigens and anti-angiogenic peptides for patients with non-small cell lung cancer. *J Transl Med*, 11, p.97.

Svane, I.M. et al., 2007. Vaccination with p53 peptide-pulsed dendritic cells is associated with disease stabilization in patients with p53 expressing advanced breast cancer;

monitoring of serum YKL-40 and IL-6 as response biomarkers. *Cancer Immunology, Immunotherapy*, 56(9), pp.1485–1499.

Takeda, K. & Akira, S., 2004. TLR signaling pathways. *Seminars in Immunology*, 16, pp.3–9.

Tesfay, M.Z. et al., 2013. PEGylation of vesicular stomatitis virus extends virus persistence in blood circulation of passively immunized mice. *Journal of virology*, 87, pp.3752–9.

Tsuruma, T. et al., 2008. Clinical and immunological evaluation of anti-apoptosis protein, survivin-derived peptide vaccine in phase I clinical study for patients with advanced or recurrent breast cancer. *Journal of translational medicine*, 6, p.24.

Uemura, H. et al., 2006. A phase I trial of vaccination of CA9-derived peptides for HLA-A24-positive patients with cytokine-refractory metastatic renal cell carcinoma. *Clinical Cancer Research*, 12, pp.1768–1775.

Vescovini, R. et al., 2007. Massive load of functional effector CD4+ and CD8+ T cells against cytomegalovirus in very old subjects. *Journal of immunology (Baltimore, Md. : 1950)*, 179, pp.4283–4291.

Visciano, M.L. et al., 2012. Effects of adjuvants on IgG subclasses elicited by virus-like Particles. *Journal of Translational Medicine*, 10, p.4.

Vollmer, J. & Krieg, A.M., 2009. Immunotherapeutic applications of CpG oligodeoxynucleotide TLR9 agonists. *Advanced Drug Delivery Reviews*, 61, pp.195–204.

De Vooght, V. et al., 2010. Choice of mouse strain influences the outcome in a mouse model of chemical-induced asthma. *PloS one*, 5(9), p.e12581.

Walton, S., Mandaric, S. & Oxenius, A., 2013. CD4 T cell responses in latent and chronic viral infections. *Frontiers in Immunology*, 4.

Walton, S.M. et al., 2011. T-cell help permits memory CD8+ T-cell inflation during cytomegalovirus latency. *European Journal of Immunology*, 41, pp.2248–2259.

Walton, S.M. et al., 2008. The dynamics of mouse cytomegalovirus-specific CD4 T cell responses during acute and latent infection. *Journal of immunology (Baltimore, Md. : 1950)*, 181, pp.1128–1134.

Watanabe, H. et al., 2004. Innate immune response in Th1- and Th2-dominant mouse strains. *Shock (Augusta, Ga.)*, 22, pp.460–466.

Watts, C., 2001. Antigen processing in the endocytic compartment. *Current Opinion in Immunology*, 13, pp.26–31.

Webster, D.P., Farrar, J. & Rowland-Jones, S., 2009. Progress towards a dengue vaccine. *The Lancet Infectious Diseases*, 9, pp.678–687.

Weekes, M.P. et al., 2004. Long-term stable expanded human CD4+ T cell clones specific for human cytomegalovirus are distributed in both CD45RAhigh and CD45ROhigh populations. *Journal of immunology*, 173, pp.5843–5851.

Weide, B. et al., 2008. Results of the first phase I/II clinical vaccination trial with direct injection of mRNA. *Journal of immunotherapy*, 31(2), pp.180–188.

Wild, T.F., Malvoisin, E. & Buckland, R., 1991. Measles virus: Both the haemagglutinin and fusion glycoproteins are required for fusion. *Journal of General Virology*, 72, pp.439–442.

Wolchok, J.D. et al., 2009. Guidelines for the evaluation of immune therapy activity in solid tumors: Immune-related response criteria. *Clinical Cancer Research*, 15, pp.7412–7420.

Wykes, M. et al., 1998. Dendritic cells interact directly with naive B lymphocytes to transfer antigen and initiate class switching in a primary T-dependent response. *Journal of immunology*, 161, pp.1313–1319.

Yanagi, Y., Takeda, M. & Ohno, S., 2006. Measles virus: Cellular receptors, tropism and pathogenesis. *Journal of General Virology*, 87, pp.2767–2779.

Yin, L. et al., 2013. CD4+ T Cells Provide Intermolecular Help To Generate Robust Antibody Responses in Vaccinia Virus-Vaccinated Humans. *J Immunol*, 190, pp.6023–6033.

Zhu, J., Yamane, H. & Paul, W.E., 2010. Differentiation of effector CD4 T cell populations. *Annual review of immunology*, 28, pp.445–489.

Zou, W., 2005. Immunosuppressive networks in the tumour environment and their therapeutic relevance. *Nature reviews. Cancer*, 5, pp.263–274.